THE JOURNAL
OF
CHEMICAL PHYSICS

VOLUME 6 DECEMBER, 1938 NUMBER 12

Diffuse Electron Diffraction Patterns

J. T. BURWELL*
Massachusetts Institute of Technology, Cambridge, Massachusetts
(Received August 15, 1938)

Diffuse electron diffraction patterns taken by reflection have in the past been cited as proof that the polished surfaces of metals are amorphous or very finely crystalline. In the present work it is shown that such patterns can be obtained from a large-grained crystalline surface and hence cannot be due to an amorphous phase but rather to the physical contour of the surface.

I. INTRODUCTION

ELECTRON diffraction patterns of the polished surfaces of metals and of some other crystalline materials show only two diffuse rings. By analogy with x-ray diffraction patterns of liquids and glasses this was assumed to prove the existence of an amorphous phase on the polished surface, as first suggested by Beilby.[1] However, Kirchner[2] and Germer[3] raised objections to this and gave alternative explanations of the observed patterns in terms of the physical contour of the surface and the refraction of the beam by the inner potential of the metal. In support of this they stated that very thin films which gave crystalline patterns by transmission yielded diffuse patterns by reflection. Independent evidence[4] and particularly some recent work by Cochrane[5] seem to indicate that the polished layer on metals is indeed either amorphous or very finely crystalline, and in the latter work the polished film is isolated and then examined by transmission so that the objections mentioned above do not arise.

Because of these objections it is now generally admitted that diffuse patterns when obtained by reflection only are not proof of the presence of an amorphous layer.[6] The following experiments support this conclusion since they show that such diffuse patterns may be obtained from samples containing relatively large crystals.

II. EXPERIMENTAL

The apparatus used was a hot filament type employing movable slits, similar to that described by Germer.[7] The sample-to-photographic plate distance was 69 cm and the accelerating voltage 30 kv.

The sample used was an alloy of iron containing 18 percent chromium, 8 percent nickel, and 0.08 percent carbon, commonly known as 18–8 stainless steel. It was fine-grained and wholly in the austenitic or face-centered cubic

* Now at the Research Laboratory, United States Steel Corporation, Kearny, N. J.

[1] G. Beilby, *Aggregation and Flow of Solids* (Macmillan Company, New York, 1921).

[2] F. Kirchner, Erg. exakt. Naturwiss. 112 (1932).

[3] L. H. Germer, Phys. Rev. **43**, 724 (1933); **49**, 163 (1936).

[4] G. I. Finch, A. G. Quarrell and J. S. Roebuck, Proc. Roy. Soc. **A145**, 676 (1934).

[5] W. Cochrane, Proc. Roy. Soc. **A166**, 228 (1938).

[6] G. I. Finch and S. Fordham, Chem. and Ind. **56**, 632 (1937); G. I. Finch, J. Roy. Coll. Sci. **7**, 32 (1937).

[7] L. H. Germer, Rev. Sci. Inst. **6**, 138 (1935).

FIG. 1. Electron diffraction pattern of stainless steel polished under benzene.

phase before treatment. It was polished on various grades of emery paper down through 0000 and finally on chamois, all carried out under benzene. It was transferred while still wet to the diffraction camera which was immediately evacuated. This procedure was followed because, as shown by Dobinski,[8] samples polished in air may give a slightly different type of diffuse pattern which could be the result of exposure to the air, although lately, however, both the results and hypotheses of Dobinski have been questioned.[9, 10] The resulting diffraction pattern showed the two diffuse rings typical of such a polished surface (Fig. 1).

The specimen was then etched electrolytically in a 10 percent solution of oxalic acid until a depth, as estimated from previous quantitative electrolysis experiments, of 18,000A, was removed. At this depth all of the alpha- or body-centered cubic phase produced by polishing has been removed. The diffraction pattern of this surface is the face-centered cubic one typical of the alloy in question and is shown in Fig. 2.

The sample was then heated inductively to a temperature of 1000°C for half an hour in a glass vacuum system. The pressure before and after heating was 1.6×10^{-5} mm of Hg. Benzene was admitted to the system until the sample was covered by the liquid so that no air could reach it and it was again transferred wet to the diffraction camera. The resulting pattern (Fig. 3) was entirely similar to that of the polished sample although there was no question of such a layer being present in this case. Pronounced grain growth had taken place and the grain boundaries were clearly revealed. A photomicrograph of the surface is shown in Fig. 4.

The experiment was repeated but this time air instead of benzene was admitted to the sample after the vacuum annealing before it was placed in the camera. The pattern obtained was the same as that of Fig. 3 and is therefore not reproduced.

III. DISCUSSION

This then is another example of a crystalline surface, in this case composed of relatively large crystals, which gives a diffuse pattern entirely similar to that from a polished surface of

FIG. 2. Electron diffraction pattern of the same sample after being etched.

[8] S. Dobinski, Phil. Mag. **23**, 397 (1937).
[9] Campbell and Thomas, Nature **142**, 253 (1938).
[10] E. Plessing, Physik. Zeits. **39**, 618 (1938).

the same material. Finch and Ikin[11] have reported that prolonged heating in a vacuum broke down the crystalline structure of a particular platinum surface to an amorphous condition. It seems to the author that this deduction from their experiment is entirely untenable and that the explanation for the experiments reported here must be looked for elsewhere. It also seems unlikely that the pattern of Fig. 3 could be due to an adsorbed layer of benzene, since the air-exposed surface where no benzene was present gave precisely the same pattern. Furthermore such gas films would not be expected to give an appreciable pattern at 30,000 volts even on as flat a surface as this one is.

The physical contour of the surface is probably responsible for the observed pattern. In this experiment considerable evaporation of the surface took place before the pattern of Fig. 3 was obtained, and the sharp ridges considered so essential for a good diffraction pattern had disappeared. The surface remained somewhat wavy as seen in Fig. 4, but on the whole was flat enough so that the beam would enter and leave the metal through essentially the same surface although making different angles with this surface at different points on the sample. In this case refraction of the beam is appreciable and because of this varying angle it could distort and blur a crystalline pattern such as Fig. 2 considerably. This has already been suggested[2, 3] and can easily be the case here.

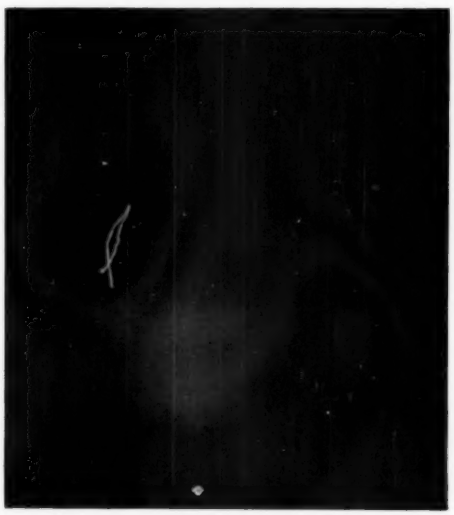

FIG. 3. Electron diffraction of the same after being vacuum annealed at 1000°C.

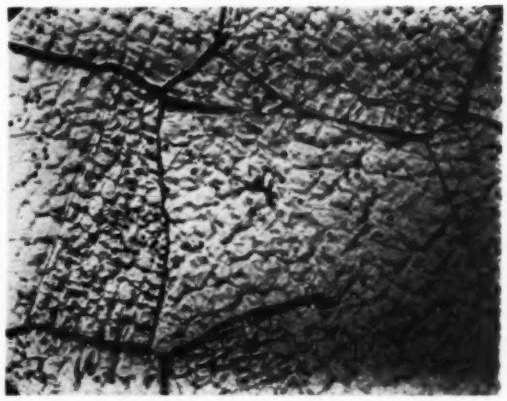

FIG. 4. Photomicrograph of vacuum-annealed surface of stainless steel, unetched, magnified 100×.

In any event this experiment shows that diffuse patterns, similar to those from the polished surface, can be obtained by reflection from large-grained crystalline materials, and hence such patterns when procured by reflection methods are not proof of the existence of an amorphous phase.

The author is much indebted to Professor J. C. Wulff for helpful discussion and encouragement in the course of the present work.

[11] G. I. Finch and A. W. Ikin, Proc. Roy. Soc. **A145**, 559 (1934).

The Ultraviolet Absorption Bands Ascribed to HNO_2

D. M. NEWITT AND L. E. OUTRIDGE
Imperial College of Science and Technology, Royal College of Science, London, England

(Received August 6, 1938)

Attention is drawn to the similarity of a series of absorption bands obtained by Melvin and Wulf as the results of experiments at normal temperatures with a $NO-NO_2-H_2O$ medium and by Bone and Newitt from the explosion of a $CO-H_2O-NO$ medium at high pressures. The formation of these bands in explosion experiments at atmospheric pressure and in static flames is described and evidence is brought forward which suggests that they may be due to the enhancement of certain bands of the normal NO_2 absorption spectrum.

OUR attention has been drawn by Professor Kondratjew to two papers[1] in which the ultraviolet absorption of a $NO-NO_2-H_2O$ medium is described and discussed. They find that mixtures of NO and NO_2 containing small amounts of water give rise to a group of bands in the near ultraviolet, lying in the same region, but not resembling, the longer wave-length NO_2 absorption. From the results of their experiments they suggest the possibility of the enhancement of certain of the NO_2 bands, but conclude that the probable carrier of the bands is the HONO molecule.

The series of bands given in Table I of their second paper appears to be identical with that described by one of us and W. A. Bone,[2] and obtained from the explosion of a $CO-N_2O-NO$ mixture at high pressures. We have since obtained the same spectrum from explosions at atmospheric pressure and from stationary flames of CO burning in various media containing N_2O and NO; and since the combustion method throws some light upon the origin of the bands, it may be of interest if we describe very briefly the conditions under which they are formed.

The radiation emitted by a gas explosion at atmospheric or high pressure may be conveniently examined in an apparatus of the form shown diagrammatically in Fig. 1. A massive cylindrical, steel, explosion vessel E, 1 meter long and 3 cm bore, is fitted with two conical quartz windows W_1 and W_2 and two ignition plugs Y_1 and Y_2. Gases from a number of storage cylinders C_1, C_2, etc., can be admitted separately to E, their respective partial pressures being indicated by a standard pressure gauge G. V_1-V_3 are valves for controlling the supply of gas. Before entering the vessel E the gases may, if so desired, be passed through a steel drying tube D containing freshly distilled phosphorus pentoxide. The vessel itself also may be heated and any water vapor removed by evacuation. In the ordinary way the gaseous mixtures are ignited at the end Y_1 nearest the spectroscope so that the radiation from the flame traverses a column of the hot products of combustion before reaching the window W_1; alternatively it may be ignited at Y_2 the radiation then only traversing a column of unburnt gas.

The apparatus employed in the stationary flame experiments is shown in Fig. 2, which is self-explanatory.

EXPERIMENTAL

(1) The spectrum given by the explosion of an equimolecular $CO-N_2O$ mixture at a pressure of several atmospheres is continuous, extending on an ordinary unsensitized plate down to about 3100A. It shows none of the characteristic OH

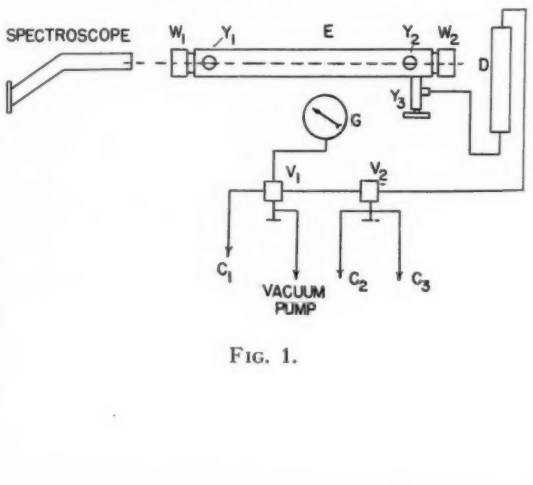

FIG. 1.

[1] E. H. Melvin and O. R. Wulf, Phys. Rev. **38**, 2294 (1931); J. Chem. Phys. **3**, 755 (1935).
[2] Proc. Roy. Soc. **115**, 41 (1927).

bands and little or no sign of the faint banded structure of the spectrum of CO burning in air or oxygen at atmospheric pressure.[3]

(2) By the addition of NO to the above mixture a series of regularly distributed absorption bands in the region 4000–3000A are superposed on the continuous $CO-N_2O$ spectrum; there are no OH bands and no trace of the ordinary absorption spectrum of NO_2. The bands are broad and ill-defined, but the regularity of their distribution is clearly shown on the negatives.

(3) When Exp. (2) is repeated at atmospheric pressure (some ten separate explosions being necessary to obtain a comparable intensity), the same spectrum is obtained together with the 3064A OH bands and the ordinary absorption spectrum of NO_2.

(4) The addition of up to 1 percent of hydrogen to the $CO-N_2O-NO$ mixture has no appreciable effect upon the intensity of the spectrum, but careful drying of the gases causes a slight diminution.

(5) The spectra obtained from the stationary flames of CO burning in N_2O and from a mixture of CO and NO in equal proportions burning in N_2O are similar to those obtained in Exps. (3) and (4).

(6) Careful drying of the gases or the addition of up to 1 percent of hydrogen has little effect upon the intensity.

Results and Discussion

In Table I the wave-lengths, wave numbers in air, and intensities are recorded. The wave-lengths were measured by comparison with an ivory scale, the spectrum of iron furnishing the necessary standards. As already mentioned the bands are in many cases broad and ill-defined and the measurements are, therefore, subject to a probable error of 5A units. The intensities are rough estimates on a scale of 3 for the brightest band and 0 for bands which are just visible. The wave-lengths are given in two columns, the first including all the bands visible on the spectrum of the high pressure explosion experiment (2), and the second, a few additional intense bands which appear in the spectra of

[3] Weston, Proc. Roy. Soc. **A109**, 176, 523 (1925).

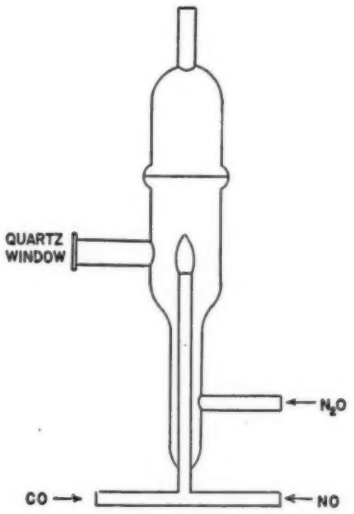

Fig. 2.

Exps. (3)–(6) and probably form part of the same system. It will be noted that the actual values differ, in some cases, from those given in the original paper by Bone and Newitt, because of better definition in the later experiments.

On account of the approximate character of the wave numbers the regularity of the distribution of the bands is not as clearly demonstrable as could be desired; nevertheless, the following partial analysis (Table II) may serve to indicate that the bands are distributed roughly in accordance with the general laws governing the

Table I.

Wave-Lengths		Wave Numbers	Intensity
High Pressure Explosion	Low Pressure Explosion and Flames		
3845		26008	1
	3800	26316	0
	3764	26567	1
3726		26838	2
3680		27173	3
3656		27352	1
	3615	27662	0
3575		27972	0
3545		28209	3
3513		28465	1
	3485	28694	1
3440		29070	0
3418		29257	3
3390		29498	1
	3330	30030	0
3305		30257	0
3270		30581	1
3202		31230	0
3183		31417	0

TABLE II. *Structure of the band spectrum.*

31417(0)	*836*	30581(1)	*1083*	29498(1)	*1033*	28465(1)	*1113*	27352(1)	*1036*	26316(0)
187		*324*		*241*		*256*		*179*		*308*
31230(0)	*973*	30257(0)	*1000*	29257(3)	*1048*	28209(3)	*1036*	27173(3)	*1165*	26008(1)
		227		*187*		*237*		*335*		
		30030(0)	*960*	29070(0)	*1098*	27972(0)	*1134*	26838(2)		
				376		*310*		*271*		
				28694(1)	*1032*	27662(0)	*1095*	26567(1)		

structure of band spectra; and the differences in the columns and rows are as nearly equal as can be expected. The heavy line serves to demarcate the additional bands which appear only in the low pressure explosion and flame spectra.

Melvin and Wulf have shown (reference 1) that under their experimental conditions the intensities of the bands depend upon the partial pressures of the three constituents NO, NO_2 and H_2O and upon temperature, and they conclude that the molecule HONO, or a polymer, acts as the band carrier. Our results, on the other hand, do not entirely support this view. In none of our experiments was NO_2 present initially although small quantities would undoubtedly be formed as the result of the thermal decomposition of any excess of N_2O present in the system.[4] Furthermore, water vapor was present only in traces, not exceeding 0.1 percent by volume, in the high pressure experiments and in the low pressure explosion and flame experiments with specially dried gases; in the latter experiments, indeed, the gases were so dry that considerable difficulty was experienced in getting them to ignite with an electric spark or heated platinum wire. In spite of the absence of any considerable quantities of water vapor, however, the greatest intensity was obtained in the explosion experiment (2), at 9 atmospheres pressure, and the addition of up to 1 percent of hydrogen to the combustible gases caused very little variation in the intensity.

It would appear, therefore, that water vapor and/or hydrogen are not essential to the formation of the bands but that, under the conditions of our experiments, they are always associated with the presence of nitric oxide and the hot products of the thermal decomposition of nitrous oxide.

If the results from the explosion experiments (1), (2) and (3) are compared, it will be noted that in (1) and (2) there is no indication of the ordinary NO_2 absorption spectrum although the cold products of the explosion contain appreciable quantities of the gas, while in (3) the NO_2 bands are quite distinct. In both (2) and (3) the bands attributed to HONO are present. The temperature of the explosion flame of a $CO-N_2O-NO$ medium exceeds 2000°C, but whereas in the low pressure experiment the products cool almost instantly to the temperature of their environment, in the high pressure explosion the rate of cooling is much slower and the flame is probably able to traverse the whole length of the vessel before the products have cooled to a temperature at which the NO_2 molecule is thermally stable. The radiation from the burning carbon monoxide, therefore, in the one case traverses a medium containing NO and NO_2 in partial thermal equilibrium, and in the other a medium containing NO and an NO−O complex which might be regarded as a transition complex or as predissociated NO_2.

This would support the view that the origin of the spectrum is the selective enhancement of certain of the NO_2 absorption bands due to a combination of temperature and the presence of a high concentration of one of the products of its dissociation, namely nitric oxide. The additional bands found in the low pressure experiments, and separately listed in Table I, might then be assigned to NO_2 in the stable state, their intensities being increased by the particular environmental conditions.

[4] Carlton-Sutton, Ambler and Wyn Williams, Phys. Soc. **48**, 189 (1936).

The Infra-Red Absorption of Carboxylic Acids in Solution

I. Qualitative Features

M. M. DAVIES AND G. B. B. M. SUTHERLAND
Departments of Colloid Science and Physical Chemistry, Cambridge, England

(Received August 22, 1938)

The absorption spectra of solutions of acetic, benzoic and trichloracetic acids in carbon tetrachloride have been studied at various concentrations and temperatures in the neighborhood of 3μ, 6μ, and 7μ. At each of these regions is a double band, one component of which is due to the monomeric, the other to the dimeric form of the molecule. The relatively small shift in each case indicates that the molecule is not radically altered on association. The absorptions in the three regions studied were due respectively to the O−H, the C=O and the C−O bonds of the COOH group. It has been possible to make a first estimate of these bond distances in the monomer and dimer, as follows (in A units):

	O−H	C=O	C−O
Monomer	0.9_{81}	1.1_{95}	1.2_{98}
Dimer	1.0_{4}	1.2_{11}	1.2_{85}

The values for the C=O and C−O distances are in satisfactory agreement with those deduced by x-ray methods for oxalic acid but not with those obtained by electron diffraction for formic acid. The general appearance and the temperature variation of the O−H "association" band in these acids appears to be very similar to that of the corresponding band in the alcohols. This is evidence in favor of Badger's explanation of the width of such bands rather than Errera's.

ATTENTION has recently been directed by the work of several authors[1] to the effects of dimeric and polymeric association on the infra-red absorption spectrum of a molecule. The majority of cases so far examined have been concerned with the absorption due essentially to the OH bond in alcohols and in water. The general result of such investigations is, briefly, that the monomeric form of the molecule gives a series of very sharp absorption bands corresponding to the fundamental and overtone frequencies of the OH bond, while the polymeric form gives very broad bands which are consistently shifted to the long wave side of the related sharp monomeric ones. Whatever may be the explanation of the great breadth of these "association bands" it was immediately obvious that the clean-cut distinction between the two types of band provided an excellent means of studying the relative degrees of association under different conditions. One of us (M. M. D.) had been interested in the type of association in the omega-hydroxy carboxylic acids,[2] and the present investigation is the outcome of a suggestion by Professor E. K. Rideal that the methods of infra-red spectroscopy might be applied to this problem. In order to do this, it was necessary first to investigate carefully the absorption spectra of molecules containing the COOH group in solution. We found on examination that the work already done on such molecules did not provide us with sufficient information, largely because it had been done under too low dispersion. Thus, Gordy[3] had shown that the position of the maximum absorption due to the C=O group varied with concentration in solutions of acetic acid in carbon tetrachloride and in benzene, while Kinsey and Ellis[4] had noted a similar effect in the OH absorption near 3μ. Gillette and Daniels[5] had studied the effect of association on the spectrum of acetic acid vapor between 3μ and 10μ. They noted a shift of 46 cm^{-1} in the maximum of the C=O absorption near 5.7μ and a shift of 37 cm^{-1} in another band (attributed by them to the C−O frequency) near 7μ. Finally, Badger and Bauer,[1d] working partly in the vapor and also in the liquid and in solution, had found a sharp monomeric and a wide association band in the region of one of the overtone frequencies of the OH group. We decided to reinvestigate the

[1] (*a*) Errera and Mollet, C. R. Acad. Sci. Paris, **204**, 259 (1937); (b) Fox and Martin, Proc. Roy. Soc. **A162**, 419 (1937); (c) R. Freyman, C. R. Acad. Sci. Paris **204**, 1063 (1937); (d) Badger and Bauer, J. Chem. Phys. **5**, 605 (1937); (e) Badger and Bauer, J. Chem. Phys. **5**, 839 (1937).

[2] Davies, Trans. Faraday Soc. **34**, 410 (1938).

[3] Gordy, J. Chem. Phys. **5**, 284 (1937).

[4] Kinsey and Ellis, J. Chem. Phys. **5**, 399 (1937).

[5] Gillette and Daniels, J. Am. Chem. Soc. **58**, 1139 (1936).

region between 2.5μ and 8μ which contains the important fundamental frequencies, using a quartz prism up to 3.5μ and a fluorite prism between 3.5μ and 8μ. A preliminary report of the main results to be described has already appeared in *Nature*.[6]

Experimental Methods

The spectrometer employed in the investigation was the standard Hilger model (D.83). Two different sources of radiation were employed. In the quartz region a tungsten filament lamp in a quartz bulb, running at 6.5 volts and 14 amp., proved steadier than, and yet of equal intensity to, a Nernst glower. The latter source was used beyond 3.5μ, running at 110 volts and 0.95 amp., with the usual hydrogen-filled iron-filament lamp in series. One great improvement in the normal steadiness of the instrument was effected by the introduction of a second exactly similar Moll low resistance thermopile, completely enclosed in a brass case, which was connected in series and in opposition to that being exposed. The zero fluctuations in both were so nearly equal as to result in a very steady reading. The absorption cells for the solutions had fluorite windows 1″ in diameter and $\frac{1}{10}$″ thick, polished to optical flatness. These were cemented into brass collars *C*, (Fig. 1) the grooves in which were such as to make the window flush with the rim of the collar. An accurately plane brass ring *D*, pierced by a small hole *B* for filling and emptying, was then cemented between both windows. A cellulose acetate adhesive (Durofix) was used throughout with complete success as this is unaffected by the solvents used. Cells with washers of 1.3, 3.05, and 6.02 mm were used at different times. A longer cell of 24 mm was also made by cementing windows into the ends of a short brass tube.

An important feature of the work was the measurement of the absorption of solutions at temperatures up to 108°C. For this purpose a length of Nichrome wire was wound on an asbestos covering around the circular edge of the cell. This was protected by further layers of asbestos tape, while loss of heat from the exposed surfaces of the cell was reduced by pasting to them a covering of asbestos board having a circular aperture. The copper-constantan thermocouple inserted through the aperture used for filling the cell, and the millivoltmeter used in conjunction with it, were calibrated with the aid of N. P. L. standardized thermometers. By means of a large scale ammeter and hand-regulation of the rheostat, the temperature of the cell could be maintained constant to ±0.5°.

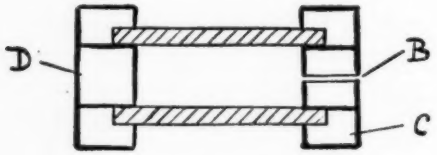

Fig. 1.

The radiation was brought to a focus at approximately the center of the cell, which could be moved out of the beam to determine the percentage absorption. The solvent correction was determined by finding the absorption when the cell (without being removed from its mount) was filled with pure solvent. The reason for not moving the cell from the mount between these runs is that the percentage absorption may vary slightly according to the position of the cell in the beam. By pipetting out of *B* and flushing the cell several times with the solution or solvent about to be examined, the transition from one absorbent to another could safely be accomplished without disturbing the position of the cell in the beam.

The numerical calculation of the solvent effect may briefly be noted. If I_0 is the original intensity, I_α that after passing through the solution and I_β that after passing through the solvent alone, then

$$I_\alpha = I_0 \cdot e^{-\{K_w d + (c_s K_s + c_t K_t) l\}}$$

and

$$I_\beta = I_0 \cdot e^{-\{K_w d + c_s K_s l\}},$$

where K_w is the absorption coefficient of the fluorite, K_s is the absorption coefficient of the solvent, whose conc. is c_s, K_t is the absorption coefficient of the solute, whose conc. is c_t.

Hence,

$$(I_\alpha/I_0)/(I_\beta/I_0) = e^{-c_t K_t l},$$

or the ratio of the percentage absorptions due to solution and solvent separately gives the practical absorption which would have been given by the solute alone. Since much of the later work

[6] Davies and Sutherland, Nature **141**, 372 (1938).

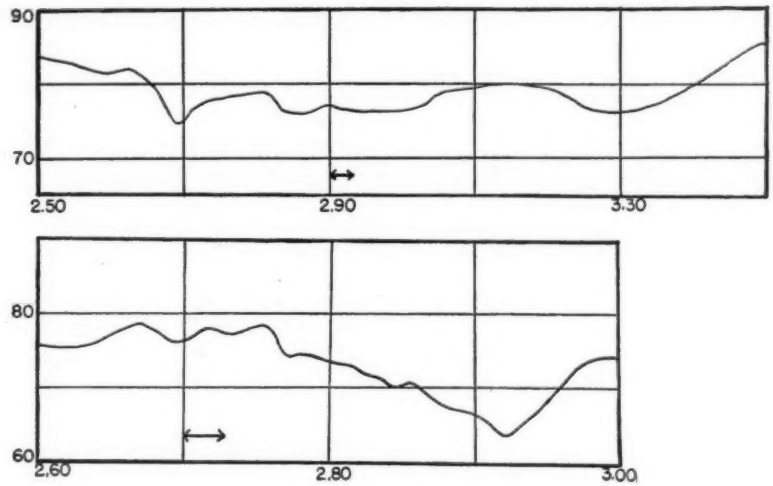

FIG. 2. Transmission curves for CCl_4 in 6.02 mm cell. Percentage transmission plotted against λ in μ. Above at 18°; below at 74°.

depended on the measurement of relative intensities it was decided to evaluate the integral absorption corresponding to each band, defined by the expression

$$\int \delta d\lambda, \quad \text{where} \quad \delta = \log_{10}(I_\beta/I_\alpha) = c_t k_t d.$$

This may be expected to bear a more satisfactory relation to the concentration of absorbing centers than the simple percentage absorption at the center of the band. The $\log_{10}(I_\beta/I_\alpha) \sim \lambda$ plots were made on squared paper and the areas under the absorption band estimated by counting squares, due allowance being made for background absorption when present. In some cases two adjacent bands overlap and the effect of one on the other had to be taken into account.

The greater proportion of the data refer to carbon tetrachloride solutions. The solvent used was the Analar reagent, given a final drying by refluxing and distilling from sodium in an all-glass apparatus. In the quartz region at room temperatures it showed a reasonably uniform transmission of about 80 percent through a 6 mm layer except for a small band at 2.70μ probably due to an overtone of a C−Cl vibration (Fig. 2). It is worth noting that even when the solvent correction was determined with considerable accuracy, a slight absorption at 2.70μ might still be recorded in the corrected curve for the solute, indicating a limitation in the accuracy of the method of applying the correction in such a region. At longer wave-lengths an intense band in the solvent made it impossible to work in the region 6.3μ to 6.8μ: fortunately, this region contained no absorption of the solutes, which was of interest. Carbon tetrabromide was used for temperatures up to 108°C. It proved somewhat difficult to work with (it does not appear to have been used previously as a solvent in this field) as it melts only at 90°C and tends to decompose on prolonged heating. Its extremely strong lachrymatory action was also troublesome.

THE QUALITATIVE NATURE OF THE RESULTS AND THEIR INTERPRETATION

The association of a carboxylic acid is well known to take place through the medium of the COOH group in some such manner as indicated,

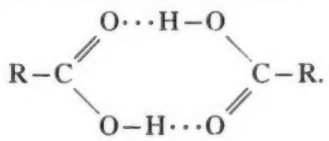

It is therefore to be expected that the O−H, C−O, and C=O bonds of the monomeric molecule will be affected. It is further known from the Raman spectra of series of compounds that any molecule containing a reasonably isolated C=O bond possesses a characteristic frequency in the neighborhood of 1750 cm^{-1}, while the C−O bond sometimes appears to be associated with a frequency of about 1400 cm^{-1} and the OH

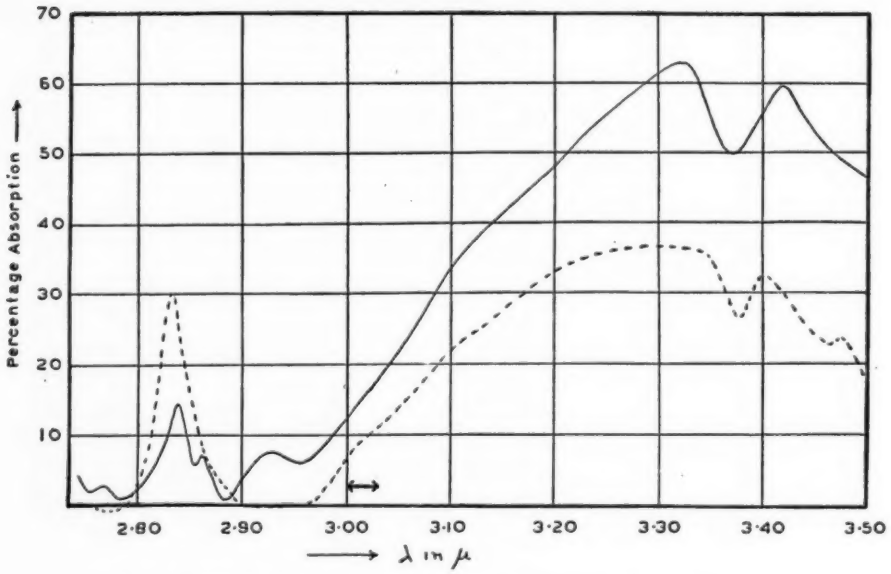

FIG. 3. 0.0100 molar acetic acid in CCl_4 6.02 mm cell. Full curve at 18°; dotted curve at 74°.

frequency is always near 3400 cm^{-1}. Accordingly, we chose the regions near 2.6–3.4μ 5.6–6.2μ and 6.7–8.0μ as most likely to yield significant results. In order to vary the proportion of monomer to dimer we either (a) varied the concentration of the acid in the solvent, or (b) varied the temperature keeping the concentration fixed. In discussing the qualitative results we shall confine our attention to (b), since (a) can only be discussed properly if quantitative measures are considered.

The region of the OH fundamental

The absorption spectra of acetic and benzoic acids were examined between 2.7μ and 3.5μ first at room temperature and then at 74°C. The result in each case (as shown in Figs. 3 and 4: in these, and in the other figures, the effective slit width is indicated by the horizontal arrow) is that a weak but sharp band at 2.84μ increases remarkably in intensity with rise in temperature, whereas a broad ill-defined band near 3.3μ decreases or remains unaffected on raising the temperature. This behavior is very similar to that of the OH absorption in alcohol solutions, with the distinction that there the broad association band can be made to disappear completely by increasing sufficiently the dilution or the temperature. In the case of the alcohols it is possible to distinguish very easily the association band (which extends roughly from 2.8μ to 3.1μ) from the CH bands occurring between 3.2μ and 3.5μ; in the case of the carboxylic acids it would appear that the association band begins at about 3μ and extends to at least 3.3μ. The consequent overlapping of the intense CH absorption would explain why its decrease is difficult to detect in some cases. Accordingly, we have also examined

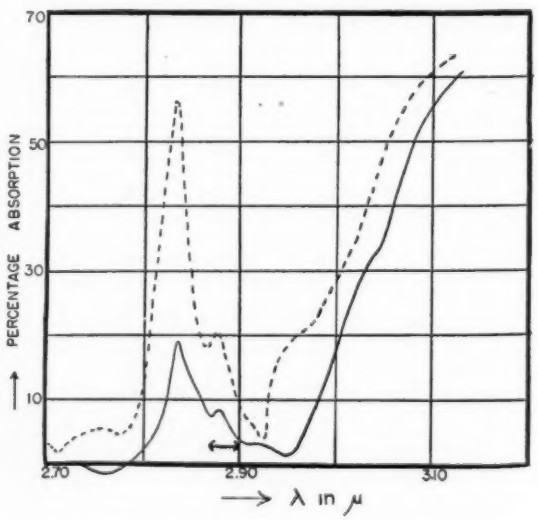

FIG. 4. 0.0167 molar benzoic acid in CCl_4 6.02 mm cell. Full curve at 18°; dotted curve at 71°.

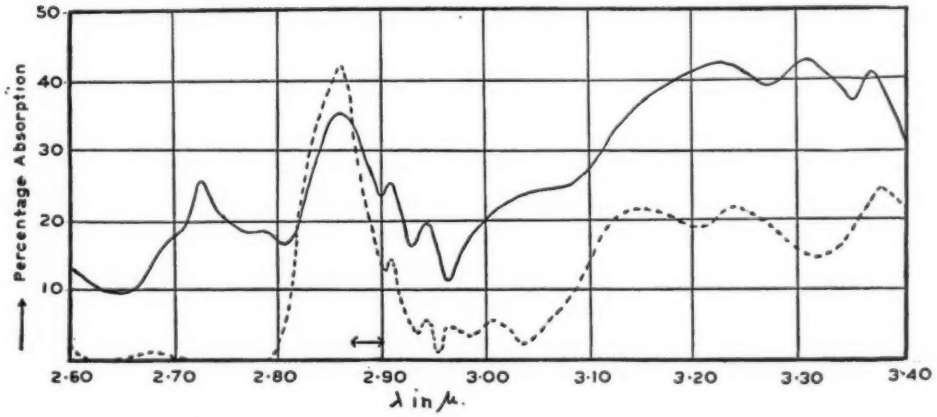

FIG. 5. 0.00565 molar trichloracetic acid in 6.02 mm cell. Full curve at 18°; dotted curve at 76°.

the absorption of trichloracetic acid in the same region. Since there is no CH bond in this molecule one would expect the diminution of the association band to be more pronounced if the above explanation is correct. The curves of Fig. 5 show exactly this behavior, and indicate that the association band extends from approximately 2.9μ to 3.3μ. This is a greater width than that found in the alcohols—roughly 420 cm^{-1} as compared with 350 cm^{-1}. It might be remarked here that the position of the monomeric OH absorption in trichloracetic acid is at a slightly longer wave-length (2.86μ) than that for acetic or benzoic acid (2.835μ). This will be more fully considered later.

Certain small but important peculiarities in the region of the OH absorption should be noted. The first is that very frequently on the long wave-length side of the sharp OH band there appear minor but very definite peaks. These occur at 2.86μ and 2.93μ in acetic, at 2.88μ in benzoic acid and at 2.91μ and 2.94μ in trichloracetic acid. This phenomenon appears to have no counterpart in the OH absorption of the alcohols. The bands in acetic acid were not recorded at the higher temperatures, but it may be that the broadening of the main monomeric band obscured one of them. The bands in benzoic and in trichloracetic acid appear to be relatively unaffected by temperature. Again, in the latter acid there is, on the short-wave side of the main monomeric OH absorption, a distinct band at 2.73μ which disappears on raising the temperature. The possible interpretation of these bands is discussed in a later section.

The region of the C=O fundamental

In this case we have studied only acetic and trichloracetic acid. The results for the former are illustrated in Fig. 6. A 0.010 molar solution in carbon tetrachloride showed two distinct bands both at room temperature and at 73.5°C. At the lower temperature the centers of the bands were at 5.66μ and 5.82μ, with the latter much more intense; at the higher temperature the centers seemed to shift to 5.64μ and 5.81μ, the bands were more clearly resolved, and their intensities were now almost equal. For a 0.0020 molar solution the 5.65μ band appeared stronger than that at 5.81μ. The slight shift of the centers is almost certainly due to the weaker band (at the lower temperature) being "attracted" by the stronger in a well-known way. The shift in the position of this band which was observed by Gillette and Daniels[5] is thus seen to be due to the change in the relative intensities of two bands, one of which is presumably due to the monomeric molecule (1768 cm^{-1}) and the other to the dimer (1719 cm^{-1}). Thus the association may be studied in the region of the C=O fundamental as well as in that of the OH, with the important distinction that here the bands do not differ so greatly in their characteristics as in the OH case.

For trichloracetic acid the two bands were not resolved at room temperature.

The region of the C–O fundamental

The absorption of a 0.010 molar solution of acetic acid was examined between the limits of 6.8μ and 7.8μ at 18°C and 73.5°C. Some of the results are seen in Fig. 7. It will be seen that there

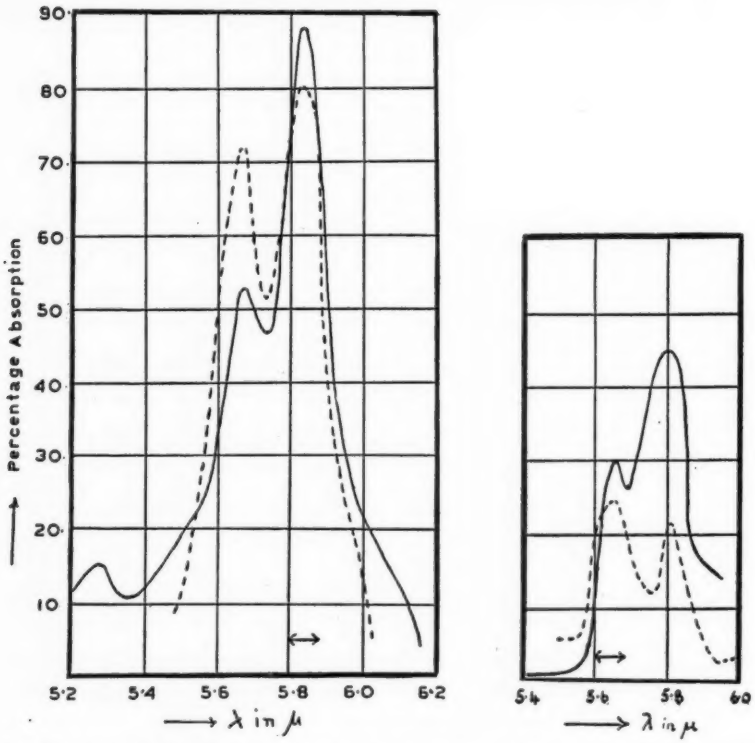

FIG. 6. (a) 0.0100 molar acetic acid in 6.02 mm cell. Full curve at 18°; dotted curve at 73.5°. (b) 0.0020 molar acetic acid.

are four distinct bands at 6.94μ, 7.05μ, 7.25μ and 7.75μ. At the higher temperature the band at 7.25μ seemed to strengthen relative to that at 6.94μ, while those at 7.05μ and 7.75μ appeared unchanged. Thus the former two exhibit the same behavior as the bands for the C=O frequency, except that in this case it is the one of shorter wave-length which weakens on increasing the temperature. Trichloracetic acid gave a more marked result (Fig. 8). At ordinary temperatures it was found that there were strong bands at 6.98μ, 7.06μ, and 7.85μ; weaker bands were noticeable at 6.82μ and 7.36μ. On raising the temperature the 6.98μ band seemed to disappear, a broad band with center near 7.2μ coming up with considerable intensity. Presumably the band at 7.06μ was unaffected although it is difficult to be certain of this in view of the obvious width of the new band. The behavior of the band near 7.8μ at high temperatures was not examined since the one in this region had shown no change in acetic acid. It might be added, however, that the band probably has a different interpretation in the two cases. In acetic acid it is probably due to the CH_3 group, whereas in trichloracetic acid it probably arises from the CCl_3 group. We shall not go into the reasons for the assignment as this point is irrelevant to the main discussion.

DISCUSSION

The first point of interest is the occurrence of the sharp OH band at a definitely longer wave-length than in the alcohols—2.84μ as against 2.76μ, (or 3521 cm^{-1}, against 3623 cm^{-1}). This has proved of great practical value in the later work where a hydroxyacid was studied and it was possible to separate easily the alcoholic OH frequency from that of the carboxylic group. This shift is also important as giving a measure of the change in the OH bond in passing from an alcohol to an acid. Thus we notice from Fox and Martin's work[1] that in a whole series of aliphatic and aromatic alcohols the monomeric OH band shifts only from 2.750μ to 2.764μ. In acetic and benzoic acids we find the same band at 2.84μ, while in trichloracetic acid (a much stronger acid)

it has moved to 2.86μ. The decrease in the OH frequency corresponds to a weakening of the OH bond and so it is not surprising to find this qualitative relation between the value of the OH frequency and the acidity of the compound. It is doubtful whether a quantitative relation can be found since the dissociation constant of an acid depends on many other factors besides the immediate energy of dissociation of the H-ion from the rest of the molecule, and it is only to the latter that the vibration frequency can even be approximately related. We have, however, computed the OH distance in the various cases using Badger's relation.[7] While the absolute values obtained cannot be considered reliable, the relative change in them is undoubtedly significant. These results are collected in Table I.

The examination of the association band in trichloracetic acid, where it is free from the CH absorption, has shown that this band is as broad if not broader, than that found for the alcohols. The cause of this broadening in the alcohols is not yet properly understood. Errera has divided the association band into two bands, one of which he suggests is due to the dimeric form of the molecule, the other to the polymeric molecules.[8]

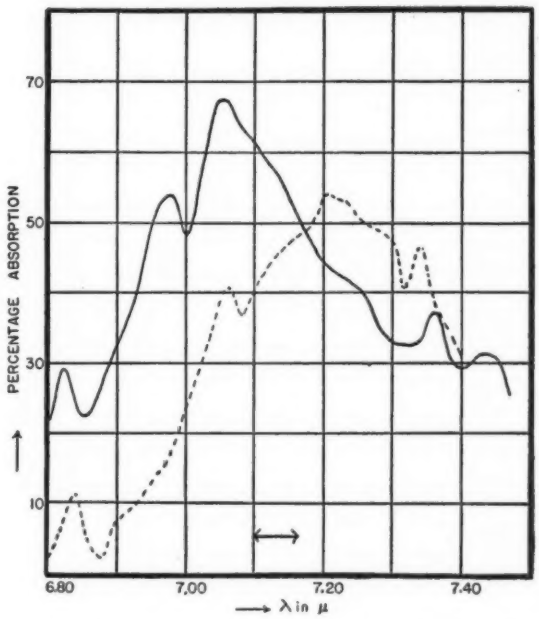

FIG. 8. 0.0195 molar trichloracetic acid in CCl_4 3.05 mm cell. Full curve at 18°; dotted curve at 72°.

[7] Badger, J. Chem. Phys. **3**, 710 (1935).

[8] Errera and Sack, Trans. Faraday Soc. **34**, 728 (1938).

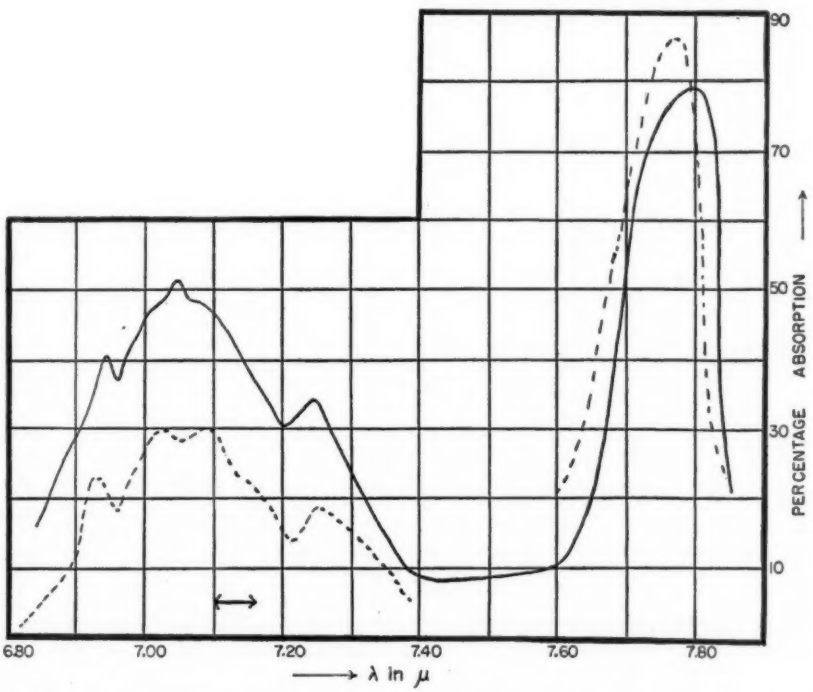

FIG. 7. 0.0100 molar acetic acid in CCl_4 3.05 mm cell. Full curve at 18°; dotted curve at 70°.

TABLE I. O–H *Distances.*

The first column under r_{OH} was calculated treating the OH group as the vibrating unit, the second column by treating XH as the vibrating unit where X represents the rest of the molecule. The true value lies between those extremes but probably much nearer the former.

MOLECULE	MONOMERIC O–H ABSORPTION		r_{O-H} A°		ACID DISSOCIATION CONSTANT
	λ in μ	ν in cm^{-1}			
n-aliphatic alcohols	2.750	3637	0.9_{68}	0.9_{60}	——
Benzyl alcohol	2.764	3618	0.9_{70}	0.9_{59}	——
Phenol	2.769	3612	0.9_{71}	0.9_{60}	1×10^{-10}
Acetic and benzoic acids	2.837	3525	0.9_{81}	0.9_{72}	1.86×10^{-5} and 1.77×10^{-4}
Trichloracetic acid	2.86	3496	0.9_{85}	0.9_{78}	2×10^{-1}

If Errera's explanation were correct, one would expect in the carboxylic acids (where association has long been accepted as purely dimeric) a narrower association band than in the alcohols, showing no sensible variation in structure with temperature. Actually, the association band is broader than in the alcohols and shows structure of the same type. Again, increase of temperature in the case of trichloracetic acid moves the position of maximum absorption to shorter wavelengths, which is exactly what Errera found for the alcohols and interpreted as due to the decrease of the polymeric relative to the dimeric form.

It would seem much more probable that the explanation of the width of these association bands lies in the presence of small combination frequencies arising from the slow vibrations of one-half of the dimer with respect to the other. Since the bond is a weak one, the restoring forces are small, and the masses being large the frequencies must be low. Similar suggestions have already been made by Badger and Bauer.[1e] It seems that the present work substantiates this idea in several ways. Thus the fact that the association band is equally broad in the carboxylic acids and in the alcohols is readily understandable on this hypothesis but not on Errera's. The variation of the contour of the association band with temperature is easily explicable as due to the variation in the number of low vibrations excited at different temperatures. Further, Errera's theory would necessitate the polymeric association of acetic acid which would lead to broad "association" bands for the C=O and C–O frequencies; the figures show them to be as sharp as the monomeric ones. This is what would be expected on the other theory, since the intermolecular bond is through the H-atom and its motion will therefore be most affected by intermolecular vibrations; in other words, the low frequency vibrations should combine strongly with the O–H but not with the C=O or C–O vibrations. The only serious difficulty for the intermolecular vibration theory is the explanation of the variation of the contour of the association band with concentration.[1b] This is not so serious as it might at first appear, since (as we shall show in the following paper) the absorption coefficient for certain vibrations shows variations with concentration. It can therefore happen that at certain concentrations some combination bands will appear more strongly than others. Physically, the effect of concentration on intermolecular vibrations will be rather similar to temperature—an increase of temperature causing increased freedom of vibration in much the same way as does increase of dilution.

The difference between the center of the association band (3.25μ) and that of the monomeric band (2.84μ) *viz.* 448 cm^{-1}, is considerably larger than that for the alcohols (about 230 cm^{-1}). This indicates that the OH bond has been more altered by association in the acids than in the alcohols. We are doubtful whether one can use the measurement of this shift to compute the energy of the association bond in the simple way Fox and Martin have employed for the alcohols. We hope to give a detailed discussion of this problem in a later paper.

Finally, an interpretation first considered for the small additional bands on the long-wave side of the main monomeric OH band was that these might arise from *cis* and *trans* forms of the COOH

group in the monomer, thus

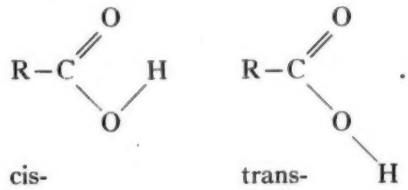

cis- trans-

Pauling has suggested such an interpretation for the weak subsidiary bands found in many of the substituted phenols.[9] This cannot be the explanation in the present instance since with the *cis* position as the more probable[10] this would require the weak band to be on the short wavelength side of the main one. It seems most likely that they are overtone bands of the C=O frequency. The interpretation of the band at 2.73μ in trichloracetic acid is also of considerable interest. It is possibly due to the $-CCl_3$ group in this acid. Remembering that such a group possesses several very low fundamentals, one can expect difference bands the intensities of which can be very sensitive to temperature changes. Thus, Fig. 2 shows that in CCl_4 itself an absorption at 2.70μ disappears on raising the temperature. The fact that it is only in trichloracetic acid that its presence has been definitely established tends to support this interpretation. Obviously, more work must be done on these subsidiary bands before their complete elucidation may be properly attempted.

The C=O frequency

In the foregoing discussion it has justifiably been assumed that one of the normal modes of vibration of any molecule containing an OH group consists essentially of the vibration of the OH group: although there is much evidence that this may also be applied to the C=O and C−O groups, one must be careful about the assignment of definite C=O and C−O frequencies, as the rest of the molecule will now be affected to an appreciable extent. Examination of the Raman spectra of esters, aldehydes, and ketones has shown that they all contain a frequency within 20 cm^{-1} of 1740 cm^{-1} and this has very properly been associated with the C=O group. In the carboxylic acids, however, although some evidence has been found for a frequency near 1730 cm^{-1} the majority of observers have agreed[11] that the Raman frequency common to all such acids which should be ascribed to the C=O group lies near 1680 cm^{-1}. Work in the infra-red has revealed no strong absorption in the latter region but instead a very strong absorption at about 1750 cm^{-1}. This is a serious difficulty which does not seem to have been satisfactorily resolved.

It might be suggested that there is a shift in the C=O frequency in going from the gaseous to the liquid state. Such shifts are well known for other molecules, and the above infra-red data refer either to the gaseous state or to weak solutions in inert solvents, while the Raman data refer to the pure liquid. Indeed, Edsall[12] and Krishnamurti[13] have both remarked on the fact that if the Raman spectrum is done in aqueous solution then a frequency does appear at 1720 cm^{-1}. In ether solutions frequencies appear at both 1666 cm^{-1} and at 1750 cm^{-1}, and Edsall has suggested that one (1650 cm^{-1}) might be associated with the dimeric form of and the other (1720 cm^{-1}) with the monomeric form of the molecule.

It seems that the point that has been overlooked is that one is dealing with a double molecule. There are therefore not one, but two C=O bonds to be considered. Presumably these are identical and are loosely coupled through the hydrogen bond. The result will be not one, but two C=O frequencies arising from the loose coupling of the two identical systems; one frequency lying a little above, the other a little below the individual frequency of either C=O bond taken separately. The best example is another case of a loosely associated molecule which has been investigated in the infra-red *viz.* N_2O_4. Here the frequencies of the two NO_2 groups are split into pairs, one of each pair being active in infra-red absorption but inactive in Raman scattering, the other having the opposite properties.[14] The essential condition for this separation into complementary pairs is that the molecule has a center of symmetry. In the car-

[9] Pauling, J. Am. Chem. Soc. **58**, 94 (1936).
[10] Bauer and Badger, J. Chem. Phys. **5**, 852 (1937); Morino and Mizushima, Proc. Inst. Phys. Chem. Research, Tokyo **32**, 33 (1937).
[11] Cf. Hibben, Chem. Rev. **18**, 38 (1936).
[12] Edsall, J. Chem. Phys. **4**, 1 (1936).
[13] Krishnamurti, Ind. J. Phys. **6**, 401 (1932).
[14] Sutherland, Proc. Roy. Soc. **A141**, 341 (1933).

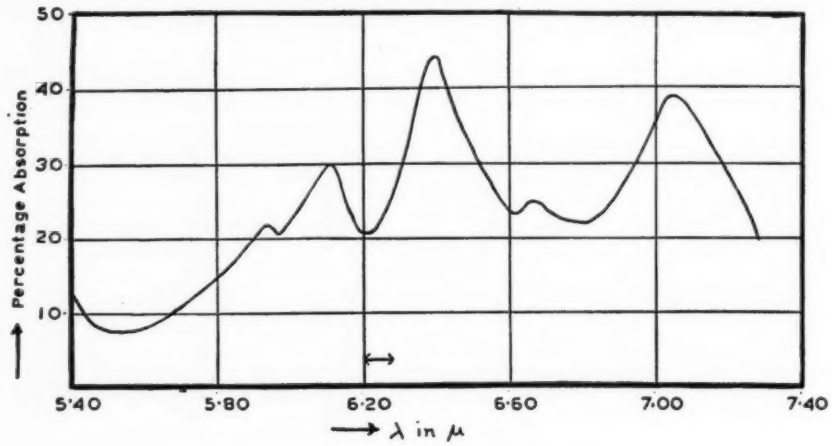

FIG. 9. Absorption of a thin layer of sodium acetate.

boxylic dimer there are two possible structures for the $(COOH)_2$ group arresponding to the cases of complete resonance[14b] (A) and incomplete resonance (B), and there is a center of symmetry in both cases.

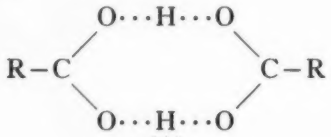

(A)

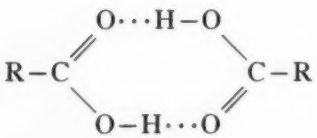

(B)

If resonance is complete and all C−O bonds are identical then one of the pairs will closely correspond to the splitting of the unsymmetrical mode of vibration of the 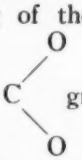 group, and another pair to the splitting of the symmetrical mode of the same group. If resonance is incomplete, then one of the pairs corresponds to the splitting of the C=O frequency and the other to the splitting of the C−O frequency. We believe the latter alternative is the correct one since the dimeric frequency in each case appears so close to the monomeric one. If resonance were complete it seems improbable that the frequencies of the 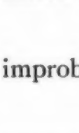 group should fall so close to the monomeric C=O and C−O frequencies.

A rough calculation may be made for the unsymmetrical mode of the group assuming a C−O force constant of 8×10^5 dynes/cm and an angle of 120° between the C−O bonds. This yields a value of 1595 cm^{-1}. In order to obtain a frequency of 1720 cm^{-1}, the value of the force constant would have to be 9.3×10^5 dynes/cm. The value of the C−O force constant is generally accepted to be very close to 4.5×10^5 dynes/cm and that of the C=O bond to be about 12 in the same units. The value of 9.3 therefore cannot be ruled out of consideration. In this connection we have investigated the absorption of a thin layer of sodium acetate where resonance is known to be complete.[15] As Fig. 9 shows there is a particularly strong band at 6.39μ or 1575 cm^{-1}. Further Edsall[16] from investigations of the Raman spectra of molecules containing the COO^- group came to the conclusion that the value for the unsymmetrical mode of

[14b] Pauling and Brockway, Proc. Nat. Acad. Sci. **20**, 236 (1934).

[15] Zachariasen, Phys. Rev. **53**, 917 (1938); Pauling and Sherman, Proc. Nat. Acad. Sci. **20**, 340 (1934).

[16] Edsall, J. Chem. Phys. **5**, 508 (1937).

this group is 1580 cm^{-1}. Although those semi-quantitative arguments cannot be regarded as conclusive without further detailed investigation, the fact that the OH frequency is not altered nearly sufficiently to bring the hydrogen atom midway between the oxygens (the separation of which is 2.67A) makes it very difficult to see how the carbon-oxygen bond to which a hydrogen is firmly attached can be equivalent to the other to which a hydrogen atom is so very weakly attached.

On the basis of incomplete resonance in the carboxylic dimer, and a frequency in the monomer for C=O equal to 1768 cm^{-1}, for C−O equal to 1379 cm^{-1}, one would expect in the dimer two C=O frequencies and two C−O frequencies. The actual value of the C=O frequency in the dimer is consequently the mean of the frequencies observed in the Raman and infra-red. These are, respectively, 1683 cm^{-1} [17] and 1719 cm^{-1}, giving a mean of 1701 cm^{-1}. This approximate method of treatment is only adopted to avoid the complication of a complete dynamical treatment of the problem at this stage. It shows sufficiently well, however, the considerable alteration in the C=O bond which occurs on association. An estimate of the approximate alteration in the interatomic distance during association is also of interest. This may be made using Clark's empirical relation between interatomic distance and vibration frequency for diatomic molecules.[18] We quite realize the approximations involved in such a procedure, and, of course, little reliance can be placed on the absolute values of the interatomic distances derived. However, the relative shift given in Table II must be very near the actual value and is of considerable use until a more complete analysis of the vibrations of the dimer can be achieved.

The C−O frequency

In the foregoing we have made the assumption that there is a definite frequency which may be associated with the C−O bond in the COOH group and that this frequency occurs in the neighborhood of 1400 cm^{-1} or, 7μ. Such an assumption is open to criticism on two grounds: specifically, (a) that many authors from examination of the Raman spectra of other compounds (alcohols, glycols, etc.) have assigned a much lower value to this frequency[19] of about 1050 cm^{-1} to 1100 cm^{-1}; more generally, (b) that one cannot associate frequencies with individual bonds. We shall not discuss (b) since this involves either a complete dynamical treatment of the problem or the quotation of a host of empirical data. Concerning (a), however, it may be remarked that the C−O bond is not necessarily the same in the alcohols as it is in the carboxylic acids.

When one comes to examine the spectra of the carboxylic acids one has the following facts to explain. The presence of a COOH group in a molecule seems to give rise to four characteristic absorptions in the infra-red, (1) near 5.8μ (2) near 7μ and 8μ, and (3) near 10.7μ.[20] The first of these we have already associated with the C=O bond; of the remaining three, the first does not seem to vary in position when one forms the ester whereas the other two do show considerable variations. This would indicate that the 7μ band is due to the C−O link whereas the 8μ and 10.7μ come from deformation vibrations (probably of the OH group, (2) in, and (3) out, of the plane of the group). A further argument in favor of the assignment of the C−O frequency at 1400 cm^{-1} in these acids is that in the Raman spectrum of pure $Cl_3C \cdot COOH$ [21] there is a line at 1413 cm^{-1}, which disappears when the acid is in aqueous solution and is also absent in trichloracetyl chloride. The latter fact provides strong evidence that it is not due to the $C \cdot Cl_3$ group; the trichlor-derivative has been quoted as otherwise there is the great difficulty that CH_3 and CH_2

TABLE II. *The change in the* C=O *distance on association.*

MOLECULE	POSITION OF ABSORPTION BAND IN μ	VIBRATION FREQUENCY IN cm^{-1}	$r_{C=O}$ IN A	$\Delta r_{C=O}$ A
Monomeric Acetic Acid	5.65	1768	1.1_{95}	0.016
Dimeric Acetic Acid	5.82	1701	1.2_{11}	

[17] This value is taken from the work of Angus, Leckie, and Wilson on the Raman spectrum of acetic acid. Proc. Roy. Soc. **A155**, 183 (1936).

[18] Clark, Phil. Mag. **18**, 459 (1934).

[19] Hibben, reference 11; Bonner, J. Chem. Phys. **5**, 293 (1937).

[20] Lecomte, "Structure des Molecules" in *Traité de Chimie Organique*, Vol. 2 (Masson et Cie., Paris, 1936).

[21] Magat, "Tables of Raman Frequencies" from Vol. 11 of *Annual Tables* (Gauthiers Villars, Paris, 1936) pp. 26–40, 26–42.

TABLE III. *The change in the* C—O *distance on association.*

MOLECULE	POSITION OF ABSORPTION BAND IN μ	VIBRATION FREQUENCY IN cm^{-1}	r_{C-O} IN A	Δr_{C-O} IN A
Monomeric Acetic Acid	7.25	1379	1.2_{98}	−0.013
Dimeric Acetic Acid	6.94	1425	1.2_{85}	

groups each have prominent frequencies in this region.

Accepting this general interpretation of the absorption near 7μ we identify the band at 6.94μ as due to the dimeric C—O and that at 7.25μ as due to the same bond in the monomer. It is to be noted that, as for the C=O frequency, the monomeric absorption is very intense compared with the dimeric. The fact that the dimeric absorption is at a shorter wave-length than the monomeric indicates that the C—O bond strengthens on association, the frequency increasing from 1393 cm^{-1} to 1435 cm^{-1}. This shift is correlated with the change in internuclear distance in the same way as for the C=O frequency (Table III). Here it will be observed that for the C—O frequency in the dimer we have taken not the frequency corresponding to 6.94μ but the mean between this frequency and that found in the Raman spectrum of trichloracetic acid *viz.* 1413 cm^{-1}. The latter is presumably the counterpart of the 1680 cm^{-1} carboxyl Raman frequency. The result should be compared with that found for the C=O distance. There we found an extension of 0.016A: here we get a contraction of 0.013A on association. Again, we would stress that the absolute values of the distances must not be regarded as within less than 3 percent of the correct value but the differences are certainly significant and of the correct order of magnitude. It is particularly interesting to compare the distances for the C=O and C—O links with those found by x-ray methods by Robertson and Woodward.[22] They found 1.24A and 1.30A, i.e., a difference of 0.06A; we get the corresponding figures to be 1.211A and 1.285A, giving a difference of 0.074A. The agreement is very satisfactory considering the nature of the approximations made in our calculations. It may be noted that if a value of 1080 cm^{-1} is used for the C—O frequency, the corresponding distance comes out as 1.376A. This is additional evidence in favor of our assignment.

[22] Robertson and Woodward, J. Chem. Soc. **4**, 1817 (1936).

The Infra-Red Absorption of Carboxylic Acids in Solution

II. Intensities

M. M. DAVIES AND G. B. B. M. SUTHERLAND
Departments of Colloid Science and Physical Chemistry, Cambridge, England

(Received August 22, 1938)

The integral absorption of the monomeric OH band has been measured for solutions of acetic, benzoic and lauric acids in CCl_4 at various concentrations and temperatures. At any given temperature the results indicate that the integrated intensity is roughly proportional to the amount of the monomer present, assuming that there is a monomer⇌dimer equilibrium. The temperature variation of the integrated absorption gave values for the heat of association varying from 6000 to 10,000 cal./g mole, which is considerably below the accepted value of 15,000 cal./g mole. This difference is attributed to the variation in the absorption coefficient with temperature. Equally anomalous results were obtained from measurements on the intensity of the monomeric C=O band. The variation of the absorption coefficient with concentration and with temperature was checked independently on solutions of cetyl alcohol in CCl_4.

A QUALITATIVE relationship between the appearance of certain absorption bands and the degree of association of the acid having been established, an attempt was made to put that relationship on a quantitative basis. Accordingly, the intensities of the monomeric bands at 2.83μ and 5.65μ were measured at varying concentrations and at two or more temperatures. The method of measuring the intensity has already been explained. (See Paper 1.) If the assumptions are correct, then the integral absorption is a direct measure of the number of absorbing centers provided the transition probability does not alter with concentration or with temperature. As we shall see, the latter conditions do not appear to be fulfilled, although the variation with concentration does not seem to be nearly so serious as that associated with temperature. It should be noted that in all the results now to be presented a constant absorption path-length of 6.02 mm was employed. The class mark provides an indication of the estimated uncertainty involved in determining the areas, this being largely dependent on the steadiness of the background absorption. When this uncertainty is less than 5 percent an α is used; for an uncertainty of 5 percent to 12 percent, β; and where greater than 12 percent, γ. The figures (1 and 2) illustrate typical examples of the procedure.

In Tables I–III c = total concentration of acid in g moles/liter, while m = computed integral absorption $\int \delta d\lambda$ for the band in question in arbitrary units maintained at the same dimension throughout. If we have a monomer⇌dimer equilibrium and α is the fraction of solute as monomer, for a total concentration of c g moles per liter, then

$$2c^2\alpha^2/c(1-\alpha) = 2c\alpha^2/(1-\alpha) = K_{(\text{Assoc})}$$

or,

$$[\text{R}\cdot\text{COOH}]_{\text{monomer}} = c\alpha = \left(\frac{K}{2}c(1-\alpha)\right)^{\frac{1}{2}} \backsimeq \left(\frac{Kc}{2}\right)^{\frac{1}{2}}$$

the final approximation being applicable when α is small compared with unity. Thus the monomer concentration, and therefore the integral absorption, should be proportional to the square root of the total concentration of acid if α is small. In Tables I to III are collected the observations on the monomer band at 2.83μ for acetic, benzoic and lauric acids at several concentrations and temperatures. (Fig. 1.)

Inspection shows that c/m^2 is very satisfactorily constant for acetic acid at 75°, but only moderately so for the other sets of observations. The only systematic variation in these values seems to be the anomalously high figures at the greatest concentrations, i.e., smaller values of m than would have been expected. A similar effect will be noted later in the case of an alcohol.

As m^2/c (proportional to $K(1-\alpha)$) gives an approximate measure, in arbitrary units, of the

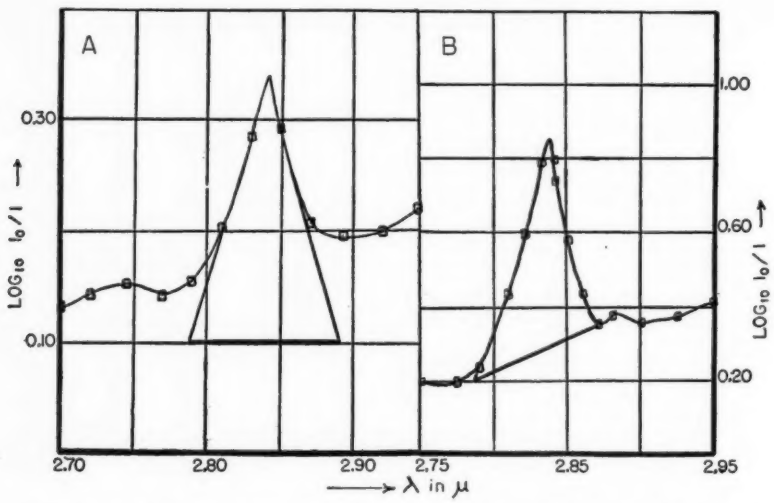

FIG. 1. A. 0.167 molar benzoic acid. Temperature: 43.0°. Area: 1458 squares ≡4.86 units. B. 0.167 molar benzoic acid. Temperature: 72°. Area: 945 squares ≡9.45 units.

association constant K, its temperature variation should allow of the heat of association being estimated. The results for acetic acid in CCl_4 give a value of $\Delta H = 9300 \pm 1000$ cal./g mole. For benzoic acid the temperature variation between 18° and 43.5° was in the wrong direction* while that between 18° and 72° gave a maximum figure of 6600 cal. per g mole. The accepted value of this heat of association, from measurements on formic and acetic acids in the gas phase, is near 15,500 cal./g mole.[1] That this value is not appreciably changed by solution in CCl_4 has been shown in the case of benzoic acid. The association of the latter was measured in CCl_4 at 19.5° by the partition method and at the boiling point by molecular weight determinations in the Cottrell apparatus.[2] The values for $K_{(\text{Assoc})}$ were 7.30×10^{-5} at 19.5°; 4.5×10^{-3} at 76.5°; giving $\Delta H = 14{,}700$ cal./g mole. The great difference between these values and those estimated from the integral absorptions can only mean that the absorption coefficient K_ι in the expression $I_\alpha = I_\beta e^{-c_\iota K_\iota l}$, itself varies with temperature, actually decreasing with rise in temperature. Again, a similar effect was found for the O−H absorption in the alcohols.

In order to pursue this point, the integral absorption of the monomeric band at 5.65μ was also measured at different temperatures. This yielded a value of $\Delta H = 1000$ cal./g mole. The obvious conclusion that the variation of absorption coefficient with temperature is even greater for the C=O than for the O−H group is not, however, justified since there is considerable uncertainty in the values of m owing to the overlapping of the two bands. Allowing for all

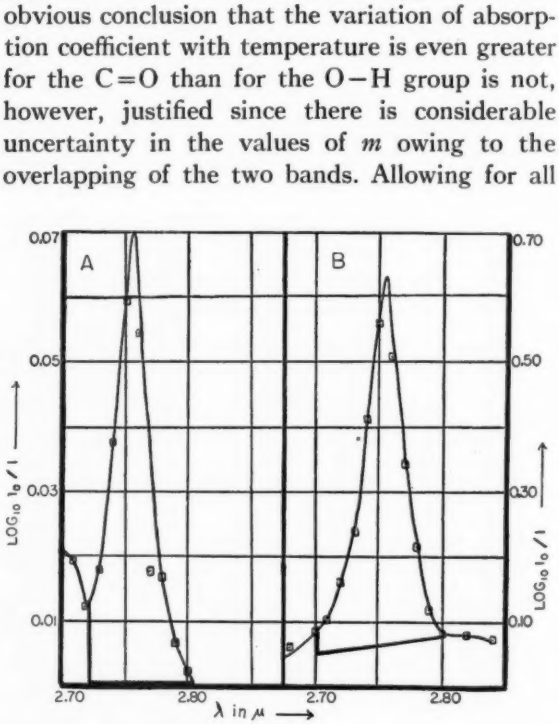

FIG. 2. 0.0033 molar cetyl alcohol. Temperature: 74°. Area: 1796 squares≡0.90 unit. B. 0.050 molar cetyl alcohol. Temperature: 74.3°. Area: 1735 squares≡8.67 units.

* Cf. the first curve on Fig. 1 where the area taken for m considerably exceeds a normal estimate, thus giving a maximum value for m.

[1] MacDougall, J. Am. Chem. Soc. **58**, 2585 (1936); Coolidge, *ibid.* **50**, 2166 (1928).

[2] Davies, Trans. Faraday Soc. **34**, 410 (1938).

TABLE I.

	Acetic Acid in CCl_4 (a) At 18°			(b) At 75°			Acetic Acid in CBr_4 (c) At 109°		
c	0.010	0.020	0.050	0.0020	0.010	0.050	0.0038	0.0204	0.224
m	1.11	1.69	2.10	1.90	4.40; 4.19	8.50	5.20	13.3	23.0
Class	β	α	β	β	β α	α	β	γ	γ
$(c/m^2)\times10^3$	8.12	7.00	11.3	0.55	0.52: 0.57	0.69	0.14	0.12	0.42

TABLE II.

	Benzoic Acid in CCl_4 At 18°			At 43.5°		At 72°		
c	0.00334	0.0167	0.167	0.0167	0.167	0.00334	0.0167	0.167
m	1.31; 1.20	1.60; 1.76	4.83; 5.21	1.21	4.86	1.86	4.36	9.43
Class	β β	β γ	β γ	γ	γ	α	α	β
$(c/m^2)\times10^3$	1.94; 2.32	6.52; 5.39	7.13; 6.13	11.4	7.10	0.96	0.88	1.87

TABLE III.

	Lauric Acid in CCl_4 at 74°			
c	0.0020	0.0100	0.050	0.25
m	1.06; 0.72	2.53; 2.85	6.42	7.17
Class	β α	α α	β	γ
$(c/m^2)\times10^3$	1.64; 3.85	1.56; 1.23	1.21	4.85

possible sources of error, the value of ΔH found from the variation of the C=O integral absorption is no higher than that found from the O−H bands. That the present is a solvent effect on the absorption coefficient is made more certain by the observations of Badger and Bauer[3] on the intensities of the O−H overtone bands in the gas phase, from which they derived a normal value of the heat of association.

A further confirmation of this effect came from a study of the OH absorption in cetyl alcohol (chosen for later use as a standard for the alcoholic OH absorption in omega-hydroxy-undecanoic acid), of which a very pure sample was available. Here we measured at 18° and at 74° the monomeric OH absorption for concentrations which were always so low that *the association band was never present.* The results are given in Table IV (Fig. 2).

It will be noticed that the integral absorption varies with concentration at each temperature. This is a real effect and not due to experimental error. Equally important is the variation with temperature of the integral absorption for a given concentration, which is even more pronounced than the former effect. We have tried whether a variation with temperature of the OH absorption coefficient in the acids of the above order would account for the low value of the heat of association. Although the correction is appreciable (corresponding to an increase in ΔH of 2100 cal./g mole in the case of benzoic acid) it is not nearly sufficient; indicating that the effect must be much more pronounced in the acids than in the alcohols.

From the above we see that it is not possible to use the integral absorption of the monomeric band of an associating molecule as a measure of the concentration of monomer present without making due allowance for the fact that the absorption coefficient varies both with the concentration of the absorbing centers and with the temperature. Provided due allowance is

[3] Badger and Bauer, J. Chem. Phys. **5**, 605 (1937).

TABLE IV.

	Cetyl Alcohol in CCl_4 (a) At 18°			(b) At 74°				
c	0.0033	0.0100	0.0033	0.010	0.0167	0.050		
m	1.22	3.23	0.90	2.67	4.40	9.52	8.67	
Class	α	α	α	α	α	α	β	
m/c	366	323	270	267	264	190	174	

made, it should be possible, however, to form a fair estimate of the concentration of free alcoholic and carboxylic OH groups in solutions of a substance the molecule of which contains one or both of these entities. The application of this to the configuration of the omega-hydroxyundecanoic acid molecule in CCl_4 solutions is considered in the next paper.

ACKNOWLEDGMENTS

One of us (M. M. D.) is indebted to the University of Wales for a Research Fellowship; the other wishes to express his thanks to the Chemical Society for a grant. We are both grateful to Professor E. K. Rideal for his original suggestion and for his interest in this work.

DECEMBER, 1938 JOURNAL OF CHEMICAL PHYSICS VOLUME 6

An Infra-Red Study of Omega-Hydroxyundecanoic Acid in Carbon Tetrachloride

MANSEL M. DAVIES
Department of Colloid Science, Cambridge, England
(Received August 22, 1938)

An infra-red examination of a long chain omega-hydroxycarboxylic acid has provided evidence as to the inter- and intramolecular association of such molecules in solution: In particular, it is believed that the occurrence of a cyclic form of the monomeric molecules in solution has been proved.

THE examination of omega-hydroxyundecanoic acid, $CH_2OH \cdot (CH_2)_9 \cdot COOH$, was suggested by the interesting behavior in its condensation reaction which was examined in different solvents.[1] Combined with data on its molecular complexity, the kinetic analysis led to a picture of the relations of this compound in solution which may be summarized as follows:

(1) At great dilutions where the simple monomeric molecules predominate it would appear that, owing to interaction between their end-groups, these tend to assume a cyclic rather than an open-chain configuration.

(2) With increasing concentration the dissolved molecules aggregate to units of higher molecular weight, a process which occurs very readily in nonpolar solvents and which proceeds until complexes of at least three or four times the normal molecular weight represent the average degree of dispersion.

The results of the study of typical alcohols and carboxylic acids in solution (see the foregoing papers) have shown how their characteristic groups, $-CH_2OH$ and $-COOH$, when free from associative interaction with others of a similar nature, can be separately identified and even estimated quantitatively. The essential feature of the present study lies in the measurement of the frequency of occurrence of these free individual groups in solutions of the hydroxyacid, on the basis of the integral intensities of the corresponding O−H absorption bands. It may be stated here that as a preliminary this method was applied to the examination of the occurrence of an acid-alcohol complex in mixed CCl_4 solutions of lauric acid and cetyl alcohol. The quantitative results showed that this interaction was certainly detectable but, as could be anticipated from independent estimates of its intensity,[2] the amount of complex so formed is very small, partly owing to the considerable self-association predominating in the case of the acid.

The present examination was confined to carbon tetrachloride solutions for this is one of the few common solvents which is free from a major absorption in the region of the hydroxyl bands. The negligible solubility of the hydroxy-acid at 18°C in CCl_4 precluded measurements at room temperatures and these are accordingly confined to 74°C. The apparent molecular

[1] Trans. Faraday Soc. **34**, 410 (1938).

[2] Trans. Faraday Soc. **33**, 335 (1937).

TABLE I. *Apparent molecular weights of* $CH_2OH \cdot (CH_2)_9 \cdot COOH$ *in* CCl_4 *at 76.5°.*

c, g moles per liter:	0.037	0.074	0.112	0.153	0.234
Mol. wt. (observed):	386	420	490	526	690

weights for $CH_2OH \cdot (CH_2)_9 \cdot COOH$ (calculated =202) determined by the elevation of the boiling point in CCl_4 are given in Table I, and show that the monomeric molecules will only predominate at very great dilutions.

Determination of the absorption spectrum of the hydroxyacid in the 2.6μ–3.5μ region showed only the anticipated features: Distinct sharp bands with peaks at 2.755μ and 2.835μ corresponding to the alcoholic and carboxylic hydroxyl absorptions, respectively, succeeded on the long wave-length side by the band arising from the associated molecules and from the C−H fundamental. In the same manner as previously, after correction for the cell and solvent absorptions, the $\log_{10}(I_\beta/I_\alpha) \sim \lambda$ curves were plotted and the areas enclosed by each of the sharp hydroxyl bands determined. The figures illustrate typical examples of the results. In the first place the discussion will be confined to the results for the alcoholic hydroxyl ($-CH_2 \cdot OH$) absorption.

The results of a systematic study of the OH absorption in cetyl alcohol at 74° in CCl_4 have been presented in the preceding paper. It was demonstrated that the integrated absorption of the 2.76μ band provides a measure of the concentration of free OH groups, the proportionality between these two factors actually being constant at dilutions greater than 0.02 molar. It must be emphasized that these similar measurements for the hydroxyacid were carried out using the same 6.02-mm absorption cell under as nearly identical conditions as those used for the alcohol. In determining the integrated absorptions it was easy to reduce these figures to the same arbitrary units as had been adopted for the alcohol. The assumption was then made that the specific absorptive power of the free alcoholic group is the same in both cetyl alcohol, $C_{16}H_{33}OH$, and in the hydroxyacid, $HOOC \cdot (CH_2)_9 \cdot CH_2OH$. The similarity of the structures in which the alcoholic OH group occurs suggests this equality, while the quantitative accuracy of this assumption may be estimated by a comparison of some results for benzyl alcohol, $C_6H_5 \cdot CH_2OH$, with those for cetyl alcohol. In the latter case an integral absorption per g mole of solute of 350 units may be taken from the results at 18°. Under the same conditions three measurements with benzyl alcohol solutions gave a value of 300±15 for this figure. The difference between these two values might safely be ascribed to the influence of the benzene nucleus in the latter molecule, in which case the practical identity of the absorptions in cetyl alcohol and the hydroxyacid would be assured. Thus, using a constant value of 270 units for the integrated absorption per g mole of free OH in dilute CCl_4 solution at 74° and interpolating, on the basis of similar values of the integral absorptions in Table IVb of the preceding paper at higher concentrations, the hydroxyacid measurements were converted into estimates of the molar concentration of free—i.e., unassociated—alcoholic hydroxyl groups. These results are summarized in Table II.

This table shows a very interesting result. Neglecting small departures which are obviously within the experimental error, the general indication is that the fraction of free hydroxyl groups, which at high concentrations is about one-half of their stoichiometric amount, at first increases with dilution but at the lowest concentrations again decreases. At the highest concentration in Table II (0.125 molar) the molecular weight data show the mean degree of association to be about 2.7. It seems very probable that the tendency to associate of the carboxyl groups, producing a dimer I, will be the first to assert itself:

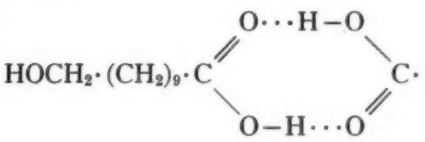

$(CH_2)_9 \cdot CH_2OH$ I

This, alone, would result in no decrease in the concentration of free alcoholic hydroxyl groups, but it is certain that before association in the sense I is complete, these latter groups come into interaction either with free carboxyl groups or with other alcoholic OH groups, producing for instance, molecular aggregates of the form II.

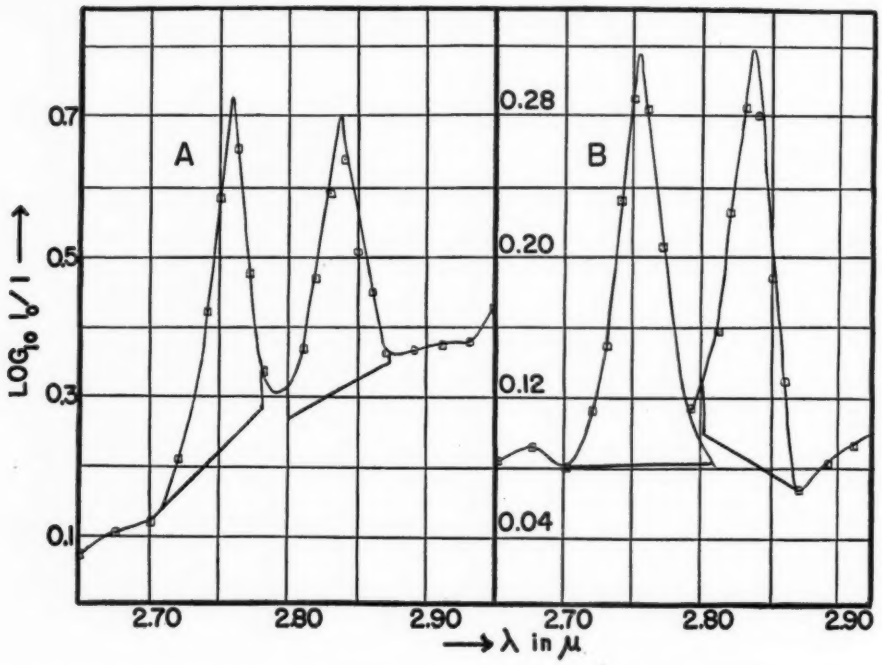

FIG. 1. Integral absorption curves. A. 0.0625 molar hydroxyacid at 74°. B. 0.0208 molar hydroxyacid at 75°.

(*a*) $HOOC\cdot(CH_2)_9\cdot CH_2OH\cdot$
$HOCH_2(CH_2)_9\cdot COOH$;

(*b*) $HOCH_2\cdot(CH_2)_9COOH\cdot$
$HOCH_2\cdot(CH_2)_9\cdot COOH$. II

All that can be said with certainty is that type I will predominate at the dimer stage (see also a later paragraph) leaving an appreciable proportion of free alcoholic OH groups. Thus, on the arbitrary, but not unreasonable, assumption that together the two types II are as frequent as I, at the dimer stage, we should expect 63 percent of free alcoholic OH groups—which is approximately the condition found. Increasing the dilution beyond the dimer stage can only result in a rise in monomer concentration. The fact that this is not accompanied by a progressive increase in the proportion of free OH groups makes it extremely probable that intramolecular interaction of the same type occurs in the monomer: this can only be formulated as a cyclization (III).

TABLE II. *The alcoholic* OH *absorption in* CCl_4 *solutions of* $CH_2OH\cdot(CH_2)_9\cdot COOH$ *at 74°.*

c = TOTAL CONC. IN g MOLES PER LITER	$\int \log_{10}\frac{I\beta}{I\alpha}d\lambda$	CLASS	c_f = CONC. FREE ALCOHOLIC OH GROUPS	% FREE OH GROUPS $=\frac{c_f}{c}\times 100$
0.125	11.33	β	11.33/160 = 0.071	56
0.0625	7.01	β	7.01/225 = 0.0312	50
0.0500	8.06	β	8.06/220 = 0.0366	73
0.0208	3.58	α	3.58/270 = 0.0132	63
0.0070	1.21	α	1.21/270 = 0.0045	64
0.0050	0.40	α	0.40/270 = 0.00148	30
0.0035	0.28	γ	0.28/270 = 0.00104	30

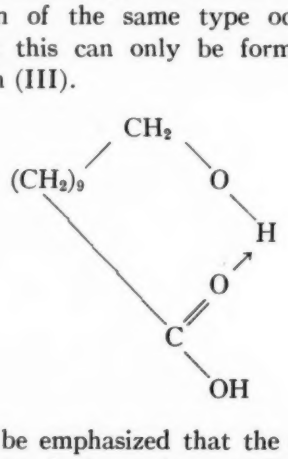

III

It should be emphasized that the order of the variations in the last column of Table II upon which this conclusion is here based, would be even more pronounced if a constant specific absorption capacity for the free OH group had been assumed throughout. Further, a careful

examination of the possible experimental errors, including that for the solvent correction, in the result for the 0.0050 molar solution showed that their cumulative operation in one direction would hardly suffice to place the correct figure above 40 percent for the free alcoholic OH groups. The values of the two last percentages in Table II suggest that the equilibrium

Open-chain monomeric molecules $\rightleftharpoons$ Cyclic molecules,

under these conditions lies with about 70 percent in the cyclic form.

The whole of the previous analysis, as far as the results at 74° in the 6.02-mm cell are concerned, has been repeated for the carboxylic OH absorption. The specific integral absorption, i.e., the integral absorption per g mole of free COOH, $=1/c \times \int \log_{10}(I_\beta/I_\alpha)d\lambda$, has been estimated for this case from the data for lauric and benzoic acids at 74°. The uncertainty in the association constants used to calculate the concentrations of monomeric molecules for these solutes undoubtedly accounts for the unsatisfactory values for this specific absorption. For lauric acid values of 1100, 580, 520, and 240 were calculated at different concentrations, while benzoic acid gave values of 1110, 965, and 590. The value of 600 chosen for this factor may thus be greatly in error, but it is important to note that we are interested not so much in the absolute values of the "free" COOH concentrations as in their variation with the total solute concentration. On this basis the following results have been obtained from the estimated integral absorptions of the 2.835μ carboxylic OH band in omega-hydroxyundecanoic acid.

It is immediately seen that these figures essentially reproduce the results for the alcoholic OH absorption, and their interpretation may be taken in the same sense. Despite the probable error in the extinction coefficient, the very definitely lower proportion of free carboxyl than free hydroxyl groups is significant. This provides a direct confirmation that the association in the first instance predominantly involves the carboxylic groups. It must be explained that on the present interpretation the proportion of free carboxyl groups should increase on dilution only in that concentration range in which there is some proportion of solute with degree of association greater than that of the dimer. Thus, on the previously assumed state of affairs for a mean degree of association, $n=2.0$ (i.e., at 0.04 molar at 76.5°), there should then be 37 percent of "free" carboxyl groups. This should represent, at least approximately, a maximum value for this figure. The results, while not in quantitative agreement with this picture, nevertheless substantially confirm its essential correctness. The eventual decrease with increasing dilution of the specific absorption in the 2.83μ band indicates that the carboxylic OH absorption in this region is also repressed when interaction with the $-CH_2OH$ group occurs: This is not obvious if the interaction is represented

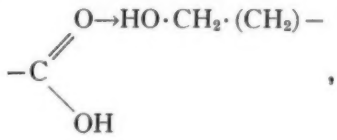

as the hydroxyl group of the COOH structure is not then directly involved in the hydrogen bond. The final value for the free carboxyl groups (20 percent) should coincide, if the solute is then all present as monomer, with that of 30 percent found for the alcoholic hydroxyl groups. The difference might easily be accounted for by a small residual association involving only the carboxyl groups and/or, by the error in estimating the absolute free concentration of the latter.

One other conclusion may be drawn from these data: It appears that in the solutions examined only a small proportion of the molecules can be associated to a "parallel" dimer of the structure IV: for if this predominated, equal proportions of alcoholic and carboxylic groups should be bound in association at the dimer

TABLE III. *The carboxylic* OH *absorption in* CCl_4 *solutions of* $CH_2OH\cdot(CH_2)_9\cdot COOH$ *at 74°.*

c = Total Conc. in g Moles per Liter	$\int \log_{10}\frac{I_\beta}{I_\alpha}d\lambda$	Class	c_f = Conc. Free Carboxylic OH Groups	% "Free" COOH
0.125	9.36	β	0.0156	12.5
0.0625	5.63	α	0.0094	15.0
0.0500	4.80	α	0.0080	15.9
0.0208	3.14	β	0.0052	25.0
0.0070	1.20	α	0.0020	28.5
0.0050	0.70	α	0.0012	23.1
0.0035	0.40	β	0.00066	18.9

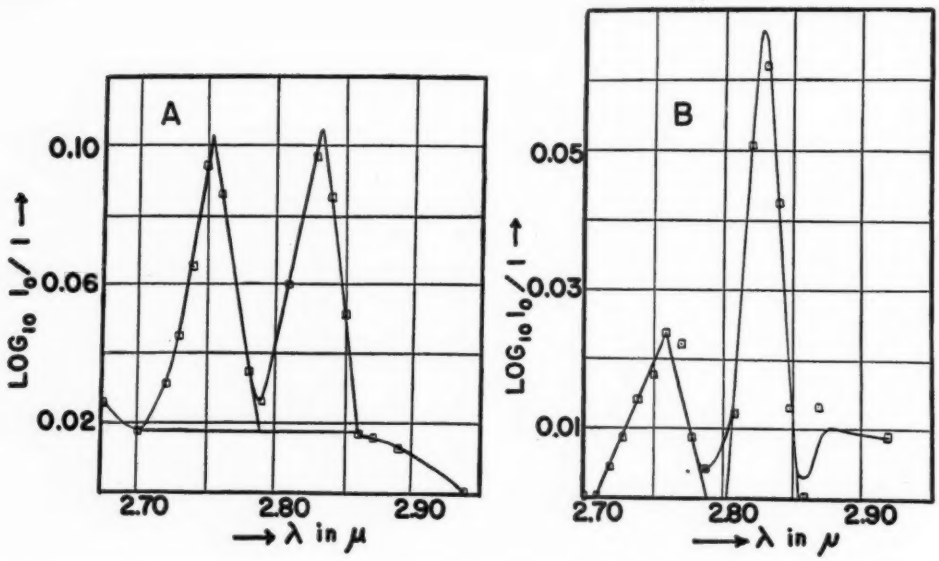

FIG. 2. Integral absorption curves. A. 0.0070 molar hydroxyacid at 74.6°. B. 0.0050 molar hydroxyacid at 74.5°.

stage. The absence of this molecular type has previously been suggested for quite different reasons.

$$\left\{\begin{matrix}\text{HOOC}\cdot(\text{CH}_2)_9\cdot\text{CH}_2\text{OH}\\ \text{HOOC}\cdot(\text{CH}_2)_9\cdot\text{CH}_2\text{OH}\end{matrix}\right\} \qquad \text{IV}$$

In conclusion, it can be said that the study of the hydroxyacid by the infra-red technique has substantiated at each stage the picture of the behavior of this solute arrived at by the more indirect indications of the kinetic analysis. Further, the method used for the detection of inter- and intramolecular group interactions would appear to be of wide applicability and its use in the present instance to establish the occurrence of ring-tied molecules of the hydroxyacid provides, we believe, a quantitative application in a very important field.

The author wishes to thank Professor E. K. Rideal for suggesting this work, Professor R. G. W. Norrish for the facilities afforded him in the Department of Physical Chemistry where the measurements were made, and Dr. G. B. B. M. Sutherland for helpful discussion.

He is also indebted to the University of Wales for a Research Fellowship.

Infra-Red Bands of Methylamine and the Phenomenon of Free Rotation

H. W. THOMPSON AND H. A. SKINNER
The Old Chemistry Department, Oxford, England

(Received September 20, 1938)

Two bands in the absorption spectrum of methylamine have been measured in the photographic infra-red. One of the bands shows rotational structure. The bands have been interpreted as involving excitation of the frequencies $3\nu_{NH}$ and $(3\nu_{CH}+\nu_{CN})$. The rotational structure of the latter band suggests that it is a perpendicular-type band, and the precise spacing of the Q branches suggests that the molecule behaves approximately like a rigid symmetric top. The inference of hindered internal rotation is in agreement with other independent data.

MUCH information about the properties and structure of simple polyatomic molecules has been obtained in recent years from the study of their infra-red spectra. The measurements fall into two classes: on the one hand the examination of the vibration bands in the far infra-red using instruments of low resolving power, and on the other the analysis of overtone or combination bands in the photographic region below 10,000A where much higher resolving power can be relatively easily applied. Comparatively few molecules have so far been studied in the latter region, since apart from possible experimental difficulties, it is necessary that the molecules shall contain at least one linkage involving a hydrogen atom, in order to bring the frequency absorbed into the accessible region. In addition to this, even with the high resolving power and dispersion of a large grating instrument, it is essential if rotational structure is to be studied, that the moments of inertia shall be relatively small.

It is, nevertheless, desirable to examine as many examples as possible using the high resolving power of the photographic method, since not only may such an analysis lead to a knowledge of the molecular structure, but also to the development of spectral theory, to the understanding of band envelopes, and to the correlation of the spectroscopic data with certain thermodynamic properties of the molecules.

In an examination of the absorption by the vapor of methylamine over the spectral range 7000–11,000A, we have recently observed two bands of methylamine, one of which has interesting structural features; and since the work must be temporarily suspended, it seems desirable to outline the main results, although it is not at present possible to give a complete interpretation of them.

In many respects methylamine resembles two other molecules, ethane and methyl alcohol, the infra-red bands of which have been recently studied. Ethane is a symmetric top, and the other two molecules, although in reality asymmetric tops, approximate closely to the symmetric top type. Also all three molecules have an axis about which free rotation, or internal torsion, might well occur. From a consideration of the bands of ethane and from the specific heat data, Howard[1] has suggested that in this molecule free rotation may be completely hindered. Badger and Bauer,[2] on the other hand, have attempted to interpret apparently abnormal rotational structure in the bands of methyl alcohol in terms of the occurrence of some degree of internal torsion. Calculations on the entropy of methyl alcohol, however,[3] suggest that in this molecule too, internal rotation is at least considerably hindered. It will be shown below that there is possible spectral evidence for very restricted rotation in methylamine, and this is interesting in view of similar conclusions reached from considerations of the entropy.[4]

The Raman spectrum of aqueous methylamine has been measured by Dadieu and Kohlrausch,[5] and of the liquid by Venkateswaran and Bhagavantam.[6] A reasonable assignment of frequencies suggests $\nu_{CH}\sim3000$, $\nu_{NH}\sim3350$, and

[1] J. Chem. Phys. **5**, 442, 451 (1937).
[2] J. Chem. Phys. **4**, 469 (1936).
[3] J. Chem. Phys. **5**, 539 (1937).
[4] Aston, Siller and Messerly, J. Am. Chem. Soc. **59**, 1750 (1937); Kistiakowsky and Wilson, J. Am. Chem. Soc. **60**, 494 (1938).
[5] Wien. Akad. **IIA**, **149**, 77 (1930).
[6] Ind. Jour. Phys. **5**, 129 (1930).

$\nu_{CN} \sim 1040$. The only measurements on the infrared spectrum appear to be those of R. and M. Freymann,[7] extending over the range 0.8–1.2μ, but using low resolution and an aqueous solution. The essential feature found was that two bands occur, at 10,420A and 10,102A or *ca.* 9600 and 9990 cm^{-1}. The band at 9600 cm^{-1}, which is by far the most intense, was attributed to the excitation of $3\nu_{NH}$ i.e., a second overtone of the N—H fundamental. When it is remembered that in solution the bands may have become somewhat displaced to lower frequencies, this assignment seems fully justified.

Experimental

The spectrograph used was a three-meter concave grating with Eagle mounting. The grating had approximately 15,500 lines to the inch and its effective width was about three inches. The spectra were studied in the first order, the dispersion being 5.8A per mm.

The methylamine was a Kahlbaum product supplied as pure, but found to contain a considerable quantity of dissolved ammonia. Repeated fractionation removed the latter perhaps completely, but in any case to such an extent that no absorption attributable to ammonia could be detected.

The absorption tube was in general a steel pipe 8 cm in diameter and 5.5 meters in length, having a side arm connected to manometer, to glass tubes containing the methylamine, and via taps to an oil pump. In some experiments an additional tube 7.5 meters in length was used in series with the above, so as to obtain a total column length of 13 meters, but in the latter case the exposure times were very considerably lengthened. The ends of the absorption tubes were closed by glass plates cemented on with suitable wax. The continuous source was a tungsten arc lamp. Higher order spectra were eliminated by means of the Ilford Infra-red or Wratten 88 filters. The plates used were Agfa 850, 950 and 1050, Kodak I R, I P, and I Q, and Ilford Infra-red, and all were hypersensitized before use. The exposures varied from 4 to 30 hours according to the type of plate used. Considerable difficulty was experienced with the Agfa 1050 and Kodak Q plates working at wave-lengths longer than 10,000A, since delivery was inconvenient and the plates seemed to have lost most of their sensitivity in transit.

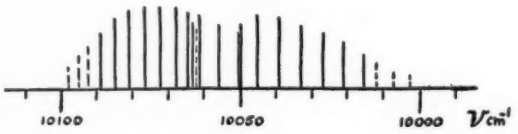

Fig. 1.

Pressures of methylamine up to one atmosphere were used. Unfortunately with the higher pressures which were necessary for the detection of the bands so far found, there appeared to be a considerable pressure broadening effect.

Results

The two bands found lie at wave-lengths *ca.* 10,300A and 9940A and are best described separately.

Band A with center at 10,300A or 9700 cm^{-1} is relatively intense, and can be observed with pressures of less than an atmosphere in columns of two meters. It has not been possible to detect any rotational structure in this band, nor even a contour suggesting *P*, *Q* and *R* branches. The band is some 100–150 cm^{-1} broad depending upon the pressure used.

Band B which is represented diagrammatically in Fig. 1, consists of a group of roughly equidistant lines centered around *ca.* 9940A i.e., 10,060 cm^{-1}. The appearance of this band is surprisingly simple, but this simplicity is almost certainly misleading. For the most part, the lines, which are broad, are separated from each other by 4–6A i.e., a mean separation of about 5A which corresponds to about 5 cm^{-1}. The spacing of the lines is, however, clearly not regular, and there is a close group of about three lines in the center which at first sight appears to divide the band into two parts. The band is far less easily detected than band *A* above and requires a column of fifteen feet at atmospheric pressure for development.

Discussion

The two bands found at 10,060 cm^{-1} (band *B*) and 9700 cm^{-1} (band *A*) with methylamine vapor agree well with those reported by Frey-

[7] Comptes rendus **202**, 1674 (1936).

mann at 9990 cm^{-1} and 9600 cm^{-1} for the aqueous solution. Band A can with reasonable certainty be attributed to the excitation of $3\nu_{NH}$ and band B is probably to be interpreted by the combination $(3\nu_{CH}+\nu_{CN})$. On the basis of the generally accepted values for the fundamentals quoted above there is good agreement.

The interpretation of the rotational structure of the two bands is less obvious. It is at once clear that considerably more spectral data, and also the relevant theory, will be required before it is possible to deduce the molecular structure from spectroscopic data alone. Therefore we must rather begin by assuming a plausible structure for the molecule and attempt to interpret the band structures found.

In methylamine the methyl group angles are roughly tetrahedral, and the C−N−H angles are close to 105°. The bond lengths have the probable values $r_{CH}=1.08$A, $r_{CN}=1.47$A, $r_{NH}=1.02$A. The possibility of free rotation about the C−N axis makes it impossible to specify the exact relative orientation of the two end groups. The molecule is in reality an asymmetric top, but like methyl alcohol[8] approaches closely to the type of symmetric top, with symmetry axis along the C−N bond. The moments of inertia about this axis of the CH_3 and NH_2 groups are respectively about 5.4×10^{-40} and 3×10^{-40} g cm^2, so that if regarded as rotating as a whole about the C−N axis, the moment is $I_x=8.4\times10^{-40}$. The moments I_y and I_z will each be about 38×10^{-40}.

The rotational energy of a symmetric top is given by

$$E_{rot}=\frac{h}{8\pi^2}\left\{\frac{J(J+1)}{I_y}-K^2\left[\frac{1}{I_x}-\frac{1}{I_y}\right]\right\},$$

in which $|K|\leqq J$ and $J=0, 1, 2, \cdots$.

Two types of band may be distinguished according to the direction of change of the electric moment with respect to the symmetry axis. For the "parallel" bands ($\Delta J=0, \pm1, \Delta K=0$) there will be a single P, Q and R branch structure, the spacing in each of the P and R branches being $h/4\pi^2I_y$. The "perpendicular" bands ($\Delta J=0, \pm1, \Delta K=\pm1$) will consist of a superposition of subbands each with P, Q and R branches of unequal intensity, so that the Q branches usually stand out against a more or less unresolved background. The separation of the Q branches will be given by

$$(h/4\pi^2)\{1/I_x-1/I_y\}.$$

Many polyatomic molecule vibrations, however, involve a change in the component of the electric moment both parallel and perpendicular to the symmetry axis, and in such cases there will be a superposition of the two types of band. Such a superposition may occur in the case of methyl alcohol, and might also occur in the excitation of vibrations in the NH_2 group in methylamine.

Unfortunately in methylamine there is an additional complication, the possibility of free rotation about the C−N axis. The effect of internal torsion on the rotational energy levels of molecules has been studied by several workers. For our present purpose we may use the result of Nielsen,[9] who showed that for a symmetric torsional oscillator,

$$E_{rot}=\frac{h}{8\pi^2}\left[\frac{J(J+1)}{I_y}-\frac{(K_1+K_2)^2}{I_y}+\frac{K_1^2}{I_x'}+\frac{K_2^2}{I_x''}\right],$$

in which $J=0, 1, 2, \cdots$.

K_1 and K_2 have values 0, ±1, ±2, subject to the rule $J\geqq(K_1+K_2)$ I_x' and I_x'' are the moments of inertia of the end groups about the symmetry axis, and I_y is the moment of the entire molecule about an axis perpendicular to the symmetry axis.

This expression refers in reality to a molecule (like ethane) having two end groups free to rotate with respect to each other, and with a coincident symmetry axis. As Badger and Bauer have shown, for a vibration in which the change in moment is parallel to the symmetry axis, $\Delta J=0, \pm1$, $\Delta K_1=\Delta K_2=0$ giving a band with P, Q and R branches as for the normal rigid symmetric top, the spacing being unaffected. For a perpendicular band, assuming the vibration to be largely localized in one of the end groups, $\Delta J=0, \pm1$, $\Delta K_2=0$ but $\Delta K_1=\pm1$ giving subbands the separation of whose centers is given by

$$(h/4\pi^2)\{1/I_x'-1/I_y\},$$

in which I_x' is the moment about the symmetry

[8] J. Chem. Phys. **4**, 469 (1936).

[9] Phys. Rev. **40**, 445 (1932).

axis of the group in which the vibration is localized. The Q branches will each be flanked with P and R branches having the same spacing as those in the parallel bands.

Finally as in the case of a rigid rotator, if the vibration under consideration leads to a change in the electric moment both parallel and perpendicular to the symmetry axis, we may expect to find a superposition of the different types of band.

Turning now to the specific case of methylamine, it is most convenient first to discuss the band at 9940A. At first sight this band may be thought to have in a modified form the simple structure of a parallel band with a crowding of lines in the center giving in some measure the appearance of a Q branch. This cannot be so. Assuming as a first approximation that the molecule is a rigid symmetric top having the moments of inertia estimated above, the separation of the lines in the P and R branches would be 1.45 cm^{-1}. With such a separation the lines would hardly have been resolved in the present measurements. The separation observed was *ca.* 5 cm^{-1}. The occurrence of free rotation could not affect the spacing of a parallel band. If, however, the lines are regarded as Q branches of a perpendicular-type band, their spacing for a rigid top should be *ca.* 5 cm^{-1}, a value surprisingly close to that found. Despite the various approximations in the above argument, and not forgetting the irregularities in the spacings, it is reasonable therefore to interpret the band as being essentially a normal perpendicular-type band. If completely free rotation were occurring the Q branch separation, assuming the vibration to be largely localized in the methyl group and the NH_2 group as fairly rigid, would be about 10 cm^{-1}. Hence we should infer that the internal rotation must be almost completely hindered.

The irregularities in the band structure do not seem such as to vitiate this conclusion. The central group of lines together with the fact that the separation of the lines to one side of the band center is about 4 cm^{-1} and to the other side about 6 cm^{-1} may suggest that the band really falls into two parts, but the broad general interpretation still seems the most probable.

Band A at 10,300A was interpreted as arising from the excitation of $3\nu_{NH}$. Now a vibration of the NH_2 radical might involve a change in the electric moment with components both parallel and perpendicular to the symmetry axis (the C—N axis). Hence we might find a superposition of bands of both types. This may be the reason for the unresolved nature of the band, and further measurements using higher resolving power and longer columns with lower pressures are clearly desirable.

The suggestion of hindered rotation in methylamine is a matter worthy of further consideration. Kemp and Pitzer[10] have recently shown that the entropy of ethane calculated from specific heat data is lower than that calculated from other molecular data (e.g. vibration frequencies), and have suggested that the discrepancy arises from a hindrance of internal rotation. Howard has also shown that the spectroscopic data with ethane lead to a similar conclusion. Aston, Siller and Messerly[11] have made similar calculations of the entropy of methylamine and found a similar discrepancy, which has been interpreted in the same manner. The spectroscopic result is not, therefore, at variance with the conclusions of other independent methods.

[10] J. Chem. Phys. **4**, 749 (1936).
[11] J. Am. Chem. Soc. **59**, 1750 (1937).

Kinetics of OH Radicals Determined by Their Absorption Spectrum

IV. Pressure Broadening and the Line Spectrum as Background

O. OLDENBERG
Research Laboratory of Physics, Harvard University, Cambridge, Massachusetts

AND

F. F. RIEKE
Department of Chemistry, University of Chicago, Chicago, Illinois

(Received August 28, 1938)

For the measurement of the concentration of OH radicals the intensity of the absorption spectrum is measured more easily with an *emission line* background than with a *continuous* background, provided that the pressure broadening is known. The total broadening of the OH absorption lines at 1473° K and 1 atmos. ($\frac{2}{3}$ O_2+$\frac{1}{3}$ H_2O) is observed to be 0.58 cm^{-1}; 36 percent of this value is Doppler broadening, the rest is pressure broadening. With this figure, recent intensity measurements of the OH bands by Avramenko and Kondratjew are reinterpreted. The resulting f values of approximately 3×10^{-4} are in reasonable agreement with our previous measurements. The conditions are discussed under which the simple method using the line spectrum as a background is applicable.

I. PROBLEM

IN a preceding paper[1] the probability of transition ("f value") of the OH bands was measured for the purpose of applying the absorption spectrum to a *quantitative* chemical test for free OH radicals in gases. A *continuous spectrum* was used as a background, and for each absorption line the absorption coefficient was measured as a function of wave number throughout the narrow region (a few cm^{-1}) in which the absorption is appreciable. For this method the resolving power of a 21-foot grating is barely sufficient. Technically it would be far simpler to apply the *sharp* OH *band spectrum* in emission as a background and observe the reduction of the total intensity of individual lines when passed through the absorbing gas. This may be measured with a medium-sized quartz spectrograph, which is much more readily available than a large grating spectrograph. Moreover, the total intensity of an emission line which may be photographed with a wide slit requires only one reading on the densitometer, whereas the accurate measurement of the contour of a narrow absorption line is far more difficult. However, this simplified method—using the line spectrum as a background—brings in a new difficulty in that it requires information regarding the line widths.

With this method Avramenko and Kondratjew[2] determined a certain constant related to the f values (see Section III) and estimated the f values to be much larger than those given subsequently in our paper. We suggest that this discrepancy is due to an incorrect assumption regarding the broadening of the OH lines by the pressure of a foreign gas. Since Avramenko and Kondratjew had no equipment for determining this broadening, they had to rely on an estimate.

Our absorption spectra, published in the paper just mentioned,[1] were taken on a continuous background with high resolving power and give direct evidence of this pressure broadening. In the present paper the broadening is evaluated and applied to a new interpretation of the absorption measurements of the Russian authors; thus an essentially new determination of the f value of the OH absorption bands is obtained.

Although we are mainly interested in the broadening of the lines for the purpose of chemical analysis by absorption spectra, these measurements are of interest also from the purely spectroscopic point of view because very few such measurements on single lines of a molecule are

[1] O. Oldenberg and F. F. Rieke, J. Chem. Phys. **6**, 439 (1938).

[2] L. Avramenko and V. Kondratjew, Acta Physicochimica **8**, 567 (1937).

known. On the broadening of electronic bands only a short note by Watson and Hull,[3] who investigated AlH bands, is known to us.

II. Width of the OH Lines

The width of the individual OH absorption line (portion of line in which the absorption coefficient exceeds 50 percent of the maximum) was measured on the spectra previously described.[1] The line $Q_1(6\frac{1}{2})$, which is free from overlapping, leads to a value 0.58 cm^{-1} at a temperature of 1473°K and a pressure of 1 atmos. ($\frac{2}{3}H_2O+\frac{1}{3}O_2$). As the Doppler broadening at this temperature amounts to 0.21 cm^{-1}, the share contributed by the pressure broadening (assumed to be additive) is 0.37 cm^{-1}. Five other lines, $Q_1(1\frac{1}{2})$ to $Q_1(5\frac{1}{2})$, were measured on the densitometer. As they are overlapped by weaker lines of other branches the resulting contours had to be separated into components. Consequently, the widths derived from these curves are less reliable. All values, however, are well consistent with the width given above. The line width is much more directly derived from the observed spectrum than the f value which was previously reported because the determination of the f value, but not of the line width, requires the computation of the thermal equilibrium. As a matter of fact, one can directly check the figure of the line width on the densitometer trace with reasonable accuracy (see reference 1, Figs. 2 and 3).

The accuracy of our result may, to a certain extent, be affected by the lack of resolving power of the spectrograph.[4] A considerable correction, however, is not to be expected since the observed line width exceeds the theoretical resolving power of the spectrograph by the factor 4. This correction cannot be computed quantitatively because our method of correction applied in the preceding paper (extrapolation to zero absorption) leads to the correct $\int \alpha d\nu$, but leaves width and minimum of intensity uncertain. Because this error can only exaggerate the width, we are certain that the real width is *not greater* than the spectra indicate. On the other hand, it is plausible that the real width is *not considerably smaller* because other lines of atoms or molecules are subject to pressure broadening of *about the same amount* (no lines of a considerably smaller amount) so that we should not expect the OH lines to be exempt from the same effect. Such a broadening effect is theoretically predicted for molecular lines by Margenau[5] as only slightly larger than the effect found for atomic lines. It is clear from our measurement that OH broadened by H_2O+O_2 does not provide an example of the anomalously large broadening theoretically predicted by Margenau for special cases.

No pressure *shift* comparable to the pressure *broadening* could be observed at 1 atmosphere. The positions of the absorption lines, both for high pressure (furnace) and low pressure (absorption spectrum of discharge tube after interrupting current), were measured against sharp Al lines emitted together with the hydrogen continuum that formed the background.

A pressure broadening of 0.37 cm^{-1} for OH is comparable to the value 0.24 for the absorption lines of AlH, observed by Watson and Hull,[6] in the atmosphere surrounding a spark discharge. It is also comparable to the broadening of many atomic lines; for instance, the Hg line 2537[7] (0.27 cm^{-1} by 1 atmos. of O_2 at 33°C). Results on the broadening of Hg 2537 and the NaD lines by various other gases—expressed by "effective cross sections"—were summarized by Weisskopf,[8] Margenau and Watson,[9] and, recently, by Schulz.[10]

It is noteworthy that the pressure broadening is of the same order of magnitude for all these lines of *different atoms and molecules* which have no first order Stark effect; they largely follow the Lorentz theory of broadening. Furthermore, the same order of magnitude is found for the broadening of the Hg line 2537 by *different foreign gases* (A, H_2, N_2, O_2, CO_2, H_2O).

---

[3] W. W. Watson and G. F. Hull, Jr., Phys. Rev. **49**, 648 (1936).

[4] See the discussion of sources of error in the preceding paper, Section IV.

[5] H. Margenau, Phys. Rev. **49**, 648 (1936).

[6] The conditions are not sharply defined in this absorption experiment because the temperature of the vapor which affects pressure broadening by the factor $1/T^{\frac{1}{2}}$ is rather uncertain in the close neighborhood of the spark.

[7] C. Füchtbauer, G. Joos, and O. Dinkelacker, Ann. d. Physik **71**, 201 (1923).

[8] V. Weisskopf, Physik. Zeits. **34**, 15 (1933).

[9] H. Margenau and W. W. Watson, Rev. Mod. Phys. **8**, 22 (1936).

[10] P. Schulz, Physik. Zeits. **39**, 420 (1938).

III. New Interpretation of the Absorption Measurements of Avramenko and Kondratjew

Avramenko and Kondratjew used the sharp lines of the emission spectrum produced in an electric discharge as a background and measured their loss of total intensity when passing through the absorbing gas. This loss strongly depends on the widths of both lines, emission and absorption. In general, one cannot even represent this loss of intensity along the absorbing path simply by an exponential function since the incident light after passing through a certain length has lost the most absorbable part (core of the line) and continues its path with the less absorbable part (wings of the line). The case of equal widths of both lines was treated by Ladenburg and Reiche.[11] Kondratjew and Ziskin[12] computed approximate formulae for the much more complicated problem of different widths for emission and absorption. By restricting their computation to weak absorption (exponential function approximated by a straight line) they gained the advantage of describing the loss of intensity by an average absorption coefficient. This is proportional to the probability of transition (f value) of the molecule; furthermore, it depends on the widths of both lines.

In Avramenko and Kondratjew's experiment, which is of importance for the determination of the f value, the absorbing medium was water vapor partially dissociated in a furnace. (The concentration of OH can be computed and so provides a calibration of the absorption spectrum of OH.) Pressures and temperatures were known in both the absorbing vapor and the emitting vapor (electric discharge through low pressure). Their great difficulty was the lack of information on the line widths. This was surmounted by the following argument. It was assumed that the widths in both cases (emitting and absorbing vapors) were caused exclusively by the pressure (Lorentz's collision broadening); that is, Doppler broadening was neglected. This approximation, which made the widths proportional to $p/T^{\frac{1}{2}}$, eliminated the line width from the final formula.

Our measurement of the line width (Section II), which was not accessible to Avramenko and Kondratjew, leads to the conclusion that the approximation just mentioned fails under the conditions of the actual experiments. In what follows, we compute the Doppler broadening from the temperature in the usual way, and determine the pressure broadening by assuming it to be proportional to $p/T^{\frac{1}{2}}$ with the constant of proportionality based on our value for 1473°K and 1 atmos. pressure. In the absorbing vapor used for the calibration (1 atmos. $\frac{2}{3}H_2O+\frac{1}{3}O_2$, 1473°K), it is true that the Doppler broadening (0.21 cm^{-1}) is smaller than the pressure broadening (0.37 cm^{-1}), but it is not negligible. In the remaining cases, in which the absorption was used by Avramenko and Kondratjew to measure an unknown concentration of OH, the Doppler broadening compared to the pressure broadening is in fact the larger of the two. In the discharge tube the Doppler broadening is 0.097 cm^{-1} and the pressure broadening is 0.00016 cm^{-1}. The same objection applies to a lesser extent to the experiment with a flame, reported by the same authors, in which the pressure was 10 mm and the temperature 1000°K. Hence their simplified method, based on a line width proportional to $p/T^{\frac{1}{2}}$, fails.

Nevertheless, their measurements with the line spectrum as a background are of great interest in that they lead to the absolute f values when we apply our line width, reported in Section II, on the basis of the following argument. The line width of 0.097 cm^{-1} in the discharge tube (background) is only one-sixth of the line width of 0.58 in the furnace. Furthermore, no appreciable shift by pressure takes place. Hence we assume as an approximation that the emission line over its whole width is uniformly affected by the coefficient of absorption that belongs to the center of the absorption line; that is, we consider the emission line to be a narrow probe measuring the maximum absorption.

From the values of width (our result) and maximum absorption (measured by Avramenko and Kondratjew) one easily computes the integral absorption coefficient, which is proportional to the number of dispersion electrons per unit volume. When a curve of the type $\alpha_\nu=\alpha_0/[1+((\nu-\nu_0)/\delta)^2]$ is assumed for the line contour (Lorentz broadening), where α_0 = maximum ab-

[11] R. Ladenburg and F. Reiche, Ann. d. Physik **42**, 181 (1913).

[12] V. Kondratjew and M. Ziskin, Acta Physiochimica **5**, 301 (1936).

TABLE I. *Comparison of f values. "old": measured with a continuous background and high resolving power; "new": measured with line background and small resolving power, the line width taken from "old" results.*

J	f VALUE (OLD)	f VALUE (NEW)
$4\frac{1}{2}$	2.42×10^{-4}	2.84×10^{-4}
$6\frac{1}{2}$	2.59×10^{-4}	3.45×10^{-4}

sorption coefficient and 2δ=half-value width, the integral absorption coefficient results from $\int\alpha_\nu d\nu=\pi\delta\alpha_0$. The computation of the thermal equilibrium of OH is, of course, the same as in the other measurement published in our previous paper.

This method presupposes that in the discharge tube there is no strong broadening *by current*. Although Avramenko and Kondratjew did not give their current density, it may be assumed that it was not excessive since for their own method they depended on having no extra broadening beyond the effect of a pressure of 1.5 mm.

IV. THE f VALUES

A comparison of our old results (continuous background and high resolving power) with these new results (their measurements of line absorptions and our values of line width) was carried through for the quantum numbers $J=4\frac{1}{2}$ and $6\frac{1}{2}$ and the temperature of 1473°K. For these figures Avramenko and Kondratjew give the measurements of the "average absorption coefficient" $(\mu l)_{Av}$. To the temperature distribution given in their paper[13] we applied the same equilibrium constants as in our preceding paper in order to make both sets of f values comparable. (The Russian authors applied other values for the equilibrium constant, which they obtained from their own set of measurements.)

The results are given in Table I. The agreement between the "old" and "new" f values confirms the surprisingly small order of magnitude.

The discrepancy between the "new" and "old" f values is presumably due for the most part to incidental errors. However, part of the error may lie in the measurement of the line width since it has not been possible to correct this measurement for lack of resolving power. The true line width may quite possibly be 10 or 20 percent less than our value of 0.58 cm^{-1}. Presumably, the "old" values are more accurate because the correction for lack of resolving power could be applied in their determination (affecting the factor $\int\alpha d\nu$), whereas the same correction (affecting the line width) could not be applied to the "new" value.

[13] H. Zeise, Zeits. f. Electrochem. **43**, 704 (1937).

V. APPLICABILITY OF THE LINE SPECTRUM AS A BACKGROUND

In order to apply the absorption spectrum as a quantitative test for free radicals, atoms, or molecules, the *line spectrum* as a background has a great technical advantage over the *continuous spectrum* (Section I). This simpler technique is applicable under the following conditions. (a) The total width of the *absorption line* must be known. This figure is given for OH in 1 atmosphere ($\frac{2}{3}H_2O+\frac{1}{3}O_2$) in Section II. For other molecular spectra no accurate figures are available at the present time. Pressure broadening is assumed to be proportional to $p/T^{\frac{1}{2}}$. (b) The *emission line* is restricted by requirements which are more difficult to meet. The simplest case is a width which is small compared to the width of the absorption line (Section IV). Even though the *pressure* and *temperature* in the discharge tube may be low enough, one must still make sure that the *current* does not cause additional broadening. That this is practicable we shall show in a subsequent paper where we shall report on experiments with a line spectrum as background in which Fabry-Pérot plates are applied as a spectrograph which offers still higher resolving power than the second-order of the 21-foot grating. Even with high current density (0.4 amp./mm^2) the broadening of the individual OH lines is unexpectedly small. Hence it seems entirely feasible to reduce the current to so low a value that current broadening is negligible. In each case, however, it must be determined whether an increase of current modifies the observed absorption and so indicates an undue current broadening. Since the current broadening can be kept negligibly small and the Doppler broadening is given by a familiar computation, the pressure broadening reported here now makes the simple method which uses the line spectrum as a background suitable for practical application in the quantitative analysis for free OH.

The Alpha-Particle Reactions in Carbon Monoxide, Oxygen and Carbon Dioxide Systems

JOSEPH O. HIRSCHFELDER
Department of Chemistry, University of Wisconsin, Madison, Wisconsin

AND

HUGH S. TAYLOR
Frick Chemical Laboratory, Princeton University, Princeton, New Jersey

(Received October 13, 1938)

The methods developed by Eyring, Hirschfelder and Taylor for the analysis of the alpha-particle reactions in hydrogen and hydrogen-bromine systems have been extended to the corresponding reactions in carbon monoxide, oxygen, and carbon-dioxide systems and to mixtures of these gases. It has been shown that experimentally known processes of ionization and of excitation, together with the probable neutralization processes, with consequent chemical reactions involving the atomic species so produced, suffice to account quantitatively for the observed experimental results. This extends the scope of the method employed to typical alpha-particle reactions of decomposition, ozonization and oxidation hitherto interpreted in terms of a clustering mechanism.

IN studying, with Eyring, the ortho-para-hydrogen conversion and the synthesis and decomposition of hydrogen bromide under the influence of alpha-particles, we came to the conclusion that the ionization occurring in hydrogen, under such conditions, eventually produced from 3 to 4 hydrogen atoms per ion pair produced in the system. Further, we concluded that, to the extent that molecular excitation processes in the track of the alpha-particle occur, these minimum yields of atomic hydrogen will be exceeded. From our analysis of the data of Lind and Livingston on the hydrogen-bromine-hydrogen bromide reaction we concluded that the total yield from ionization and molecule excitation may reach 6 hydrogen atoms measured in terms of ion pairs produced.[1-3]

The experimental demonstration of reaction due to the excitation of molecules, in addition to ionization, by alpha-particles has recently been achieved by Smith and Essex.[4] They have shown that, in the decomposition of ammonia by alpha-rays, as much as two-thirds of the total reaction is due to mechanisms other than those involving ions and their recombination. This research can be recorded as supporting the additional formation of atomic hydrogen which we found it necessary to assume in our previous studies. To test our conclusions, Mund and van Tiggelen,[5] in 1937, undertook to find the number of hydrogen atoms, per ion pair, produced by an alpha-particle in hydrogen containing a small amount of hydrogen sulfide. They measured the number of molecules of hydrogen sulfide disappearing per ion pair. In two series of data they found mean values of 2.14 and 2.2, respectively, with extreme values of 3.16 and 1.7. They assumed the reactions to be $H+H_2S \rightarrow H_2+HS$ followed by $2HS=H_2+S_2$, following a mechanism agreeing with photochemical quantum yield measurements of Stein.[6] A quite recent research by Forbes, Cline and Bradshaw[7] indicates, however, that the quantum yield is 1.02 ± 0.05 molecules of hydrogen per quantum, independent of pressure over the range 8–1400 mm, and of light intensity over a fourteen-fold range. They are thus led to a mechanism $H+H_2S \rightarrow H_2+HS$ followed by $HS+HS=H_2S+S$ from which it would follow that the Mund-van Tiggelen data indicate mean yields of 4.28 and 4.4 with individual determinations indicating as high as

[1] Eyring, Hirschfelder and Taylor, J. Chem. Phys. **4**, 479 (1936).
[2] Eyring, Hirschfelder and Taylor, J. Chem. Phys. **4**, 570 (1936).
[3] Lind and Livingston, J. Am. Chem. Soc. **58**, 612 (1936).
[4] Smith and Essex, J. Chem. Phys. **6**, 188 (1938).
[5] Mund and van Tiggelen, Bull. Soc. Chim. Belg. **46**, 129 (1937).
[6] Stein, Trans. Faraday Soc. **29**, 583 (1933).
[7] G. S. Forbes, Cline and Bradshaw, J. Am. Chem. Soc. **60**, 1431 (1938).

6.3 atoms of hydrogen per ion pair. This modification of the Mund-van Tiggelen results brings the work on alpha-particles in hydrogen-hydrogen sulfide mixtures into good agreement with our computations in the ortho-parahydrogen reaction and the hydrogen bromide synthesis.

Quite recently Gunther has re-examined[8] his earlier data[9] on the hydrogen-chlorine reaction under ionizing influences and has concluded that they can better be reconciled with our theory of such processes than with the "cluster-theory" on which his earlier interpretation was based. He shows, further, that new experiments on the decomposition of azomethane under ionization cannot be reconciled with the cluster theory but require such a treatment as we have given for their interpretation.

The cumulative effect of these several researches in support of our theoretical analysis of the alpha-ray reactions in hydrogen-containing systems encourages us to present our analysis of the alpha-particle reactions in the systems carbon monoxide, carbon dioxide and oxygen. The system carbon monoxide-oxygen can be employed to illustrate the general applicability of our methods to oxidation processes under ionization conditions.

Any theory which is proposed for the radiochemical oxidation of carbon monoxide must explain the following experimental facts. Carbon dioxide is the sole product[10–13] of alpha-particle bombardment of carbon monoxide-oxygen mixtures. The yield is practically independent of the ratio of the two reactants until these species approach exhaustion, and four molecules of carbon dioxide are formed per ion pair produced by impact of alpha-particles with the reactants. Radiation absorbed by the carbon dioxide has little effect on the reaction kinetics and the reaction proceeds at a rate influenced to only a minor degree by the ions produced by impact of alpha-particles with the carbon dioxide product. The oxidation process under ionizing influence continues even with the reaction bulb immersed in liquid air.

Pure carbon dioxide, under alpha-radiation, remains practically unchanged, and the ion efficiency is practically zero. With pure carbon monoxide, about two molecules of carbon monoxide disappear per ion pair formed. Carbon suboxide is deposited, and carbon dioxide appears equal to about two-thirds of that required by a reaction $2CO = CO_2 + C$. The empirical formula of total solid deposited is C_2O. Pure oxygen, under alpha-ray ionization, yields ozone with low yields in static systems, reaching at least 1 to 1.25 molecules of ozone per ion pair in flow systems.[14] Lind and Bardwell[15] found 1.7 molecules of ozone per ion pair and two results in excess of 2 were obtained in flow systems. The yield is evidently dependent on the reverse process of de-ozonization.

We now proceed to an analysis of these experimental data, resolving the total process into three component parts, (a) the ionization and excitation processes caused by the alpha-particle and its secondary electrons, (b) the neutralization process and the reactive species thus produced, and (c) the chemical reactions which such species may induce. We consider first these several stages in the several pure gases and then we shall consider gaseous mixtures of the three.

I. Radiochemical Reactions in Pure Carbon Monoxide

1. Ionization processes

Excellent investigations are available of the processes of ionization, excitation and negative ion formation in carbon monoxide from mass-spectrographic data of the products formed in electrical discharges[16–20] and from the data of electron impacts of controlled speeds.[21] In electrical discharges, the ions CO^+, C^+ and CO^{++}

[8] P. Gunther and H. Theobald, Zeits. f. physik. Chemie **B40**, 1 (1938).
[9] P. Gunther and G. Cohn, Zeits. f. physik. Chemie **B26**, 8 (1934); P. Gunther and K. Holm, *ibid.* **B33**, 407 (1936).
[10] S. C. Lind, *Chemical Effects of Alpha-Particles* (Chemical Catalog Co., 1928), p. 165.
[11] S. C. Lind and D. C. Bardwell, J. Am. Chem. Soc. **47**, 2675 (1925).
[12] S. C. Lind and C. Rosenblum, Proc. Nat. Acad. Sci. **18**, 374 (1932).
[13] C. Rosenblum, J. Am. Chem. Soc. **55**, 220 (1933).
[14] J. D'Olieslager, Bull. Acad. Roy. Belg. **12**, 719 (1925).
[15] S. C. Lind and D. C. Bardwell, J. Am. Chem. Soc. **51**, 2751 (1929).
[16] Hogness and Harkness, Phys. Rev. **32**, 936 (1928).
[17] Kallmann and Rosen, Zeits. f. Physik **61**, 61 (1930).
[18] H. D. Smyth, Rev. Mod. Phys. **3**, 347 (1931).
[19] A. L. Vaughan, Phys. Rev. **38**, 1687 (1931).
[20] W. W. Lozier, Phys. Rev. **46**, 268 (1934).
[21] Savard, de Hemptinne and Capron, Comptes rendus **204**, 354, 1039 (1937).

are all found, but CO^+ ions, at the low pressures of these experiments, were of the order of 1000 to 100 times more numerous than the other species. Thus, the primary ionization is, in major part,

$$CO = CO^+ + \epsilon - 13.5 \text{ ev.} \quad (1)$$

The energy consumed, 13.5 ev, is derived from the electron impact data. The same source indicates that, at 16.1 ev and 19.1 ev, two excited states of the CO^+ ion may be formed, while the direct formation of $C^+ + O$ requires 20 ev. For the dissociation of the carbon monoxide molecule into neutral atoms, Savard, de Hemptinne and Capron deduce an energy of 8.8 ev. Faltings, Groth and Harteck, in a review of the spectroscopic data, coupled with their own observations of the photodissociation of carbon monoxide,[22] conclude that, at present, the most reliable value is that given by Herzberg,[23] 9.097 ev. Hogness and Harkness obtained good evidence that an ionic reaction occurs:

$$CO^+ + CO = C^+ + CO_2. \quad (2)$$

However, a simple calculation shows that this reaction will require excited CO^+ ions:

$$\begin{aligned} CO^+ + \epsilon &= CO + 13.5 \text{ ev} \\ CO &= C + O - 9.1 \text{ ev} \\ C &= C^+ + \epsilon - 11.3 \text{ ev} \\ CO + O &= CO_2 + 5.5 \text{ ev} \end{aligned}$$

whence $CO^+ + CO = C^+ + CO_2 - 1.4$ ev.

The excited state formed at 16.1 ev would convert this endothermic process to an exothermic one. Experimentally, it would be difficult to determine how much of the CO^+ current is due to each of the three states of the species and, therefore, we cannot make any estimate of the frequency with which the reaction (2) forming C^+ and CO_2 occurs. Since Hogness and Harkness were able to distinguish the reaction at pressures lower than 1 mm Hg, it must occur frequently at atmospheric pressure.

2. Excitation processes

These are known through the absorption spectra observed in the ultraviolet by Hopfield and Birge[24] and by Leifson.[25] There are a large number of excited states of carbon monoxide but, when the molecule dissociates, a normal carbon and a normal oxygen atom are produced,

$$CO \rightarrow C + O - 9.1 \text{ ev.} \quad (3)$$

The energy consumed is taken as 9.1 ev as indicated above, but the exact magnitude does not concern us here.

3. Negative ion formation

The formation of negative ions in carbon monoxide has been investigated by Wahlin,[26] Bradbury,[27] Tate and Lozier,[28] and Lozier.[20] All concur in the conclusion that the carbon monoxide molecule has negligible electron affinity. No negative ions are formed in it until the energy of the impacting electron exceeds 19.5 volts. Savard, de Hemptinne and Capron[21] assign a value of 21.4 ev to the reaction

$$CO + \epsilon = C^+(^4P) + O^- + \epsilon. \quad (4)$$

Lozier arrives at a value of 20.9 ev for the same process, and, for the reaction,

$$CO + \epsilon = C + O^-, \quad (5)$$

a value of 9.5 ev. In the radiochemical reaction, where the available energy is great, both (4) and (5) are possible. However, when Lozier plots the ion currents of CO^+, O^- and C^+ as a function of the electron energy, it appears that the magnitude of the O^- current is of the order of 10^{-3} of the positive ion current. Therefore, we conclude that, whilst negative ions are formed, the number of them is negligible for our purposes.

4. The total processes and chemical reactions

The alpha-particle and its fast secondary electrons use about 30 ev in producing each ion pair. We know that 13.5 ev is used up in reaction (1). The remainder is principally consumed in reaction (3) and unfruitful excitation processes. Thus, the primary stage yields,

$$2CO + \alpha = CO^+ + \epsilon + C + O + \alpha. \quad (6)$$

[22] K. Faltings, W. Groth and P. Harteck, Zeits. f. physik. Chemie **B41**, 15 (1938).
[23] G. Herzberg, Chem. Rev. **20**, 145 (1937).
[24] J. J. Hopfield and R. T. Birge, Phys. Rev. **29**, 922 (1927).
[25] S. Leifson, J. Astrophys. **63**, 82 (1926).
[26] H. B. Wahlin, Phys. Rev. **19**, 173 (1922).
[27] N. Bradbury, J. Chem. Phys. **2**, 827 (1934).
[28] J. T. Tate and W. Lozier, Phys. Rev. **39**, 254 (1932).

There is a certain chance, w, that the CO^+ will undergo reaction (2). Hence,

$$wCO^+ + wCO = wC^+ + wCO_2. \quad (7)$$

The possible neutralization processes are given in the following equations:

$$CO^+ + \epsilon = C + O \quad (8)$$

$$C^+ + \epsilon + CO = 2C + O. \quad (9)$$

The neutralization of CO^+ will yield a carbon and an oxygen atom, the excess energy appearing either as excitation energy of the atoms or as mutual kinetic energy. The neutralization of C^+ might be expected to yield a carbon atom. However, the energy of this process would have to be emitted in the form of radiation and such radiation processes are of small probability. We, therefore, indicate a neutralization process involving a simultaneous collision with a molecule which, in this case, must be carbon monoxide. Reaction (9) is favorable since not more than 2.5 ev excess energy remain to be converted into the kinetic energy of the fragments.

After the neutralization processes, we therefore obtain, for each ion pair formed in the carbon monoxide,

$$2(1+w)CO + \alpha = wCO_2 + 2O + (\lambda + w)C.$$

The excess of atomic carbon is the origin of the carbon suboxides found in the experimental observations. Some carbon atoms may reach the vessel walls to form solid carbon. Others, doubtless the major portion, react with monoxide to form suboxide, $C + 2CO = C_3O_2$ which polymerizes on the wall. The oxygen atoms can combine with carbon monoxide to form carbon dioxide. The work of Jackson[29] and of Groth[30] has shown this to be a slow three-body process, forty times slower than the three-body reaction $O + O_2 + M \rightarrow O_3 + M$. Oxygen atoms can oxidize either the carbon suboxide or the solid carbon. It is therefore impossible to predict the ratio of the products obtained but the analysis shows definitely that, in nature, they are as experimentally found, and that in the neighborhood of two molecules of carbon monoxide will disappear per ion pair formed. This analysis of the ion reaction is in best agreement with the results of the recent research by Faltings, Groth and Harteck[22] who found that carbon monoxide, dissociated photochemically by light of wave-length $\lambda = 1295$A, causes the decomposition of one molecule of carbon monoxide per absorbed quantum and a similar distribution of reaction products between carbon dioxide and carbon suboxide.

[29] W. F. Jackson, J. Am. Chem. Soc. **56**, 2631 (1934).
[30] W. Groth, Zeits. f. physik. Chemie **B37**, 315 (1937).

II. Radiochemical Reactions in Pure Carbon Dioxide

1. Ionization processes

In carbon dioxide, these processes have been studied by Smyth and Stueckelberg,[31] Kallmann and Rosen,[32] and reviewed by Smyth.[18] The ions CO_2^+, CO^+, O^+ and C^+ are found. At low pressures and moderately high voltages, the relative numbers are of the order 100, 20, 7 and 3, respectively. We shall treat the ions CO_2^+ and CO^+. They are formed in the reactions,

$$CO_2 + \epsilon = CO_2^+ + 2\epsilon - 14.4 \text{ ev} \quad (10)$$

$$CO_2 + \epsilon = CO^+ + O + 2\epsilon - 20.4 \text{ ev}. \quad (11)$$

There is some evidence for the exchange reaction,

$$CO + CO_2^+ = CO^+ + CO_2, \quad (12)$$

and its reverse, in mixtures of the two gases. This does not involve any large energy change since the ionization potentials differ by a fraction of a volt. We shall discuss, later, the possibility of this reaction in connection with the effect of carbon dioxide on the carbon monoxide oxidation.

2. Excitation processes

The ultraviolet absorption spectrum has been studied by Leifson[25] and by Lyman.[33] Bonhoeffer and Harteck[34] conclude from the data that the continuous absorption spectrum corresponds to a dissociation into carbon monoxide and a normal oxygen atom

$$CO_2 = CO + O - 5.5 \text{ ev}. \quad (13)$$

[31] H. D. Smyth and E. C. G. Stueckelberg, Helv. Phys. Acta **2**, 303 (1929); Phys. Rev. **36**, 472 (1930).
[32] Kallmann and Rosen, Zeits. f. Physik **58**, 52 (1929); **61**, 61 (1930).
[33] Lyman, *Ultravioletts pektroscopie*, cited by Bonhoeffer and Harteck.
[34] Bonhoeffer and Harteck, *Grundlagen der Photochemie* (T. Steinkopff, Dresden and Leipzig, 1933), p. 133.

3. Negative ion formation

Loeb,[35] Wahlin[26] and Bradbury and Tatel[36] find that carbon dioxide does not have an appreciable electron affinity and no negative ions were observed even at the highest electron velocities attained. There is a possibility that some O^- ions might be formed for electron velocities in excess of the 5.5 ev required to dissociate carbon dioxide to carbon monoxide and oxygen. It is, however, evident that the process

$$CO_2+\epsilon=CO+O^- \tag{14}$$

only occurs infrequently.

4. The total processes and chemical reactions

The majority of the positive ions are formed through reaction (10). Let p represent the fraction of times that reaction (11) occurs. There is enough energy available per ion pair formed that reaction (13) can take place with a probability equal to that of positive ion formation. On this basis, for each ion pair produced, we have

$$2CO_2+\alpha=(1-p)CO_2^++pCO^+ +(1+p)O+CO+2\epsilon+\alpha. \tag{15}$$

The neutralization processes will, in this case, be simply

$$CO^++\epsilon=C+O \tag{16}$$

$$CO_2^++\epsilon=CO+O. \tag{17}$$

The neutralization of CO_2^+ to yield three atoms is impossible, requiring 15.5 ev where only 14.4 ev are available. Thus, for each ion pair,

$$2CO_2+\alpha=(2-p)CO+(2+p)O+pC. \tag{18}$$

Under the conditions of the experiment, the carbon atoms will be oxidized by the carbon dioxide present. Lind[37] cites experimental evidence of the oxidation of suboxide in presence of pure carbon dioxide. We have also seen that the recombination of oxygen atoms and carbon monoxide is a slow process. Some of these atoms will therefore reach the wall and undergo two competitive heterogeneous reactions

$$O+O=O_2 \tag{19}$$

$$O+CO=CO_2, \tag{20}$$

the latter also occurring as a three-body gas reaction.[30] When the concentration of O_2 becomes appreciable, the oxygen will act as catalyst for the recombination of CO and O

$$O+O_2=O_3 \tag{21}$$

$$O_3+CO=CO_2+O_2. \tag{22}$$

Both these reactions are reasonably fast. Thus, under the influence of alpha-particles, an equilibrium state between CO_2 and $CO+O_2$ is reached after a small quantity of molecular oxygen is formed in the reaction vessel. It is, therefore, easy to understand the experimental observation that, when alpha-particles pass through pure carbon dioxide gas, there is no appreciable decomposition of the gas.

III. Radiochemical Reactions in Pure Oxygen

1. Ionization processes

Three primary processes are of importance:[38, 39]

$$O_2=O_2^++\epsilon-12.5 \text{ ev} \tag{23}$$

$$O_2=O_2^{+\prime}+\epsilon-16.1 \text{ ev} \tag{24}$$

$$O_2=O^++O+\epsilon-19.5 \text{ ev}. \tag{25}$$

There is no evidence for secondary reactions in oxygen or for the formation of complex ions of the type O_3^-.

2. Excitation processes

From spectral data[34] it is seen that the most important transitions are $^3\Sigma_g^-$ to $^3\Sigma_u^-$. When the latter is excited it decomposes to a ^3P and a $'D$ oxygen atom

$$O_2\rightarrow O(^3P)+O(\prime D)-7.05 \text{ ev}. \tag{26}$$

3. Negative ion formation

Two types of negative ion are formed, O_2^- and O^-. The molecular ion is formed with electrons of low kinetic energy. The atomic ions result from collisions between molecules and electrons of sufficient energy to disrupt the molecule. This emerges from the studies of Bradbury,[40] Loeb,[41] Block and Bradbury[42] and

[35] L. B. Loeb, Phys. Rev. **17**, 89 (1921).
[36] N. Bradbury and E. Tatel, J. Chem. Phys. **2**, 836 (1934).
[37] S. C. Lind, reference 10, p. 153.
[38] H. D. Smyth, Proc. Roy. Soc. **A105**, 116 (1924).
[39] J. Tate and P. Smith, Phys. Rev. **39**, 270 (1932).
[40] N. Bradbury, Phys. Rev. **44**, 883 (1933).
[41] L. Loeb, Phys. Rev. **48**, 684 (1935).
[42] F. Bloch and N. Bradbury, Phys. Rev. **48**, 689 (1935).

Lozier.[20] According to Lozier, there are two types of dissociation yielding atomic negative ions:

$$O_2+\epsilon=O+O^- -2.9 \text{ ev} \quad (27)$$

$$O_2+\epsilon=O'+O^- -12.0 \text{ ev}. \quad (28)$$

The electron affinity of molecular oxygen is estimated by Loeb to be less than 0.34 ev, while Block and Bradbury set the limits between 0.07 and 0.19 ev. It is sufficiently small that the electron can be removed from the molecule ion in neutralization processes at distances from the positive ion so large that the residual O_2 molecule is not affected.

4. The total processes and chemical reactions

The energy of the alpha-particle is sufficient to form one positive ion, O_2^+ or O^+, and, in addition, to break up another molecule to form a negative ion and an atom or two neutral atoms. In case the electron uses up its energy in excitation processes it can finally attach itself to an oxygen molecule to form O_2^-. All the neutralization processes possible lead to the same products, four oxygen atoms per ion pair, some normal and others excited

$$2O_2+\alpha\rightarrow 4O. \quad (29)$$

On the basis of the photochemical ozone yield of 1.3–2 molecules per quantum, the maximum ozone yield in the alpha-particle reaction should lie between 2.6 and 4. The experimental values average 1.7, with Lind reporting two results greater than 2. It is evident that the reverse deozonization reaction reduces the experimental yield below the maximum theoretical yield, as is further evident from the minimal ion yields of ozone in static systems. The maximum oxygen atom yield in the process assumes importance in the alpha-particle oxidation now to be considered.

IV. Radiochemical Reactions in Carbon Monoxide-Oxygen Mixtures

In a mixture of gases the energy of the alpha-particle is used by the different species according to the specific stopping power, S_i, the specific ionization, I_i, and the partial pressure, p_i. If N_{CO} is the number of ions produced in carbon monoxide and N_{O_2} the number in oxygen, then

$$N_{CO}/N_{O_2}=S_{CO}I_{CO}p_{CO}/S_{O_2}I_{O_2}p_{O_2}.$$

According to Lind, $S_{CO}I_{CO}=100$ and $S_{O_2}I_{O_2}=110$ so that, to a good approximation, the ratio of ions produced and energy consumed in the two gases respectively is proportional to the partial pressures. To the approximation to which the law of mixtures for ionization is valid, the ratio of the energy consumed by the various components will be equal to the ratio of the number of ions formed in each. Thus, we obtain, from the data in Sections I and III, the following yield per ion pair in a mixture of the gases before neutralizations set in:

$$\frac{p_{CO}}{p_{CO}+p_{O_2}}[(1-w)CO^+ + wC^+ + C + O + wCO_2]$$

$$+\frac{p_{O_2}}{p_{CO}+p_{O_2}}[aO_2^+ + bO^+ + cO + dO^- + fO_2^-], \quad (30)$$

where $0.5a+b+c+d=4$. Since all neutralizations now involve at least two atoms, we expect, on neutralization of charges:

$$\frac{p_{CO}}{p_{CO}+p_{O_2}}[2C+(2-w)O+wCO_2]$$

$$+\frac{p_{O_2}}{p_{CO}+p_{O_2}}[4O]. \quad (31)$$

Since each atom of oxygen will eventually oxidize one molecule of carbon monoxide to dioxide (see Eqs. (21) and (22)), and since, under the experimental conditions, with oxygen and carbon dioxide present, each carbon atom finally produces a carbon dioxide molecule:

$$C+CO=C_2O$$
$$C_2O+O_2=CO_2+CO$$

or, in sum,

$$C+O_2=CO_2,$$

it follows that the yield from the species present in *either* of the two square brackets in (31) will be exactly four molecules of carbon dioxide. Therefore, the ion pair yield will be $4CO_2$ independent of the concentrations of carbon monoxide or oxygen. This result is in exact agreement with the experimental result of Lind and Bardwell. The more recent value of Lind and Rosen-

blum which yielded $2.5CO_2$ per ion pair was based on a calculation including ions produced not only from the reactants, but also those from the carbon dioxide product, the latter with an assumed fractional efficiency (see Section V). We have had access to some recalculations of the data by Rosenblum which reveal that all the experiments are in best agreement with the result deduced above, that the carbon dioxide yield is $4CO_2$ per ion pair produced from the carbon monoxide and oxygen present. The work of Brewer and Kueck,[43] in which carbon monoxide was oxidized in a glow discharge, showed that the yield per ion pair was about two molecules of carbon dioxide. In agreement with Gunther,[8] and with Lunt,[44] we emphasize the difficulties involved in this technique and expect therefrom only the order of magnitude of the yield.

V. The Effect of Carbon Dioxide on the Oxidation Yield

The energy used in pure carbon dioxide per ion pair formed has been shown to result in the break-up of two molecules of carbon dioxide and the production, after neutralization, of

$$(2-p)\mathrm{CO}+(2+p)\mathrm{O}+p\mathrm{C},$$

where p is the fraction of the carbon dioxide ionized to yield CO^+ and $1-p$ is the fractional yield of CO_2^+. Each oxygen atom and each carbon atom ultimately converts one molecule of carbon monoxide into dioxide. There are thus produced $2+2p$ molecules of dioxide or $2p$ molecules per ion pair in excess of those which disappear in the ionization process. If p had a value of unity, the yield from carbon dioxide would be $2CO_2$ per ion pair or 50 percent of the yield of four obtaining in carbon monoxide-oxygen mixtures free from carbon dioxide. Experimentally, Lind and Rosenblum[12] found that the ionization in carbon dioxide was approximately 15 percent as efficient as that in the carbon monoxide-oxygen mixtures. This figure points to a value of $p=0.3(2p/4\times100=15)$. A low value of p such as this is very reasonable since, in the studies of electric discharge through carbon dioxide at low pressures and moderate voltages, the yield of CO^+ was approximately one-fifth that of CO_2^+, or a value of $p=0.17$. Alternatively expressed, a ratio of 5 : 1 in ionization to yield CO_2^+ and CO^+ indicates an efficiency of ionization for carbon dioxide, expressed on the Lind-Rosenblum basis, of 8.3 percent. Further, the exchange reaction already discussed, $CO_2^+ + CO = CO^+ + CO_2$, would tend to raise the efficiency of the carbon dioxide added over and above that calculable from its own primary ionization products. Calculations carried out by Dr. C. Rosenblum, with the available measurements, to determine a definitive value of p on the basis of the present method of treatment revealed that the precision of the experimental data was not adequate to assign a reliable value for the quantity p. The ionization products of carbon dioxide indicate quite definitely, if qualitatively, that the addition of this gas to carbon monoxide-oxygen mixtures can only exercise a minor influence on the velocity of oxidation under the influence of alpha-particles.

VI. The Effect of Added Nitrogen on the Oxidation Yield

The ionization processes in nitrogen were reviewed by Smyth[18] and there is recent work by Tate, Smith and Vaughan.[45] Two processes occur:

$$N_2 = N_2^+ + \epsilon - 15.65 \text{ ev}$$

and

$$N_2 = N^+ + N + \epsilon - 24 \text{ ev}.$$

At 100 ev the ratio of N_2^+ to N^+ is about 10 : 1. These later workers observed no negative ion formation but Smyth and Hogness and Lunn[46] observed minute traces of N_2^-. Bradbury considers negative ion formation in nitrogen very improbable.

The excitation processes in nitrogen have been abundantly studied.[47] As is well known, in discharge tubes, active nitrogen is formed, known to be chemically very reactive, and containing both nitrogen atoms and excited metastable nitrogen molecules.[48] Three-body recombination

[43] K. Brewer and P. D. Kueck, J. Phys. Chem. **35**, 1281 (1931).
[44] R. W. Lunt, Trans. Faraday Soc. **32**, 1691 (1936).
[45] J. T. Tate, P. Smith and A. Vaughan, Phys. Rev. **48**, 525 (1935).
[46] Hogness and Lunn, Phys. Rev. **26**, 786 (1925).
[47] See H. Sponer, *Molekülspektren*, Vol. II (Julius Springer, Berlin, 1936), p. 458.
[48] Cario, Zeits. f. Physik **89**, 523 (1934).

of nitrogen atoms may occur:

$$N+N+M=N_2+M+7.35 \text{ ev.}$$

The metastable molecules have 6.14 ev energy of excitation, and active nitrogen is known to react with oxygen.[49] Further, there is the possibility of exchanges in ionization such as:

$$N_2^+ + CO = CO^+ + N_2 + 2.15 \text{ ev,}$$

which may contribute to the initiation of the oxidation reactions. In a complex of products from an ionization process such as this it is obviously impossible to subject the system to a quantitative treatment. It is, however, quite evident that the addition of nitrogen to the carbon monoxide-oxygen system cannot fail to influence the velocity of the process as was actually found by Rosenblum.

[49] Wansborough-Jones, Proc. Roy. Soc. **A127**, 511 (1930).

The present analysis abundantly supports the point of view put forward by Eyring, Hirschfelder and Taylor in the ortho-parahydrogen conversion and the synthesis of hydrogen bromide as an explanation of alpha-particle reactions alternative to the older "cluster-theory." The preceding data indicate that the alternative is equally applicable to typical processes of alpha-particle decompositions, ozonization and oxidation processes. With increasingly available data on the primary products of ionization processes it may lead to satisfactory interpretation of all such processes.

ACKNOWLEDGMENT

Our thanks are due to Professor H. Eyring and to Dr. C. Rosenblum with whom we have had occasion frequently to discuss these topics.

DECEMBER, 1938 JOURNAL OF CHEMICAL PHYSICS VOLUME 6

Slow Electron Scattering and the Apparent Electron Affinity of Mercury

J. H. SIMONS AND R. P. SEWARD
Department of Chemistry, Pennsylvania State College, State College, Pennsylvania

(Received July 28, 1938)

The scattering of slow electrons by gaseous molecules is discussed with the object of explaining the curves obtained when the apparent scattering area is plotted against a function of the electron velocity. The peaks frequently observed at about the ionization potential for most substances and the abnormally high values for the alkali metals are explained as being due to the formation or presence of positive ions. The rise in the curves for some substances, as the accelerating potential is diminished below the ionization potential, is explained as the result of an attractive force between the electron and the neutral molecule. It is shown that this attractive force for mercury approximates an inverse fourth-power law. From this law and an assumption of the diameter of the negative mercury ion, a reasonable value for the apparent electron affinity of mercury is calculated.

THE scattering of slow electrons in gases at low pressure has been studied by several investigators whose experiments have been summarized by Brode.[1] The effects are usually expressed in terms of α, the apparent cross section for scattering in square centimeters per cubic centimeter at 1 mm pressure and 0°C. Curves showing how α varies with the electron velocity show three distinct types. For argon, methane, etc., α is small for very slow electrons, increases to a maximum, and then decreases gradually as the electron speed increases. In some cases two or more maxima appear. For the alkali metals α at all electron speeds has a much greater value, and maxima and minima appear at lower electron velocities. Curves for the variation of α in zinc, cadmium, and mercury vapors show a very high value at the lowest electron speeds studied, a rapid falling off at higher velocities, and followed

[1] Brode, Rev. Mod. Phys. **5**, 257 (1933).

by a less marked maximum. Inspection of the curves seems to indicate a connection between the ionization potential of the molecule and the appearance of a maximum in the curve. The maximum is in many cases very near to the ionization potential, and with molecules of lower ionization potential the maxima appear at lower electron voltages. It is entirely reasonable to expect a maximum at about the ionization potential; for at this velocity of the electron, it has sufficient energy to produce positive ions. The positively charged particles thus formed would have a much greater scattering effect on the beam of electrons than neutral atoms or molecules and consequently a much greater apparent cross section. As the electron velocity increases above the ionization potential, its greater energy results in a smaller angle of deflection with the same scattering particles in its path, and a smaller apparent cross section results. At very high velocities the electron may approach close to the nuclei of the atoms with but a small deflection and the apparent cross section becomes less than the kinetic theory value. As the electron velocity is decreased below the ionization potential, the apparent cross section should decrease. However, should the neutral molecules exert a small attractive force on the electrons, a rise in α should be expected as the velocity is reduced to zero, for this force would produce a relatively large angle of deflection for low velocities. This is similar to the rise as the velocity is reduced from high values to the ionization potential.

The very high values reported for the apparent cross section of the alkali metals may be due to the positive ions present in the vapor. At the temperatures at which the experiments are performed thermal energy will cause some ionization. A variation of α with temperature should be found, if this explanation is correct.

Since α varies with electron speed in such a markedly different way for different substances, for example, argon on the one hand and mercury on the other, it is apparent that the interaction is different in the two cases. A study of the chemical properties of the two substances indicates the difference to be due to a much greater electron affinity, or ability to form a stable negative ion by addition of an electron, in the case of mercury. It is known that sodium and mercury react with

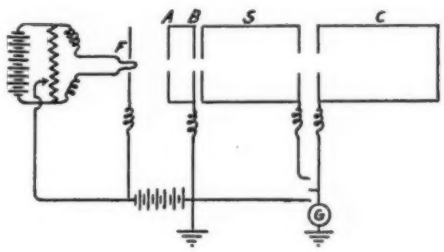

FIG. 1.

evolution of considerable energy, in which reaction the mercury presumably captures the valence electron of the sodium. Glockler[2] has calculated the electron affinity of mercury by an extrapolation method to be 1.8 electron volts. Quantitatively, the electron affinity is the energy consumed in removing to infinity an electron from a negative ion.

If energy is required to remove an electron from a negative ion, it would seem reasonable to assume that there is a force of attraction on an electron in the neighborhood of a neutral atom such as mercury that has the ability to form a stable negative ion. How this force of attraction would vary with the distance between electron and atom is, of course, unknown, but it may be assumed to vary as some inverse power of the distance.

It will be shown that the experimentally determined values of α for mercury are consistent with the assumption that the electron is attracted to the atom by a force varying as the inverse fourth power of the distance and that by assuming a value of the radius of the negative ion a reasonable numerical value for the electron affinity can be calculated. Because of the energy which would have to be dissipated in the formation of a negative ion, it is not likely that there will be actual attachment of electrons under the conditions of the experiments. Nor is this necessary to account for the scattering, since a force of attraction which simply deflects the electron somewhat from its path will cause it to be counted as scattered.

EXPERIMENTAL

A straight tube similar to that employed by T. J. Jones[3] was used. It is shown diagrammatically in Fig. 1.

[2] Glockler, Phys. Rev. **46**, 111 (1934).
[3] Jones, Phys. Rev. **32**, 464 (1928).

Electrons are drawn from the heated tungsten filament, F, and accelerated by varying positive potentials to A and B in the center of which are 2-mm holes. A and B are 1.5 cm apart. The electron beam thus produced passes through the scattering chamber S, 5 cm in length, with a hole at the further end 1.2 cm in diameter and into the collecting chamber C, 8 cm long. These chambers were 3.0 cm in diameter. The metal parts were nickel and enclosed in a Pyrex tube connected to a trap and the vacuum system. A galvanometer was used to measure the currents, connected by a switch so that either the current to the collecting chamber or the combined current to scattering chamber and collecting chamber could be measured. The currents were of the order of 10^{-7} ampere. Mercury vapor in the tube at known pressures was obtained by holding the trap at a given temperature. The pressures used varied from 2 to 20×10^{-4} mm. Reasonably straight lines were obtained by plotting the logarithm of the ratio of collector current to total current against the mercury vapor pressure. The values of α, the apparent cross section for scattering, were calculated from the equation,

$$\alpha=\frac{2.3}{l(p_2-p_1)}\log\,(R_1/R_2),$$

where l is the length of the scattering chamber, p_1 and p_2 the mercury vapor pressures in mm corrected to 0° and R_1 and R_2 the ratio of collector to total current at the pressures p_1 and p_2, respectively. The voltages corresponding to the velocity of the electrons passing through the scattering chamber were determined from graphs showing the relation of the current to the collecting chamber and opposing potentials applied to it. As is usual with this type of tube, a velocity spread amounting to a few tenths of a volt was indicated by the curves.

TABLE I.

Electron Velocity in Volts V	α_{Hg}	α_{Hg} Brode
2	260	230
4	157	150
6	123	100
8	93	77
10	79	64
12	63	56
14	59	51
16	58	50

In Table I are given the values of α obtained for mercury vapor and for comparison those reported by Brode.[4]

It will be noted that our values are somewhat higher than those of Brode. He states, however, that had he used the *International Critical Table* values of the vapor pressure of mercury, which were employed in our calculations, his values of α would have been increased by about ten percent. This would make the agreement good.

Discussion

The experimental values of α will be interpreted in terms of classical mechanics, assuming that the moving electron is attracted toward the atom center by a force varying as some inverse power, n, of the distance. From the known number of mercury atoms per cc in the scattering chamber and α, the effective cross section in square cm per cu. cm of space, the effective radius of a single atom to scattering may be calculated. Let this be r_0. An electron passing farther than r_0 from the atom center will not be sufficiently deflected to fail to get to the collecting chamber, while one which approaches within this distance will be sufficiently deflected. Hence the distance r_0, and therefore a definite value of α, corresponds to the average angle, θ, of deflection, which is just sufficient to make the electron miss the collector. This may be determined by the dimensions of the apparatus.

Since the mass of the atom is very great compared with that of the electron, and its motion at room temperature relatively slow, it will be considered at rest. The initial kinetic energy of the electron, V, is known and will be expressed in electron volts. The potential energy, P, of the electron owing to its attraction toward the atom is $-K/r^{n-1}$ where K is an unknown constant. Exact solution of the problem of the motion of the electron involves mathematical difficulties, but an approximate solution may be made as follows: For small angles of deflection

$$\tan\,\theta=CP/V, \qquad (1)$$

where θ is the angle of deflection, C is a constant,

[4] Brode, Proc. Roy. Soc. (London) **A125**, 134 (1929).

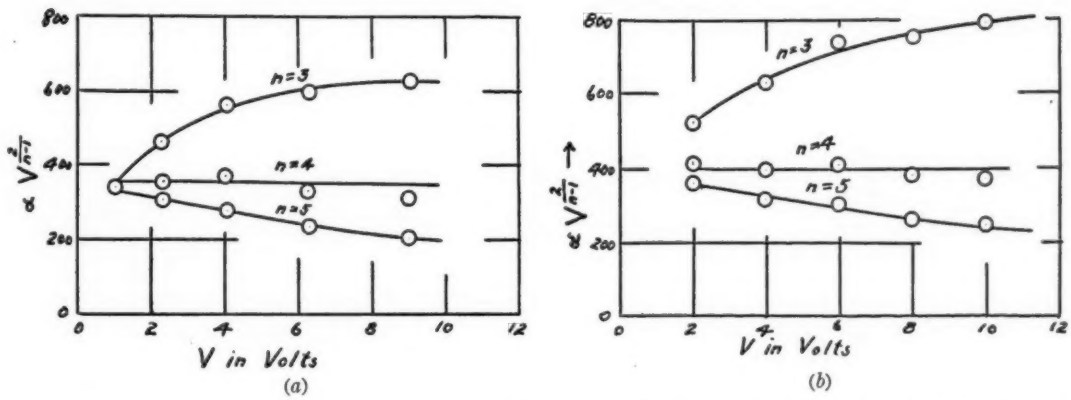

FIG. 2. (*a*) Calculated from results published by Brode. (*b*) Calculated from results of Simons and Seward.

P is the potential energy at the least distance r_0, and V is the initial kinetic energy. Inserting the previously mentioned energies—

$$\tan\theta = C\left(\frac{-K}{{r_0}^{n-1}}\right)\frac{1}{V},$$

r_0 and α are related by the equation $\alpha = \pi {r_0}^2 N$, where N is the number of atoms per cc;

hence $$ {r_0}^2 = \alpha/\pi N $$

and $$ {r_0}^{n-1} = (\alpha/\pi N)^{(n-1)/2}; $$

substituting $$ \tan\theta = \frac{C(-K)}{\alpha^{(n-1)/2}}\frac{(\pi N)^{(n-1)/2}}{V}; $$

rearranging $$ \alpha^{(n-1)/2} V = \frac{C(-K)(\pi N)^{(n-1)/2}}{\tan\theta}, $$

all quantities on the right being constant:

$$ \alpha^{(n-1)/2} V = k_1 \quad \text{or} \quad \alpha \cdot V^{2/(n-1)} = k_2, $$

which equation may be employed to find n.

Assuming an inverse 3-, 4-, and 5th-power force of attraction, the values in Table II have been calculated from the experimental values. Similarly using Brode's values, we obtain the values in Table III.

In both of these tables it may be seen that the product $\alpha V^{\frac{1}{2}}$, corresponding to inverse fourth-power attraction, is most nearly constant. Fig. 2 shows this graphically. Fig. 3 shows how a curve, based on the assumption that $\alpha V^{\frac{1}{2}}$ is constant, compares with the experimental points.

The relation between α, the initial energy of the electron, and the angle through which the electron must be deflected to be counted among those scattered, requires that, other things being equal, if the angle θ is increased α must decrease. It follows that a scattering chamber having a larger hole on the collector end should give a smaller value of α. In the Ramsauer type of apparatus used by Brode, the angle of deflection required for scattering is much smaller than that in the straight tube method. Hence the former should give larger α values. The experimental values cited indicate that the opposite is true. This was likewise found by Jones, who used both methods. It is not certain, however, that the two methods are strictly comparable. Experimental evidence contrary to the above-mentioned discrepancy is found in the work of Palmer[5] on the variation of α

TABLE II.

α	V	$V^{\frac{1}{3}}$	$V^{\frac{1}{4}}$	αV	$\alpha V^{\frac{1}{3}}$	$\alpha V^{\frac{1}{4}}$
260	2	1.59	1.41	520	413	362
157	4	2.53	2.00	628	397	314
123	6	3.31	2.46	738	407	302
93.0	8	4.00	2.84	745	372	267
79.2	10	4.65	3.16	790	368	250

TABLE III.

α	V	$V^{\frac{1}{3}}$	$V^{\frac{1}{4}}$	αV	$\alpha V^{\frac{1}{3}}$	$\alpha V^{\frac{1}{4}}$
340	1	1	1	340	340	340
205	2.25	1.72	1.5	462	353	308
150	4.00	2.53	2.0	560	379	280
95	6.25	3.40	2.5	594	325	238
70	9.00	4.34	3.0	630	304	210

[5] Palmer, Phys. Rev. **37**, 72 (1931).

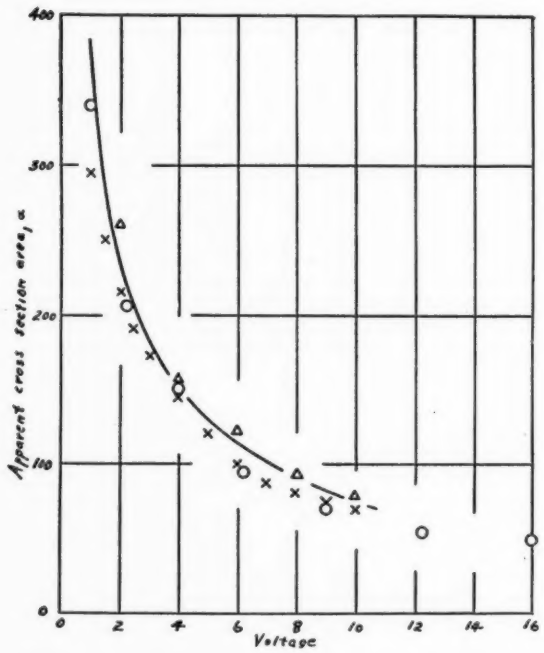

FIG. 3. Apparent cross-section area, α, of mercury at low voltages. The full line represents the theoretical fourth-power attraction. The points are from experiments of different investigators: O, Brode; ×, Jones, and △, Simon and Seward.

with the size of the aperture in the scattering chamber. A decrease in α with increase in aperture was found. However, Palmer did not use electrons below 20 volts, so his results can not be applied in the region discussed here. Experimental work on this point is planned.

The apparent electron affinity of mercury may now be calculated. For inverse fourth-power attraction the constant C of Eq. (1) is found following the method of Zwicky[6] to be -2.

$$\tan\theta = -2P/V = 2(K/r_0^3)(1/V).$$

$\alpha V^{\frac{1}{2}}$ has been previously found to equal approximately 400.

$$\alpha V^{\frac{1}{2}} = (2K/\tan\theta)^{\frac{1}{2}}\pi N = 400.$$

Solving this equation for K,

$$K = (400/\pi N)^{\frac{1}{2}} \tan\theta/2.$$

For the apparatus used the tangent of the average angle of deflection is 0.17 and substituting this and a numerical value of N:

$$K = \left(\frac{400\times 22.400\times 760}{3.14\times 6.06\times 10^{23}}\right)^{\frac{1}{2}} \frac{0.17}{2}$$

$$= 17.3\times 10^{-24}.$$

The potential energy of the electron in its equilibrium position in an ion will now be calculated. The radius of a negative mercury ion is not known. Presumably it would be larger than that of the negative iodide ion 2.16×10^{-8}, from crystal measurements. Assuming it to be 2.25×10^{-8} we find

$$P = -\frac{K}{r_i^3} = -\frac{17.3\times 10^{-24}}{(2.25\times 10^{-8})^3} = -1.53,$$

where r_i is the ion radius.

The apparent electron affinity would be the negative of this or 1.53 electron volts. The uncertainty of the experimental values and the assumptions made preclude the possibility of an accurate value for the electron affinity, but this value seems to be a reasonable one. In the calculations it is assumed that the inverse fourth-power attraction holds down to the equilibrium position of the electron in the negative ion. This, of course, is not justified by the experimental data, since they are weighted in favor of those electrons which pass at large rather than small distances from the center of attraction. Theoretically, also, this law would be expected to change close to an atom or molecule. It may be argued that the total and not the potential energy of the atom-electron system is a measure of the electron affinity. Calculation of the total energy is uncertain however. Employing the virial theorem one obtains a positive total energy. This leads to the apparent absurdity of a negative electron affinity. On the other hand not enough is known of the quantum conditions obtaining in the interaction of an electron with a neutral atom or molecule to permit calculation of electron affinities.

Because of the uncertainties discussed above we have called the quantity which we calculated the *apparent* electron affinity. Although this may not be an accurate measure of the electron affinity it should be valuable, if only for the purpose of comparing the attraction which different atoms or molecules have for electrons.

[6] Zwicky, Physik. Zeits. **24**, 171 (1923).

The Energy of the Triatomic Hydrogen Molecule and Ion, V.

JOSEPH O. HIRSCHFELDER
Chemistry Department, University of Wisconsin, Madison, Wisconsin

(Received July 25, 1938)

In previous papers, the energy of H_3 and of H_3^+ has been obtained by the variational method for linear configurations. In this treatment we are able to evaluate the difficult three center integrals for nonlinear configurations with the aid of the differential analyzer and to compute the energy of H_3 and of H_3^+ as a function of the angle between the nuclei. The excited states as well as the ground states are considered. Direct comparison of calculated energy values for the equilateral triangle show that the molecular orbital approximation is inferior to the method of homopolar bond functions. The triatomic hydrogen molecule has its lowest energy for linear configurations. The angle dependence calculated by the variational method agrees well with that calculated on the basis of the Eyring semi-empirical scheme. By the theorem of Jahn and Teller there could not be a minimum in the energy for the equilateral triangle, as here the lowest electronic state is doubly degenerate. The triatomic hydrogen ion, H_3^+, is very stable (when left to itself) and has an energy lower by more than 184. kcal. than two separated hydrogen atoms and a proton. Thus the chemical reaction:

$$H_2+H_2^+\rightarrow H_3^++H$$

is certainly exothermic by more than 11 kcal. and probably is exothermic by 38 kcal. The triatomic hydrogen ion has a stable configuration corresponding to separation between the nuclei of about 1.79A with the nuclei lying intermediate between a right and an equilateral triangle. The vibration frequencies of H_3^+ are estimated but their exact value as well as the exact configuration of the stable state are somewhat in doubt. Two of these frequencies should be infra-red active and susceptible to direct experimental measurement.

I. INTRODUCTION

THE triatomic hydrogen ion, H_3^+, is formed in rather large quantities whenever hydrogen gas is ionized; the neutral triatomic hydrogen molecule is the metastable complex formed when a hydrogen atom collides with a hydrogen molecule. The difficulties which arise in the calculation of their energies are met quite generally in molecular quantum mechanics. Throughout this work we have used the variational method and computed some of the difficult integrals on the differential analyzer of the Moore School of Electrical Engineering. A discussion of these integrals is given in the following article. In previous communications[1] the energies were computed for linear configurations of the nuclei. In this paper, we consider the triangular configurations for both the ground and the excited states. A direct comparison of energy levels shows that the molecular orbital approximation is inferior to that of the homopolar bond treatments. This is in accord with the recent work of Coulson[2] on H_2. The triatomic hydrogen molecule has its lowest energy for linear configurations and has the same dependence on the bending angle when the variational method is used as is obtained on the Eyring semi-empirical scheme.[3] The triatomic hydrogen ion has its stable configuration intermediate between a right and an equilateral triangle.

II. THE ENERGY OF H_3^+ AND OF H_3 IN THE EQUILATERAL TRIANGLE CONFIGURATION

A. Simplifications due to symmetry

The symmetry of the equilateral triangle simplifies the problem of forming the eigenfunctions for H_3^+ and for H_3. In this particular configuration the Hamiltonian operator is symmetrical with respect to all of the reflections and rotations whose net result is to interchange the like nuclei: a, b, and c. These molecules belong to the D_{3h} symmetry point group[4] and their eigenfunctions

[1] Hirschfelder, Eyring and Rosen, J. Chem. Phys. **4**, 121 and 130 (1936); Hirschfelder, Diamond and Eyring, J. Chem. Phys. **5**, 695 (1937); Stevenson and Hirschfelder, J. Chem. Phys. **5**, 933 (1937).

[2] C. A. Coulson, Proc. Camb. Phil. Soc. **34**, 204 (1938).

[3] Eyring and Polanyi, Zeits. f. physik. Chemie **B12**, 279 (1931); Hirschfelder, Topley and Eyring, J. Chem. Phys. **4**, 170 (1936).

[4] Group theory is the mathematical treatment of symmetry properties. Without it we would obtain the same results but require more work. Some of the most useful references on group theory are; (a) Eugen Wigner, *Gruppentheorie* (Vieweg, 1931). (b) Jenny Rosenthal and G. M. Murphy, Rev. Mod. Phys. **8**, 317 (1936). (c) Eyring, Frost and Turkevitch, J. Chem. Phys. **1**, 777 (1933). (d) J. E. Lennard-Jones, Trans. Faraday Soc. **30**, 70 (1934). (e) Mulliken, Phys. Rev. **41**, 49 (1932).

must transform under the various symmetry operations as eigenvectors of the corresponding representations. Here D_{3h} is the Schönfliess notation to indicate that the molecule possesses three vertical and one horizontal symmetry planes. There are altogether twelve operations under which the Hamiltonian remains invariant —six of these consist in pure rotations and reflections about the vertical symmetry plane, the other six involve reflections about the horizontal plane. In this treatment we are limited to a discussion of only those approximate eigenfunctions which can be formed from 1*s*-hydrogen-like atomic orbitals. Such functions are necessarily symmetrical with respect to a reflection about the nuclear plane and belong to the C_{3v} subgroup of the D_{3h}. In order to obtain eigenfunctions with a nodal plane passing through the nuclei it would be necessary to use p, d, $\cdots$ atomic orbitals. The states which we do not consider for this reason are presumably states of high energy and are therefore relatively unimportant.

There are three classes of eigenfunctions belonging to the D_{3h} group which are symmetrical with respect to a reflection about the nuclear plane. Any satisfactory function must fall into one of the three Mulliken[4e] classifications:

(1) A_1. Eigenfunctions of this class are easily recognized because they remain invariant when the coordinates of the nuclei are interchanged.

(2) A_2. Functions of this class change sign when the coordinates of any two of the nuclei are interchanged.

(3) E. Unlike the functions of the A_1 and A_2 classes these eigenfunctions do not obey a simple law of transformation. They come in pairs (i.e., the corresponding energy states are doubly degenerate) and are partially converted into one another under the symmetry operations.

In this paper, we form our eigenfunctions as the sum of parameters times products of atomic orbitals. The requirement that these approximate eigenfunctions transform in one of the above three manners, provides very stringent restrictions on the values of these parameters. In other words, group theory enables us *a priori* to partially diagonalize the secular equations.

One-electron eigenfunctions which satisfy the symmetry conditions are termed molecular orbitals. These can be formed by taking the right linear combinations of the 1*s*-hydrogen-like atomic orbitals:

$$\begin{aligned} a(1) &= (z^3/\pi)^{\frac{1}{2}} \exp(-zr_{a1}), \\ b(1) &= (z^3/\pi)^{\frac{1}{2}} \exp(-zr_{b1}), \\ c(1) &= (z^3/\pi)^{\frac{1}{2}} \exp(-zr_{c1}). \end{aligned} \tag{1}$$

Here r_{a1}, r_{b1}, and r_{c1} are the distances of electron 1 to nuclei a, b, and c, respectively and z is a parameter which is varied so as to give the lowest energy for the system. In the case of one electron in the field of three protons arranged in an equilateral triangle, i.e., H_3^{++}, there are three molecular orbitals which can be formed in this way:

$$A_1 \qquad \chi(1) = a(1) + b(1) + c(1), \tag{2}$$

$$E \qquad \begin{cases} \varphi_o(1) = a(1) - c(1), & (3) \\ \varphi_e(1) = 2b(1) - a(1) - c(1). & (4) \end{cases}$$

Throughout this paper the subscript o will indicate that the eigenfunction is antisymmetrical (odd) with respect to a permutation of nuclei a and c and the subscript e will indicate that the function is symmetrical (even) in this sense. The $\chi(1)$ orbital belongs to the A_1 class since it is symmetrical with respect to an interchange of any of the nuclei. It is often referred to as an s orbital as it corresponds to a state having no angular momentum for the electron and in this respect it is similar to the s state of an atom. The $\varphi_0(1)$ and $\varphi_e(1)$ belong to the E class and we shall designate them as ω orbitals. Both of these orbitals correspond to states having the same angular momentum but two linear combinations of them will have the electrons revolving in opposite directions. Both states have the same energy. Fig. 1 shows graphically the symmetry of these orbitals. The values of the orbitals are plotted as a function of the angle as we proceed around the circle passing through the three nuclei and having the center of the molecule for its center. The s orbital has no nodes. The ω orbitals have a more complicated structure. It is impossible to form an A_2 orbital out of just one type of atomic function. For the case of just one electron or H_3^{++} we have only three atomic orbitals at our disposal and these are combined to form the three mutually orthogonal molecular

orbitals. Here there is no ambiguity as to the best linear combinations of atomic orbitals (LCAO); they are equivalent to the molecular orbitals.

B. The energy of H_3^+

The problem of H_3^+ where we have two electrons in the field of trigonal symmetry is more difficult than the one-electron case, H_3^{++}. The additional complications are caused by the mutual repulsion of the electrons and by the Pauli Exclusion Principle. Coulson[5] studied the triatomic hydrogen ion, and obtained some very interesting qualitative results as to the relative positions of the various energy states, etc. But he was unable to compute the integrals arising from the mutual repulsion of the electrons and make his results quantitative. These integrals are of a very difficult nature and it was only with the aid of the differential analyzer at the Moore School of Electrical Engineering that we were able to evaluate them. A complete discussion of these integrals is given in the following article by C. N. Weygandt and the author. For two electrons, the Pauli exclusion principle divides the states into two divisions. Those having spatial eigenfunctions symmetrical with respect to an interchange of electrons are multiplied by spin functions characteristic of singlets, whereas those spatial eigenfunctions which are antisymmetric with respect to an interchange of electrons are multiplied by triplet spin functions. The spatial eigenfunctions are formed by taking linear combinations of products of either the atomic or of the molecular orbitals. Since there are three atomic orbitals (or three molecular orbitals) there are altogether (3×3) nine products, or nine mutually orthogonal approximate eigenfunctions which we can form. Three of these functions are for triplets and the other six are for singlets. A little algebra or group theory suffices to further decompose the linear combinations, so that they transform according to the irreducible representations A_1, E, and A_2. The eigenfunctions for the singlet states are:

$$\psi(^1A_1; s^2)=\chi(1)\chi(2), \tag{5}$$

$$\psi(^1A_1; \omega, \omega)=-\tfrac{2}{3}\varphi_u(1)\varphi_u(2)-\tfrac{1}{3}\varphi_g(1)\varphi_g(2), \tag{6}$$

$$\psi_o(^1E; s, \omega)=\chi(1)\varphi_u(2)+\chi(2)\varphi_u(1), \tag{7}$$

$$\psi_o(^1E; \omega, \omega)=\tfrac{1}{2}\varphi_u(1)\varphi_g(2)+\tfrac{1}{2}\varphi_u(2)\varphi_g(1), \tag{8}$$

[5] C. A. Coulson, Proc. Camb. Phil. Soc. **31**, 244 (1935).

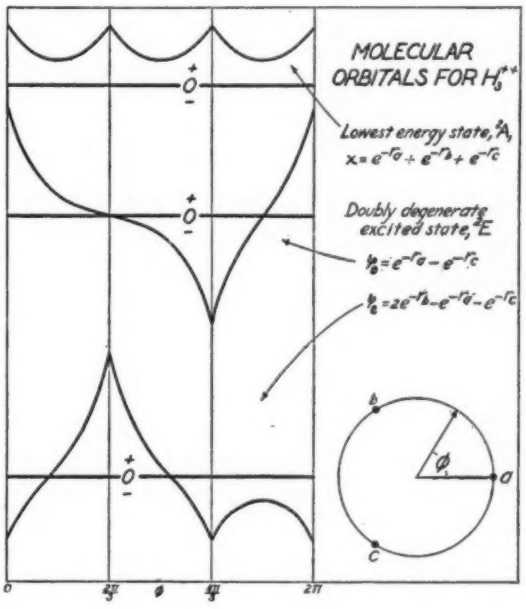

FIG. 1.

$$\psi_e(^1E; s, \omega)=\chi(1)\varphi_g(2)+\chi(2)\varphi_g(1), \tag{9}$$

$$\psi_e(^1E; \omega, \omega)=\tfrac{2}{3}\varphi_u(1)\varphi_u(2)-\tfrac{1}{3}\varphi_g(1)\varphi_g(2). \tag{10}$$

The triplet states for H_3^+ are:

$$\psi_o(^3E; s, \omega)=\chi(2)\varphi_u(1)-\chi(1)\varphi_u(2)=2[a(1)c(2)-a(2)c(1)]+[a(1)b(2)-a(2)b(1)]+[b(1)c(2)-c(1)b(2)], \tag{11}$$

$$\psi_e(^3E; s, \omega)=\tfrac{1}{3}[\chi(2)\varphi_g(1)-\chi(1)\varphi_g(2)]=[b(1)a(2)-b(2)a(1)]+[b(1)c(2)-b(2)c(1)], \tag{12}$$

$$\psi_e(^3A_2; \omega, \omega)=\tfrac{1}{2}[\varphi_u(1)\varphi_g(2)-\varphi_u(2)\varphi_g(1)]=[a(1)b(2)-a(2)b(1)]+[c(1)a(2)-a(1)c(2)]+[b(1)c(2)-c(1)b(2)]. \tag{13}$$

The three triplet states each have different symmetries and therefore have no matrix components between them. The best eigenfunctions for the singlet states are linear combinations of two molecular orbital functions. Thus the lowest energy state for H_3^+ is a linear combination of $\psi(^1A_1; s, s)$ and of $\psi(^1A_1; \omega, \omega)$. The eigenfunctions for the degenerate ^1E state are a linear combination of $\psi_u(^1E; s, \omega)$ and of $\psi_u(^1E; \omega, \omega)$ or of $\psi_g(^1E; s, \omega)$ and of $\psi_g(^1E; \omega, \omega)$. The best energies for these states can be determined by solving second-order secular equations and the best linear combinations (LCAO) can be determined in a similar fashion. However, it has been the practice of many investigators in molecular quantum mechanics to guess what these best linear combinations should be. There are two schools of thought—the molecular orbitalists

(Hund, Mulliken, Lennard-Jones, etc.) and the homopolarists (Heitler, London, etc.). The former take for their eigenfunctions the functions formed from the lowest orbitals. Thus they would take for the normal state of the H_3^+ ion $\psi(^1A_1; s, s)$ and neglect the effect of the $\psi(^1A_1; \omega, \omega)$. The homopolarists, however, would take that linear combination which does not contain any polar terms, i.e., products such as $a(1)a(2)$ which connote in a sense that two electrons are revolving about the same nucleus at the same time. The homopolar and polar eigenfunctions may be written as linear combinations of the molecular orbital functions. Thus:

$$\psi(^1A_1; \text{homo}) = \tfrac{2}{3}\psi(^1A_1; s, s) + \tfrac{1}{3}\psi(^1A_1; \omega, \omega) = a(1)b(2) + a(2)b(1) + a(1)c(2) + a(2)c(1) + b(1)c(2) + b(2)c(1), \quad (14)$$

$$\psi(^1A_1; \text{polar}) = \tfrac{1}{3}\psi(^1A_1; s, s) - \tfrac{1}{3}\psi(^1A_1; \omega, \omega) = a(1)a(2) + b(1)b(2) + c(1)c(2), \quad (15)$$

$$\psi_o(^1E; \text{homo}) = \tfrac{1}{3}\psi_o(^1E; s, \omega) + \tfrac{2}{3}\psi_o(^1E; \omega, \omega) = a(1)b(2) + a(2)b(1) - b(1)c(2) - b(2)c(1), \quad (16)$$

$$\psi_o(^1E; \text{polar}) = \tfrac{1}{3}\psi_o(^1E; s, \omega) - \tfrac{1}{3}\psi_o(^1E; \omega, \omega) = a(1)a(2) - c(1)c(2), \quad (17)$$

$$\psi_e(^1E; \text{homo}) = \tfrac{1}{3}\psi_e(^1E; s, \omega) + \tfrac{2}{3}\psi_e(^1E; \omega, \omega) = a(1)b(2) + a(2)b(1) + b(1)c(2) + b(2)c(1) - 2[a(1)c(2) + a(2)c(1)], \quad (18)$$

$$\psi_e(^1E; \text{polar}) = \tfrac{1}{3}\psi_e(^1E; s, \omega) - \tfrac{1}{3}\psi_e(^1E; \omega, \omega) = 2b(1)b(2) - a(1)a(2) - c(1)c(2). \quad (19)$$

From the above equations it is clear how we pass from the molecular orbital or Hund-Mulliken description to the homopolar-polar or Heitler-London approach. The real test of these two approximations is the accuracy of the energy levels which they predict. We will compare these energies with those obtained by solving the secular equations and using the best linear combination of atomic orbitals (LCAO).

Having decided upon the approximate eigenfunctions for the various states of the triatomic hydrogen ion, the corresponding energies are calculated by substituting these functions into the expression:

$$E = \int\int \bar{\Psi} H \Psi d\tau_1 d\tau_2 \Big/ \int\int \bar{\Psi}\Psi d\tau_1 d\tau_2. \quad (20)$$

From the variational principle, it follows that the energies calculated in this manner will be too high. For this reason we vary the effective nuclear charge, z, and the composition of the eigenfunctions so as to get as low an energy as possible for a particular state.

When $z=1$ and the separation between the nuclei is $R\,a_0$ (where a_0 is the radius of the first Bohr orbit), the numerator of (20) for each of the states or types of approximations is a linear combination of the six energy components:

$$a^2b^2 = \int\int a(1)b(2)Ha(1)b(2)d\tau_1 d\tau_2 = (3/R-1) - 4G(R) + L(aa, bb), \quad (21)$$

$$a^2a^2 = \int\int a(1)a(2)Ha(1)a(2)d\tau_1 d\tau_2 = (3/R-1) - 4G(R) + L(aa, aa), \quad (22)$$

$$a^2bc = \int\int a(1)b(2)Ha(1)c(2)d\tau_1 d\tau_2 = (3/R-1)I(R) - 2I(R)G(R) - [J(R) + K(a, bc)] + L(aa, bc), \quad (23)$$

$$a^2ab = \int\int a(1)a(2)Ha(1)b(2)d\tau_1 d\tau_2 = (3/R-1)I(R) - 2I(R)G(R) - [J(R) + K(a, bc)] + L(aa, ab), \quad (24)$$

$$ab\,ab = \int\int a(1)b(2)Hb(1)a(2)d\tau_1 d\tau_2 = (3/R-1)I^2(R) - 2I(R)[J(R) + K(a, bc)] + L(ab, ab), \quad (25)$$

$$ab\,ac = \int\int a(1)b(2)Hc(1)a(2)d\tau_1 d\tau_2 = (3/R-1)I^2(R) - 2I(R)[J(R) + K(a, bc)] + L(ab, ac). \quad (26)$$

Here the unit of energy is $e^2/a_0 = 627.4$ kcal. per mole. Table I shows the linear combinations of energy components occurring for the various states. The integrals which occur in equations (21) through (26) are defined in the following article and tables of them are given for the convenience of anyone working in molecular quantum mechanics. The integrals

$$L(aa, bc) = \frac{1}{\pi^2}\int\int \frac{1}{r_{12}} \times \exp(-2r_{a1} - r_{b2} - r_{c2}) d\tau_1 d\tau_2 \quad (27)$$

and

$$L(ab, ac) = \frac{1}{\pi^2}\int\int \frac{1}{r_{12}} \times \exp(-r_{a1} - r_{b1} - r_{a2} - r_{c2}) d\tau_1 d\tau_2 \quad (28)$$

are the only ones novel to this particular problem and these were evaluated with the aid of the differential analyzer as described in the following article. The denominator of (20) is the same as the numerator when a^2b^2 and a^2a^2 are replaced by 1, a^2bc and a^2ab are replaced by $I(R)$, and $ab\,ab$ and $ab\,ac$ are replaced by $I^2(R)$.

The variation of the effective nuclear charge, z, is very simple if at the same time the internuclear separations are changed to $R\,a_0/z$. Then

the energy components in the numerator of (20) become:

$$a^2b^2 = z[(a^2b^2)_{z=1} + (z-1)], \tag{29}$$

$$a^2a^2 = z[(a^2a^2)_{z=1} + (z-1)], \tag{30}$$

$$a^2bc = z[(a^2bc)_{z=1} + (z-1)J(R)], \tag{31}$$

$$a^2ab = z[(a^2ab)_{z=1} + (z-1)J(R)], \tag{32}$$

$$ab\ ab = z[(ab\ ab)_{z=1} + (z-1)(-I^2(R) + 2I(R)J(R))], \tag{33}$$

$$ab\ ac = z[(ab\ ac)_{z=1} + (z-1)(-I^2(R) + 2I(R)J(R))]. \tag{34}$$

When the above expressions for the energy components are used, the denominator of Eq. (20) remains the same as for $z=1$.

The results of these computations are shown in Fig. 2 and in Table I. The states lie in order of increasing energy: $^1A_1$, ^3E, ^1E, and $^3A_2$. The zero of energy is for two normal H atoms and a proton infinitely far apart. Only the $^1A_1$ state has a minimum and can correspond to a stable ion in the equilateral configuration. In the other states the nuclei are repelled. In Fig. 2, the energies are given for the LCAO approximation. The black dots correspond to the values of the energy when $z=1$. The fine curves are obtained by varying the value of z. The heavy curves are then drawn tangent to the fine curves and represent the best energy which we can obtain for these states. The variation of z results in a considerable improvement of the energy of the stable $^1A_1$ but has little effect on the excited states.

Using the best linear combination of atomic orbitals and varying z to get the lowest energy, we find that when the internuclear separation is $1.79\,a_0$ the binding energy of the $^1A_1$ is more than 184 kcal. This is the energy which would be required to separate the triatomic hydrogen ion into two hydrogen atoms and a proton. Because of the variational principle we know that this value is too small. If we use the correct values for the binding energies of H_2 and of H_2^+ (respectively 108.6 and 64.0 kcal. neglecting zero point energies), the reaction

$$H_2 + H_2^+ \rightarrow H_3^+ + H \tag{35}$$

is exothermic by more than 11.2 kcal. (neglecting zero point energies). A much more probable estimate for this energy of reaction can be obtained by using our binding energy for H_3^+

TABLE I.

State	$\int \bar{\Psi} H \Psi d\tau$	Energy in kcal. per Mole $R=2.0\,a_0$	$R=2.5\,a_0$	$R=3.0\,a_0$
A. Lowest State for H_3^+; Singlet A_1 (Symmetrical in Nuclei)				
LCAO		−115.9, $z=1$	−119.5, $z=1$	−100.9, $z=1$
		−172.6, $z=1.37$	−183.8, $z=1.40$	−153.9, $z=1.36$
($^1A_1$; Homo)	$2\,[a^2b^2 + ab\ ab + 2\,a^2bc + 2\,ab\ bc]$	−115.8, $z=1$	−119.5, $z=1$	−100.5, $z=1$
		−171.6, $z=1.36$	−179.3, $z=1.37$	−147.1, $z=1.38$
($^1A_1$; Polar)	$[a^2a^2 + 2\,ab\ ab]$	− 3.1, $z=1$	+ 43.5, $z=1$	+106.8, $z=1$
		− 16.8, $z=1.17$	+ 38.9, $z=1.10$	+106.8, $z=1$
($^1A_1$; s, s)	$3\,a^2a^2 + 6\,a^2b^2 + 12\,a^2bc + 24\,a^2ab + 24\,ab\ ac + 12\,ab\ ab$	−100.6, $z=1$	− 99.7, $z=1$	− 75.0, $z=1$
		−157.6, $z=1.37$	−164.6, $z=1.48$	−128.9, $z=1.43$
($^1A_1$; ω, ω)	$2\,[a^2b^2 + 2\,a^2a^2 + 2\,a^2bc - 8\,a^2ab + 5\,ab\ ab - 2\,ab\ bc]$	+577.7, $z=1$	+421.8, $z=1$	+333.6, $z=1$
		+308.3, $z=.50$	+258.38, $z=.60$	+228.2, $z=.66$
B. Doubly Degenerate Excited Singlet (^1E) State for H_3^+				
LCAO		+238.1, $z=1$	+140.1, $z=1$	+ 86.83, $z=1$
(^1E; Homo)	$2\,[a^2b^2 + ab\ ab - a^2bc - ab\ bc]$	+253.3, $z=1$	+148.9, $z=1$	+ 91.3, $z=1$
(^1E; Polar)	$a^2a^2 - ab\ ab$	+341.0, $z=1$	+273.9, $z=1$	+251.0, $z=1$
(^1E; s, ω)	$2\,[a^2b^2 + 2\,a^2a^2 + 2\,a^2ab - a^2bc - 3\,ab\ bc - ab\ ab]$	+268.9, $z=1$	+189.0, $z=1$	+157.3, $z=1$
(^1E; ω, ω)	$[2\,a^2b^2 + a^2a^2 - 2\,a^2bc - 4\,a^2ab + ab\ ab + 2\,ab\ bc]$	+507.4, $z=1$	+343.4, $z=1$	+250.1, $z=1$
C. Doubly Degenerate Triplet (^3E) State for H_3^+				
(^3E; s, ω)	$[a^2b^2 - ab\ ab + a^2bc - ab\ ac]$	+123.4, $z=1$	+ 42.5, $z=1$	+ 7.5, $z=1$
D. Nondegenerate Triplet ($^3A_2$) State for H_3^+				
($^3A_2$; ω, ω)	$[a^2b^2 - ab\ ab + 2\,ab\ bc - 2\,a^2bc]$	+436.9, $z=1$	+265.1, $z=1$	+166.5, $z=1$

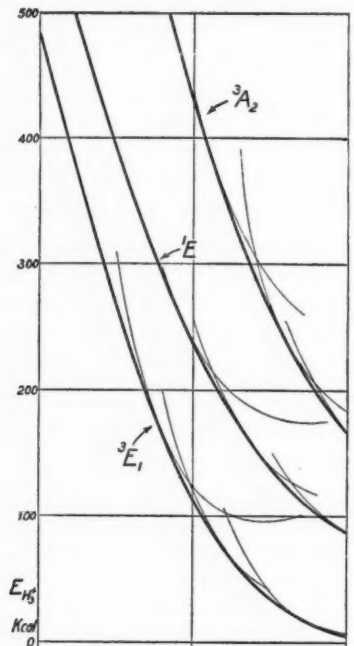

FIG. 2. The energy of H_3^+ in the equilateral triangle configuration as a function of the separation between the nuclei. The zero of energy corresponds to two normal hydrogen atoms and a proton separated by an infinite distance.

together with the binding energies of H_2 and of H_2^+ computed by the same LCAO method (92.2 and 51.9 kcal., respectively). This leads to an exothermic heat of reaction of 39.7 kcal. In any case this reactions is perfectly possible from energy considerations and experimentally[6] it is found to take place with great frequency.

Let us return to a discussion of the relative merits of the homopolar and molecular orbital approximations. For the $^1A_1$ state at the equilibrium separation corresponding to $R=2.5(a_0/z)$ the energies are

LCAO -183.8
Homopolar -179.3
Molecular orbital -164.6

and for the ^1E state for $R=2.5\ a_0$ and $z=1$, the energies are:

LCAO $+140.1$
Homopolar $+148.9$
Molecular orbital $+189.0$.

It is clear from the above figures that *the homopolar approximation is much closer to the best linear combination than is the molecular orbital.* The strongest argument in favor of the molecular orbital picture is that the energy of a state formed from the lowest orbitals such as $\Psi(^1A_1; s, s)$ has a much lower energy than does the excited orbital state $\Psi(^1E; \omega, \omega)$ and therefore we would expect their interaction to be small. From Table I we see that even though their energy difference is roughly 500 kcal., their interaction lowers the best energy by 19.2 kcal. The reason seems to be that the overlapping of these charge distributions is particularly large when the electrons are close to each other. Thus when $R=2.5a_0$ and $z=1$, the energy of interaction between these states is

$$\int\int \bar{\Psi}(^1A_1; s, s) H \Psi(^1A_1; \omega, \omega) d\tau \Big/ \left[\left(\int \Psi^2(^1A_1; s, s) d\tau\right)\left(\int \Psi^2(^1A_1; \omega, \omega) d\tau\right)\right]^{\frac{1}{2}} = -185 \text{ kcal.} \quad (36)$$

This interaction between the molecular orbital states is zero when the nuclei are very close together and increases as the nuclei are separated. Finally when the nuclei are infinitely far apart the total energy of the $\Psi(^1A_1; s, s)$ is 104.6 kcal., the energy of the $\Psi(^1A_1; \omega, \omega)$ is 209.1 kcal., and yet their interaction is strong enough to improve the best energy by 104.6 kcal. So we see that the argument in favor of the molecular orbital picture is not satisfactory in the case of H_3^+ and should be investigated very carefully in other cases. At a first glance we would expect the polar states to give strong interactions with the homopolar, since their energies are close together.

[6] H. D. Smyth, Rev. Mod. Phys. **3**, 347 (1931); Phys. Rev. **4**, 452 (1925).

However, the polar states are not orthogonal to the homopolar, i.e.,

$$\int \bar{\Psi}(\text{polar})\Psi(\text{homopolar})d\tau \neq 0,$$

and therefore these energies give us no information as to the strength of the interaction.

Recently, Coulson[2] computed the energy of the normal hydrogen molecule, H_2, using molecular orbitals. The lowest energy which he was able to calculate on this basis (with a five-term function) was 26.2 kcal. too high and he reached the conclusion that the best possible molecular orbital would have an energy only 0.7 kcal. lower than this. So the best possible molecular orbital would not give as good an approximation to the charge distribution as even the simple homopolar bond function of Wang.[7] This bears out the conclusions of the previous paragraph.

C. The energy of H_3 in the equilateral triangular configuration

The triatomic hydrogen molecule is the intermediate complex in the simplest chemical reactions, i.e., the *ortho-para* hydrogen conversion or the reaction of a deuterium atom with hydrogen. The semi-empirical scheme predicts the energy of this metastable collision complex and therefore it is interesting to see how well the variational calculations agree with these prognostications. The computations of the energy is similar to that for the triatomic ion. No further integrals are required and we obtain the energy of the neutral molecule as a corollary to that for the ion. Again the eigenfunctions must transform according to the three symmetry classes: A_1, E, and A_2. Since H_3 has three electrons, these eigenfunctions will correspond to both doublet and quartet spin states. The Pauli exclusion principle makes it no longer possible to separate the eigenfunctions for three electrons into a product of a space function times a spin function, but this difficulty is alleviated by the use of Slater determinants. A little consideration shows that there are twenty of these determinants which do not vanish identically, and which can be formed from our three atomic or three molecular orbitals. These correspond to one quartet ($^4A_2$), three doubly degenerate (^2E) and two nondegenerate ($^2A_1$, and $^2A_2$) doublet states. The lowest energy state for H_3 is the doubly degenerate ^2E. Altogether there are six combinations of Slater determinants which have the ^2E symmetry and a spin component of $(\frac{1}{2})h/2\pi$. Three of these are symmetric and three antisymmetric with respect to an interchange of the nuclei a and c. The symmetric functions do not combine with the antisymmetric ones and this provides a natural division between the degenerate states. In the homopolar-polar description, the states antisymmetric with respect to an interchange of a and c are:

$$\Psi_o(^2E;\ \text{homo}) = 2\begin{pmatrix} a & b & c \\ \alpha & \beta & \alpha \end{pmatrix} - \begin{pmatrix} a & b & c \\ \beta & \alpha & \alpha \end{pmatrix} - \begin{pmatrix} a & b & c \\ \alpha & \alpha & \beta \end{pmatrix}, \tag{37}$$

$$\Psi_o(^2E;\ \text{polar}_1) = 2\begin{pmatrix} a & a & c \\ \alpha & \beta & \alpha \end{pmatrix} - 2\begin{pmatrix} c & c & a \\ \alpha & \beta & \alpha \end{pmatrix} + \begin{pmatrix} a & a & b \\ \alpha & \beta & \alpha \end{pmatrix} - \begin{pmatrix} c & c & b \\ \alpha & \beta & \alpha \end{pmatrix} + \begin{pmatrix} b & b & c \\ \alpha & \beta & \alpha \end{pmatrix} - \begin{pmatrix} b & b & a \\ \alpha & \beta & \alpha \end{pmatrix}, \tag{38}$$

$$\Psi_o(^2E;\ \text{polar}_2) = 2\begin{pmatrix} a & a & b \\ \alpha & \beta & \alpha \end{pmatrix} - 2\begin{pmatrix} c & c & b \\ \alpha & \beta & \alpha \end{pmatrix} + \begin{pmatrix} a & a & c \\ \alpha & \beta & \alpha \end{pmatrix} - \begin{pmatrix} c & c & a \\ \alpha & \beta & \alpha \end{pmatrix} + \begin{pmatrix} b & b & a \\ \alpha & \beta & \alpha \end{pmatrix} - \begin{pmatrix} b & b & c \\ \alpha & \beta & \alpha \end{pmatrix}. \tag{39}$$

Here the brackets such as $\begin{pmatrix} a & b & c \\ \alpha & \beta & \alpha \end{pmatrix}$ represent Slater determinants where the electrons have spacial orbitals as given by the top line and spin functions according to the bottom line. α is the spin function corresponding to an electron spin in the preferred direction and β corresponds to a spin in the opposite direction. The normal state of the H_3 molecule is made up of a linear combination of two polar and one homopolar state. The lowest value for the energy which we can obtain is for the LCAO approximation and this gives the best linear combination of these three states. As in the case of H_3^+ we should discuss the relative merits of the homopolar and molecular orbital approximations obtained by neglecting the polar states in the former method and by taking a particular linear combination of these states in the second case. The molecular orbital eigenfunction of lowest energy is:

$$\Psi_0(^2E;\ s,\ s,\ \omega) = \begin{pmatrix} \chi & \chi & \varphi_u \\ \alpha & \beta & \alpha \end{pmatrix} = -\Psi_0(^2E;\ \text{homopolar}) - 2\Psi_0(^2E;\ \text{polar}_1). \tag{40}$$

For the states other than ^2E, there is only one way in which we can form an approximate eigen-

[7] S. C. Wang, Phys. Rev. **31**, 579 (1928).

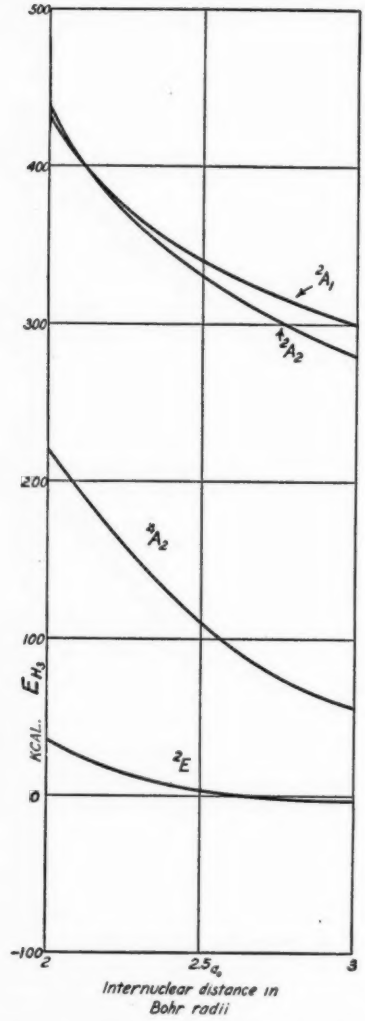

FIG. 3. The energy of H_3 in the equilateral triangle configuration as a function of the distance between the nuclei. The zero of energy corresponds to three normal hydrogen atoms separated infinitely far apart.

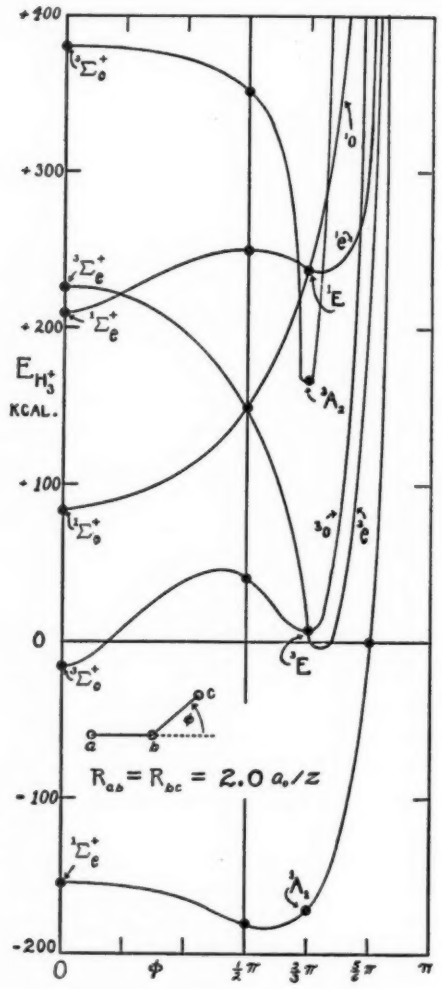

FIG. 4. The energy of H_3 ion as a function of the angle between the nuclei. The black dots represent calculated points.

function out of atomic orbitals and there is therefore no question as to the proper linear combinations. The eigenfunctions for these states are:

$$\Psi(^2A_2)=\begin{pmatrix}a&a&c\\ \alpha&\beta&\alpha\end{pmatrix}-\begin{pmatrix}c&c&a\\ \alpha&\beta&\alpha\end{pmatrix}+\begin{pmatrix}b&b&a\\ \alpha&\beta&\alpha\end{pmatrix}-\begin{pmatrix}a&a&b\\ \alpha&\beta&\alpha\end{pmatrix}+\begin{pmatrix}c&c&b\\ \alpha&\beta&\alpha\end{pmatrix}-\begin{pmatrix}b&b&c\\ \alpha&\beta&\alpha\end{pmatrix}, \tag{41}$$

$$\Psi(^2A_1)=\begin{pmatrix}a&a&b\\ \alpha&\beta&\alpha\end{pmatrix}+\begin{pmatrix}a&a&c\\ \alpha&\beta&\alpha\end{pmatrix}+\begin{pmatrix}b&b&a\\ \alpha&\beta&\alpha\end{pmatrix}+\begin{pmatrix}b&b&c\\ \alpha&\beta&\alpha\end{pmatrix}+\begin{pmatrix}c&c&a\\ \alpha&\beta&\alpha\end{pmatrix}+\begin{pmatrix}c&c&b\\ \alpha&\beta&\alpha\end{pmatrix}, \tag{42}$$

$$\Psi(^4A_2)=\begin{pmatrix}a&b&c\\ \alpha&\alpha&\alpha\end{pmatrix}=\frac{1}{6}\begin{pmatrix}\chi&\varphi_0&\varphi_e\\ \alpha&\alpha&\alpha\end{pmatrix}. \tag{43}$$

In Fig. 3 we have plotted the energy in kcal. of the various states for H_3 as a function of the internuclear separation, R/z. The zero of energy is taken to be the energy of three hydrogen atoms separated to infinity. The ^2E has the lowest energy but it has no minimum and therefore corresponds to a repulsion between the three atoms. The energy of the H_3 in the linear configuration is about 80 kcal. lower than for the equilateral triangle. This agrees with the prediction of the semi-empirical scheme and adds additional weight to the assertion that the reaction:

$$H+H_2\ (ortho)\rightarrow H_2\ (para)+H \tag{44}$$

proceeds most often when the hydrogen atom collides with the molecule close to the line of nuclei. The absolute quantitative agreement between the semi-empirical and the LCAO schemes is not so good as might be desired, but the difference in the energies for the equilateral triangular configuration and for the linear is about the same for the two methods of computation (101–67 = 34 kcal. is the difference in energy of semi-empirical and variational methods for H_3 in a straight line and 34+4 = 38 kcal. is the difference for the equilateral triangle).

For the ground state of H_3, the homopolar state has an energy between 4 and 12 kcal. higher than the LCAO so that it is not very satisfactory. However, the molecular orbital state has an energy lying between 12 and 60 kcal. higher than the homopolar which shows that this approximation is even worse. The energy of the molecular orbital state is a minimum at $R=2.5\,a_0$. For larger separations this energy increases rather than decreases and approaches a limiting value of 261.4 kcal. (instead of zero) when the nuclei are separate by an infinite distance.

The $^4A_2$ lies considerably lower than does the $^2A_2$ which follows the general rule of spectroscopy that, everything else equal, the state of the greatest multiplicity will have the lowest energy. The energy of the $^2A_2$ is almost equal to that of the $^2A_1$ and in fact, the two levels cross. Because these states have different symmetries such a crossing is permissible.

III. Variation of the Energy of H_3^+ and of H_3 with the Angle Between the Nuclei

In previous papers[1] we have considered both the energy of the triatomic hydrogen molecule and ion for linear configurations and their force constants for bending from the straight line. With this information at our disposal, it is easy to obtain four terms interpolation formulae for evaluating the difficult three center integrals as functions of the bending angle. These integrals are discussed in the following article. With these integrals we were able to compute the energy of the configurations where $r_{ab}=r_{bc}=2.0\,a_0/z$ and the angle abc was taken to be 90° (right triangle) and 151° 3′ (this angle makes $r_{ac}=1.0\ (a_0/z)$). Figs. 4 and 5 show the variation of the energy levels in H_3^+ and H_3 as a function of the angle abc between the nuclei.

The energy of the ground state of H_3^+ is lower for the right triangle (−180 kcal.) than for the equilateral triangle (−173 kcal.) which indicates that the stable configuration for the H_3^+ lies between the right and the equilateral

Table II. *Energy* H_3 (*Equilateral triangle*).

$z=1$

State	$\int \bar{\Psi} H \Psi d\tau$	Energy in Kcal. per Mole $R=2.0\,a_0$	$R=2.5\,a_0$	$R=3.0\,a_0$
A. Lowest State for H_3; Doubly Degenerate Doublet ^2E				
(^2E; LCAO)		+ 38.2	+ 4.2	− 3.2
(^2E; Homo)	$12\,[a^2b^2c^2-ab\ bc\ ca]$	+ 50.5	+ 12.6	+ 1.4
(^2E; *s*, *s*, *w*)	$12\,[a^2b^2c^2+2\ a^2a^2b^2+6\ a^2b^2ac$ $+2\ a^2b^2ab+a^2a^2bc-2\ a^2ab\ ab$ $-a^2ac\ ab+a^2bc\ bc+2\ a^2ab\ bc$ $-2\ ab\ bc\ ca-8\ ab\ ab\ ac-2\ ab\ ab\ ab]$	+ 62.5	+ 41.6	+ 61.0
(^2E; Semi-Empirical, 20% Coulombic)		− 49	− 34	− 20
B. Excited Doublet States for H_3				
($^2A_2$)	$a^2a^2b^2-a^2ab\ ab-ab\ ab\ ab$ $+a^2b^2ab+b^2ab\ bc-b^2b^2ac$ $-b^2ac\ ac+ab\ bc\ ca+2\ ab\ ab\ ac$ $-2\ a^2ab\ bc$	+439.2	+330.2	+280.9
($^2A_1$)	$a^2a^2b^2-a^2b^2ab-a^2ab\ ab$ $+a^2a^2bc-b^2ab\ bc+ab\ ab\ ab$ $+b^2ac\ ac-ab\ bc\ ca+2\ ab\ ab\ ac$ $-2\ a^2ab\ bc$	+434.3	+340.4	+298.2
C. Quartet State for H_3				
($^4A_2$)	$a^2b^2c^2-3\ a^2bc\ bc+2\ ab\ bc\ ca$	+220.8	+110.4	+ 56.2

triangular configurations. It would be difficult to ascertain the exact angle as the approximation to which these calculations have been made is not sufficiently accurate. Furthermore, we would like to stress the fact that the three center integrals for the right triangle were estimated, not calculated directly so that there is a chance for small error arising from this source. The electron binding is strongest for the equilateral triangle but the energy of nuclear repulsion decreases as the molecule is bent into a straight line. The position of minimum energy is therefore a compromise between these two tendencies.

According to the theorem of Jahn and Teller,[8] we know that the position of lowest energy of the ground state for the neutral triatomic hydrogen molecule cannot correspond to the equilateral triangle. This theorem states that, barring unlikely numerical coincidences, "All non-linear nuclear configurations are unstable for an orbitally degenerate electronic state of a polyatomic molecule." The ground state for H_3 in the equilateral triangle is the doubly degenerate ^2E and falls into this classification. Fig. 5 shows that indeed the energy for this state decreases as the molecule approaches a straight line and the degeneracy is removed.

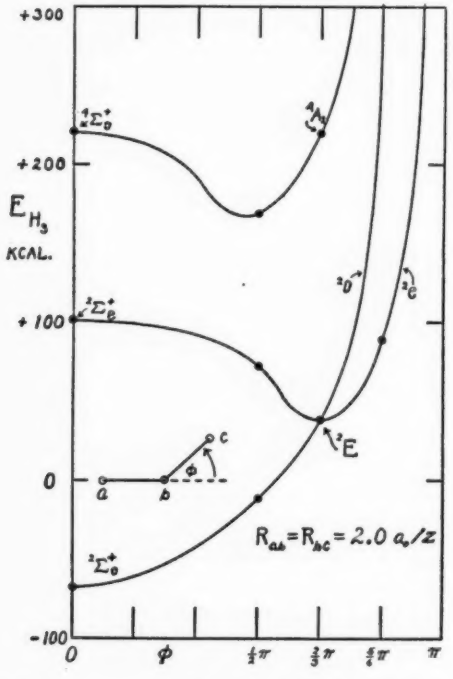

FIG. 5. The energy of the metastable H_3 molecule as a function of the angle between the nuclei. The black dots represent calculated points.

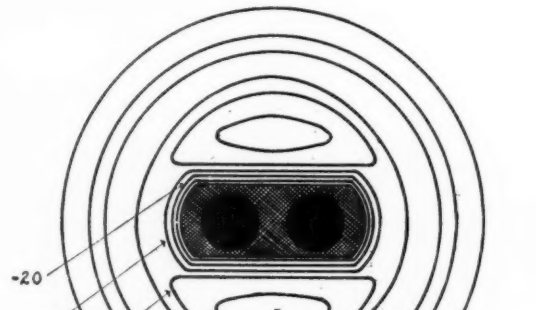

FIG. 6. The energy of attraction of a proton to a hydrogen molecule. The contour lines give the energy of the system when the proton is brought up to a position and the hydrogen molecule is held fixed. The black circles (roughly one Bohr radius in size) outline the location of the hydrogen molecule. The cross-hatched region corresponds to configurations which would be energetically difficult to attain.

When the three nuclei are in a straight line, all of the states given for H_3^+ and for H_3 are either Σ_g^+ or Σ_u^+. This does not mean that there are not Π and minus states as well, but only that our method of using 1*s*-hydrogen-like atomic orbitals cannot lead to the eigenfunctions for these states. Presumably these states would have rather high energies. In all cases for both the ion and the neutral molecule, when an odd and an even state have the same energy for the equilateral triangle, the odd one has the lower energy when ϕ is less than $2\pi/3$ and the even state has the lower energy when the nuclei *a* and *c* approach each other. As the nuclei *a* and *c* come together, the H_3^+ goes into HeH^+ and the H_3 becomes HeH. The even states become Σ^+ and Π^+ states for the diatomic molecule with any nodal planes perpendicular to the line of nuclei whilst the *ungerade* become minus states with a nodal plane passing through the line of nuclei. Our calculations indicate that the states with the node perpendicular to the line

[8] H. A. Jahn and E. Teller, Proc. Roy. Soc. **A161**, 220 (1937).

of nuclei has a lower energy than the states with the nodal plane passing through the nuclei.

IV. Physical Properties of H_3^+

A. Approach of a proton to a hydrogen molecule

Let us consider the forces which are acting upon a proton as it approaches a hydrogen molecule.[9] Fig. 6 shows the lines of equal potential energy for the system when we keep the two nuclei of the hydrogen molecule (shown as big black circles) fixed at their equilibrium separation, and let the proton explore the field. At large separations, the hydrogen molecule is polarized by the electric charge on the proton and attracted to it with a force whose potential is:

$$E(H_3^+)-E(H_2)=\alpha(H_2)e^2/2R^4 \qquad (45)$$

where R is the separation between the proton and the center of the hydrogen molecule and $\alpha(H_2)$ is the mean polarizability of H_2. At large separations the equipotential lines are very nearly circular. At smaller separations (starting with the -60 kcal. contour line) we must use the results of our present computations and take into account the complicated forces of valency as well as the pure electrostatic interactions. We see that for these close separations, the proton is pulled into an energy trough roughly parallel to the line of nuclei. Here it can oscillate rather freely in a long narrow path. The results of our present computations leave the question open as to whether the position of lowest energy is an equilateral triangle, but the best evidence at hand points to a stable configuration lying halfway between the equilateral and the right triangles. If the proton moves even closer to the hydrogen molecule it is repelled. The cross-hatching indicated the region in which the proton is most strongly repelled.

B. Vibration frequencies of H_3^+

Let us assume for the sake of simplicity that the triatomic hydrogen ion is an equilateral triangle with separations of $r=1.79$A between the nuclei. Because of symmetry, the most general expression for the expansion of the potential energy of the system in powers of the displacements of the nuclei from their equilibrium positions is

$$V=V_0+(\tfrac{1}{2})k_1[(\Delta r_{ab})^2+(\Delta r_{bc})^2+(\Delta r_{ac})^2] +k_2[\Delta r_{ab}\Delta r_{bc}+\Delta r_{ab}\Delta r_{ac}+\Delta r_{ac}\Delta r_{bc}], \qquad (46)$$

where k_1 and k_2 are force constants to be determined from our calculations. In the central-force approximation k_2 is taken to be zero.[10] In order to evaluate the force constants, it is convenient to express the potential energy in terms of the lengthening of two sides, Δr_{ab} and Δr_{bc}, and the change in the angle between them, $\Delta\phi$. To do this we substitute the relation

$$\Delta r_{ac}=(\tfrac{1}{2})(\Delta r_{ab}+\Delta r_{bc})+\frac{\sqrt{3}}{2}r\Delta\phi \qquad (47)$$

into Eq. (46). The potential energy then becomes:

$$V=V_0+(\tfrac{1}{2})\left(\frac{5}{4}k_1+k_2\right)\{(\Delta r_{ab})^2+(\Delta r_{bc})^2\} +(\tfrac{1}{2})k_1\frac{3r^2}{4}(\Delta\phi)^2+(\tfrac{1}{4}k_1+2k_2)\Delta r_{ab}\Delta r_{bc} +((\tfrac{1}{2})k_1+k_2)\frac{\sqrt{3}}{2}r\Delta\phi(\Delta r_{ab}+\Delta r_{bc}). \qquad (48)$$

It is interesting to see that in this case of equal masses located in an equilateral triangle, there are no possible choices for the general force constants k_1 and k_2 which would lead to the form of potential energy used by Cross and Van Vleck[11] in which the cross-terms $\Delta r_{ab}\Delta r_{bc}$ and $\Delta\phi(\Delta r_{ab}+\Delta r_{bc})$ do not appear. Using our expression (48) for the potential energy in the Routh function as given by Cross and Van Vleck we find that the normal modes of vibration, x, y, and z are given by the relations:

$$\begin{aligned}\Delta r_{ab}&=x+y+z,\\ \Delta r_{bc}&=x-y+z,\\ \frac{\sqrt{3}}{2}r\Delta\phi&=\quad -3z.\end{aligned} \qquad (49)$$

[9] This was considered in the case of the proton approaching the hydrogen molecule along the line of nuclei in the paper of Hirschfelder, Diamond and Eyring, J. Chem. Phys. **5**, 695 (1937).

[10] The vibrations of three particles of equal mass located in an equilateral triangle was considered in the central-force approximation by Bhagavantam (Indian J. Phys. **5**, 73 (1930)). Radakovic has considered the general problem of three particles in a triangle to this central force approximation (M. Radakovic, Wien Ber. **139**, 107 (1930)).

[11] P. C. Cross and J. H. Van Vleck, J. Chem. Phys. **1**, 350 (1933).

The normal mode, x, corresponds to an alternate expansion and contraction of the molecule without distortion. From the group theory point of view the displacement x is an eigenvector for the A_1 representation of the symmetry group C_{3v}. The normal modes y and z correspond to distortions of the molecule in which one angle remains 60° while one side is lengthened and the other shortened. They belong to the doubly degenerate E representation. In the special case of the equilateral triangle with equal masses, we see that the normal modes of vibration are independent of the values of the force constants. Substituting x, y and z into the Routh function, we easily obtain the equations of motion and from them the vibration frequencies:

$$\nu_x=\frac{1}{2\pi}\left(\frac{3(k_1+k_2)}{m_H}\right)^{\frac{1}{2}}, \quad \nu_y=\nu_z=\frac{1}{2\pi}\left(\frac{3(k_1-k_2)}{2m_H}\right)^{\frac{1}{2}}. \tag{50}$$

The real test whether or not the H_3^+ ion is an equilateral triangle would be a determination of its vibration spectrum. If H_3^+ has only two fundamental frequencies (ν_x and $\nu_y=\nu_z$) it is equilateral. If the degeneracy is removed, it is in some other configuration.

The force constants should be evaluated in the following manner. First set $\Delta\phi=0$ and let $\Delta r_{ab}=\Delta r_{bc}=\Delta r$. Then $V=V_0+(\frac{1}{2})(3k_1+6k_2)(\Delta r)^2$. This variation corresponds to Fig. 2. Second, we keep $\Delta r_{ab}=\Delta r_{bc}=0$ and vary $\Delta\phi$. In this case,

$$V=V_0+(\tfrac{1}{2})\frac{3r^2}{4}k_1(\Delta\phi)^2.$$

This variation of the potential energy with the angle is given in Fig. 4. Unfortunately, our calculations of the variation with angle is not sufficiently accurate for this purpose but as closely as we can tell, $k_2=0$ (agreeing with the central force approximation) and $k_1=4.8\times10^4$. From these force constants, it follows that

$$\nu_x=1550\ \text{cm}^{-1}, \qquad \nu_y=\nu_z=1100\ \text{cm}^{-1} \tag{51}$$

and the zero point energy of H_3^+ is

$$(\tfrac{1}{2})h\nu_x+(\tfrac{1}{2})h\nu_y+(\tfrac{1}{2})h\nu_z=5.4\ \text{kcal}. \tag{52}$$

The z and y modes of vibration should be infra-red active and therefore susceptible to direct experimental observation.

The author wishes to express his appreciation to Professor Henry Eyring under whom this research project was first undertaken and to Mr. Bertrand Mayland who assisted materially in making the computations. We are very glad to acknowledge a Grant-in-Aid from the Penrose Fund of the American Philosophical Society which financed the preliminary investigations, the trip to Philadelphia, and the services of Mr. Mayland. We would like to thank the Wisconsin Alumni Research Foundation for financial support during the remainder of this work.

DECEMBER, 1938 JOURNAL OF CHEMICAL PHYSICS VOLUME 6

Integrals Required for Computing the Energy of H_3 and of H_3^+

JOSEPH O. HIRSCHFELDER
Chemistry Department, University of Wisconsin, Madison, Wisconsin
AND
CORNELIUS N. WEYGANDT
Moore School of Electrical Engineering, University of Pennsylvania, Philadelphia, Pennsylvania

(Received July 25, 1938)

Some of the difficult integrals required for the variational method calculation of the energy of the triatomic hydrogen molecule and positive ion were evaluated with the aid of the differential analyzer. The integral $\int_0^\pi \exp(-B(1-A\cos\theta)^{\frac{1}{2}})d\theta$ is tabulated for a complete range of the parameters, A and B. The integral $K(c, ab)=(1/\pi)\int r_c^{-1}\exp(-r_a-r_b)d\tau$ is tabulated for many configurations of the three electrons or nuclei: a, b, and c. Numerical tables are given of all of the integrals occurring in the Sugiura treatment of the ground state of H_2. The values of all of the other integrals used in the calculation of the energy of H_3 and of H_3^+ are given. It is expected that these tables will be useful for many problems of molecular quantum mechanics.

THE success of a variation method calculation depends on the ability to evaluate the definite integrals which arise. At the present time we are very much limited in the types of charge distributions which we can consider because of the difficulties of integration. Machines such as the differential analyzer at the Moore School of Engineering at Philadelphia and at the Massachusetts Institute of Technology at Cambridge, make it possible to integrate with ease certain functions which would be extraordinarily difficult to handle by the more orthodox mathematical methods. In this work on the triatomic hydrogen ion and molecule we required the evaluation of a two-parameter family of definite integrals which were quite unmanageable from any analytical point of view. In a period of two weeks work on the differential analyzer, we were able to evaluate these integrals for over 200 values of the parameters with an accuracy which was well within the limits required for our present purposes. This shows that the differential analyzer can be used to good advantage in molecular quantum mechanics and should be extremely useful in improving the charge distributions which have been used heretofore.

The two integrals $L(aa, bc)$ and $L(ab, ac)$ (see Eqs. (27) and (28) of preceding article) were the ones which required special consideration. The integrations over the coordinates of the first electron gives:

$$L(aa, bc) = K(a, bc) - T(a, bc), \tag{1}$$

where

$$T(a, bc) = -\frac{1}{\pi}\int e^{-2r_{a2}-r_{b2}-r_{c2}}\left[1+\frac{1}{r_{a2}}\right]d\tau \tag{2}$$

and $K(a, bc)$ is defined as

$$K(a, bc) = -\frac{1}{\pi}\int \frac{1}{r_a} e^{-r_b-r_c} d\tau. \tag{3}$$

Similarly integrating $L(ab, bc)$ over the coordinates of the first electron,

$$L(ab, bc) = -\frac{1}{\pi}\int K(2, ab) e^{-r_{b2}-r_{c2}} d\tau_2. \tag{4}$$

Here,

$$K(2, ab) = -\frac{1}{\pi}\int \frac{1}{r_{12}} e^{-r_{a1}-r_{b1}} d\tau_1. \tag{5}$$

TABLE I. $K(c, ab) = (1/\pi)\int r_c^{-1} \exp(-r_a - r_b) d\tau = K_0(R, x) + \mu^2 K_2(R, x)$ where $x = R(\lambda - 1)/2$.

$K_0(R, x)$

x	$R=1.0$	$R=1.5$	$R=2.0$	$R=2.5$	$R=3.0$	$R=4.0$	$R=5.0$	$R=6.0$	$R=8.0$	$R=12.0$
0.0	.78245 5391	.61627 6976	.46460 541	.33941 6318	.24216 665	.11708 805	.05391 823	.02399 5317	.00443 1661	.00012 79176
0.25			.41379 6561	.30096 1124	.21413 066					
0.50	.63770 6403	.49354 2942	.36833 08	.26748 2122	.19017 84	.09168 849	.04221 922	.01881 202	.00348 8202	.00010 158319
0.75	.57007 1472	.44052 3495	.32867 1972	.23876 8881	.16880 800					
1.00	.50968 6841	.39424 0636	.29456 15	.21432 7444	.15273 62	.07399 680	.03423 458	.01532 147	.00286 2951	.00008 437508
1.25				.19357 4804						
1.50	.41156 9661	.32021 7155	.24058 18	.17593 8601	.12595 40	.06150 429	.02864 126	.01288 899	.00242 9807	.00007 250517
2.00	.33926 0520	.26602 4077	.20122 34	.14802 1433	.10651 15	.05245 363	.02459 248	.01112 862	.00211 6220	.00006 389365
2.25			.18559 96							
2.50		.22599 9	.17207 89	.12729 907						
2.75			.16030 65							
3.00	.24608 9478	.19583 1135	.14999 0	.11151 9340	.08099 023	.04049 475	.01921 476	.00878 053	.00169 5143	.00005 222460
4.00	.19154 9414	.15412 2753	.11916 05	.08931 7112	.06532 490	.03304 682	.01582 820	.00728 889	.00142 4175	.00004 459231
6.00	.13237 041	.10796 6230	.08447 10	.06398 0646	.04723 073	.02427 394	.01177 849	.00548 359	.00109 0301	.00003 497475
8.00			.06548 55		.03705 70	.01923 701	.00941 434	.00441 531	.00088 8598	.00002 900735

$-K_2(R, x)$

x	$R=1.0$	$R=1.5$	$R=2.0$	$R=2.5$	$R=3.0$	$R=4.0$	$R=5.0$	$R=6.0$	$R=8.0$	$R=12.0$
0.0	.04669 6505	.05845 1574	.05859 957	.05211 8824	.04301 838	.02550 986	.01349 055	.00664 4052	.00141 2498	.00004 80428
0.25			.03955 2640	.03586 8080	.03007 5405					
0.50	.01950 5634	.02599 0962	.02730 9	.02520 9253	.02145 2	.01334 46	.00731 673	.00370 893	.00082 3802	.00002 96750
0.75	.01316 441	.01798 054	.01927 291	.01808 583	.01560 513					
1.00	.00911 2644	.01272 4932	.01389 08	.01323 6898	.01157 15	.00751 69	.00426 372	.00222 115	.00051 4415	.00001 95827
1.25				.00987 6067						
1.50	.00468 0411	.00679 2965	.00766 05	.00750 4961	.00671 92	.00453 865	.00265 483	.00141 807	.00034 1352	.00001 36764
2.00	.00261 3074	.00391 8596	.00454 5	.00456 0118	.00416 87	.00291 44	.00175 21	.00095 705	.00023 8500	.00001 00063
2.25			.00358 71							
2.50		.00241 92	.00287 29	.00294 28						
2.75			.00233 28							
3.00	.00100 2710	.00158 2296	.00191 5	.00199 8320	.00188 84	.00139 55	.00087 717	.00049 705	.00013 1185	.00000 594563
4.00	.00047 472	.00077 620	.00096 88	.00103 8792	.00100 55	.00077 358	.00050 285	.00029 295	.00008 0793	.00000 388900
6.00	.00015 764	.00026 809	.00034 1	.00038 5637	.00038 61	.00031 22	.00021 223	.00012 847	.00003 7715	.00000 198486
8.00			.00016 2		.00018 84	.00015 71	.00010 959	.00006 803	.00002 0821	.00000 116630

The expression for $K(2, ab)$ was given in closed form in a previous paper,[1] but it requires considerable work to evaluate it for any particular configuration. This integral is required for many problems in molecular quantum mechanics and the tabulation of it, in Table I should be useful. The integration over the coordinates of the second electron in $T(a, bc)$ and $L(ab, bc)$ could not be carried out in closed form when the nuclei were fixed in a triangular configuration, and the rest of the integrations proceeded numerically. Introducing ellipsoidal coordinates with foci at a and at b:

$$d\tau_2=(R_{ab}^3/8)(\lambda^2-\mu^2)d\theta d\mu d\lambda,$$
$$r_{a2}=(R_{ab}/2)(\lambda+\mu),\quad r_{b2}=(R_{ab}/2)(\lambda-\mu),$$
$$r_{c2}=\frac{R_{ab}}{2}[(\lambda^2+\mu^2-6\mu\lambda+8)+8(\sin^2\phi/2)(\mu\lambda-1)-8\cos\theta\cos\phi/2\times|\sin\phi/2|((\lambda^2-1)(1-\mu^2))^{\frac{1}{2}}]^{\frac{1}{2}} \quad (6)$$

where ϕ is defined as the angle abc. When a, b, c are in a line, $\phi=0$ and for the equilateral triangle $\phi=2\pi/3$. Thus in $T(a, bc)$ and $L(ab, bc)$ for the equilateral triangle:

$$r_{c2}=\frac{R_{ab}}{2}[(\lambda^2+\mu^2+2)-2\sqrt{3}((\lambda^2-1)(1-\mu^2))^{\frac{1}{2}}\cos\theta]^{\frac{1}{2}}. \quad (7)$$

Now it is only in r_{c2} that the angle of rotation about the line a–b appears in these integrals. The integration over θ has the form:

$$Q=\int_0^\pi \exp[-B(1-A\cos\theta)^{\frac{1}{2}}]d\theta, \quad (8)$$

where A and B are functions of λ and of μ. For a satisfactory numerical evaluation of $T(a, bc)$ and of $L(ab, bc)$ it is necessary to carry through the above integrations for a great many values of the parameters. A careful study of the function Q showed that it was a new type of transcendental function having some of the characteristics of Bessel functions and some properties of elliptical integrals. For small values of A an expansion of the integrand into a power series in $\cos\theta$ is useful, but for larger values of A this series does not converge sufficiently rapidly, if it converges at all. This family of integrals was evaluated on the differential analyzer of the Moore School of Electrical Engineering, in the following manner. The $(1-A\cos\theta)^{\frac{1}{2}}$ was plotted on a large sheet of graph paper for ten values of A. These curves were fed into the machine manually. A gear ratio multiplied them by the factor B. One integrater formed the exponential $\exp(-B(1-A\cos\theta)^{\frac{1}{2}}$ as the solution to a first-order differential equation. A second integrater performed the final integration over θ. The indefinite integral was obtained as a by-product and we should like to know some applications for it. Table II shows the values of the definite integrals which were obtained on the machine. These values will be useful in computing many of the exchange

[1] C. A. Coulson, Proc. Comb. Phil. Soc. **34**, 204 (1938).

TABLE II. $Q(A, B)=\int_0^\pi \exp[-B(1-A\cos\theta)^{\frac{1}{2}}]d\theta$.

A	$B=.5$	$B=1.0$	$B=1.5$	$B=2.0$	$B=2.25$	$B=2.44141$	$B=2.60417$	$B=2.88$	$B=3.0$	$B=3.33333$
1.0	2.0549	1.4146	1.0249	.7804	.6917	.6342	.5907	.5311	.5072	.4533
.95	2.0236	1.3555	.9456	.6853	.5907	.5292	.4838	.4183	.3937	.3349
.90	2.0053	1.3232	.9026	.6354	.5395	.4784	.4313	.3657	.3407	.2831
.80	1.9769	1.2753	.8412	.5687	.4706	.4088	.3642	.2994	.2752	.2199
.70	1.9583	1.2380	.8007	.5251	.4278	.3664	.3222	.2592	.2359	.1833
.60	1.9423	1.2168	.7705	.4948	.3974	.3371	.2932	.2322	.2098	.1593
.50	1.9283	1.1938	.7461	.4696	.3734	.3144	.2711	.2123	.1905	.1419
.40	1.9202	1.1800	.7291	.4531	.3576	.2983	.2560	.1980	.1780	.1300
.30	1.9124	1.1683	.7162	.4395	.3446	.2866	.2453	.1877	.1675	.12177
.20	1.9091	1.1615	.7076	.4315	.3372	.2793	.2377	.1809	.1611	.11613
.10				.4280					.1577	

A	$B=3.75$	$B=4.26667$	$B=5.33333$	$B=6.0$	$B=7.5$	$B=8.53333$	$B=10.0$	$B=12.0$	$B=13.33333$	$B=20.0$
1.0	.3993	.3484	.2727	.2423	.2031		.1501	.1231	.11136	.0740
.95	.2780	.2252	.1488	.1160	.07221		.03515			
.90	.2266	.1742	.1057	.07797	.04185		.015818			
.80	.1658	.1200	.06401	.04376	.01929		.005166			
.70	.1346	.09256	.04383	.02821	.01067	.005624				
.60	.1134	.07512	.03286	.01984	.006612	.003201				
.50	.09874	.06333	.02580	.01489	.004453					
.40	.08809	.05554	.02128	.011815	.003205					
.30	.08162	.05002	.01831	.009827	.002466					
.20	.07726	.04662	.01648	.008649	.002031					
.10										

integrals which arise in molecular quantum mechanics as well as in entirely different applications which we cannot foresee at the present time. For large values of B, the value of Q decreases inversely proportionally to B when A is unity and exponentially with B when A is small.

Using the values of Q computed on the differential analyzer, we evaluated the integrands of $T(a, bc)$ and of $L(ab, bc)$ for 230 values of λ and of μ for each nuclear configuration. The problem was then reduced to one of a double numerical integration. This numerical integration was carried out analytically. It has been the experience of practical workers such as the Statistical Laboratory at Edinburgh that greater accuracy can be obtained with less work in this way than by the use of graphical methods. Interpolation formulae were developed for fitting cubics to successive sequences of four points. These interpolation formulae were then integrated over the central segment of the regions which they fit and the total value of the integral was obtained by adding up all of these sub-integrals. Thus the integration of $T(a, bc)$ and of $L(ab, bc)$ over μ gives:

$$\int_{-1}^{1} I(\lambda, \mu)d\mu = \sum_i G(\mu_i)I(\lambda, \mu_i), \qquad (9)$$

where I is the value of the corresponding integrands and the $G(\mu_i)$ are numbers corresponding to the particular values of μ where the integrand was evaluated. For the values of μ_i which we considered $G(\mu) = G(-\mu)$ and:

$$\begin{array}{llll} G(1.0) = .018229, & G(\ .95) = .046626, \\ G(\ .9) = .069791, & G(\ .8) = .165104, \\ G(\ .6) = .165178, & G(\ .5) = .086111, \\ G(\ .4) = .098958, & G(\ .3) = .100833, \\ G(\ .2) = .099479, & G(\ .1) = .084375, \\ G(\ .05) = .040833, & G(0,0) = .048958. \end{array}$$

These G's may be thought of as the coefficients in an improved Simpson's rule. The integration over λ (or $x = (\frac{1}{2})R(\lambda - 1)$) required even more care than that over μ because there were less points at which we knew the value of the function. Then too, the integration over λ or x is extended to infinity whereas the integration over μ is over finite limits. In the region between $x = 0$ and $x = 1$, the integrand of $L(ab, bc)$ passes through a flat maximum and looks like a parabola. Throughout this region, the integrand is fitted by cubics passing through sequences of four points and only the central segment of each region is integrated. From $x = 1$ to infinity, the integrand of $L(ab, bc)$ behaves very nearly as $\exp(-1.5\,x)$. For this reason we multiplied the integrand by $\exp(1.5\,x)$ and fit cubics to every successive sequence of four points, multiplied these approximating cubics by $\exp(-1.5\,x)$ and integrated over the central section of the region fitted. Adding up all of the sub-integrals, we obtained the value of $L(ab, bc)$:

$$L(ab, bc) = \frac{R^2}{4\pi} \sum_{i,\,j} k(x_j)G(\mu_i)l(x_j, \mu_i), \qquad (10)$$

where $l(x_j, u_1)$ is the value of

$$(\lambda^2 - \mu^2)K(2, ab)e^{-r_{b2}} \int_0^{2\pi} e^{-r_{c2}}d\theta$$

when $\lambda = 1 + 2x_j/R$ and $\mu = \mu_i$. For the values of x_j which we considered, the $k(x_j)$ are:

$$\begin{array}{llll} k(0) = .08333333, & k(\ .25) = .32291667, \\ k(\ .50) = .20572917, & k(1.0) = .35858510, \\ k(1.5) = .51497398, & k(2.0) = .66439253, \\ k(4.0) = 1.11010116, & k(6.0) = 3.02627612, \\ k(\ .75) = .24851861, & k(3.0) = 1.17182926. \end{array}$$

Similarly, an improved Simpson's rule was obtained for the integration of $T(a, bc)$ over x. For this purpose we observe that the integrand of $T(a, bc)$ decreases as $\exp(-3.5\,x)$ so that our best curve fitting is obtained by multiplying the integrand through by $\exp(3.5\,x)$ and fitting cubics to successive sequences of four points, then these cubics are multiplied by $\exp(-3.5\,x)$ and integrated over the central section of the region fitted. Adding up all of these sub-integrals we finally obtain for the value of $T(a, bc)$:

$$T(a, bc) = \frac{R^2}{4\pi} \sum_{i,\,j} p(x_j)G(\mu_1)t(x_j, \mu_1), \qquad (11)$$

where $t(x_j, \mu_1)$ is the value of

$$(\lambda^2 - \mu^2)e^{-2r_{a2} - r_{b2}} \left[1 + \frac{1}{r_{a2}}\right] \int_0^{2\pi} e^{-r_{c2}}d\theta$$

for the configuration of electron 2 corresponding to x_j, μ_1. Here the $p(x_j)$'s were the numbers:

$$\begin{array}{llll} p(0) = .0715969, & p(\ .25) = .3874184, \\ p(\ .50) = .0904707, & p(1.0) = .4167317, \\ p(1.5) = .4094224, & p(2.0) = .7813404, \\ p(\ .75) = .2956447, & p(3.0) = 1.243573. \end{array}$$

It is interesting to note the differences in the values of the $k(x_j)$ from the corresponding $p(x_j)$ which are due to the difference in the method of curve fitting. If $l(x_j, u_1)$ were exactly a cubic from $x = 0$ to $x = 1$ and a cubic times $\exp(-1.5\,x)$

TABLE III.

R/a_0	$I(R)$	$J(R)$	$G(R)$	$L(aa, bb)$	$L(ab, ab)$	$L(aa, ab)$
1.0	.85838 53627	.73575 88e^2/a_0	.72932 94e^2/a_0	.55452 13e^2/a_0	.43665 1e^2/a_0	.50704 485
1.5	.72517 30203	.55782 55	.58368 82	.49033 75	.29683 5	.40536 896
2.0	.58645 28938	.40600 59	.47252 65	.42597 43	.18415 6	.30803 646
2.5	.45830 79088	.28729 75	.39056 69	.36838 78	.10662 2	.22559 548
3.0	.34850 948	.19914 83	.33002 83	.31980 35	.05850 83	.16074 246
4.0	.18926 160	.09157 820	.24958 067	.24755 392	.01562 72	.07698 167
5.0	.09657 7238	.04042 768	.19994 552	.19956 908	.00371 704	.03495 3043
6.0	.04709 6292	.01735 126	.16665 949	.16659 267	.00081 4027	.01531 1456
8.0	.01017 5699	.00301 91637	.12499 987	.12499 7955	.00003 28959	.00273 87379
12.0	.00037 47970	.00007 9874761	.08333 333	.08333 3331	.00000 00354836	.00007 4658581

$$I(R)=\frac{1}{\pi}\int \exp(-r_a-r_b)d\tau \qquad L(aa,bb)=\frac{1}{\pi^2}\int\int\frac{1}{r_{12}}\exp(-2r_{a1}-2r_{b2})d\tau_1 d\tau_2$$

$$J(R)=\frac{1}{\pi}\int\frac{1}{r_a}\exp(-r_a-r_b)d\tau \qquad L(ab,ab)=\frac{1}{\pi^2}\int\int\frac{1}{r_{12}}\exp(-r_{a1}-r_{b1}-r_{a2}-r_{b2})d\tau_1 d\tau_2$$

$$G(R)=\frac{1}{\pi}\int\frac{1}{r_a}\exp(-2r_b)d\tau \qquad L(aa,ab)=\frac{1}{\pi^2}\int\int\frac{1}{r_{12}}\exp(-2r_{a1}-r_{a2}-r_{b2})d\tau_1 d\tau_2.$$

from $x=1$ to infinity, the $k(x_j)$'s would make (62) exactly true. Similarly, if $t(x_j, u_1)$ were really a cubic times $\exp(-3.5\,x)$, the $p(x_j)$ would make (63) exactly true. So it is evident that the method of curve fitting makes a considerable amount of difference in the result which we obtain. The careless use of interpolation formulae could easily result in an error of one to two percent in the final answer. We believe that our method of integration should give the values of the integrals to within a half of one percent.

In this way we obtained the values for the equilateral triangular configuration:

R/a_0	$L(ab, bc)$	$L(aa, bc)$	$K(a, bc)$
2.0	.169845 e^2a_0	.258356 e^2/a_0	.294562 e^2/a_0
2.5	.095383	.177685	.193575
3.0	.050862	.119193	.125954

Comparing the values of $L(aa, bc)$ with the corresponding $K(a, bc)$ we see that the difference $T(a, bc)$, is small and therefore requires less accuracy in the computations than does the $L(ab, bc)$. The last two figures of $L(ab, bc)$ and of $L(aa, bc)$ are probably not significant. These integrals are given in units of e^2/a_0 or 627.4 kcal. per mole so that an error of 0.001 (which is certainly larger than any which we have made in these computations) would still give the values of these integrals to within 0.6 kcal. and would be sufficiently accurate for the purposes of this problem.

The other integrals which occur in this problem are integrals involving the distances of the electrons to only two nuclei. These integrals arise in a consideration of H_2 as well as in the triatomic molecule and ion. In spite of the fact that they have been used in many computations, we do not believe that they have ever been published in a tabular form. Table III gives the values of these integrals for many internuclear separations, R.

Next, we wish to discuss the dependence of the three center integrals on the angle between the nuclei. For the internuclear separation corresponding to $R = 2.0$, Stevenson and Hirschfelder[2] have computed the second derivatives of the integrals with respect to the angle of bending, ϕ. In addition, we know the values of the integrals for $\phi=0$, i.e., when the three nuclei are in a line; the values for $\phi=\pi$, when nucleus a coincides with nucleus c to make these integrals equal to the two center integrals which we have tabulated; and the values for $\phi=2\pi/3$, which is the equilateral triangle model which we have just been considering. With these four pieces of information we can express the angle dependence of the integrals in the form:

$$L=L_0+L_1\cos\phi+L_2\cos^2\phi+L_3\cos^3\phi$$

and evaluate the four constants L_0, L_1, L_2, L_3 to agree with the facts at our disposal. Thus or $R=2.0\,a_0$

$$L(ab,bc)=.155966-.025373\cos\phi+.006715\cos^2\phi+.003898\cos^3\phi,$$
$$L(ab,ac)=.098042-.094281\cos\phi+.081583\cos^2\phi-.034130\cos^3\phi,$$
$$L(bb,ac)=.165902-.128456\cos\phi+.094192\cos^2\phi-.037424\cos^3\phi,$$
$$L(aa,bc)=.225658-.052216\cos\phi+.022556\cos^2\phi-.007606\cos^3\phi.$$

For $R=2.5$ and $R=3.0$, we do not know the derivatives of ϕ as we depart from a straight line, but from the values of the integrals for $\phi=0$, π, and $2\pi/3$ we could evaluate three constants.

The Reaction of Hydrogen Atoms with Carbon Tetrachloride*

JOHN E. VANCE AND W. C. BAUMAN†
Department of Chemistry, Yale University, New Haven, Connecticut
(Received September 28, 1938)

Reaction rate constants have been obtained at seven temperatures between 21° and 200° for the reaction $H+CCl_4=HCl+CCl_3$. The change of reaction rate with temperature is satisfactorily represented by the classical bimolecular reaction theory with a steric factor of 0.007 and an activation energy of 3.45 kcal. per mole. A comparison of the amount of HCl formed with the number of hydrogen atoms entering indicates that complete conversion of atomic hydrogen into HCl by the reaction may be attained at 150–200° under conditions which are determined in the experiments.

SINCE the original work of Wood on the production of hydrogen atoms in a high voltage discharge, and of Bonhoeffer on the properties of hydrogen atoms, many studies have been made of the various reactions involving them. These reactions, and exchange reactions, seem to be the most suitable ones for testing reaction rate theories. The work on hydrogen atoms, however, has been handicapped to a considerable extent by the difficulty of measuring, conveniently and accurately, the concentration of hydrogen atoms entering a reaction on one hand, and of estimating the concentration gradient of the atoms in the reaction zone on the other. As a consequence of these difficulties, most of the experimental work on atomic reactions involving hydrogen and deuterium has resulted in the determination of the energies of activation rather than in the estimate of the specific reaction rate constants. A few years ago Polanyi,[1] in a study of the reactions of hydrogen atoms with saturated alkyl halides, discovered that the reaction between hydrogen atoms and carbon tetrachloride led to but one product, HCl, within the limits of accuracy of such experiments, and suggested that this reaction might be a convenient means of determining more exactly the concentration of hydrogen atoms entering into a gas reaction. Polanyi and his co-workers were unable to measure the rate or the activation energy of the reaction exactly, due to the limitations of their apparatus, but were able to make an estimate of the activation energy as being less than 2.8 kcal. The present investigation had as its aims the study of this same reaction over a wider range of conditions of temperature, pressure and relative hydrogen-carbon tetrachloride concentrations in order to determine the conditions necessary for the reaction $H+CCl_4=HCl+CCl_3$ to take place quantitatively. In order to obtain an independent check on the previous results of Polanyi, a different method for the determination of the hydrogen atom concentration was used, namely, the calorimetric method. Further, it was hoped to obtain a more accurate measure of the energy of activation and of the specific rate constant.

APPARATUS

Figure 1 is a scale drawing of the apparatus used in the experiments. Since the primary aim at the beginning of the experiments was to determine the conditions for the complete conversion of hydrogen atoms into HCl, the reaction flask *A* was made as large as the glass-blowing facilities would allow. This flask was surrounded by an electrically heated furnace whose temperature was manually controlled within ±0.5° of the desired temperature. The H_2+H and the CCl_4 entered concentrically at *B*, the hydrogen mixture through the inner tube and out through a tapered tip with a minimum inside diameter of 3.5 mm, and the CCl_4 through the outer coiled tube and out through an orifice with an inside diameter of 8 mm. With the assumption that the rate of radiation from the furnace to these tubes

* From a dissertation presented by W. C. Bauman to the faculty of the Graduate School of Yale University in partial fulfillment of the requirements for the degree of Doctor of Philosophy.

† Present address, Dow Chemical Company, Midland, Michigan.

[1] E. Cremer, J. Curry and M. Polanyi, Zeits. f. physik. Chemie **23B**, 445 (1933).

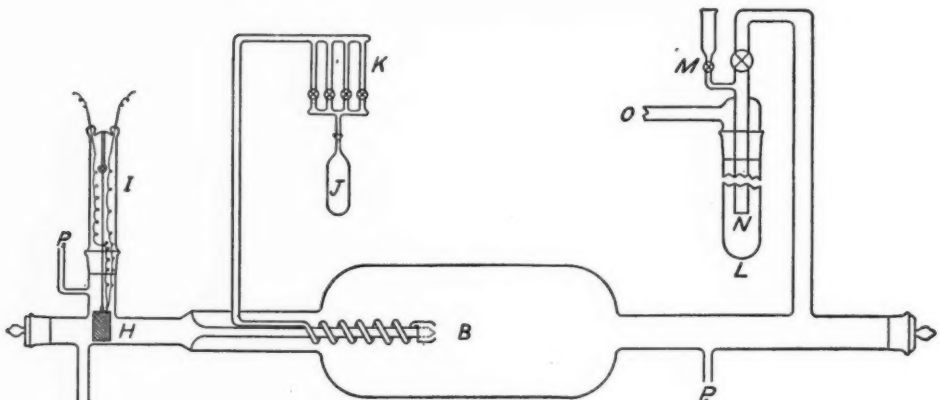

FIG. 1.

was sufficient to maintain the tubes at the furnace temperature, the inlet tubes for both gases were longer than necessary to heat the gases to the furnace temperature before they entered the reaction flask.

Molecular hydrogen entered the system at *C* and passed through the discharge tube *D*, the electrodes *E* of which were mounted in side compartments to prevent spattering of the metal into the main part of the tube. It was found that a discharge tube of this design could be used indefinitely with but a small decrease in efficiency. The discharge tube was cooled by water in the trough *F*. After leaving the discharge tube, the mixture of H_2+H flowed through a tube *G* which was 76 cm long and 11 mm inside diameter. This tube was put into the apparatus in order to prevent diffusion effects between the calorimeter bob *H* and the discharge tube, and was wrapped with asbestos cord.

The calorimeter bob *H* was a solid piece of silver weighing 116.525 grams and was plated with 0.767 gram of platinum. A copper-constantan thermocouple was soldered into a hole in the bob, and the whole bob was suspended by a cord as shown in the figure. The tube *I* surrounding the calorimeter bob was also wrapped in order to prevent irregularities in the temperature of the thermocouple due to air drafts. The whole assembly of bob and thermocouple could be removed and replaced with a ground stopper.

All glass surfaces in the hydrogen line were coated with phosphoric acid to prevent the recombination of hydrogen atoms on the walls.

CCl_4 was drawn from the reservoir *J* through the capillaries *K*. The reservoir was immersed in a beaker thermostat maintained at a constant temperature within $\pm 0.1°$. The flow of hydrogen entering the discharge tube was similarly controlled by capillaries which were calibrated as described by Amdur[2] and were checked at regular intervals. Measurements of the hydrogen flow were reproducible to ± 1 percent. Tank hydrogen was used without purification. It was saturated with water vapor at room temperature before entering the discharge tube and was kept at atmospheric pressure by an overflow device. CCl_4 was purified by washing with 10 percent NaOH which was then removed by washing with distilled water. After drying, the

[2] I. Amdur, J. Am. Chem. Soc. **57**, 588 (1935).

CCl_4 was distilled, the first and last 200 cc portions of a liter distillation being discarded.

All thermocouples were calibrated against a standardized platinum resistance thermometer. Thermocouple leads were shielded from stray electric fields. The thermocouples were read on a Leeds & Northrop type K potentiometer of 0–16 mv range.

Experimental Procedure

The range of flows studied was, for the hydrogen atoms 0.5 to 3.5×10^{-3} mole per min., and for the CCl_4 from 8×10^{-5} to 9×10^{-3} mole per min.

With the bob in place the hydrogen atom concentration was determined under conditions of hydrogen flow, pressure, discharge voltage and amperage identical with those in a given experiment. This procedure was particularly satisfactory since it was found empirically that the hydrogen atom concentration varied simply with the pressure in the hydrogen line, making possible small corrections for differences in pressure between actual experiments on the reaction and those experiments on the determination of hydrogen atom concentrations. It was possible to reproduce the hydrogen atom concentrations to within 3 percent for the higher concentrations and to within 5 or 10 percent, at the worst, for lowest concentrations. Over a period of five months it was found that under the same conditions the concentration of hydrogen atoms remained the same, providing that after a period of disuse the discharge was allowed to run for an hour before the measurement. The calculation of the concentration of hydrogen atoms from the temperature rise of the thermocouple was made in the usual way, using the data of Beutler[3] on the heat of dissociation of the hydrogen molecule.

Since it has been indicated in the literature[4] that it is difficult to freeze out HCl quantitatively, careful tests were made. According to the work of Giauque and Wiebe[5] the vapor pressure of solid HCl at liquid-air temperature must be of the order of 10^{-3} mm, so that any difficulty must be that of entraining the gas. Several runs were made in which a known volume of standardized HCl solution were evaporated into the system with the pumps running and the HCl frozen out. These experiments gave titrations agreeing within a small fraction of a percent of the HCl taken, so that it may be said definitely that in the presence of an excess of water vapor, HCl is taken out completely in a liquid-air trap. In a typical experiment on the reaction, however, only a small amount of water vapor is present. In this case the HCl may be taken out quantitatively by placing a quantity of snow in the trap. Two sets of experiments checked this. First, an excess of water vapor was introduced into the vacuum line just before the liquid-air trap. This did not increase the amount of HCl frozen out during an experiment. Second, when two successive traps were cooled with liquid air, the second trap showed no trace of HCl. The trap L used in the experiments had a special design, shown in Fig. 1, so that it could be isolated from the system by stopcocks at the conclusion of an experiment. A second large stopcock adjoined the trap at the point O. After an experiment the trap was warmed and the HCl absorbed in the water as the snow melted. When the snow melted more water was introduced through the stopcock M and finally air admitted until the pressure became atmospheric. The trap was then removed and the inner tubes N and O washed. The HCl was titrated with 0.1 N $Ba(OH)_2$.

The procedure in a typical experiment was as follows: Hydrogen was admitted into the system through the desired capillary and was permitted to flow until the pressures at P_1 and P_2 became constant. Then the CCl_4 capillary was opened and again the pressures allowed to become constant. When this had occurred the discharge was turned on and allowed to run for exactly five minutes, following which time the CCl_4 was turned off and a minute later, the hydrogen. After cutting off the discharge the pressures were again read and recorded. The liquid-air trap was then removed and the acid titrated, the whole procedure consuming approximately thirty minutes.

Separate experiments were made to measure the amount of the thermal reaction between H_2 and CCl_4. At the highest temperature studied in

[3] H. Beutler, Zeits. f. physik. Chemie **B29**, 315 (1935).
[4] H. M. Chadwell and T. Titani, J. Am. Chem. Soc. **55**, 1363 (1933).
[5] W. F. Giauque and R. Wiebe, J. Am. Chem. Soc. **50**, 101 (1928).

TABLE I. *The reaction of hydrogen atoms with* CCl_4 *at* 21°.

Exp. No.	n_{HCl} ×10⁵	n_H ×10⁵	P_1 mm	n_C ×10³	n ×10³	f	ρ_c ×10⁹	k_c ×10⁻¹⁰	k_s ×10⁻¹⁰
322	17.9	45.3	0.78	0.079	3.96	0.396	0.85	7.2	10.6
323	21.4	43.1	.81	.225	4.09	.496	2.44	3.4	4.9
324	22.3	42.5	.82	.295	4.16	.524	3.17	2.9	4.1
325	22.7	41.8	.83	.417	4.27	.543	4.41	2.2	3.1
326	23.2	41.1	.84	.580	4.43	.565	6.02	1.7	2.4
327	24.0	40.4	.86	.783	4.63	.593	7.92	1.4	2.0
328	24.3	38.6	.88	1.265	5.10	.629	11.94	1.0	1.4
329	24.5	38.6	.89	1.433	5.26	.634	13.21	0.91	1.3
330	24.5	38.0	.91	1.655	5.48	.645	14.89	0.82	1.2
161	25.0	35.2	.92	1.980	5.75	.711	17.29	0.90	1.3
163	22.5	31.5	.99	2.980	6.73	.716	23.99	0.61	0.86

the regular experiments, the correction for the amount of HCl due to the thermal reaction was approximately 0.1 cc of 0.1*N* base.

DATA AND CALCULATIONS

In order to make an estimate of the specific reaction rate, it is necessary to determine the distribution of the reactants in the reaction zone. This involves a study of the stationary state in a streaming, diffusing and reacting gas mixture. The mathematical treatment of this phase of the problem was carried out under the direction of Dr. Lars Onsager, and is described in full in the dissertation of W. C. Bauman on file in the Yale University Library; it will appear in print at a later date. Briefly, the assumptions are that a reacting gas *A* (in the present instance, CCl_4) is streaming through the reaction zone with a certain linear velocity, and that a second reacting gas *B* (in the present instance, hydrogen atoms) is introduced into the reaction flask at the center of the vessel and is carried into the reaction flask by component *A*. It is assumed further that the gas *A* is in great excess, so that its concentration may be taken as constant throughout the vessel, and that any remaining atoms of *B* are destroyed by collision with the walls of the vessel. Linear flow is also assumed. While Hartel and Polanyi[6] have studied the stationary state for spherical flames, and Förster and Geib[7] have discussed the distribution of reactants longitudinally in a tube, both of these treatments assume the absence of a wall reaction.

Two cases were considered: the case in which the reaction vessel is a cylinder, the length of which is much greater than the radius, and the case in which the reaction vessel is a sphere.

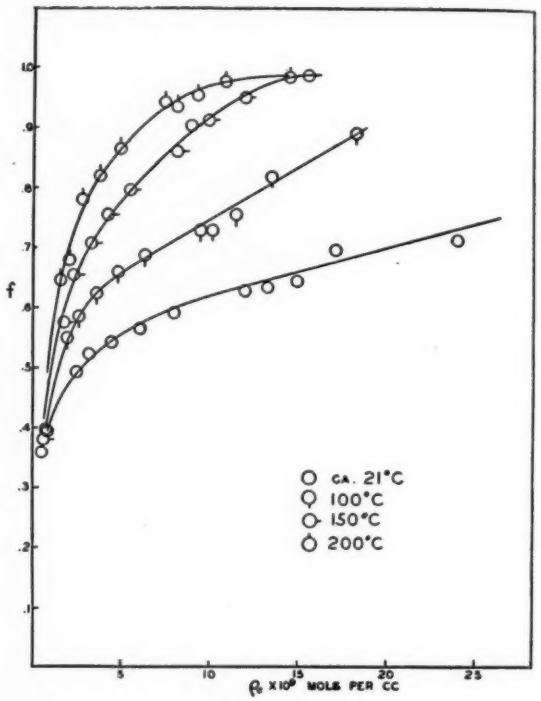

FIG. 2.

The experimental data and the calculated results are shown in Tables I–IV. The experiments included in the tables are all with an approximately constant flow of H_2. Further experiments, not included, with a lower H_2 flow give the same value of the constants. Checking experiments are not shown in the tables. These agreed within 5 percent in the value of f. n_{HCl}, n_H, n_C, and n refer respectively to the mole per minute of HCl, H atoms, CCl_4 and total mole flowing in a given experiment. f is the fraction of hydrogen atoms entering which were converted to HCl, as measured by the titration, thus $f = n_{HCl}/n_H$. ρ_c is the

TABLE II. *The reaction of hydrogen atoms with* CCl_4 *at* 100°.

Exp. No.	n_{HCl} ×10⁵	n_H ×10⁵	P_1 mm	n_C ×10³	n ×10³	f	ρ_c ×10⁹	k_c ×10⁻¹⁰	k_s ×10⁻¹⁰
303	15.2	38.3	0.80	0.079	3.81	0.398	0.71	12.2	17.5
304	20.8	37.8	.81	.225	3.95	.550	1.97	7.3	10.5
305	21.5	36.6	.82	.295	4.02	.586	2.59	6.1	8.9
306	22.8	36.6	.82	.417	4.14	.624	3.55	5.1	7.2
307	23.5	35.6	.84	.580	4.34	.660	4.80	4.2	5.9
308	24.1	35.0	.84	.783	4.54	.688	6.26	3.6	4.9
309	25.1	34.4	.87	1.265	5.01	.730	9.40	2.6	3.7
310	25.5	35.0	.85	1.433	5.18	.729	10.12	2.5	3.4
311	26.0	34.4	.87	1.655	5.40	.756	11.40	2.4	3.3
103	27.6	33.6	.88	1.980	5.62	.821	13.36	2.6	3.5
110	27.8	31.2	.95	2.980	6.65	.893	18.18	2.5	3.4

[6] H. v. Hartel and M. Polanyi, Zeits. f. physik. Chemie **11B**, 97 (1931).
[7] v. Th. Förster and K. H. Geib, Ann. d. Physik **20**, 250 (1934).

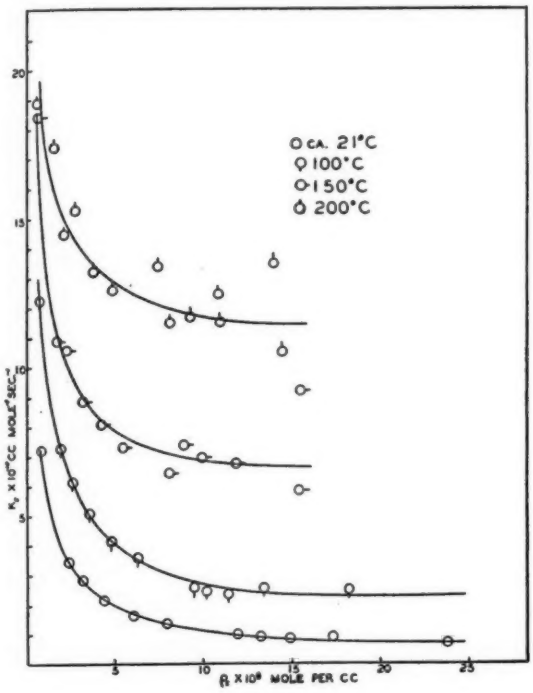

FIG. 3.

concentration of CCl_4 in mole/cc; k_c and k_s are the specific reaction rate constants calculated on the basis of the theoretical equations. Depending upon the two limiting cases for the shape of the reaction flask, two equations were derived. In the case of a spherical flask the result is:

$$\frac{n_H}{n_H - n_{HCl}} = \frac{1}{1-f} = \frac{\sinh(\sqrt{M}R)}{\sqrt{M}R}, \qquad (1)$$

where R is the radius of the reaction flask = 7.62 cm. In the case of an infinitely long cylinder, the result is,

$$1/(1-f) = I_0(\sqrt{M}R), \qquad (2)$$

where $I_0(x)$ is the Bessel function of zeroth order and of imaginary argument and is given by:

$$I_0(x) = 1 + \frac{x^2}{2^2} + \frac{x^4}{2^2 \cdot 4^2} + \frac{x^6}{2^2 \cdot 4^2 \cdot 6^2} + \cdots.$$

In either case, $M = (k \cdot \rho_c)/\delta$, where δ is the diffusion coefficient of H in cm²/sec. The constant calculated from the first equation is designated as k_s and that calculated from the second equation as k_c. For the reaction flask actually used one might expect the proper treatment to be intermediate between these two cases. The difference actually found between k_s and k_c is, however, not large.

If Exp. 261 is taken as a typical caculation, it is found that n_H is 27.1×10^{-5} mole/min. and the HCl found is 9.72×10^{-5} mole/min., giving a value of $f = 0.359$ and of $1/(1-f) = 1.560$. According to Eq. (1) this gives a value of $M = 0.0501$ and according to Eq. (2) a value of $M = 0.0342$ cm^{-2}. Since $k = M\delta/\rho_c$ it is necessary to estimate the diffusion coefficient of hydrogen atoms through almost pure H_2 at a pressure P_1 and at the particular temperature. Taking the values of Steiner[8] at 760 mm and 300°K for the diffusion coefficient of H_2 in H_2 as 1.31 cm²/sec. and for the diffusion coefficient of H in H as 2.2 cm²/sec., as well as the diameter of the H_2 molecule, determined from viscosity measurements, as 2.46A,[9] it is possible to calculate the diffusion coefficient of H atoms through H_2. The assumption necessary is that the diffusion coefficient is inversely proportional to the square of the diameter of the diffusing molecule.[10] The values thus obtained are: for the diameter of the H atom, 1.91A; and

TABLE III. *The reaction of hydrogen atoms with* CCl_4 *at* 150°.

Exp. No.	$n_{HCl} \times 10^5$	$n_H \times 10^5$	P_1 mm	$n_C \times 10^3$	$n \times 10^3$	f	$\rho_c \times 10^9$	$k_c \times 10^{-10}$	$k_s \times 10^{-10}$
284	13.6	35.7	0.77	0.079	3.67	0.380	0.63	18.4	23.6
285	20.2	35.0	.79	.225	3.82	.575	1.77	10.9	15.4
286	22.0	33.6	.81	.295	3.89	.655	2.32	10.6	14.9
287	23.3	33.0	.82	.417	4.02	.706	3.23	8.9	12.5
288	24.9	33.0	.82	.580	4.26	.755	4.23	8.1	11.3
289	26.2	33.0	.82	.783	4.46	.795	5.46	7.3	10.2
290	27.6	32.0	.84	1.265	4.93	.861	8.12	6.5	8.8
291	28.5	31.6	.84	1.433	5.10	.903	8.91	7.4	10.0
292	28.4	31.1	.84	1.655	5.33	.912	9.92	7.0	9.4
64	24.7	26.0	.83	1.980	5.18	.950	11.97	8.0	10.6
70	25.3	25.6	.91	2.980	6.60	.988	15.50	9.2	11.8

TABLE IV. *The reaction of hydrogen atoms with* CCl_4 *at* 200°.

Exp. No.	$n_{HCl} \times 10^5$	$n_H \times 10^5$	P_1 mm	$n_C \times 10^3$	$n \times 10^3$	f	$\rho_c \times 10^9$	$k_c \times 10^{-10}$	$k_s \times 10^{-10}$
341	11.7	32.4	0.80	0.079	3.79	0.360	0.57	18.9	27.5
342	20.3	31.5	.82	.225	3.93	.646	1.59	17.4	24.6
343	21.1	31.0	.84	.295	4.00	.679	2.09	14.5	20.4
344	24.2	31.0	.84	.417	4.17	.780	2.84	15.3	21.4
345	25.1	30.6	.84	.580	4.32	.819	3.83	13.2	18.3
346	26.4	30.6	.84	.783	4.53	.863	4.94	12.6	17.2
347	27.6	29.3	.87	1.265	5.07	.941	7.42	13.4	17.9
348	27.4	29.3	.87	1.433	5.17	.934	8.14	11.5	15.4
349	27.1	28.5	.89	1.655	5.39	.953	9.25	11.7	15.2
219	27.1	27.8	.94	1.980	5.79	.975	10.84	12.5	16.3
220	25.9	26.3	.97	2.980	6.77	.983	14.47	10.5	13.7

[8] W. Steiner, Trans. Faraday Soc. **31**, 623, 962 (1935).
[9] L. Page, *Introduction to Theoretical Physics* (D. Van Nostrand Co., Inc., New York, 1932), p. 309.
[10] H. S. Taylor, *Treatise on Physical Chemistry* (D. Van Nostrand Co., Inc., New York, 1932), Vol. I, p. 214.

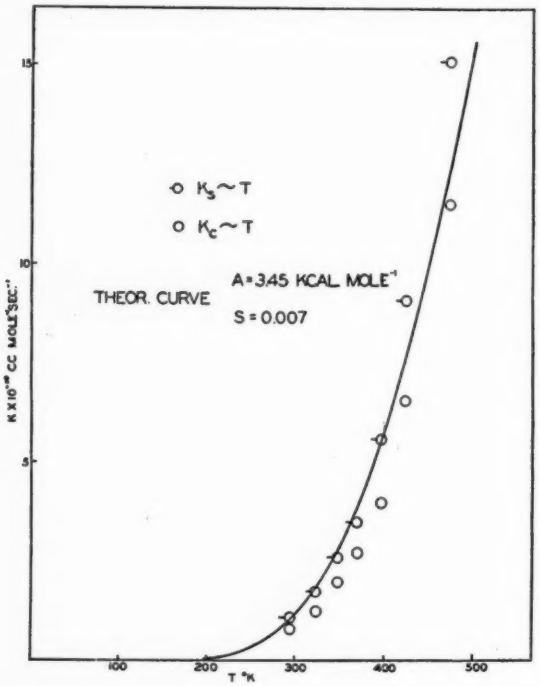

FIG. 4.

for the diffusion coefficient of H atoms through H_2 at 760 mm and 300°K, 1.66 cm²/sec. This leads to a general expression $\delta=0.2428T^{3/2}/P_1$ cm²/sec. With the values of M obtained above, it is at once possible to calculate k_s and k_c.

DISCUSSION OF RESULTS

Figure 2 is a plot of f against ρ_c at the four temperatures and for the experiments given in the tables, these being all at an approximately constant flow of H_2 of 3.4×10^{-3} mole/min. The experimental points lie on a smooth curve within 5 percent. This may be considered fair accuracy since f depends upon two independent measurements and ρ_c upon three. The results shown in the tables are also plotted in Fig. 3 where the values of k_c are shown as a function of ρ_c. It is entirely evident from Fig. 3 that at the lower values of ρ_c the reaction rate constant increases. This apparent deviation might be expected since the derivation of the equations assumes that ρ_c remains constant, and this, of course, will be true only at higher values of the concentration of CCl_4. Hence the rate constant as calculated from the theoretical expressions will be constant only for these higher values of ρ_c, and this is seen in Fig. 3. On the basis of a changing and decreasing concentration of CCl_4, we would expect the value of k to decrease, whereas it is actually observed to increase. The explanation is found in the experimental data for those experiments with lowest CCl_4 concentrations, namely Exps. 341, 284, 303 and 322, in which it is seen that the number of mole of HCl found is actually greater than the number of mole of CCl_4 put into the reaction. This evidence would indicate that secondary reactions of the type $H+CCl_3=HCl+CCl_2$ probably enter at these lower concentrations of CCl_4. Exp. 322 in particular shows that the decomposition of CCl_4 must go beyond the CCl_2 stage at these very low concentrations of CCl_4, since in that experiment the amount of HCl found is more than twice as large as the amount of CCl_4 put into the reaction. While the direct evidence for the existence of such reactions is found only at the lowest concentrations of CCl_4 used, it would be expected that they would occur in all those experiments with low concentrations of CCl_4 and would decrease as the ratio of CCl_4/H increases. These considerations suggest that the limit of k_c or k_s is the actual rate constant for the reaction $H+CCl_4=HCl+CCl_3$. A plot of k_s against ρ_c gives an exactly similar figure.

Figure 3 shows that there are some appreciable deviations from a smooth curve, particularly at the higher temperatures. This is not because of the failure of the theoretical equations, but rather because of the quantities used in the calculation. The deviations occur in that region where f approaches unity (cf. Fig. 2) and in that region a small experimental error of 5 percent may give rise to an error in the quantity $(1-f)$,

TABLE V. *The specific rate constants at the various temperatures.*

T, °K	k_c cm³ mole^{-1} sec.$^{-1}$	k_s cm³ mole^{-1} sec.$^{-1}$
294	0.8×10^{10}	1.1×10^{-10}
323	1.3	1.8
348	2.0	2.6
373	2.7	3.5
398	4.0	5.6
423	6.6	9.1
473	11.5	15.1

used in the calculations, of 100 percent or more. This difficulty in the determination of the rate constant may be obviated by changing the design of the apparatus in such a way that f never approaches unity. This change was not made in the present report since one of the principal aims was to determine those conditions which would allow complete conversion of the hydrogen atoms into HCl. Experiments along this line are now in progress.

Experiments exactly similar to those shown in Tables I–IV and in Figs. 1 and 2 were also performed at 50, 75 and 125°. Since the values for f and k show precisely the same dependence upon ρ_c, the data have not been given. In Table V, however, the values of the two constants are given for all seven temperatures as obtained from plots similar to those in Fig. 3. In Fig. 4 the reaction rate constants at all temperatures are plotted as a function of temperature. The curve is the function $k=SZe^{-A/RT}$, S being the steric factor and A the energy of activation, with $Z=3.1\times10^{13}\sqrt{T}$, this latter value being calculated on the usual basis using the values $d_H=1.91$A and $d_{CCl_4}=4.8$A. The values of the constants S and A were obtained from Fig. 5. The straight line in Fig. 5 has been drawn to favor the results at the lower five temperatures and to favor the results calculated on the basis of a spherical flask. This type of weighting, however, does not appreciably alter the values of S and A. The results are $S=0.007$ and $A=3.45$ kcal./mole.

It is difficult to make an estimate of the effect of the difference between the actual flow conditions used in the experiments and those assumed in the theoretical derivation of the equations. The primary simplifying assumption of linear flow, which is quite necessary to avoid extreme complexities in the solution of the equations, has not been entirely fulfilled in the present experiments. Further, the glass surface around the jet may recombine some hydrogen atoms. Both effects would tend to make the values of the specific rate constants somewhat too low. These effects would be approximately the same in all experiments.

In all, over two hundred experiments were performed. Those with lower flow rates of H_2 have been mentioned. Other experiments were

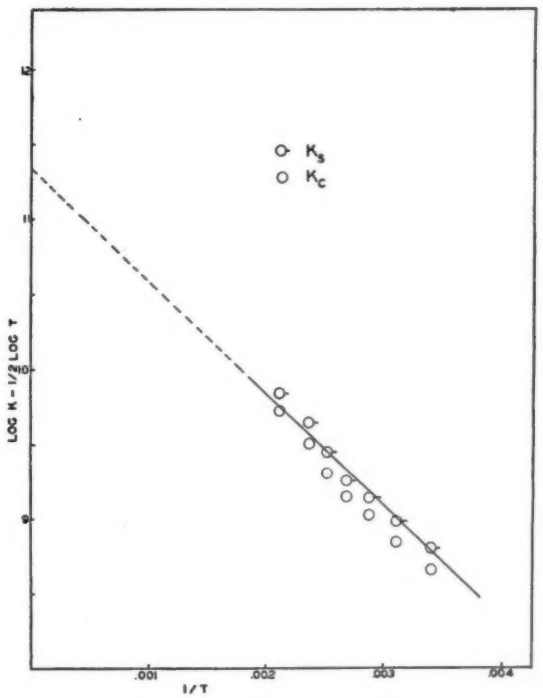

FIG. 5.

carried out in which the concentration of CCl_4 was increased very markedly above the limits of those experiments shown in the tables. In the experiments shown the lower limit of the ratio of CCl_4 : H is approximately 1 : 4, while the upper limit is about 11 : 1. When this ratio, or in general, when the concentration of CCl_4 is increased indefinitely, f suffers a decrease and correspondingly the value of k falls off. For example, when the ratio CCl_4 : H has been increased to 32 : 1, f is found to have decreased by about 17 percent. This decrease is almost certainly because of increased recombination between the calorimeter bob and reaction flask brought about by the increase in pressure. In fact, when the amount of recombination between these two points is calculated from the decrease in f, and plotted against the appropriate function of P_2 and n_{H_2}, the slope obtained agrees with that predicted by Steiner's results[8] within very narrow limits, although the line is displaced by an appreciable amount. This displacement may be partly accounted for by diffusion of hydrogen atoms into the flask, since their concentration is effectively reduced

to zero as they enter, or it might conceivably be due to a constant defect in the calorimetric method of measuring the hydrogen atom concentration.

In a very careful and exhaustive paper by Poole[11] on the general subject of hydrogen atoms, B.S.V.R. Rao points out that Bichowsky and Copeland[12] were in error in their direct determination of the heat of dissociation of the H_2 molecule. In that case there is no longer a direct proof of the correctness of the calorimetric method for estimating hydrogen atom concentrations. It may be pointed out, however, that the agreement between the results of the present paper and the general conclusions of Polanyi,[1] in which the ortho- and parahydrogen conversion was used as a measure of the hydrogen atom concentration, indicates that the calorimetric method is sound. It seems inconceivable that the reaction of hydrogen atoms with CCl_4 should reach the same limit, namely, 100 percent conversion of the hydrogen atoms into HCl in the range 150–200°, as a result of counter-balancing errors.

The previous discussion of the reaction rate and its calculation may obscure the fact that at intermediate CCl_4 concentrations, the absolute value of n_{HCl} is essentially determined by the absolute value of n_H. In other words, the reaction may be used to determine the concentration of hydrogen atoms actually entering into a reaction with good accuracy and little difficulty. The conditions necessary for apparatus of this design are: a pressure of approximately 0.8 mm, a temperature of 150–200° and a CCl_4 : H ratio of about 10 : 1.

[11] H. G. Poole, Proc. Roy. Soc. (London), **163**, 404 (1937).
[12] F. R. Bichowsky and L. C. Copeland, J. Am. Chem. Soc. **50**, 1315 (1928).

DECEMBER, 1938 JOURNAL OF CHEMICAL PHYSICS VOLUME 6

The Calculation of Bond Strengths from Photochemical Evidence

MILTON BURTON[1]
Departments of Chemistry, University of California, Berkeley, California, and New York University, New York, N. Y.
(Received October 14, 1938)

When predissociation manifests itself in polyatomic molecules by a sudden broadening of the rotation lines of a discrete absorption spectrum, a close correspondence is to be expected between the beginning of the predissociation region and the strength of the bond involved. This principle is used to calculate the bond strengths of C—C in ethane, acetaldehyde, acetone and free acetyl (values: 72.1, 93.1, 96.5 and −19.4 kcal., respectively) and of C—H in methane, acetaldehyde ($CH_3\overset{O}{\overset{\|}{C}}-H$), formaldehyde and free formyl (values: 94.8, 114.7, 103.3, and 0.1 kcal., respectively), where the bond strength is defined in reference to the state of the molecule at 0°K. Assuming the validity of the method, the bond strength values given are shown to be accurate within 1.0 kcal. The limitations of the method as well as some implications of the results are indicated.

IT is frequently observed in the absorption spectra of diatomic molecules that within the vibrational bands a sudden blurring occurs because of broadening of the rotational lines as the wave-length is decreased. It has been shown that when predissociation is of this kind in polyatomic molecules a close correspondence may be expected between the beginning of the diffuse region and the strength of the bond ruptured in the attendant photochemical process.[2] This type of spectrum appears to be present in the cases of formaldehyde, acetaldehyde and acetone. It is proposed in this paper to make the assumption

[1] This paper was begun when the writer was a visitor at the University of California and completed at New York University, which is his present address.

[2] Cf. Burton and Rollefson, J. Chem. Phys. **6**, 416 (1938).

that correspondence between the threshold of predissociation and the bond strength is exact in these cases and to deduce therefrom the strength of the C−H and C−C bonds in several other compounds and free radicals. The photochemical data alone, of course, are insufficient for this purpose. Such data must be supplemented by the various thermochemical values already available.

Definition of Bond Strength

The strength of a bond in a particular compound may be defined as the energy difference (per mole) between the lowest energy state of that compound and the (summed) lowest energy state of the products formed by rupture of that bond. It is essential in giving the bond strength to indicate the products. If, for example, we consider the free acetyl radical, CH_3CO, decomposing into CH_3 and normal CO we find a negative bond strength although a positive heat of activation is required for the process of rupture. On the other hand, if we consider the *immediate* products to be CH_3 and CO in the latter of which there are two unpaired electrons, the bond strength comes out to be positive. In ordinary stable compounds the bond strength will very frequently come out to be the same as the energy required to rupture a bond (the energy of activation for the rupture process) but this equality is not required by the definition. It is evident that the bond strength cannot exceed the energy of activation from the lowest state.

Since the bond strength is defined in reference to the lowest energy states it is necessary that the calculation be conducted in reference to the states of the original compound and of the product atoms or free radicals at 0°K, i.e., for particles devoid of translation and in the lowest vibrational and rotational states.

The predissociation process, already referred to, at its threshold is assumed to yield radicals in their lowest rotational and vibrational energy states. It will appear that no correction need be applied to the predissociation data in such compounds to allow for the contribution of energy from available degrees of freedom in the molecule at normal temperatures.

Fundamental Data

In the estimation of these bond strengths the reliability of the following thermochemical data has been assumed.[3]

$$C(gr)+\tfrac{1}{2}O_2\rightarrow CO;\qquad \Delta H=-26.395\pm0.021 \text{ kcal.} \quad (1)[4]$$

$$C(gr)+O_2\rightarrow CO_2;\qquad \Delta H=-94.030\pm0.011 \text{ kcal.} \quad (2)[4]$$

$$2O\rightarrow O_2(g,\ 0°K);\qquad \Delta H=-116.4\pm0.8 \text{ kcal.} \quad (3)[5,6]$$

$$2H\rightarrow (n)H_2(g,\ 0°K);\qquad \Delta H=-102.48\pm0.02 \text{ kcal.} \quad (4)[7]$$

The following heats of formation of substances from their elements in their standard states are given by Bichowsky and Rossini.[8]

$CH_3CHO(g)$	44.0 kcal.	(5)
$HCHO(g)$	28.7±0.01 kcal.	(6)
$H_2O(l)$	68.370±0.010 kcal.	(7)
$CH_4(g)$	18.24±0.10 kcal.	(8)
$C_2H_6(g)$	20.96±0.15 kcal.	(9)

The following values are obtained from the *International Critical Tables.*

$$(CH_3)_2CO(l)+4O_2\rightarrow 3CO_2+3H_2O(l);\qquad \Delta H=-427 \text{ kcal.} \quad (10)$$

$$(CH_3)_2CO(g)\rightarrow (CH_3)_2CO(l);\qquad \Delta H=-7.7 \text{ kcal.} \quad (11)$$

It has already been mentioned that bond strengths are properly defined in relationship to the molecules at 0°K. To perform the calculations the following data were assumed. The basis on which they were calculated is discussed immediately below.

---

[3] Unless otherwise indicated all chemically stable compounds and carbon, C (gr), are to be presumed to be in their standard states. Radicals and atoms are to be presumed to be in the states corresponding to 0°K.

[4] Rossini, J. Chem. Phys. **6**, 569 (1938).

[5] Knauss and Ballard, Phys. Rev. **48**, 796 (1935).

[6] Herzberg, Chem. Rev. **20**, 145 (1937).

[7] Beutler, Zeits. f. physik. Chemie **B29**, 315 (1935).

[8] Bichowsky and Rossini, *The Thermochemistry of the Chemical Substances* (Reinhold Publishing Corp., New York, 1936).

$$H_2(g, 0°K)+\beta\rightarrow H_2; \quad \beta=1.9 \text{ kcal.} \quad (12)$$

$$CH_3CHO(g, 0°K)+\partial\rightarrow CH_3CHO(g); \quad \partial=3.0 \text{ kcal.} \quad (13)$$

$$HCHO(g, 0°K)+\epsilon\rightarrow HCHO; \quad \epsilon=2.5 \text{ kcal.} \quad (14)$$

$$(CH_3)_2CO(g, 0°K)+\mu\rightarrow(CH_3)_2CO(g); \quad \mu=3.3 \text{ kcal.} \quad (15)$$

$$CH_4(g, 0°K)+\phi\rightarrow CH_4; \quad \phi=2.0 \text{ kcal.} \quad (16)$$

$$C_2H_6(g, 0°K)+\psi\rightarrow C_2H_6 \quad \psi=2.6 \text{ kcal.} \quad (17)$$

$$CO(g, 0°K)+\sigma\rightarrow CO; \quad \sigma=2.0 \text{ kcal.} \quad (18)$$

Hydrogen.—Giauque's figures[9] yield 528.1 cal. as the vibrational and rotational energy of $(n)H_2$ at 291.1°K. To this is added $3RT/2$ for translational energy plus RT for the pressure volume term.

Methane.—The specific heat of methane gas is given by Millar,[10] over the range 142–278°K. Straight-line extrapolation on the high side yields a value for $C_p=8.37$ cal./mole/deg. at 291.1°K. At 142°K, $C_p=7.2$. The assumption was made in the calculation that the specific heat from there down fell off linearly to $C_p=5.0$ at 0°K. The heat content of CH_4 at 291.1°K relative to the *gas* at 0°K was then calculated from $\int C_p dT$. Such a method of extrapolation is, of course, extremely rough and subject to theoretical criticism. The defense of the method is simply that the error so introduced is small, probably not exceeding 0.2 kcal.

Ethane.—Kemp and Pitzer give a theoretical curve for the specific heat of ethane extending from ~140°K to high temperatures.[11] As in the case of methane, it is here assumed that C_p equals 5.0 at 0°K and increases linearly to 140°K. The values used for 140°K and 291.1°K were 9.2 and 12.25 cal./mole/deg. respectively.

Carbon monoxide.—Specific heats are available over the range 83°K to 300°K.[12] They range from 7.27 at the lower temperature to 7.01 cal./mole/deg. at 291.1°K. As before, the rough assumption (adequate for the present purpose) was made that at 0°K, $C_p=5.0$, rising linearly to 7.27 at the lower limit of measurement at 83°K.

Acetaldehyde.—Very limited data are available for this compound.[13] C_p/C_v is given as 1.14 at 30°. From this information a value of $C_p=16.3$ cal./mole/deg. at 30°C was calculated. The *very* rough assumption was then made that C_p fell linearly to 5.0 at 0°K and the heat content of gaseous CH_3CHO at 291.1°K relative to the gas at 0°K was calculated on this basis.

Acetone.—The only specific heat data available for this compound are for greater than normal room temperatures.[14] From these data a value of $C_p=17.8$ cal./mole/deg. at 291.1°K was calculated on the assumption that the specific heat fell off linearly to 5.0 at 0°K. This is undoubtedly the least justifiable of the approximations so far made. Again the excuse is that the error is not too large; in this case the resultant relative heat content value is probably not more than ~0.5 kcal. too low.

Formaldehyde.—No data at all are available for this compound. The value of ϵ was simply guessed at by comparison of methane with ethane and of acetaldehyde with acetone.

The following data are not essential to the calculation of bond strengths but are included for the purpose of reference so that those who may be interested in the heats of formation of compounds and radicals from their gaseous atoms may find such information here. In such calculations it is necessary to know the heat of sublimation of graphite and, in turn, the heat of formation of CO from the gaseous atoms. The values favored by Herzberg[6] (and which are by no means uncontested) are

$$C+O\rightarrow CO(g, 0°K); \quad \Delta H=-209.7 \text{ kcal.} \quad (19)$$

and the consequent

$$C(gr, 0°K)\rightarrow C(g, 0°K); \quad \Delta H=125.1 \text{ kcal.} \quad (20)^{14a}$$

[9] Giauque, J. Am. Chem. Soc. **52**, 4816 (1930).
[10] Millar, J. Am. Chem. Soc. **45**, 874 (1923).
[11] Kemp and Pitzer, J. Am. Chem. Soc. **59**, 276 (1937).
[12] *International Critical Tables;* Scheel and Heuse, Ann. d. Physik **40**, 473 (1913).
[13] *International Critical Tables.* Wüllner, Ann. d. Physik **4**, 321 (1878).
[14] *International Critical Tables;* Regnault, Ann. chim. phys. **24**, 342 (1871).
[14a] The value of 124.1 kcal. actually given by Herzberg depends on an earlier value for ΔH in reaction 1 than that given here.

The value for the reaction

$$C(gr, 0°K)+\alpha \rightarrow C(g); \quad \alpha = 0.2 \text{ kcal.} \quad (21)$$

is obtained from Nernst.[15] The value for

$$O_2(g, 0°K)+\gamma \rightarrow O_2; \quad \gamma = 2.1 \text{ kcal.} \quad (22)$$

is obtained by a calculation similar to that used for carbon monoxide.[12]

Calculations

The above data have been used to calculate the heats of formation of various gaseous substances from their *atomic* elements. These values are assembled in Table I together with an indication (in the column labeled "Source of Data") of the method of calculation. The heats of formation given in the column headed C(gr, 0°K) are based on graphite as the reference state for carbon; those given in the column headed C(g, 0°K) are based upon the assumptions of Herzberg already noted. The nature of the approximations is clearly indicated in both cases. As to the relative accuracy of the two sets of data, the former are probably correct within 1.0 kcal. Although the latter may be just as accurate, it is not likely that they will be accepted without opposition by all the workers interested in this field.

For further calculations it is now necessary to use our knowledge of the predissociation limits of CH_3CHO, HCHO and $(CH_3)_2CO$. The discrete absorption spectrum of acetaldehyde extends to

Table I. *Heats of formation of several gaseous substances at 0°K from their atoms.*[a]

Substance	Heat, kcal. per mole		Source of Data	Ref.
	C(gr, 0°K)	C(g, 0°K)		
CH_3CHO	$307.2-2\alpha-2\beta-(\gamma/2)+\delta$ $=305.0$	$557.4+\Sigma^{23}$ $=555.2$	3, 4, 5; 12, 13 21, 22; 20	23
HCHO	$189.4-\alpha-\beta-(\gamma/2)+\epsilon$ $=188.8$	$314.5+\Sigma^{24}$ $=313.9$	3, 4, 6; 12, 14 21, 22; 20	24
CH_4	$223.2-\alpha-2\beta+\phi$ $=221.2$	$348.3+\Sigma^{25}$ $=346.3$	4, 8; 12, 16 21; 20	25
C_2H_6	$328.4-2\alpha-3\beta+\psi$ $=325.1$	$578.6+\Sigma^{26}$ $=575.3$	4, 9; 12, 17 21; 20	26
$(CH_3)_2CO$	$418.1-3\alpha-3\beta-(\gamma/2)+\mu$ $=414.1$	$793.4+\Sigma^{27}$ $=789.4$	2, 3, 4, 7, 10 11; 12, 15; 21, 22 : 20	27

[a] The Σ term in the column headed C(g, 0°K) is the sum of the Greek letter terms in the column headed C(gr, 0°K).

[15] *International Critical Tables;* Nernst, Ann. d. Physik **36**, 395 (1911).

λ3050A[16] at which wave-length corresponding to 93.1 kcal. per mole, the diffuse spectrum begins. This value can be taken as the strength of C−C bond in CH_3CHO.[2] There is indirect evidence for slight free radical production[17] at wave-lengths of 3130A and less but this can be attributed[2] to the contribution from available vibrational degrees of freedom of the acetaldehyde molecule.[18] It is a reasonable assumption that the time required for the transfer of such energy is so long as to yield a discrete absorption spectrum and that the predissociation limit would be practically the same in a molecule devoid of vibrational or rotational energy. We therefore write

$$CH_3CHO(0°K) \rightarrow CH_3+HCO; \quad \Delta H = 93.1 \text{ kcal.} \quad (28)$$

Similarly the sharp line absorption spectrum of formaldehyde becomes diffuse at λ2750A[19] ($\approx$103.3 kcal.). There is fairly good evidence [2, 20] that the light absorbed in the diffuse region results in the formation of free hydrogen atoms. We therefore write

$$HCHO(0°K) \rightarrow H+HCO; \quad \Delta H = 103.3 \text{ kcal.} \quad (29)$$

In acetone, discrete absorption fades out at λ2945A[21] ($\approx$96.5 kcal.). The evidence[22] indicates that the decomposition in the diffuse region is exclusively via a free radical mechanism, whereas in the discrete region ultimate molecules are formed in the primary act. We write

$$CH_3COCH_3(0°K) \rightarrow CH_3+CH_3CO; \quad \Delta H = 96.5 \text{ kcal.} \quad (30)$$

The heats of formation of some free radicals shown in Table II are calculated from these three equations and from the data given in Table I. As before, the method of calculation is indicated in the column titled "Source of Data."

[16] Schou, J. Chem. Phys. **27**, 27 (1929); Leighton, Chem. Rev. **17**, 393 (1935).
[17] Blacet and Roof, J. Am. Chem. Soc. **58**, 278 (1936). Cf. Rollefson, J. Phys. Chem. **41**, 259 (1937), Burton, ibid. **41**, 322 (1937).
[18] Cf. Franck and Herzfeld, J. Phys. Chem. **41**, 97 (1937).
[19] Henri and Schou, Zeits. f. Physik **49**, 774 (1929).
[20] Patat, Zeits. f. physik. Chemie **B25**, 208 (1934); Löcker and Patat, ibid. **B27**, 431 (1934).
[21] Noyes, Duncan and Manning, J. Chem. Phys. **2**, 717 (1934).
[22] Spence and Wild, J. Chem. Soc. 352 (1937).

It is now possible to calculate several bond strengths from the data thus far given. The results of such calculation are assembled in Table III. Assuming the validity of the method, and taking into account the fact that the errors in the approximations (the Greek-letter terms) cancel each other to a large extent, it follows that the bond strengths given are accurate within 1 kcal.

TABLE III. *Bond strengths.*

BOND	COMPOUND OR FREE RADICAL	STRENGTH, KCAL./MOLE	SOURCE OF DATA	REF.
C–C	C_2H_6	$72.4-\beta+\psi-2\partial+2\epsilon=72.1$	26, 32	34
	CH_3CHO	93.1	28	35
	CH_3COCH_3	96.5	30	36
	CH_3CO	$-18.2-\beta-\sigma+\mu-\partial+\epsilon=-19.4$	1, 32, 33	37
C–H	CH_4	$95.2-\beta+\phi-\partial+\epsilon=94.8$	25, 32	38
	$CH_3C(=O)-H$	$114.5+2\partial-\mu-\epsilon=114.7$	23, 33	39
	HCHO	103.3	29	40
	HCO	$1.5-\beta-\sigma+\epsilon=0.1$	1, 31	41

DISCUSSION

Significance of the bond strength values

In one sense there is nothing new in the ideas suggested by Table III. We are already accustomed to the notion that there is some difference in the strength of a particular bond in different types of compounds.[23] On the other hand, it is not usual to have in one table a listing for the C–C bond ranging from −19.4 kcal. (for CH_3CO) to 96.5 kcal. (for CH_3COCH_3). However, these two values are not really as far apart as they seem. The CO formed in the decomposition of CH_3CO[37] does not have the same electron configuration as the CO in the CH_3CO radical. In fact, it seems that approximately 100 kcal. are liberated in the conversion of CO from a free radical (with two unpaired electrons) to a stable molecule (with all electrons paired).[24] The potential energy relationships involved are shown in Fig. 1. Curve *a* represents the normal repulsive curve between a methyl radical and an unactivated carbon monoxide molecule. At values of r approaching infinity the potential energy of this system is ∼100 kcal. less than that of the methyl plus activated carbon monoxide (CO*) system. Thus, the strength of the C–C bond in the CH_3CO relative to CH_3+CO^*, is ∼100−19.4 or ∼80.6 kcal., a value more consistent with its strength in such compounds as ethane.

An estimate as to the value of A in Fig. 1 may be gleaned from the fact[22, 25] that although CH_3CO is stable at room temperatures it is apparently completely unstable above 60°. If we assume that the rate of the decomposition $CH_3CO \rightarrow CH_3+CO$ is 10^6 to 10^{12} times greater at 60° than at 0°, it appears that the energy of activation of the decomposition (i.e., A) is 4.2 to 8.4 kcal., which may be compared with Rice and Herzfeld's estimate[26] of ∼10 kcal.

The potential energy relationships for HCO are similar to those for CH_3CO. However, the strength of the H–C bond (relative to H+CO*) is much greater than that of the C–C bond (relative to CH_3+CO^*). The value of A in this case, estimated from the great stability of HCO,[27] appears to be rather large. On the other hand, the readiness with which H and CO combine,[28] indicates that $A-0.1$ kcal. may not be very great. It is possible, however, to arrive at a false estimate from these latter data, for the combination reaction is probably a three-body process.

TABLE II. *Heats of formation of some free radicals from their atoms.*

SUBSTANCE	HEAT, KCAL./MOLE: C(gr, 0°K)	HEAT, KCAL./MOLE: C(g, 0°K)	SOURCE OF DATA	REF.
HCO	$86.1-\alpha-\beta-(\gamma/2)+\epsilon=85.5$	$211.2+\overset{31}{\Sigma}=210.7$	24, 29	31
CH_3	$128.0-\alpha-\beta+\partial-\epsilon=126.3$	$253.1+\overset{32}{\Sigma}=251.4$	23, 28, 31	32
CH_3CO	$193.7-2\alpha-2\beta-(\gamma/2)+\mu-\partial+\epsilon=191.0$	$443.9+\overset{33}{\Sigma}=441.2$	27, 30, 32	33

[23] Cf. Kistiakowsky, J. Phys. Chem. **41**, 175 (1937).
[24] Cf. Norrish, Trans. Faraday Soc. **30**, 103 (1934).

JUSTIFICATION OF BOND STRENGTH VALUES

The values of 72.1 kcal. for the bond strength of C–C in ethane and of 94.8 kcal. for C–H in methane are quite in line with those generally accepted at the present time.[14] They are to be compared with the values of 72–76 and ∼95 kcal., respectively, employed by Rice and Herzfeld in their calculation of the chain decomposition of

[25] Glazebrook and Pearson, J. Chem. Soc. 567 (1937).
[26] Rice and Herzfeld, J. Am. Chem. Soc. **56**, 284 (1934).
[27] Cf. Burton, J. Am. Chem. Soc. **58**, 1655 (1936); J. Phys. Chem. **41**, 322 (1937); J. Am. Chem. Soc. **60**, 212 (1938).
[28] Cf. Frankenburger and co-workers, Zeits. f. Elektrochem. **36**, 757 (1930).

ethane. It is interesting that the method of calculation employed in this paper involves the assumption of three values, for C−C in acetaldehyde (35) and acetone (36) and for C−H in formaldehyde (40), which might be subject to criticism. Their best justification is that they are consistent with the C−C value in C_2H_6 and with the C−H value in CH_4.

The values for C−C in acetaldehyde and acetone disagree with those determined by Rice and Johnston[29] from mirror experiments at ~1100°K. Their values are 69.4 and 70.9 kcal., respectively. It is possible that similar experiments conducted at lower temperatures might yield information as to the cause of the disagreement with the values here quoted. Nevertheless, it is interesting to see under what conditions their values may be made to fit the values of 72.1 kcal. for C−C in ethane and 94.8 kcal. for C−H in methane. Simple calculation shows that a value of ~80 kcal. for the C−H bond in formaldehyde is all that is necessary. However, it is apparent that this is an extraordinarily low value for the strength of the C−H bond in a stable compound, particularly in view of the assumed strength of the C−C bond in acetaldehyde. Patat and Sachsse,[30] for example, have assumed the much higher value of 92 kcal.

One interesting result of the view of the bond strengths in HCHO, CH_3CHO and CH_3COCH_3 presented in this paper is that it would entail a much lower steady-state concentration of free atoms and radicals in the pyrolyses of those compounds. This result would be consonant with the findings of Patat and Sachsse, who used the

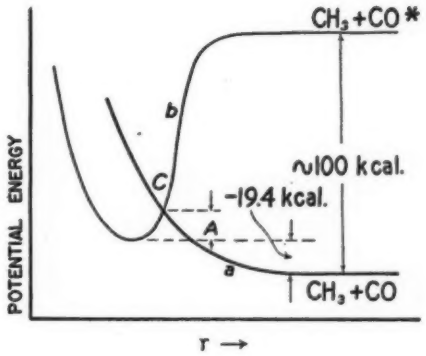

FIG. 1.

para-ortho hydrogen conversion method for the counting of free radicals in the steady state.[30]

Limitations of the method

This method of calculating bond strengths can only be used in those cases in polyatomic molecules where the predissociation process manifests itself in a sudden broadening of the rotation lines in a clearly defined portion of the spectrum. Furthermore, it is essential to know the chemical process involved. Thus, in the case of benzene, predissociation is observed but we are not informed as to the process involved (there is no net yield of products) and the spectrum itself[31] is not suitable to our purpose.

In the case of benzaldehyde, although the products of the photolysis are well known the diffuse spectrum appears sharply at λ2428A after a transparent region extending from 2599 to 2428A.[32] This type of spectrum is unsuited for these calculations.

[29] F. O. Rice and W. R. Johnston, J. Am. Chem. Soc. **56**, 214 (1934).
[30] Patat and Sachsse, Zeits. f. physik. Chemie **B31**, 105 (1935).
[31] Cf. Henri, J. de phys. et rad. (6) **3**, 181 (1922).
[32] Henri, *The Structure of Molecules*, P. Debye, Editor (Blackie and Son, Ltd. London, 1932), p. 124.

The Optical Activity of Secondary Butyl Alcohol

EVERETT GORIN, JOHN WALTER AND HENRY EYRING
Frick Chemical Laboratory, Princeton, New Jersey

(Received September 17, 1938)

A calculation of the optical activity of secondary butyl alcohol is presented based upon a one-electron model. The chromophoric electron is considered to be one of the nonbonding electrons on the oxygen atom. This electron is considered to be moving in a field of the other nuclei and electrons considered as charge distributions. The fields of the other electrons are obtained from the Slater type eigenfunctions for the various atoms. This amounts to a rough solution of the Hartree approximation for the chromophoric electron. The results obtained are somewhat larger or somewhat smaller than the experimental value depending on the exact orientation of the groups in their rotation about single bonds. The assignment of an absolute configuration in these calculations follows provided the exact orientation of the rotating groups is known. The orientations which we consider most likely lead to an assignment of the absolute configuration in agreement with that of Kuhn.

INTRODUCTION

IF the electric moment $\mathbf{p}$ of a molecule is given by

$$\mathbf{p}=\alpha\mathbf{E}'-(\beta/c)\dot{\mathbf{H}}, \tag{1}$$

where α, $\mathbf{E}'$, $\dot{\mathbf{H}}$, and c, are the polarizability, effective electric field on the molecule, time derivative of the magnetic field, and the velocity of light, respectively, then the rotatory power of the medium is given by

$$\varphi=\frac{16\pi^3 N_1\beta}{\lambda^2}\frac{n^2+2}{3}, \tag{2}$$

where N_1, λ, and n are the number of molecules per cc, the wave-length, and the index of refraction, respectively. Using quantum mechanics, Rosenfeld[1] obtained the relationship

$$\beta_a=\frac{c}{3\pi\nu h}\sum_b \frac{\nu Im\{(a|\mathbf{p}|b)\cdot(b|\mathbf{m}|a)\}}{\nu_{ba}^2-\nu^2}, \tag{3}$$

where ν, ν_{ba}, $(a|\mathbf{p}|b)$, $(b|\mathbf{m}|a)$, are the frequency of the light used, the frequency corresponding to the transitions between levels b and a, the matrix component for the electric moment and the matrix component for the magnetic moment for the transition from level a to b, respectively. Finally we have

$$\beta=\sum_a p_a\beta_a, \tag{4}$$

where p_a is the probability of a molecule lying in the state a. For most substances the number of molecules in any but the lowest electronic level may be neglected, but unless the molecule is rigid it is necessary to average over the various possible internal configurations. As written, both β_a and β are already averaged over all possible orientations with respect to the polarized beam passing through the material. Condon[2] has given a detailed derivation of these equations in his presentation of the theories of optical rotatory power. In any quantum mechanical treatment of optical activity it is convenient to start with (3). Kirkwood[3] has based his interesting theory on this equation and the same is true of a treatment by Condon, Altar, and Eyring.[4] These latter authors showed that a single electron moving in a field of suitable dissymmetry gives rise to optical activity. Previous theories of optical activity, aside from the first treatment by Drude, are based on coupled oscillators. Drude's model has been rejected by Born and Kuhn.[5] Kuhn's proof[6] that one electron cannot show optical activity on the basis of classical theory requires the further assumption that the electronic displacement be infinitesimal, as he has recently emphasized.[7] For the finite displacements always involved in actual transitions, the carrying over of the quantum mechanical formula to the clas-

[1] Rosenfeld, Zeits. f. Physik **52**, 161 (1928).

[2] Condon, Rev. Mod. Phys. **9**, 432 (1937).
[3] Kirkwood, J. Chem. Phys. **5**, 479 (1937).
[4] Condon, Altar, and Eyring, J. Chem. Phys. **5**, 753 (1937).
[5] See: Lowry, *Optical Rotatory Power*, p. 372.
[6] Kuhn, Zeits. f. physik. Chemie **B20**, 235 (1933).
[7] Kuhn, Naturwiss. **19**, 289 (1938).

sical case by the use of the correspondence principle yields optical activity for one electron.[3] The necessary condition for optical activity to result from a single electron in a properly dissymmetric field is thus that finite displacements be involved. Finite displacements always occur in actual molecules and are automatically considered in quantum mechanics, but were ordinarily not considered in classical theory.

The chief concern of Condon, Altar and Eyring[4] was to demonstrate one-electron optical activity. A simple three-dimensional harmonic oscillator in a perturbing field was chosen because it permitted a comparatively simple calculation. The perturbation considered was that which arose by assigning such charges to the various atoms as would account for the known dipole moments associated with the bonds. The contributions of these atomic charges to the field in which the chromophoric electron moved was then expressed in the usual series expansion and only the leading terms retained. Although in certain cases the results obtained are of the order of magnitude of those found experimentally, this was not true in the case of secondary butyl alcohol where the calculated value was about one five-hundredths of that found experimentally.

A rigorous application of Eq. (3) requires a knowledge of the exact eigenfunctions for secondary butyl alcohol in its normal and excited states. Unfortunately these are not available at the present time and one is forced to use approximate models. Kuhn has extended Born's coupled oscillator treatment and has treated secondary butyl alcohol. Boys[8] has proposed a model consisting of four isotropic polarizable groups situated at the vertices of an irregular tetrahedron. The rotation of the plane of polarization is assumed to arise from the way the scattered secondary wavelets from each group reinforce one another. Such a model can at most apply at very long wave-lengths since it does not take explicit account of the various electronic transitions involved, which dispersion data show are intimately connected with optical activity. Kirkwood[3] has improved upon Boys' model by taking into account the anisotropy of the component groups and by employing a quantum mechanical treatment based upon Eq. (3). He treats the OH groups, however, as isotropic, which our results show to be quite unjustifiable. Kirkwood's treatment has the merit of summing over the contributions of all transitions involved in the four groups surrounding the central carbon. However, Kuhn[7] * concludes from a survey of the experimental rotatory dispersion data that in the case of secondary butyl alcohol the sign and magnitude of the rotation in the visible is controlled by the transitions nearest the visible which in this case are associated with the hydroxyl group. It thus seems feasible to center our attention on the transitions in the hydroxyl group. This is an important simplification of the problem and forms the basis for our subsequent treatment.

A One-Electron Model

In actual atomic transitions, although the quantum number of only one electron is usually represented as changing, the orbits of the remaining electrons are modified to a certain extent. This may be thought of as due to a change in the screening constant of the electron which jumps and also of the other electrons.[9] Optical transitions involving an electron outside a closed shell can be treated, however, as a one-electron transition to a good approximation.[10]

We have considered that the transitions in the OH group involve the nonbonding electrons on the oxygen atom. The configurations of the normal and excited states in the C−O−H part of the molecule can be represented as:

Normal State		$(2t_i \cdot 2pz')$	$(1s \cdot 2py')$	$(2px \cdot 2px)$
Excited States	I	$(2t_i \cdot 2pz')$	$(1s \cdot 2py')$	$(2py \cdot 2px)$
	II	$(2t_i \cdot 2pz')$	$(1s \cdot 2py')$	$(2pz \cdot 2px)$
	III	$(2t_i \cdot 2pz')$	$(1s \cdot 2py')$	$(3s \cdot 2px)$

The first, second, and third parentheses represent the electrons forming the C−O bond, the O−H bond, and the two nonbonding electrons on the oxygen, respectively. The z direction lies along the O−C bond. The y direction lies in the C−O−H plane and the x direction is perpendicular to this plane. Due to the distortion of the C−O−H valence angle from ninety degrees, the

[8] Boys, Proc. Roy. Soc. London **A144**, 655, 675 (1934).

* Levene and Rothen (*Gilman Organic Chemistry*, Vol. II, p. 1801) do not agree with this conclusion. In any case, if other electrons need be considered, their contributions can be simply added to the value already calculated.

[9] Slater, Phys. Rev. **34**, 57 (1930).

[10] McDougall, Proc. Roy. Soc. **A138**, 550 (1932).

TABLE I.

	O	H_1	H_2	H_3	H_4	H_5	H_6	H_7	H_8	H_9	H_0	C_1	C_2	C_3	C_4
x	0	1.85	0.96	−0.92	−0.92	0.92	−0.92	0.92	0.0	0.0	1.85	1.24	0.0	0.0	0.0
y	0	1.08	1.60	0.53	−1.60	−1.60	−3.05	−3.05	−1.85	0.94	0.04	0.77	0.0	−1.43	−2.40
z	0	1.08	2.55	1.80	2.55	2.55	0.78	0.78	−0.18	−0.24	2.55	1.94	1.42	1.94	0.76

function $2pz'$ is nearly equal to $2pz$ but is a linear combination with $2py$. $2py'$ is the corresponding orthogonal linear combination.[11] $2t_i$ is the carbon tetrahedral bonding eigenfunction.

For the usually measured wave-lengths those transitions will be most important which require the least energy. The bonding electrons are more tightly held than the nonbonding electrons, as is shown by the fact that in H_2 it requires about two more volts to ionize an electron than in the hydrogen atom, and over a volt more to reach the first resonance potential than does the hydrogen atom. On the other hand, the nonbonding electrons of oxygen are a little more easily ionized than in the free atom as is shown by the fact that the ionization potential of water is at least a half volt less than in the oxygen atom.[12] The transition $^3P \rightarrow {}^3S$ in the oxygen atom requires about 9.0 volts, while judging from the dispersion data on alcohols the optically active absorption band lies at about 7.5 volts above the normal state.[13] The fact that the measured excited level is lower in the alcohols than in the oxygen atom indicates that a nonbonding electron is involved. This conclusion is somewhat different from that of Kuhn, who interprets the greater polarizability of the CH_3OH molecule in the C−O−H plane to mean that in his treatment the important transition of the three dimensional oscillator lies in the C−O−H plane.[14] In our treatment the eigenfunction is initially nearly odd, and ends up by being nearly even, with respect to the C−O−H plane.

Our procedure consists in obtaining a rough solution to the Hartree equation for the nonbonding oxygen electron moving in the Hartree field of the rest of the molecule.

$$\nabla^2\psi+\frac{h^2}{8\pi^2 m}\Big((E-V(r)-\sum_i\sum_k\Big[e^2\int\frac{\varphi_{ik}^2}{r_{ik}}d\tau_k-\frac{ze^2}{r_i}\Big]\Big)\psi=0. \quad (5)$$

$V(r)$ is the potential field for the oxygen atom and was assumed to be hydrogen-like for the various series electrons. The values of Z were 2 for the s and p series, and 1.5 for the d series. These values of Z were necessary if one is to obtain the right ionization and resonance potentials, and still neglect all changes in the remaining electrons. The first resonance potential was chosen to correspond to that in alcohol and the separation between the $3s$ and $3d$ levels, although unknown for alcohols, was taken from the value in atomic oxygen.

The last set of terms in Eq. (5) corresponds to the potential of the atomic kernels, while the next to the last set arises from the electrostatic potential of the electron clouds around each kernel. The index i refers to the kernels and the index k to the electrons. The eigenfunctions φ_{ik} were taken to be the ordinary atomic functions for the hydrogens and the functions for the carbon valence electrons were taken after Slater with the difference that the two $1s$ electrons were assumed to screen the nucleus perfectly. This slight modification somewhat simplified the calculations without materially affecting the results. The carbon atom in its ^5S valence state is spherically symmetric so that the potential energy is simply a function of the distance r from the carbon kernel.

$$V_C=-\frac{4e^2}{a_0}e^{-2.95r_i/a_0}\Big[\frac{1.070r_i^2}{a_0^2}+2.175\frac{r_i}{a_0}+2.213+\frac{a_0}{r_i}\Big].$$

[11] We wish to thank Professor R. S. Mulliken for a very helpful discussion in connection with the assignment of possible transitions.

[12] Smyth, Rev. Mod. Phys. **3**, 347 (1931).

[13] Lowry, *Optical Rotatory Power*, p. 265; Levene and Rothen, J. Biol. Chem. **116**, 209 (1936).

[14] Kuhn, Zeits. f. physik. Chemie **B31**, 23–57 (1935).

The potential function of the hydrogen atom is likewise spherically symmetric.

$$V_H = -\frac{e^2}{a_0} e^{-2r_i/a_0}\left[1+\frac{a_0}{r_i}\right].$$

r_i is the distance from the ith atom and a_0 is the Bohr radius. The exact configuration first investigated was that of Condon, Altar and Eyring.[4] The coordinates are given in Table I since it was convenient to use a coordinate system in which the signs of the y and z coordinates were reversed and also to correct a misprint in the original table. We will refer to this as orientation I. (In general we propose to use the word orientation for an exact configuration in which the relative positions of all the atoms are specified and use the word configuration in the usual sense to specify merely the general positions of the groups with respect to the asymmetric carbon.) It corresponds to the following absolute configuration. Dotted lines indicate groups below the plane.

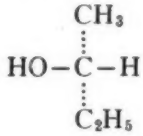

The carbon atoms are numbered in order along the chain with the O−H group on C_2. Hydrogen atoms 0, 1, 2 are on C_1, 3 is on C_2, 4, 5 are on C_3, 6, 7, 8 on C_4, while H_9 is the hydrogen of the hydroxyl group.

Orientation II corresponds to a small rotation of the hydroxyl hydrogen such that C_2, O, H_9, and H_3 become coplanar. Thus all the atoms have the same coordinates as in orientation I except H_9 which has the coordinates (−0.82, +0.47, −0.24). In addition the case of free rotation of the O−H group was considered.

The last two terms in Eq. (5), which we will indicate by the symbols H' and H'', were treated by a perturbation method. H' refers to the perturbations due to the carbon and hydrogen atoms bound to the oxygen, while H'' refers to the perturbations due to the remaining atoms. The unperturbed normal state is given by the hydrogen-like eigenfunction

$$\psi_1 \equiv \psi_{2pz} = \frac{1}{4(2\pi)^{\frac{1}{2}}}\left(\frac{2}{a_0}\right)^{\frac{1}{2}} \frac{2r}{a_0} \exp\left(-\frac{r}{a_0}\right)\left(\frac{x}{r}\right).$$

The unperturbed excited levels are given by the three hydrogen-like functions which are even with respect to reflection in the C−O−H plane

$$\psi_2 \equiv \psi_{3s} = \frac{1}{81(3\pi)^{\frac{1}{2}}}\left(\frac{2}{a_0}\right)^{\frac{1}{2}}\left(27-\frac{36r}{a_0}+8\left(\frac{r}{a_0}\right)^2\right) \times\exp\left(-\frac{2r}{3a_0}\right),$$

$$\psi_3 \equiv \psi_{3py} = \frac{2^{\frac{1}{2}}}{81\pi^{\frac{1}{2}}}\left(\frac{2}{a_0}\right)^{\frac{1}{2}}\left(\frac{12r}{a_0}-4\left(\frac{r}{a_0}\right)^2\right) \times\exp\left(-\frac{2r}{3a_0}\right)\left(\frac{y}{r}\right),$$

$$\psi_4 \equiv \psi_{3pz} = \frac{2^{\frac{1}{2}}}{81\pi^{\frac{1}{2}}}\left(\frac{2}{a_0}\right)^{\frac{1}{2}}\left(\frac{12r}{a_0}-4\left(\frac{r}{a_0}\right)^2\right) \times\exp\left(-\frac{2r}{3a_0}\right)\left(\frac{z}{r}\right).$$

The odd function ψ_{3px} was not considered since to include it would considerably complicate the calculation without giving an important contribution to the optical activity. The functions ψ_2, ψ_3, and ψ_4 all correspond to the same energy. The degeneracy is removed by the perturbations of the term in brackets. The usual proper linear combination is determined by solving the usual set of linear equations which lead to the secular determinant

$$\begin{vmatrix} H_{22}-W & H_{23} & H_{24} \\ H_{32} & H_{33}-W & H_{34} \\ H_{42} & H_{43} & H_{44}-W \end{vmatrix} = 0 \qquad (6)$$

$$H_{ij} = \int \psi_i H' \psi_j d\tau.$$

We thus obtain three eigenfunctions

$$\psi_n' = c_{n2}\psi_2 + c_{n3}\psi_3 + c_{n4}\psi_4, \qquad (7)$$

where n goes from 1 to 3. After removal of the degeneracy these functions are combined by the perturbation H' with the functions $\psi_5 \equiv \psi_{2py}$ and $\psi_6 = \psi_{2pz}$. These wave functions are then

$$\psi_n'' = \psi_n' + c_{n5}\psi_5 + c_{n6}\psi_6,$$

where $c_{n5} = \dfrac{\int \psi_n' H' \psi_5 d\tau}{E_n - E_5}$, $\quad c_{n6} = \dfrac{\int \psi_n' H' \psi_6 d\tau}{E_n - E_6}$

and where $E_5=E_6=E_1$ is the energy of the normal state and E_n is the energy of the unperturbed eigenfunctions ψ_2, ψ_3, or ψ_4. The functions ψ_n'' are all even with respect to the C−O−H plane and consequently transitions to them would not be optically active. If however, we consider linear combinations of these functions with the odd functions $\psi_7\equiv\psi_{3dxz}$ and $\psi_8\equiv\psi_{3dxy}$, the resulting wave functions χ_1, χ_2, and χ_3 lead to optically active transitions from the ground state.

$$\chi_n=c_{n2}\psi_2+c_{n3}\psi_3+c_{n4}\psi_4+c_{n5}\psi_5+c_{n6}\psi_6+c_{n7}\psi_7+c_{n8}\psi_8,$$

where n goes from 1 to 3 and

$$c_{ni}=\frac{\int\psi_n'H''\psi_i d\tau}{E_n-E_i},$$

where $i=7$ or 8. The f, g, and higher functions are omitted since they do not contribute to the optical activity. The reason for omitting the higher d levels will be discussed later.

The perturbation H'' acting upon the eigenfunction for the normal state may be omitted to a good approximation. Considering only the perturbation H' we have for ψ_1'

$$\psi_1'=\psi_1+a_9\psi_9,$$

where $\psi_9\equiv\psi_{3pz}$ and

$$a_9=\int\psi_1H'\psi_9 d\tau/(E_1-E_9).$$

The matrix components for magnetic and electric moments calculated with these wave functions are

$$(b|\mathbf{m}|a)\equiv(\chi_n|\mathbf{m}|\psi_1')=\frac{eh}{4\pi mci}[(c_{n6}\mathbf{j}-c_{n5}\mathbf{k})+(c_{n4}\mathbf{j}-c_{n3}\mathbf{k})], \quad (8)$$

$$(b|\mathbf{p}|a)\equiv(\chi_n|\mathbf{p}|\psi_1')=ea_0\{D\{c_{n7}\mathbf{j}+c_{n8}\mathbf{k}\}+Fa_9\{c_{n7}\mathbf{j}+c_{n8}\mathbf{k}\}+Cc_{n2}\mathbf{i}\}, \quad (9)$$

where $D=\int\psi_{3dxy}y\psi_{2pz}d\tau$; $F=\int\psi_{3dxy}y\psi_{3pz}d\tau$; $C=\int\psi_{3s}x\psi_{2px}d\tau$.

The operators m and p are

$$\mathbf{m}=\frac{eh}{4\pi mci}\left\{\left(y\frac{\partial}{\partial z}-z\frac{\partial}{\partial y}\right)\mathbf{i}+\left(z\frac{\partial}{\partial x}-x\frac{\partial}{\partial z}\right)\mathbf{j}+\left(x\frac{\partial}{\partial y}-y\frac{\partial}{\partial x}\right)\mathbf{k}\right\}$$

$$\mathbf{p}=e(x\mathbf{i}+y\mathbf{j}+z\mathbf{k}).$$

Substituting Eqs. (8) and (9) in Eq. (3) we get for the rotatory parameter

$$\beta=\frac{e^2a_0}{12\pi^2m}\frac{1}{\nu_n^2-\nu^2}\{D(c_{n5}c_{n8}-c_{n6}c_{n7})+a_9(c_{n3}c_{n7}-c_{n4}c_{n8})+Fa_9(c_{n5}c_{n8}-c_{n6}c_{n7})+Fa_9^2(c_{n3}c_{n8}-c_{n4}c_{n7})\}, \quad (10)$$

$$\nu_n=\frac{E_2-E_1+W_n}{h},$$

where W_n is the nth root of the secular Eq. (6).

The justification for omitting d levels with principal quantum number greater than 3 is that the integral D corresponding to the electric moment for a transition from the state $2p$ to nd falls off very rapidly as n becomes greater than 3.

The evaluation of the matrix components involved the usual transformation to elliptic coordinates

$$u=(r_a+r_b)/R,\quad v=(r_a-r_b)/R,$$

$$r_a=\frac{R}{2}(u+v),\quad r_b=\frac{R}{2}(u-v),\quad z_a=\frac{R}{2}(1+uv),$$

$$d\tau=(R^3/8)(u^2-v^2)du\,dv\,d\varphi$$

with the limits of integration

$$-1\leq v\leq 1,\quad 1\leq u\leq\infty,\quad 0\leq\varphi\leq 2\pi.$$

The potentials of the hydrogen and carbon atoms become

$$V_H=-\frac{e^2}{a_0}\exp\left(-\frac{R(u-v)}{a_0}\right)\left(1+\frac{2a_0}{R(u-v)}\right),$$

$$V_C=-\frac{4e^2}{a_0}\exp\left(-\frac{1.475R}{a_0}(u-v)\right)\times\left\{\frac{1.07}{4}\left(\frac{R}{a_0}\right)^2(u-v)^2+\frac{2.175}{2}\left(\frac{R}{a_0}\right)+2.213+\frac{2a_0}{R(u-v)}\right\}$$

where R is the distance from the oxygen atom to the atom under consideration. c_{n7} may be written, for example, in terms of its component integrals as follows:

$$c_{n7}=\frac{\sum_i\sum_j\int(c_{n2}\psi_2+c_{n3}\psi_3+c_{n4}\psi_4)(V_{Hi}+V_{Cj})\psi_7}{E_n-E_7}; \quad (11)$$

where the indices i and j refer to the various hydrogen and carbon atoms, respectively. Take for example the integral $\int\psi_2 V_{Hi}\psi_7 d\tau$ (12) contributing to c_{n7}. We write the radial parts of ψ_2 and ψ_7 in elliptic coordinates

$$\psi_2\equiv\psi_{3s}=\frac{1}{81(3\pi)^{\frac{1}{2}}}\left(\frac{2}{a_0}\right)^{\frac{3}{2}}\left(27-18\left(\frac{R_i}{a}\right)(u+v)+2\left(\frac{R_i}{a_0}\right)^2(u+v)^2\right)\exp\left(-\frac{R_i(u+v)}{3a_0}\right),$$

$$\psi_7\equiv\psi_{3dxz}=\frac{(2)^{\frac{1}{2}}}{324\pi^{\frac{1}{2}}}\left(\frac{1.5}{a_0}\right)^{\frac{3}{2}}(1.5)^2\left(\frac{R_i}{a_0}\right)^2(u+v)^2\times\exp\left(-\frac{1.5}{6}\frac{R_i}{a_0}(u+v)\right)\frac{xz}{r^2}.$$

The factor xz/r^2 in ψ_7 refers to the angular part in the original polar coordinates. It is now convenient to transform to a new set of coordinates such that the new z axis lies along the line joining the two atomic centers. The old coordinates in terms of the new are then given by

$$x=\alpha_1x'+\beta_1y'+\gamma_1z',$$
$$y=\alpha_2x'+\beta_2y'+\gamma_2z',$$
$$z=\alpha_3x'+\beta_3y'+\gamma_3z'.$$

γ_1, γ_2, and γ_3 are the direction cosines of the new z axis in the old coordinate system and are equal to X_i/R_i, Y_i/R_i, and Z_i/R_i, respectively. X_i, Y_i, and Z_i are the coordinates of the ith atom in the initial coordinate system, since the oxygen atom is at the center of coordinates. Since the directions of the new x and y axes are immaterial, the α's and β's can be left arbitrary, and as we shall see do not enter into the final expression for the integral. By symmetry considerations only even powers of x' and y' contribute. Therefore the contributing terms in xz are

$$xz=\alpha_1\alpha_3x'^2+\beta_1\beta_3y'^2+\gamma_1\gamma_3z'^2.$$

Since the integral with x'^2 is the same as with y'^2 and since $\alpha_1\alpha_3+\beta_1\beta_3+\gamma_1\gamma_3=0$, this can be simplified to $xz=\gamma_1\gamma_3(z'^2-x'^2)$. The integral (12) can then be written in the form

$$I_{12}=\gamma_1\gamma_3\int F(u,v)\exp(-au-bv)(z'^2-x'^2)dudv.$$

$F(u,v)$ is a polynomial in u and v and consequently the integral can be easily evaluated in terms of the elementary integrals

$$A_m=\int_1^\infty u^m\exp(-au)du,$$

$$B_n=\int_{-1}^1 v^n\exp(-bv)dv.$$

The values of the various integrals in electron volts contributing to c_{n7} and c_{n8} are given in Table II for various distances. The calculation of the coefficients c_{n7} and c_{n8} involve a knowledge of the coefficients c_{n2}, c_{n3}, and c_{n4} obtained from a solution of the secular Eq. (6). The matrix components H_{mn} in (6) are computed in the way described for I_{12}. Their values along with those of the three roots of the determinant in electron volts and the corresponding three sets of coefficients are given in Table III.

The coefficient a_9 in Eq. (10) turned out to be very small so that all but the first term in (9) could be neglected. The contributions to β_α due to transitions to the three levels χ_1, χ_2, and χ_3, corresponding to W_1, W_2, and W_3, are listed below:

$$\beta_{\alpha_1}=2.18\times10^{-35},$$
$$\beta_{\alpha_2}=-1.02\times10^{-35},$$
$$\beta_{\alpha_3}=-3.86\times10^{-35}.$$

Summing over the levels we have

$$\sum\beta_\alpha=-2.70\times10^{-35},$$

to be compared with the experimental value $\beta=-1.4\times10^{-35}$ for laevo-secondary butyl alcohol. In calculating the rotatory parameter for a new configuration where the H atom is rotated through an angle θ it should be remembered that the coordinate system was so defined that the z axis was coincident with the C–O bond and the x axis normal to the C–O–H plane. Keeping this choice of coordinates such a rotation can be represented as a rotation around the z axis through an angle $-\theta$ of all except the three atoms C–O–H. The calculation remains the same except that we use a new set of γ's in calculating the coefficients c_{n7} and c_{n8} defined by

$$\gamma_1'=\gamma_1\cos\theta+\gamma_2\sin\theta,$$
$$\gamma_2'=-\gamma_1\sin\theta+\gamma_2\cos\theta,$$
$$\gamma_3=\gamma_3.$$

TABLE II.

R	$V=V_H$ 2.09	$V=V_H$ 2.40	$V=V_H$ 3.16	$V=V_C$ 2.43
$\int\psi_2 V\psi_7$	$-0.0935\gamma_1\gamma_3$	$-0.1859\gamma_1\gamma_3$	$-0.2278\gamma_1\gamma_3$	$-0.8836\gamma_1\gamma_3$
$\int\psi_3 V\psi_7$	$.3219\gamma_1\gamma_2\gamma_3$	$.4122\gamma_1\gamma_2\gamma_3$	$.3759\gamma_1\gamma_2\gamma_3$	$1.931\gamma_1\gamma_2\gamma_3$
$\int\psi_4 V\psi_7$	$.3564\gamma_1\gamma_3^2$ $+ .0115\gamma_1(1-3\gamma_3^2)$	$.4452\gamma_1\gamma_3^2$ $+ .0110\gamma_1(1-3\gamma_3^2)$	$.4053\gamma_1\gamma_3^2$ $+ .0098\gamma_1(1-3\gamma_3^2)$	$2.083\gamma_1\gamma_3^2$ $+ .0507\gamma_1(1-3\gamma_3^2)$
$\int\psi_2 V\psi_8$	$- .0935\gamma_1\gamma_2$	$- .1859\gamma_1\gamma_2$	$- .2278\gamma_1\gamma_2$	$- .8836\gamma_1\gamma_2$
$\int\psi_3 V\psi_8$	$.3564\gamma_1\gamma_2^2$ $+ .0115\gamma_1(1-3\gamma_2^2)$	$.4452\gamma_1\gamma_2^2$ $+ .0110\gamma_1(1-3\gamma_2^2)$	$.4053\gamma_1\gamma_2^2$ $+ .0098\gamma_1(1-3\gamma_2^2)$	$2.083\gamma_1\gamma_2^2$ $+ .0507\gamma_1(1-3\gamma_2^2)$
$\int\psi_4 V\psi_8=\int\psi_3 V\psi_7$				

The results for orientation II are then

$$\beta_{\alpha 1}=-0.934\times10^{-35},$$

$$\beta_{\alpha 2}=-0.248\times10^{-35},\quad \sum\beta_\alpha=-9.67\times10^{-35},$$

$$\beta_{\alpha 3}=-8.493\times10^{-35}.$$

In the case of free rotation of the hydroxyl hydrogen about the C−O axis it is necessary to average the expression $c_{n5}c_{n8}-c_{n6}c_{n7}$ in Eq. (10), over the angle of rotation θ from 0 to 2π. (As before we neglect the remaining small terms containing a_9.) The result is

$$\begin{aligned}\beta_{\alpha n}=\sum_{ij} & D_{ni}E_{nj}\gamma_{3i}(\pi/2)(\gamma_{1i}\gamma_{2i}\gamma_{2j}^2\\ & -\gamma_{1i}\gamma_{2i}\gamma_{1j}^2+\gamma_{1i}^2\gamma_{1j}\gamma_{2j}-\gamma_{2i}^2\gamma_{1j}\gamma_{2j})\\ & +\pi(\gamma_{1i}\gamma_{2j}-\gamma_{2i}\gamma_{1j})[(A_{ni}\gamma_{3i}\\ & +B_{ni}\gamma_{3i}^2+C_{ni})(G_{nj}+F_{nj}\gamma_{3nj})]\\ & -\pi E_{nj}\gamma_{3j}\{(B_{ni}/4)[-\gamma_{1i}^2\gamma_{1j}\gamma_{2i}\\ & +\gamma_{1i}^3\gamma_{2j}-\gamma_{2i}^3\gamma_{1j}+\gamma_{2i}^2\gamma_{1i}\gamma_{1j}]\\ & +C_{ni}(\gamma_{1i}\gamma_{2j}-\gamma_{1j}\gamma_{2i})\},\end{aligned}$$

where the summation i and j extends over all the atoms except the three atoms C−O−H. The quantities A_j to E_j are derived from integrals similar to those in Table II and are defined below.

$$A_{ni}=\frac{-c_{n2}\int\Psi_{3s}V_i\Psi_{3d}(Z_i^2-X_i^2)}{2.95},$$

$$B_{ni}=\frac{-c_{n4}\int\Psi_{3p}V_i\Psi_{3d}(Z_i^3-3Z_iX_i^2)}{2.95},$$

$$C_{ni}=\frac{-c_{n4}\int\Psi_{3p}V_i\Psi_{3d}X_i^2}{2.95},$$

$$D_{ni}=\frac{-c_{n3}\int\Psi_{3p}V_i\Psi_{3d}(Z_i^3-3Z_0X_i^2)}{2.95},$$

$$E_{nj}=\frac{+c_{n3}\int\Psi_{3p}V_j\Psi_{2p}(Z_j^2-X_j^2)}{7.54},$$

$$F_{nj}=\frac{+c_{n4}\int\Psi_{3p}V_j\Psi_{2p}(Z_j^2-X_j^2)}{7.54},$$

$$G_{nj}=\frac{c_{n2}\int\Psi_{3s}V_j\Psi_{2p}Z_j}{7.54},$$

where V_i refers to the potential of the ith atom. Z_i and X_i refer to the coordinates defined such that the z axis lies along the line joining the atom i with the oxygen atom. The functions Ψ_{3s}, Ψ_{3p}, Ψ_{2p} and Ψ_{3d} are the functions Ψ_{3dzz}, Ψ_{3py}, etc., with the factors xz, y, etc., omitted. The result is then $\beta_\alpha=+0.68\times10^{-35}$. If one should neglect the small parts of c_{n5} and c_{n6} which arise from the atoms outside of the C−O−H plane the result would be identically zero.

DISCUSSION OF RESULTS

It is clear from the above results that the magnitude as well as the sign of the rotation for a given absolute configuration depends upon the relative orientation of the groups about the single bonds. Thus to determine the absolute configuration we must know how to weight the various orientations. Further, since the above calculations took no account of the neighboring molecules the question arises as to whether the gaseous value so calculated corresponds to that of the liquid. In a series of ten compounds inves-

tigated by Guye and Amarel[15] the value for the specific rotation always shows agreement in sign between liquid and vapor and agrees always within a factor of two in magnitude. One of these compounds, amyl alcohol, which is very similar to our case, changed from 5.1 in the liquid to 6.5 in the vapor. There are cases known, however, where the sign changes. Thus Kenyon[16] found a value for $[\varphi]$ of 20.1 for β-hexyl stearate in alcohol as compared to -8.93 in carbon disulfide. The effect of solvents has been reviewed by Condon[2] and by Lowry in *Optical Rotatory Power*.

Since orientations I and II correspond to the maximum hydrogen bonding with the oxygen in the gas phase, our calculations lead to the assignment of our configuration in the figure to the laevo form. This happens to agree with Kuhn[7] and to disagree with Boys[8] and Kirkwood.[3] Had we used the result calculated on the basis of free rotation of the hydroxyl the assignment would have agreed with Boys and Kirkwood. This would be equivalent to Kirkwood's assumption of axial symmetry of the O−H group. However the evidence is against the possibility of free rotation.[17, 18]

We should expect that optically active molecules in the vapor phase should show very small temperature coefficients unless the various orientations were separated by small energy differences. If the minima of potential energy for the rotations about single bonds are deep and sharp then the temperature coefficient would be very small due to the very small number of freely rotating molecules at ordinary temperatures. The temperature coefficient in the liquid may be enhanced due to association. The value of the optical rotation should approach that of the vapor as the critical temperature is reached, aside from the small field effect due to the factor $(n^2+2)/3$.

Alternative Calculations

Replacing the term in brackets in (5) by the potential energy due to dipole charges as assigned by Condon, Altar, and Eyring[3] we obtain $\beta_\alpha = +5.7\times10^{-37}$ for orientation I. In this calculation no expansion was made of the potential of the dipoles around the oxygen atom since it was found that the series rapidly diverged in this case. This result is much smaller and even of opposite sign.

A value of $\beta_\alpha = -1.2\times10^{-35}$ was obtained upon considering the same perturbations as previously in the C−O−H group but only the dipoles in the rest of the molecule. This is of the same order of magnitude as that obtained above. It should be pointed out that in the dipole calculation the carbon atoms being negative give contributions of opposite sign to those of the hydrogen atoms. In the electron cloud distribution calculation (i.e., the calculation first described) both carbon and hydrogen atoms contribute with the same sign. This is in agreement with the fact discussed by Kuhn that the sign of the rotation remains fixed if one replaces the largest group by one greater in mass than the next largest one. Mulliken[19] has pointed out that the electron cloud distribution corresponding to homopolar bonds gives rise to an assignment of dipoles to the bonds. Smyth[20] quotes a calculation by Hirschfelder which shows that in the case of the C−H bond this calculation agrees with previous estimations. In the case of large dipoles or ions arising from polar eigenfunctions the corresponding charge distribution and potential can be calculated in the same way and the calculation of the rotatory power carried through as before. Our procedure is thus a general one, applicable to any molecule or crystal.

Our eigenfunction for the chromophoric electron in the normal state spreads out more than the function calculated by Hartree and Black[21] for oxygen. This arises from the screening constants which were necessary in order to give the observed ionization and resonance potentials. Exact eigenfunctions for two states associated

Table III.

H_{22}	−.6502	W_1	−.7629	W_2	−.5593	W_3	−.4177
H_{23}	.1025						
H_{24}	.0489	c_{12}	−.6923	c_{22}	.6822	c_{32}	.2359
H_{34}	−.1155	c_{13}	.5460	c_{23}	.2835	c_{33}	.7975
H_{33}	−.5314	c_{14}	.4718	c_{24}	.6740	c_{34}	−.5555
H_{44}	−.5585						

[15] Guye and Amarel, Arch. Sci. Phys. Nat. Geneva **33**, 409, 513 (1895).
[16] Pickard and Kenyon, J. Chem. Soc. **105**, 830 (1914).
[17] Schumann and Aston, J. Chem. Phys. **6**, 480 (1938).
[18] Borden and Barker, J. Chem. Phys. **6**, 553 (1938).
[19] Mulliken, J. Chem. Phys. **3**, 573 (1935).
[20] Smyth, J. Phys. Chem. **41**, 214 (1937).
[21] Hartree and Black, Proc. Roy. Soc. **A139**, 311 (1933).

with transitions would no doubt show changes in more than one electron. Treatments such as that of Zener and Slater take care of this by assigning different screening constants to electrons which do not change quantum numbers. Our treatment which attributes to a single electron the entire change in a transition should give better results for properties in which the operators can be broken into a sum of terms depending on single electrons such as optical activity than for operators such as the energy where such a decomposition into terms depending upon single electrons is not possible.

In considering the excited states the $2py$ and $2pz$ functions of the oxygen have been treated as though they were completely available to the excited chromophoric electron whereas these states are at least partly filled by the two valence electrons contributed by the adjacent C and H atoms. However, there are effects which at least partly compensate for this deficiency in our treatment. (1) The effect of these valence electrons on the chromophoric electron is at least partly taken care of by the assumed charge distribution. (2) If the screening constant of these bonding electrons were changed the $2pz$ and $2py$ functions would automatically become included in the upper state. (3) The removal of the $2px$ antibonding electron will modify the bonding electrons such that the $2pz$ and $2py$ states will be somewhat more empty.

Whether or not this term or the term calculated by Kirkwood is the more important will be one of the subjects of further investigation.

In the case of one electron transitions it is easy to assign a unique center about which to calculate the magnetic moment. However, for a multiple electron transition the calculated optical activity will depend upon the center chosen unless the functions used to represent the initial and final states are eigenfunctions of some Hamiltonian operator. With our present knowledge of one-electron eigengunctions this is difficult to insure in practice. That this is true may be seen from the following.

The magnetic moment for the transition from the state a to the state b may depend upon the center of coordinates chosen. If $\mathbf{r}_k$ is the position vector in the first coordinate system and $\mathbf{r}_i$ that in the new system, then

$$\mathbf{r}_i=\mathbf{r}_k-\mathbf{R}_{ik}, \tag{12}$$

where $\mathbf{R}_{ik}$ is the vector joining the two centers. The magnetic moment for the transition about the new center is then

$$(b|\mathbf{m}|a)=\frac{e}{2mc}(\mathbf{r}_i\times\mathbf{P})_{ba}$$

$$=\frac{e}{2mc}\{(\mathbf{r}_k\times\mathbf{P})_{ba}-\mathbf{R}_{ik}\times\mathbf{P}_{ba}\}, \tag{13}$$

where the large $\mathbf{P}$ is the electronic momentum. Using the relation

$$(h/2\pi i)\dot{r}=H\mathbf{r}-\mathbf{r}H, \tag{14}$$

one finds that

$$\mathbf{P}_{ba}=\frac{2\pi imv_{ba}}{e}(b|\mathbf{p}|a), \tag{15}$$

provided that the functions b and a are eigenfunctions for some Hamiltonian operator H. The second term in (13) is therefore perpendicular to the electric moment vector $(b|\mathbf{p}|a)$, and on forming the dot product with $(b|\mathbf{p}|a)$ will give no contribution to the optical activity. However, this is contingent on relationship (15) which depends upon b and a being eigenfunctions for some Hamiltonian operator. If, for example, we consider the case where a is an eigenfunction for some Hamiltonian operator H and b is some linear combination of eigenfunctions of H, then in place of $\mathbf{P}_{ba}$ in (13) we have a sum of terms connecting state a with a linear combination of eigenstates b. The orthogonality between this sum of terms and the corresponding sum of terms for the electric moment will now no longer hold and we will get a contribution which will depend upon where the center for calculating the magnetic moment is chosen. This illustrates, from the present point of view, one of the more serious difficulties in considering more than one electron transitions such as one would have if one used bond functions for the upper and lower states.

A Kinetic Approach to the Theory of Conductance of Infinitely Dilute Solutions, Based on the "Cage" Model of Liquids

MILTON J. POLISSAR
Department of Chemistry, San Francisco Junior College, San Francisco, California

(Received October 6, 1938)

Attention is called to the disparity between the hydrodynamic model of an electrolytic solution and its physical counterpart. The "cage" theory of liquids is reviewed, and some of its equations developed with the purpose of bringing to the surface the underlying assumptions. A quantitative comparison is carried out between the behavior of an ion subject to Brownian motion and that of the placidly moving ion of the hydrodynamic theory. The conclusion is drawn that the tremendous difference between the two models casts doubt upon the validity of the hydrodynamic equations. The possibility is mentioned that the hydrodynamic theory, while giving fortuitously approximately correct values of ionic radii, may still be incorrect in its theoretical implications. Stress is laid on the desirability of a kinetic theory of electrolytic conductance. An approach to a kinetic theory is made, based on the cage model of liquids. In this method, the ionic migration is considered as the cumulative effect of a feeble, sporadic, but directed perturbation of the violent but random Brownian movement. The method leads to an experimentally substantiated relation between the diffusion and the conductivity of an electrolyte. It offers a plausible explanation of the high temperature coefficient of the slow-moving ions. For the ions of an infinitely dilute aqueous solution of potassium chloride, the method yields the following data: Heat of activation for a cage-to-cage jump, 4230 calories; frequency of cage-to-cage jumps, 1.12×10^{11} sec.$^{-1}$; frequency of oscillation within the cage, 8.3×10^{13} sec.$^{-1}$; average number of oscillations in each cage, 740.

THE hydrodynamic theory of electrolytic conductance treats the ion as a charged sphere moving with a steady velocity in the direction of the field. The Brownian movement of the ion is treated as an unimportant, self-canceling perturbation of the rectilinear motion. The object of the present paper is to compare the behavior of the hydrodynamic model with the model of an ion offered by the latest theories of liquid structure; to discuss the validity of the hydrodynamic equations; and to offer an approach to a *kinetic* theory of conductance, in which the migration of the ion along the field is considered as the result of a rather feeble but persistent perturbation of the vigorous Brownian movement.

I. THE HYDRODYNAMIC THEORY

In 1888 Nernst[1] derived a theoretical relation between the diffusion coefficient of a salt and the mobilities of its ions. Nernst assumed that a diffusing ion is acted upon by a force which in solution theory was called osmotic pressure. He assumed that the ion moves at a constant velocity because of the resistance offered by the medium. He further assumed that the same friction coefficient operates to restrict to a steady velocity the movement of an ion in an electric field. Eliminating the unknown friction coefficient from his diffusion and conductance equations, Nernst obtained the relation between the diffusion coefficient and the mobility of the ion. Eq. (1) is a modification of the Nernst relation:

$$v=(nE\epsilon D)/kT. \qquad (1)$$

In this equation n is the valence of the ion, E is the intensity of the field, D is the diffusion coefficient of the ion, ϵ is the electronic charge, and kT is the Boltzmann constant multiplied by the absolute temperature. v is the absolute mobility of the ion in a field of unit intensity.

Nernst showed that in the case of a salt whose ions possess unequal mobilities u and v the diffusion of the slower ion will be accelerated by the faster ion; the diffusion of the latter will be retarded. The equation for the diffusion of a salt retains the simple form shown in Eq. (1) if v is replaced by an average mobility, equal to $2uv/(u+v)$. The agreement between observed diffusion coefficients and those calculated from the known mobilities is highly satisfactory (Taylor, reference 1, p. 1024).

[1] Nernst, Zeits. f. physik. Chemie **2**, 613 (1888); Taylor, *Treatise on Physical Chemistry* (D. Van Nostrand Co., 1930), p. 690, 1022. For several further references, see Taylor, p. 690.

In 1905, Einstein,[2] assuming that a large Brownian particle is also subject to the influence of osmotic force, added the assumption that the friction coefficient is given by Stokes law. This led to the now familiar equation:

$$D=kT/(6\pi\eta r). \tag{2}$$

In this equation η is the ordinary macroscopic coefficient of viscosity of the medium, and r is the radius of the particle. The assumption that a suspended particle or molecule is subject to an "osmotic force" in the direction of the concentration gradient is somewhat disturbing. Einstein meets this possible objection as follows:[3]

"In this calculation osmotic pressure is treated as a force acting on the individual molecules, which evidently does not correspond with the conceptions of the kinetic-molecular theory, since, according to the latter, the osmotic pressure in the case under discussion must be thought of as a virtual force only. However, this difficulty vanishes if we reflect that (dynamic) equilibrium with the (virtual) osmotic forces, which correspond to the differences in concentration of the solution, can be established by the aid of a numerically equal force acting on single molecules in the opposite direction."

In 1910, Lorenz[4] contributed the assumption that, despite the small size of an ion, its friction coefficient is given by the Stokes formula. He suggested that the extended Einstein-Stokes equation may be used for the determination of ionic radii in solution. Lorenz's equation, slightly modified, reads as follows:

$$v=n\epsilon E/(6\pi\eta r). \tag{3}$$

Eliminating Stokes friction coefficient from Eqs. (2) and (3), we obtain the modified form of Nernst's Eq. (1).

In conclusion, we may state briefly the nature of the model offered by the hydrodynamic theory of electrolytic conductance, as it is known at the present time:[5, 6] When an electric field is turned on, each ion begins to move under the influence of the force $n\epsilon E$. The resistance, $6\pi\eta rv$, increases with the velocity. Eventually, the ion reaches a steady velocity, given by Eq. (3).

II. The Relation Between the Assumptions of the Hydrodynamic Theory and the Validity of the Derived Equations

We have seen that the hydrodynamic theory calls for an initial period of acceleration. The question may be raised: Why is the conductivity of an electrolyte in an alternating electric field independent of the frequency of the field? This question is taken up in some of the reference books. Ulich (reference 6, p. 224) estimates that the period of acceleration is of the order of magnitude of 10^{-13} sec. and is much shorter than the periods of the fields ordinarily used. Newman,[7] discussing the same question, gives the following equations in support of the statement that the period of acceleration must be extremely short:

$$m\frac{dv}{dt}=nE\epsilon-6\pi\eta rv;$$
$$v=\frac{nE\epsilon}{6\pi\eta r}(1-e^{-6\pi\eta rt/m}). \tag{4}$$

It is obvious that for large values of t Eq. (4) is reduced to Eq. (3). To check Ulich's estimate, we shall calculate the value of t at which v will have reached 90 percent of its maximum velocity. Solving the equation: $e\exp(-6\pi\eta rt/m)=0.1$, and assuming a molecular weight 100 for the ion, $\eta=0.01$, $r=3\times10^{-8}$ cm, we find that $t=6.7\times10^{-14}$ sec., in fair agreement with Ulich's value.

If the frictional force were absent, the freely accelerated ion would have acquired in the same time interval a velocity 2.303 times as great as its steady limiting velocity given by Eq. (4). In other words, the velocity of the ion at the end of an interval of 6.7×10^{-14} second is 0.9/2.303, or 39 percent of the value it would have had if friction were completely absent. This last calculation, which does not appear in reference books on electrolytic conductance, leads to a very

[2] Einstein, Ann. d. Physik **17**, 549 (1905).
[3] Einstein, *Investigations of the Theory of the Brownian Movement*, edited by Fürth, translated by Cowper (Methuen & Co., London, 1926), p. 58.
[4] Lorenz, Zeits. f. physik. Chemie **73**, 252 (1910).
[5] Baars, *Handbuch der Physik*, Vol. XIII (Julius Springer, Berlin, 1928), p. 399, 437.
[6] Ulich, Eucken-Wolf's *Hand- und Jahrbuch der chemischen Physik*, Vol. VI (Leipzig, Akademische Verlagsgesellschaft, 1933), pp. 152–181.
[7] Newman, *Electrolytic Conduction* (Wiley, 1931), p.367.

puzzling conclusion. The absolute velocity of an ion in a field of 1 volt/cm is of the order of magnitude of 1×10^{-3} cm/sec. Therefore, in 6.7×10^{-14} sec. the distance covered by the accelerated ion is less than 6.7×10^{-17} cm. We find, then, that, while the ion covered this distance, frictional forces operated to give it a velocity which was only 39 percent of the velocity it would have acquired in the absence of friction!

This is a startling conclusion. We are accustomed to think that the distance between the particles of a liquid are of the order of magnitude of 10^{-9} cm. How could the friction of the solvent affect the ion while it was moving through a distance equal to approximately one-ten-millionth of its mean free path?

The difficulty may be resolved in one of two ways. First, we may try to apply the Heisenberg principle of uncertainty. The momentum of the ion moving at full speed is approximately 16.5×10^{-26}. Since we are trying to define the momentum of the ion within 10 percent of this value, or 1.65×10^{-26}, we can localize its position with an uncertainty equal to $h/1.65\times10^{-26}$, or 0.386 cm. (Taylor, reference 1, p. 1354). We could say that the problem should have been approached with the methods of quantum mechanics. This, however, would be too much like changing the rules of the game after the cards had been dealt. Since we have been using classical dynamics, it is desirable to discover, with the use of simple ideas of classical dynamics, the contradiction which has crept into our discussion of the problem.

The alternative explanation is based upon an inherent weakness of any model intended to represent a complicated physical system. To be amenable to theoretical treatment, the model must be simpler than the system it represents, and therefore different from it. Any calculation in which the difference between the system and its model is of crucial importance is apt to bring contradictory results. Stokes law is based on the assumption that the sphere is moving in a continuous viscous medium, the latter extending from the very surface of the sphere. In Lorenz's model of an electrolytic solution the coarse-grained solvent was replaced by a viscous, placid, continuous medium. The restless ions were replaced by steadily moving charged spheres. It should be clear that any argument based on the coarse-grained structure of the solution is almost bound to conflict with the deductions based on the Lorenz model. In the opinion of the writer, it is not unfair to the hydrodynamic theory to state that it cannot give the correct answer to the question of initial acceleration of ions in a real solution. As a matter of fact, in a subsequent section it will be shown that this question, perfectly definite as it is when applied to a Lorenz model, is meaningless when applied to a real solution.

The paradox discussed in this section represents one case in which the difference between a solution and its hydrodynamic model is of enough importance to invalidate the conclusions of the theory. In the light of this example it would be desirable to carry out a careful quantitative comparison between the behavior of ions in solution and that of ions in the hydrodynamic model, with a view to examining critically the validity of the hydrodynamic equations. In some discussions of the hydrodynamic theory the Brownian movement of the ions is mentioned parenthetically. In others, it is mentioned with real concern. In all cases, however, it is assumed that the randomness of the movement operates to leave unimpaired the applicability of Stokes law. In this paper the writer intends to reopen this discussion in the light of a *quantitative* comparison between the behavior of a Lorenz ion and its physical counterpart. This quantitative treatment is made possible by recent progress in the theory of liquids. Some of the latest developments of the theory will be discussed in the next two sections, after which it will be possible to return to the main subject of this paper.

III. The "Cage" Model of Liquids and Solutions

In 1926, Frenkel[8] called attention to an important aspect of the motion of molecules and of ions in a liquid. He pointed out that the particles do not "crawl" past each other; that they oscillate about an equilibrium position; and that they jump from one equilibrium position to another on infrequent occasions. The same idea was ad-

[8] Frenkel, Zeits. f. Physik **35**, 652 (1926).

vanced by the writer in 1932.[9] Bradley[10] brought forth the same idea in his interesting paper on the rate of reactions in solution. Since then several papers appeared which deal, in whole or in part, with the idea of "caged" molecules.[11–16]

To quote from the writer's earlier paper: "There is good evidence that molecules in the liquid phase are fairly closely packed. Thus, if we calculate the molecular diameters of molecules in the liquid phase on the assumption of close packing, we obtain values which are in fair agreement with those obtained by other methods.[17] It follows from what has been said that the application of the gas-kinetic formula to the case of solutions may be incorrect not only in degree but also in kind.

"The question may be raised as to the nature of the process whereby molecules in a closely packed system change position and neighbors. The answer will probably be supplied by the statistical theory of fluctuations. As long as the molecules are not solidly packed, there is room for fluctuation in density. The density fluctuation in a system consisting of a large number of molecules is very small. However, in a system consisting of from ten to fifty molecules the fluctuation may be violent enough to allow individual molecules a frequent change of neighbors and position."

The present view is that in a liquid each particle is surrounded by a "cage" consisting of approximately 12 molecules and that the central molecule or ion cannot escape from this "cage" unless it possesses energy of activation of the order of magnitude of 5000 calories. Since a great portion of the discussion in this paper will depend on the assumption of caged molecules, it will be of interest to form an estimate of the distance between the molecules in a liquid.

Lorenz,[18] after a careful study of the available data, estimated that the volumes of an "average" liquid, at its melting point and at its boiling point, are 21 percent and 41 percent, respectively, greater than the extrapolated volume at 0°K. Volume expansions in the ratios 1.21 and 1.41 correspond to linear expansions in the ratios 1.065 and 1.120, respectively. This means that in an "average" liquid the average distance between the surfaces of two adjacent molecules is equal to something like 6.5 percent to 12 percent of the molecular diameter. It seems plausible that under such conditions a molecule or an ion must possess more than its average share of kinetic energy before it can squeeze through a "gate" or exchange places with one of its neighbors.

IV. Calculation of the Frequency of Cage-to-Cage Jumps

The calculations in this section will be based on the following assumptions and definitions: (1) In an ordinary liquid or solution each particle (molecule or ion) is oscillating in a cage made up of the surrounding particles, approximately twelve in number. (2) When the central particle has suddenly changed positions in such a way as to exchange about half or more of its former neighbors, we shall say that it has made a cage-to-cage jump. We need not specify the precise mechanism of the process. The molecule may exchange places with one of the cage molecules; it may occupy a hole created by the departure of one of the cage molecules; it may squeeze past two of the cage particles. (3) We shall assume that long jumps are extremely rare and that the average distance between two successive equilibrium positions is of the order of magnitude of the average distance between the centers of two neighboring particles.

Suppose we fix our attention on a single particle and study its progress through space in the course of n cage-to-cage jumps. Its vector-displacement will be given by the following vector equation:

$$\mathbf{S}_n = \sum_{p=1\cdots n} \mathbf{L}_p, \qquad (5)$$

[9] Polissar, J. Am. Chem. Soc. **54**, 3105 (1932).
[10] Bradley, J. Chem. Soc. 1910 (1934). Bradley was unaware of the two papers published earlier, just as the author was unaware in 1932 of Frenkel's paper published 6 years earlier.
[11] Wheeler, Proc. Ind. Acad. Sci. **1**, 795 (1935); **4**, 291, 298, 466 (1936); Trans. Nat'l. Inst. of Sci. of India **1**, 333 (1938).
[12] Rabinowitch and Wood, Trans. Faraday Soc. **32**, 1381 (1936).
[13] Eyring, J. Chem. Phys. **4**, 283 (1936).
[14] Bradley, Trans. Faraday Soc. **33**, 1185 (1937).
[15] Rabinowitch, Trans. Faraday Soc. **33**, 1225 (1937).
[16] Fowler and Slater, Trans. Faraday Soc. **34**, 81 (1937).
[17] Jeans, *The Dynamical Theory of Gases* (Cambridge University Press, 1925), p. 332.
[18] R. Lorenz, *Raumerfüllung und Ionenbeweglichkeit* (Leopold Voss, Leipzig, 1922.)

where $\mathbf{L}_p$ is the vector displacement in jump number p. Taking the dot product of each side against itself, we obtain the following equations:

$$\mathbf{S}_n \cdot \mathbf{S}_n = S_n^2 = \sum_{\substack{p=1\cdots n \\ q=1\cdots n}} \mathbf{L}_p \cdot \mathbf{L}_q = \sum_{p=1\cdots n} \mathbf{L}_p^2 + \sum_{p \neq q} \mathbf{L}_p \cdot \mathbf{L}_q. \quad (6)$$

If we repeat the experiment m times, where m is a very large number, we obtain m equations similar to Eq. (6). On adding the left sides of the m equations and dividing by m, we shall obtain the average of the square of the vector displacement after n jumps. The sum of the right sides of the m equations, divided by m, will be equal to $n\bar{L}^2$, where $\bar{L}^2$* is the average of the square of a cage-to-cage displacement[1]

$$\bar{S}_n^2 = n\bar{L}^2. \quad (7)$$

The terms of the type $\mathbf{L}_p \cdot \mathbf{L}_q$ will add up to zero, since the cosine of the angle between the two vectors has an equal chance of being positive or negative. This last statement is dependent on the reasonable assumption, to be verified later, that in each cage the particle completes several oscillations, thus making the directions of two successive jumps completely independent of each other.

Let j be the number of cage-to-cage jumps per second. Then the average of the square of the displacement after a time t is given by the following equation:

$$\bar{S}_t^2 = jt\bar{L}^2. \quad (8)$$

The relations between L, S, and the components of the latter along three mutually perpendicular directions are given by the following equations:

$$S^2 = X^2 + Y^2 + Z^2; \quad \bar{S}_t^2 = 3\bar{X}_t^2;$$
$$\bar{X}_t^2 = (jt\bar{L}^2)/3. \quad (9)$$

Einstein[2] has derived the following equation, in which D is the coefficient of diffusion of a particle:

$$\bar{X}_t^2 = 2Dt. \quad (10)$$

This equation is completely independent of any physical assumptions, such as the application of Stokes law to molecules, except the assumption of completely random motion. Combining Eqs. (9) and (10), we obtain the following relation:

$$j = 6D/\bar{L}^2. \quad (11)$$

Equation (11) makes it possible to calculate the value of j in terms of the diffusion coefficient. It is applicable to neutral molecules of a solute, to molecules of a solvent (in which case D is the coefficient of self-diffusion), and to electrolytes, such as potassium chloride, whose ions possess equal mobilities.

We can now calculate the approximate value of the frequency, j, of cage-to-cage jumps in ordinary liquids. D is of the order of magnitude of 10^{-5} cm^2/sec.; L^2 is of the order of magnitude of 10^{-15} cm^2; j must be of the order of magnitude of 6×10^{10} sec.$^{-1}$.[a]

* Because of typographical difficulties the overbar does not extend beyond the letter. In this and in the other equations, $\bar{A}^2$ is to be taken as the average of the square of A and not as the square of the average of A.

[a] *Note:* Equation (11) has been used by preceding writers on the subject. Bradley (reference 9, 13) used the familiar method of derivation involving two planes separated by a distance L. Rabinowitch (reference 14) employed a method similar to that given here. His equations involve an error of a factor of 3, caused by the use of $\bar{X}^2$ in place of $\bar{S}^2$. The complete derivation of Eq. (7) is given here, since it is not given in any of the papers perused by the writer. The purpose is twofold: First, to show that it can be used with equal rigor for any value of n, from $n=1$ and up; secondly, to bring to the surface all the underlying assumptions.

To start with, we may note that the derivation is independent of the shape of the molecule. It is also independent of the mechanism of the cage-to-cage jump, as long as $\bar{L}^2$ is recognized as the weighted average of the squares of the possible single displacements. The derivation is based on the assumption that the directions of two successive jumps are mutually independent. This assumption does not hold true in the case of an ion jumping in the vicinity of another ion. It holds true for the ions of an infinitely dilute solution.

There is one hidden assumption which should be discussed at this point. In the derivation of Eq. (7) it has been assumed that the vector displacement S was due solely to the cage-to-cage jumps of the particle. This need not necessarily be correct and is most probably incorrect to a small extent. To make this point clear, we shall assume the extreme case of a hypothetical liquid containing semi-crystalline molecular swarms. In such a liquid an individual molecule may be buried in a single cage for a relatively long time, while the swarm is subject to Brownian motion. The Brownian motion of the swarm and not the cage-to-cage jumps of the molecule would serve as the chief contributor to the diffusion of the molecule, and Eq. (11) would be incorrect.

Even in a liquid with no localized rigid structure, the whole cage must be subject to Brownian movement, because of fluctuations in density of the environment. In a loosely packed liquid, this motion would be more violent than in a tightly packed one. But in a loosely packed liquid the frequency of jumps would be greater than in a tightly packed one. For this reason, the relative importance of the two types of displacement would be roughly the same in all liquids. Furthermore, the Brownian displacement of a group of molecules must be smaller than that of a single one.

There cannot be any doubt that Eq. (11) will give the correct order of magnitude of the value of j, despite the neglect of the Brownian movement of the cage as a whole.

V. A Comparison Between the Hydrodynamic Model of an Electrolytic Solution and its Physical Counterpart

In carrying out a comparison between the behavior of an electrolytic solution in an electrical field and that of its hydrodynamic model, it would be desirable to avoid a discussion of those differences which are not essential to the validity of the hydrodynamic equations. In order to provide both direction and emphasis to our line of inquiry, we shall consider the differences in the light of the assumptions underlying the derivation and the use of Stokes law. We need not consider all the assumptions.[19] Two of them are of particular interest in the present case: The motion of the sphere must be steady; and there must be no slipping at the surface of the sphere. It will be most pertinent to the present discussion to quote Herzfeld and Smallwood's interpretation, given in Taylor's treatise (reference 1, p. 183). After showing that a small particle subject to a constant force will move through a gas with a speed which is inversely proportional to the *square* of its radius, they state that a large particle will obey Stokes law. Their explanation follows:

"The physical difference between the two cases is as follows: In the case of *small* particles (or ions), it was assumed that the motion of the particle had no effect on the motion of the molecules in front of it prior to the actual collision. . . . In Stokes' case, however, the motion of the gas molecules is changed throughout the entire surrounding region by the motion of the particle. That is to say, so many molecules are reflected from the particle that they might be said to prepare the molecules in front of them, due to their altered distribution of velocities. The entire body of gas in front of the particle has therefore a component of velocity parallel to the velocity of the particle."

The hydrodynamic model satisfies all the requirements underlying the use of Stokes equation. In examining the behavior of an actual solution, we shall attempt to answer the following questions: Is the motion of the ion steady? Is there slippage at the surface? Is the motion of the ion under the influence of the field a dominating factor in the region surrounding the ion?

For the sake of concreteness we shall study the behavior of potassium ions in a dilute solution of potassium chloride, at 18°C, in a field of 1 volt/cm. This electrolyte has the convenient, but unessential, characteristic that its ions possess approximately equal mobilities. For the convenience of the reader, the data and derived quantities are assembled in Table I.

(1) We shall estimate the number of jumps per second. The diffusion coefficient in very dilute solutions cannot be much different from that of a 0.001-molal solution (1.69×10^{-5} cm²/sec.). The value of L will be taken quite arbitrarily as 3×10^{-8} cm. This value is certainly correct as to order of magnitude. No effort is made to obtain a more accurate value, since none of the arguments of this paper are based on the exact value of L. Substituting in Eq. (11), we get: $j=1.12\times10^{11}$ jumps per second.

(2) We shall compare the migration velocity of the ion with its kinetic velocity. The former is 6.75×10^{-4} cm/sec.; the latter is of the order of magnitude of 300 meters/sec. The ratio of these two quantities is approximately 4.5×10^{7}. It would seem, then, that the introduction of a field of 1 volt/cm would not affect greatly the behavior of the ion.

(3) We shall compare the energy acquired by the ion as it moves along the field with the mean thermal energy per degree of freedom. We shall make the usual assumption that the ion picks up energy while it is free to move with the field. Assuming that the ion can cover even as large a distance as 3×10^{-8} cm without losing its energy, we find that the energy so acquired is 3×10^{-8} volt-electron, or 4.77×10^{-20} erg. The value of kT is 3.99×10^{-14} erg. The ratio of these two quantities is 8.35×10^{5}. This is another indication that the electrical field cannot be very effective in helping the ion to batter its way through the surrounding molecules!

(4) It will be even more significant to compare the activation effected by the electrical field with the energy of activation needed for a cage-to-cage

It is highly probable that this equation is satisfactory within an error of a very few percent. This assumption is supported by the fact that equations derived in a later section and based on Eq. (11) are in agreement with experimental observations.

[19] For a list of assumptions, see Ulich, reference 6, p. 152, or Millikan, *Electrons* (The University of Chicago Press, 1935), p. 95.

jump. This latter quantity is calculated in a later section and is equal to 4230 calories per mole, or 2.92×10^{-13} erg per ion. The ratio between this and the activation energy of the field is 6.12×10^{6}. The electric field supplies only one-six-millionth, approximately, of the energy needed to push the ion from one cage to another.

(5) The migration velocity of the ion is 6.75×10^{-4} cm/sec. This is equivalent to 22,500 jumps per second along the field. Although the absolute number is large, it should be compared with the total number of jumps per second (paragraph 1). The ratio is 5×10^{6}. In the absence of an electrical field the average numbers of jumps in two opposite directions must be equal. Our calculations show that in the presence of a field of 1 volt/cm, the net gain along the field is only one for every five million jumps.

(6) It will be of interest to compare the average Brownian displacement in the line of the field with the average gain along the field. It takes the ion 4.45×10^{-5} second to make a net gain of 3×10^{-8} cm along the field. During this time, the average Brownian displacement along the line of the field (given by the equation: $\bar{X}^2=2Dt$) is equal to 3.87×10^{-5} cm. The Brownian displacement along the field is 1290 times as large as the net gain. (The distance along the zig-zag path is 5×10^{6} times as large, as shown in the preceding paragraph.)

(7) Since the net gain along the field is proportional to the time, whereas the Brownian displacement is proportional to the square root of the time, the relative magnitude of the Brownian displacement decreases with time. For use in a subsequent discussion, it will be of interest to calculate how long the ion must be "under observation" before its average Brownian displacement is only 1 percent of the gain along the field. Solving the equation: $v^2t^2=10{,}000\bar{X}^2=20{,}000Dt$, we find $t=7.41\times10^{5}$ sec., or 206 hours.

We have seen that for the validity of Stokes law it was necessary to ascribe a dominant role to the moving ion. The ion was supposed to plow its way through the surrounding medium, pushing it out of the way and in turn being retarded by it. From a consideration of the behavior of an ion in solution we learned that the role of the electrical field is much more humble than the hydrodynamic theory assumes it to be. An imaginary observer deriving his information by watching an individual ion would hardly be able to detect any change on the introduction of a potential gradient of 1 volt/cm. Only by keeping

TABLE I. *Some of the symbols used and the values of these quantities in a dilute solution of potassium chloride, at 18°C, and under a potential gradient of 1 volt per centimeter.*

1. $T=291°K.$
2. E: Intensity of electrical field
   $E=1$ volt/cm.
3. ϵ: Electronic charge; $\epsilon=4.77\times10^{-10}$ e.s.u.
4. n: Valence of ion.
5. S: Vector displacement of ion.
6. η: Viscosity of solvent.
   $\eta=0.0106$ poise.
7. D: Diffusion coefficient of ion.
   $D=1.69\times10^{-5}$ cm²/sec.
8. r: Hydrodynamic value of the ionic radius.
   $r=1.18\times10^{-8}$ cm.
9. Crystal theory value of the radius of potassium ion:
   $r'=1.33\times10^{-8}$ cm.
   $(r'/r=1.13$, despite hydration!).
10. Approximate time necessary for "hydrodynamic" ion to reach 90 percent of migration velocity:
    $t_{0.9}=6.7\times10^{-14}$ sec.
11. Distance covered in that time:
    $S_{0.9}=6.7\times10^{-17}$ cm, approx.
12. Compare with mean free path of ion:
    $F=0.1$ to 3×10^{-5} cm.
    $(S_{0.9}/F=6.7\times10^{-7}$, approx.!).
13. L: Cage-to-cage distance.
    $L=3\times10^{-8}$ cm, approx.
14. v: Migration velocity of ion.
    $v=6.75\times10^{-4}$ cm/sec.
15. This corresponds to a net gain of j_{Field} jumps per second along the field:
    $j_{\text{Field}}=22{,}500$ sec.$^{-1}$
16. j: Total number of cage-to-cage jumps per second.
    $j=1.12\times10^{11}$ sec.$^{-1}$
    $(j/j_{\text{Field}}=5\times10^{6})$.
17. 1 volt-electron $=1.59\times10^{-12}$ erg.
18. Q_E: Activation due to field operating through a distance L.
    $q_E=4.77\times10^{-20}$ erg/electron
    $Q_E=6.91\times10^{-4}$ calorie/faraday.
19. kT: Thermal energy per degree of freedom.
    $kT=3.99\times10^{-14}$ erg. $RT=578$ calories
    $(kT/q_E=8.35\times10^{6})$.
20. Q: Energy of activation for a cage-to-cage jump.
    $q=2.92\times10^{-13}$ erg. per ion
    $Q=4230$ calories per mole
    $(Q/Q_E=6.12\times10^{6})$.
21. Time in which ion migrates through distance L:
    $t_L=4.45\times10^{-5}$ sec.
22. Brownian displacement along the field in the same time:
    $X_L=3.87\times10^{-5}$ cm.
    $(X_L/L=1290)$.
23. Distance covered along field in 206 hours:
    $v\cdot t=500$ cm.
    Average Brownian displacement in the same time:
    $(2Dt)^{\frac{1}{2}}=5.00$ cm, or 1 percent of former.
24. Temperature Coefficient of mobility:
    Simple hydrodynamic theory:
    2.54% per degree for all ions.
    Lindemann's theory:
    0.13% per degree for potassium ion.
    Observed values:
    2.65% for lithium ion
    2.17% for potassium ion
    2.12% for cesium ion.
25. $A/2$: Frequency of oscillation within the cage.
    $A/2=8.3\times10^{13}$ sec.$^{-1}$, approx.
26. Average number of oscillations per cage:
    $A/2j=740$ (for potassium ion).

his records to an accuracy of seven significant figures, would he be able to observe that in every five million jumps there is a discrepancy of one, between the number of jumps with the field and the number of jumps against it.

The motion of the ion is admittedly not constant and rarely in the direction of the field. If the idea of "caged" molecules is approximately correct, then the motion is not even smooth and continuous, but intermittent and jerky. Furthermore, the electric field, while acting on the ion all the time, succeeds in influencing the direction of the jump on extremely rare occasions. This is contrary to one of the assumptions underlying Stokes law, namely that the force operates continuously on the moving sphere. This assumption is so obvious that it is never even mentioned in a discussion of the applicability of Stokes law.

The question as to whether there is any slippage at the surface of the moving ion would appear to be meaningless. Furthermore, the question as to the time interval during which the ion is accelerated to its "steady" velocity, discussed in Section II, also loses physical significance.

VI. A Critical Discussion of the Validity of the Hydrodynamic Equation

The conclusions reached in the preceding section are not such as to inspire confidence in the validity of Eqs. (2) and (3) when applied to ions. Whereas, to the best of the writer's knowledge, the quantitative comparison is here carried out for the first time, the qualitative objections lying in the way of acceptance of the hydrodynamic theory have been taken up before. It is not improbable that the hydrodynamic equations would not have gained acceptance if it were not for the fact that they are supported, more or less accurately, by experimental results. For this reason, before taking up the theoretical arguments adduced in support of these equations, we shall consider the nature of the experimental evidence.

Lorenz[4] compared several ionic radii obtained from Eq. (3) with the Reinganum values. He found that, whereas individual values showed high discrepancies, the two averages of all the radii agreed to within 2.5 percent. When one considers the tremendous simplification of model offered by the hydrodynamic theory, it is amazing to find that the calculated radii are correct as to order of magnitude, let alone to an accuracy of a few percent.

Ulich,[6] who is a supporter of the hydrodynamic theory, devotes about twenty-five pages to a discussion of the applicability of the Stokes friction coefficient to the diffusion of ions and molecules and to the conductance of ions. He cites numerous cases in which the calculated radii are correct to within a few percent. On the other hand, among those listed there are quite a few where the value is correct only as to order of magnitude.

The fact that Eq. (3) gives approximately correct values of the radii of many ions cannot be taken as so many independent verifications of the equation. The sizes of ordinary ions do not vary greatly. It is to be expected that larger ions migrate more slowly. Under such circumstances it is almost unavoidable that if the equation gives fortuitously an approximately correct value for one ion, it will also give approximately correct values for all other ions, with a good correlation between the values so obtained and those obtained by other means.

There is no doubt at the present time that Eq. (3) gives approximately correct ionic radii. Controversy arises when an attempt is made to give this equation a strict interpretation, namely, to assume that it is correct to, say, 5 percent and that all the theoretical implications deduced from this equation are correct. Serious objections must be met before such a conclusion can be accepted. For instance, aside from the discrepancy between the values of ionic radii obtained with the use of Eq. (3) and those obtained by other means, there is the question of temperature coefficient of mobility.[20] If Eq. (3) is correct, then the temperature coefficients of mobility of all ions should be equal to the coefficient of fluidity, which for water is 0.0254 per degree, at 18°C. Actually, the slow ions show this coefficient, whereas the faster ones exhibit lower coefficients, the faster the ion, the lower the temperature coefficient. To account for this fact it was necessary to assume that the degree of solvation of the fast ions *increases* with increase in temperature.

Herein lies the importance of a critical examination of the validity of Eq. (3). Whereas addi-

[20] Davies, *The Conductivity of Solutions* (John Wiley & Sons, New York, 1933), p. 210.

tional assumptions are needed to bring the theory in alignment with the experimental facts, once the equation is accepted as essentially correct, the very assumptions used for its support become far-reaching conclusions based on an accepted theory. In this connection, it is of interest to mention that Kraus[21] after considering the various assumptions necessary to square the theory with observed values, concludes that the Einstein-Stokes equation should be applied with caution to systems of particles of molecular dimensions.

We shall now consider the theoretical arguments adduced in support of the application of the Einstein-Stokes equation to ions. It will suffice to refer to Ulich's review.[6] Two of the difficulties offered by the coarse-grained structure are listed: (1) The ion may be able to slip between the molecules of the solvent. (2) The velocity of the medium may fall off discontinuously. The errors introduced by these two factors are opposite in sign, and the assumption is made that they will cancel each other. It should be pointed out that this assumption need not necessarily be correct. As a matter of fact, a similar assumption is definitely incorrect in the case of a Brownian particle falling through a gas. Millikan and his co-workers found (reference 19, p. 115) that when the size of the particle is equal to the mean free path of the gaseous molecule, the friction coefficient in Stokes' formula must be multiplied by the factor 1/1.874.

In support of the assumption that the Brownian motion of the ion does not invalidate the applicability of Stokes law, Ulich[6] cites the experimental work of Fürth[22] on the rate of fall of microscopic particles through water and the rate of movement of charged metallic particles through a gas, in an electric field. To this evidence we may add the work Fletcher and Millikan (reference 19, p. 154), who verified the applicability of Stokes law to large particles falling through a gas. Unfortunately, this evidence is not convincing when applied to a molecular system. Millikan states quite definitely that in these experiments the irregular Brownian displacements were much smaller than the orderly displacement of the falling particle. On the other hand, the calculations given in Section V, paragraphs 6 and 7, show that ordinarily the Brownian displacement of an ion is very much greater than its displacement along the field. A potassium ion, moving in a field of one volt per centimeter would have to be "under observation" for 206 hours before its displacement along the field is one hundred times as great as its irregular Brownian displacement.

In conclusion, we must state that the validity of the hydrodynamic equation is still in doubt. We must recognize the existence of two possibilities: Either Eq. (3) yields approximately correct values of ionic radii fortuitously, through a favorable set of cancellations of errors: or the equation is correct, through the operation of an even more magnificent set of cancellations of error. In either case the hydrodynamic model is admittedly very much different from its physical counterpart. The writer is of the opinion that it would not be unscientific to accept the simpler alternative, namely, that the agreement is fortuitous.[a]

VII. An Approach to a Kinetic Theory of Electrolytic Conductance

Independently of whether the strict interpretation of the Einstein-Stokes-Lorenz equation is correct, it would be desirable to develop a theory of electrolytic conductance based on a model which resembles the kinetic theory picture of a liquid much more closely than the hydrodynamic model does. The desirability of such an approach has been expressed by others who doubted the validity of the hydrodynamic equation.[23] The theories of Lindemann[24] and of

[21] Kraus, *Properties of Electrically Conducting Systems* (The Chemical Catalog Co., New York, 1922), p. 202.

[22] Fürth, Ann. d. Physik **59**, 409 (1919); **60**, 77 (1919); **63**, 521 (1920).

[a] It is of interest to note that the theory of solutions offers another case in which an erroneous hypothesis yields theoretical equations which are in good agreement with experimental results. The hypothesis that the osmotic pressure of a solution is due to the pressure of the solute, considered as a gas, with the solvent merely supplying the space, will give correct equations for dilute solutions. According to Hildebrand (*Solubility*, Second edition, (1936), p. 21), the limitations of the van't Hoff law were clearly stated by van't Hoff himself; yet the failure of later writers to recognize these limitations obscured certain important aspects of solutions and retarded progress in the theory of solutions.

[23] Davies, reference 20, p. 211; Baars, reference 5, p. 437.

[24] Lindemann, Zeits. f. physik. Chemie **110**, 394 (1924); reference 20, p. 211.

Magnus[25] offered a step in the right direction, and will be discussed later.

The cage model of pure liquids and of solutions offers a simple method of attack of this problem. The temperature coefficient of diffusion is of the order of magnitude of 2 percent to 3 percent per degree. This is much larger than the temperature coefficient of T (0.34 percent at 18°) or of $\bar{L}^2$ ($\frac{2}{3}$ of the coefficient of expansion of the solvent, or, for water, approximately 0.014 percent per degree.) On inspection of Eq. (11), we must conclude that j is the chief contributor to the high value of the temperature coefficient of diffusion. We shall therefore, follow the procedure, quite customary in chemical kinetics, of ascribing the high temperature coefficient to a need for a high heat of activation. In accordance with this well-established practice, we shall represent j in the form of an Arrhenius equation:

$$j=Ae^{-Q/RT}. \tag{12}$$

The physical interpretation of Eq. (12) is as follows: Q is the energy of activation per mol necessary to break through the walls of the cage. A is twice the frequency of oscillation within the cage (since the ion may break through twice in a complete oscillation, each time it reaches the wall). The exponential term gives the fraction of collisions with the wall in which the energy is sufficient to break through it.

Suppose a potential gradient, E, is established in the solution along the X direction in such a sense as to tend to propel the positive ions to the right. It was shown in Section V that the activation effected by the field is exceedingly small as compared with the energy of activation needed for a cage-to-cage jump. Thus, the effect of the field will be wasted on all but two very small classes of ions. There will be a small class of ions whose oscillatory motion is carrying them to the right and whose energy is just a trifle smaller than that necessary to carry them over the summit of the potential barrier. These ions will be carried across the barrier, thanks to the contribution of the electrical field. There will be another class of ions, moving to the left, with only a trifle more energy than that necessary to carry them across the potential barrier. These ions will be prevented by the field from crossing the barrier. The net result will be a very slow migration of each positive ion in the direction of the field. Using modern terminology, we shall state that the introduction of an electrical field lowers slightly the height of the potential barrier for positive ions moving to the right, and raises slightly the height of the barrier for those ions which jump to the left. In each case the change in energy is equal to the product of the force, $n\epsilon E$, by the distance from the average position of the ion in the cage to the summit of the barrier. This distance, for reasons of symmetry, must be equal to $L/2$.

To carry out a quantitative calculation, we shall make the simplifying assumption that one-third of all the ions jump in the X direction and that all the others jump in the plane of $Y-Z$. A more careful analysis, allowing for distribution amongst all possible directions leads to the same final result. We have, then, in the absence of the field:

$$j_{+X}=j_{-X}=\frac{Ae^{-Q/RT}}{6}=\frac{j}{6}. \tag{13}$$

When the field is turned on, the following equations hold:

$$\begin{aligned} j_{+X}&=\frac{Ae^{(-Q+0.5nN\epsilon EL)/RT}}{6};\\ j_{-X}&=\frac{Ae^{(-Q-0.5nN\epsilon EL)/RT}}{6}. \end{aligned} \tag{14}$$

The difference between the two expressions of Eq. (14) gives the net gain along the field, or the net number of jumps per second along the field:

$$j_{+X}-j_{-X}=j_{\text{Field}}=j(n\epsilon EL)/6kT. \tag{15}$$

In the expansion of the exponentials, the higher terms were disregarded. R/N was replaced by the Boltzmann constant. Multiplying the number of jumps along the field by the length of a jump, L, we obtain the absolute velocity of the ion along the field:

$$v=j(n\epsilon E\bar{L}^2)/6kT.^{a} \tag{16}$$

[25] Magnus, Zeits. f. physik. Chemie **174A**, 262 (1935).

[a] There may be some ambiguity in this derivation whether the numerator of the right side of Eq. (16) should contain the average of the square of L or the square of the average of L. In a gas, where the mean free paths vary greatly, the ratio of these two quantities is equal to 2. In a liquid, where the jumps do not vary greatly, the two quantities would be more nearly equal. Nevertheless, to avoid any ambiguity,

Combining Eq. (16) with Eq. (11), we arrive at Eq. (1), obtained by Nernst in 1888 with the use of a hydrodynamic model! The application of the cage method to the more general case of a uni-univalent salt whose ions possess different mobilities leads to Nernst's more general equation:

$$2uv/(u+v)=(E\epsilon D)/kT. \qquad (18)$$

Nernst and others have tested Eq. (18) and have found that it agrees with experimental observations to within a very few percent (Taylor, reference 1, p. 1024). A casual consideration of Eqs. (1), (2), and (3) may lead to the conclusion that the validity of Eq. (1) serves as an indirect proof of the validity of the other two, since the former can be obtained directly from the latter by elimination of the friction coefficient. It should be pointed out, however, that even if the friction coefficient were incorrect as to order of magnitude, its elimination from Eqs. (2) and (3) would leave Eq. (1) unaffected.

VIII. Temperature Coefficients of Mobility, of Diffusion, and of the Frequency of Cage-to-Cage Jumps. The Theories of Lindemann and of Magnus

With the use of Eqs. (1) and (12) we obtain the following relations between the various temperature coefficients and the energy of activation of a cage-to-cage jump:

$$\frac{dv}{v\,dT}=\frac{d\ln v}{dT}=\frac{d\ln D}{dT}-\frac{1}{T}=\frac{Q}{RT^2}-\frac{1}{T}. \qquad (19)$$

In the derivation, the temperature coefficients of A and of L^2 were neglected. Eq. (19) offers a plausible explanation, both of the high temperature coefficients of mobility and of the difference between the temperature coefficients of slow and of fast ions. A large ion requires a higher energy of activation for a cage-to-cage jump than a small ion does. Therefore, the mobility of the former is smaller, but the temperature coefficient of mobility is larger.

The temperature coefficient of mobility of potassium ion is 2.17 percent per degree (Davies, reference 20, p. 205). Substituting this value in Eq. (19), we find that Q is 4230 calories.

it should be stated here that the more rigorous derivation of Eq. (16) demands the use of the mean-squared value of L.

We can now discuss the theories of Lindemann and of Magnus. Both writers emphasized the desirability of substituting the hydrodynamic model by a kinetic one. Since their models are essentially the same, the two theories may be discussed simultaneously. In the model adopted by each the ion moves in a zigzag path. The electrical field contributes a displacement component in the direction of the field in the course of every mean free path. Lindemann's further assumptions lead to a theoretical mobility which is proportional to the length of the free path and inversely proportional to the square root of the temperature. Magnus' assumptions lead to a mobility which is proportional to the square root of the mean free path.

If the behavior of an electrolytic solution approximates that of its cage model, then it follows that the effect of the electric field is wasted on all ions except the very small fraction which happens to reach the potential barrier summit with approximately zero energy. In this fundamental assumption the cage method differs radically from the Lindemann-Magnus methods. However, their approach to the problem need not be judged in the light of the cage theory. A more serious objection is that these two theories predict entirely too low temperature coefficients of mobility.

The mobility of a Lindemann ion is proportional to $L\cdot T^{-\frac{1}{2}}$, where L is the mean free path. These are the only temperature-variable quantities. According to Lindemann's own calculations, the temperature coefficient of L for potassium ion should be approximately 44 times the coefficient of linear expansion of water. The latter is approximately equal to 0.007 percent per degree, at 18°. Allowing for the variation of $T^{-\frac{1}{2}}$, we find that Lindemann's theory leads to the value 0.13 percent per degree for the temperature coefficient of the mobility of potassium ion. This is 16.5 times smaller than the observed coefficient. Magnus' theory would lead to approximately the same value as Lindemann's does.

IX. The Frequency of Oscillation Within the Cage. The Number of Oscillations between Jumps

In Eq. (12), A is double the frequency of oscillation of the ion within a cage. Since j and Q are known, A can now be calculated. Substituting

$j = 1.12 \times 10^{11}$ sec.$^{-1}$ and $Q = 4230$ calories, we get: $A/2 = 8.3 \times 10^{13}$ oscillations per second. Since there is an approximately twofold uncertainty in the value of L, there is a fourfold uncertainty in the value of A.

It is possible to carry out a rough check of this calculation. The "mean free path" of the ion within its cage is given by the ratio of its mean thermal velocity and A, Assuming that the mean thermal velocity of potassium ion is the same as that of a gaseous ion ($M = 39$), its value at 18°C is 4.3×10^4 cm/sec. The "mean free path" is equal to $4.3 \times 10^4 / 16.6 \times 10^{13}$, or 2.6×10^{-10} cm. This value is approximately ten times smaller than the value one would be inclined to predict. However, allowing for the uncertainty in the value of A and for the crudity of the assumption regarding the mean thermal velocity, the agreement is fairly satisfactory.

The number of oscillations between jumps is given by $A/2j$. For potassium ion at 18° this number is 740. It follows that the assumption of complete independence between the directions of two successive jumps is justifiable.

Conclusions

When we attempt to discover the physical significance of the term "steady migration velocity," as applied to a real solution, we conclude that the term has no meaning, since the ions move violently to and fro and respond to the guiding influence of the electrical field during only a very short fraction of their turbulent existence. We suspect that the discussion of the rate of approach to a steady velocity is meaningless *a fortiori* (Table I, items 10, 11, 12).

When we consider the viloence of the Brownian movement and compare it with the placid behavior of the hydrodynamic model (Table I, ratios 16, 19, 20, 22), we are apt to suspect that the violation of some of the fundamental assumptions underlying the derivation of Stokes law would tend to invalidate the conclusions of the hydrodynamic theory. Unfortunately, calculations based on Eq. (3) are not decisive. The computed ionic radii are neither so inaccurate as to discredit this equation, nor are they accurate enough to support it without the introduction of additional assumptions. Under these circumstances, we have two courses open to us: We may make further attempts to strengthen our confidence in the validity of Eq. (3) by means of mathematical analysis, necessarily complicated. Or we may strike out in a different direction, attempting to build a theory based on a model which approximates more closely a real electrolytic solution. The cage model of liquids offers an approach to such a theory.

The hydrodynamic theory offered a promise of yielding the radii of ions. What promise does the cage model offer? First, the model conforms with the spirit of the times; instead of giving a definite description of the path of an ion, as the hydrodynamic theory does, it describes the migration of the ion in terms of its probable behavior in an electric field.

The hydrodynamic theory cannot possibly be depended on to shed any light on the Brownian movement of either the ion or the solvent molecules. The cage method, based on a recognition of the Brownian movement, offers a promise in this direction. It gives immediately the frequency of cage-to-cage jumps.

The cage method offers a plausible explanation of the high temperature coefficient of slow-moving ions. In hands more expert than the writer's, it may throw light on the nature of hydration and on the mechanism of solvent transport by an electric current. It offers the tempting prospect of discovering a kinetic theory approach to the calculation of the effects of inter-ionic attraction, to supplement the hydrodynamic method of the Debye-Hückel-Onsager theory.

If the present paper succeeds in accelerating even slightly the growing interest in the possibilities inherent in the cage model of liquids, it will have served its purpose.

Acknowledgments

The writer deems it a pleasure to acknowledge his indebtedness to Professor William C. Bray, for his encouragement in undertaking this problem; and to Professor Joel H. Hildebrand, for stimulating discussions, in his seminar on the theory of liquids, of some of the ideas expressed in this paper.

An Equation for Transference Numbers

THEODORE SHEDLOVSKY
Laboratories of The Rockefeller Institute for Medical Research, New York, New York
(Received October 4, 1938)

The following transference number equation is proposed,

$$1/t=1/t_0+AC^{\frac{1}{2}}-BC.$$

The values for the constant A are in accord with the Onsager theory for most uni-univalent electrolytes in water, but not for abnormal salts, such as silver nitrate, or for higher valence salts. However, the transference equation appears to have quite general applicability.

SEVERAL years ago the author proposed an equation for electrolytic conductance[1] which reduces to Onsager's[2] theoretical formulation at high dilutions and is useful for extrapolation purposes. It is applicable to most strong uni-univalent electrolytes up to a concentration of about one-tenth normal. An analogous equation for transference numbers has been proposed by Longsworth.[3] However, these equations have forms which are somewhat unwieldy for practical computations and they fail in the case of higher valence salts. In the present communication a simpler transference number equation is presented.

The Onsager theory for conductance yields the following limiting transference number equation

$$t=\frac{\lambda}{\Lambda}=\frac{\lambda_0(1-\alpha C^{\frac{1}{2}})-\beta(Z_1/Z_1+Z_2)C^{\frac{1}{2}}}{\Lambda_0(1-\alpha C^{\frac{1}{2}})-\beta C^{\frac{1}{2}}}, \qquad (1)$$

in which t is the transference number, λ the equivalent conductance of the corresponding ion species of valence Z_1, Z_2 the valence of the other ion species, and α and β are the Onsager constants for the "time of relaxation" and electrophoretic effects, respectively. Neglecting terms of higher order than $C^{\frac{1}{2}}$ in an expansion yields

$$t=t_0-\frac{\beta t_0}{\Lambda_0}\left(\frac{Z_1}{(Z_1+Z_2)t_0}-1\right)C^{\frac{1}{2}}, \qquad (1')$$

in which $t_0=\lambda_0/\Lambda_0$. It will be noted that only the electrophoretic term appears in this equation. Plots of t against $C^{\frac{1}{2}}$, however, generally show considerable curvature. To account for this fact, Longsworth[3] proposed the equation

$$t_0'=\frac{t\Lambda'+(\beta/2)C^{\frac{1}{2}}}{\Lambda'+\beta C^{\frac{1}{2}}}=t_0+BC, \qquad (2)$$

in which $\Lambda'=\Lambda_0-(\alpha\Lambda_0+\beta)C^{\frac{1}{2}}$, based on the modified Onsager formula[1]

$$\Lambda_0=\frac{\Lambda+\beta C^{\frac{1}{2}}}{1-\alpha C^{\frac{1}{2}}}-BC.$$

He found it applicable to his very accurate measurements on strong uni-univalent electrolytes up to $C=0.10N$.

A simpler equation, also reducing to the theoretical limiting Eq. (1'), is the following

$$1/t=1/t_0+AC^{\frac{1}{2}}-BC, \qquad (3)$$

in which $A=(\beta/l_1)[Z_1/(Z_1+Z_2)t_0-1]C^{\frac{1}{2}}$ and B is an empirical constant. For uni-univalent electrolytes in water at 25° $A=(59.79/l_0)(1/2t_0-1)$.

Using Longsworth's[4] transference measurements on NaCl, HCl, LiCl, KCl, KBr, KI, NH_4Cl and $NaC_2H_3O_2$, linear graphs result when the function $(1/t-AC^{\frac{1}{2}})$ is plotted against C, from which the empirical constants B are obtained. In every case the intercepts give values for the limiting transference number, t_0, in accord with those chosen by Longsworth. The comparison in Table I shows the excellent agreement between the experimentally determined values for the transference numbers and the corresponding ones computed from Eq. (3). It is interesting to note that the equation reproduces the slight minima observed for KI, KBr and NH_4Cl.

[1] T. Shedlovsky, J. Am. Chem. Soc. **54**, 1405 (1932).
[2] L. Onsager, Physik. Zeits. **27**, 388 (1926); **28**, 277 (1927).
[3] L. G. Longsworth, J. Am. Chem. Soc. **54**, 2741 (1932). See also, B. B. Owen, *ibid.* **57**, 2441 (1935).
[4] L. G. Longsworth, J. Am. Chem. Soc. **57**, 1185 (1935).

TABLE I. *Cation transference numbers of strong 1−1 electrolytes in water at 25°.*

$1/t^+ = 1/t^+ + AC^{\frac{1}{2}} - BC$; $A = (\beta/l_0^+)1/2t_0^+ - 1$; $\beta = 59.79$.

ELECTROLYTE	C EQUIV./LITER	t^+ CAL.	t^+ OBS.
KCl	0.01	0.4903	0.4902
$A = 0.012$	.02	.4902	.4901
$B = .002$	.05	.4900	.4899
$t_0^+ = .4906$	.10	.4897	.4898
	.20	.4894	.4894
	.50	.4888	.4887
	1.00	.4882	.4883
NaCl	.01	.3918	.3918
$A = 0.312$	.02	.3903	.3902
$B = .250$	.05	.3875	.3876
$t_0^+ = .3963$	.10	.3851	.3854
	.20	.3827	.3821
LiCl	.01	.3290	.3289
$A = 0.749$	.02	.3262	.3261
$B = .453$	.05	.3211	.3211
$t_0^+ = .3368$	.10	.3164	.3168
	.20	.3112	.3112
HCl	.01	.8252	.8251
$A = -0.067$	.02	.8267	.8266
$B = -.058$	.05	.8293	.8292
$t_0^+ = .8210$	.10	.8315	.8314
	.20	.8336	.8337
NaAc	.01	.5538	.5537
$A = -0.110$	.02	.5550	.5550
$B = -.070$	.05	.5572	.5573
$t_0^+ = .5507$	.10	.5593	.5594
	.20	.5616	.5610
KI	.01	.4884	.4884
$A = 0.019$	.02	.4883	.4883
$B = .043$	.05	.4882	.4882
$t_0^+ = .4887$	.10	.4883	.4883
	.20	.4887	.4887
KBr	.01	.4832	.4833
$A = 0.027$	.02	.4831	.4832
$B = .069$	.05	.4831	.4831
$t_0^+ = .4837$	.10	.4833	.4833
	.20	.4841	.4841
NH_4Cl	.01	.4906	.4907
$A = 0.015$	.02	.4906	.4906
$B = .039$	.05	.4906	.4905
$t_0^+ = .4909$	.10	.4907	.4907
	.20	.4912	.4911

For higher valence electrolytes and certain abnormal uni-univalent salts such as silver nitrate, Eq. (3) is not in accord with the transference data if the theoretical Onsager values for the coefficients A are used. However, if A, as well as B, is taken as an empirical constant, the equation is useful in many cases. This is shown by the examples listed in Table II for $CaCl_2$,[4] $AgNO_3$[5] and K_2SO_4.[6] The values for t_0^+ in the "observed" columns were obtained from the limiting conductances and ionic mobilities for these salts,[4, 6] while the constants A and B for Eq. (3) were found from the transference data by the method of least squares. Although the coefficients A are in all these cases considerably lower than would be expected from the Onsager theory, the equation is well in accord with the measurements and gives the correct limiting transference number values. For example, in the case of calcium chloride $t_0^+ = 1 - l_0Cl^-/\Lambda_0 = 1 - 76.34/135.84 = 0.4380$, which is in close agreement with the value 0.4376 obtained from the transference data alone, but the value of $A = 0.6113$ is quite different from the theoretical value $A = 0.965$.

TABLE II. *Cation transference numbers for calcium chloride, silver nitrate and potassium sulfate in water at 25°.*

$1/t^+ = 1/t_0^+ + AC^{\frac{1}{2}} - BC$.

	t^+					
	$CaCl_2$		$AgNO_3$		K_2SO_4	
C EQUIV./LITER	OBS.	CALC.	OBS.	CALC.	OBS.	CALC.
0	(0.4380)	0.4376	(0.4643)	0.4643	(0.480)	0.4780
0.01	.4264	.4264	.4648	.4648	.4829	.4826
.02	.4220	.4221	.4652	.4652	.4848	.4843
.05	.4140	.4141	.4664	.4664	.4870	.4871
.10	.4060	.4057	.4682	.4682	.4890	.4895
.20	.3953	.3952	—	—	.4910	.4916
.50	—	—	—	—	.4909	.4909
A	.6113		−.0085		−.2192	
B	.1411		.155		−.2001	

[5] D. A. MacInnes and L. G. Longsworth, Chem. Rev. **11**, 209 (1932).

[6] G. S. Hartley and G. W. Donaldson, Trans. Faraday Soc. **33**, 457 (1937).

Molecular Interaction in Mixed Monolayers on Aqueous Subsolutions

I. Mixtures of Alcohols, Acids and Amines

WILLIAM D. HARKINS AND ROBERT T. FLORENCE
George Herbert Jones Chemistry Laboratory, University of Chicago, Chicago, Illinois

(Received August 1, 1938)

Mixed films are of fundamental importance in biological systems, so mixtures of long chain alcohols, acids, and amines on acidic and basic subsolutions have been investigated. The principal effect of mixing is to change the conditions with respect to the pressure, area, and temperature at which one surface phase changes into another.

In general a mixture of two liquid films gives a monolayer of the same type, with the mean molecular area: a liquid expanded film is made more condensed by admixture of a substance which gives a condensed film, and the condensing action increases with the length of the hydrocarbon chain; an alcohol condenses an acid more than the corresponding acid. The interaction, or departure from the mean value may be either positive or negative, and on acid subsolutions is greatest when one of the components is an amine. Only in amine-acid mixtures is there an indication of chemical action. The 1 : 1 mixture of stearyl alcohol and stearic acid "freezes" at a much larger area than the film given by either component, so the area of the solid mixed film is abnormally high. The area interaction with an amine present is negative, and the potential interaction has a high value and is positive. Calcium ions in a basic subsolution condense a Type II to a solid Type I monolayer.

1. INTRODUCTION

THE properties of mixed films, that is those which consist of two or more components in addition to water, are of fundamental importance for biology, since membranes are undoubtedly structures built up on one or more mixed monolayers as a foundation. Indeed, the first investigation of mixed films was undertaken by Leathes[1, 2] on account of the supposed importance in biology of monolayers of this type. He found that when the proportions were one (large) molecule of lecithin to two to four of myristic or another fatty acid which gives an expanded film, the effect of the large molecules was to condense the film.

The mutual effect of alcohols and stearic acid in mixtures was one of the topics in an investigation by Harkins and Morgan,[3] and in the present work mixtures of alcohols, acids, and amines of from 14 to 18, and in some cases up to 20 carbon atoms, per molecule have been studied both on acidic and basic subsolutions. A paper by Marsden and Schulman,[4] received after our communication was written, considers two of the mixtures investigated by us, but in no case did they vary the length of the hydrocarbon chain. That we were able to do so is due to the generosity of Emmet E. Reid and Jane E. Meyer, who contributed the large number of extremely pure organic compounds used in this work.

[1] Leathes, Zeits. f. Physiol. Chemie **130**, 113 (1923).
[2] Leathes, Lancet **2**, 853 (1925).
[3] W. D. Harkins and J. W. Morgan, Proc. Nat. Acad. Sci. **11**, 631 (1925).
[4] J. Marsden and J. H. Schulman, Trans. Far. Soc. **34**, 748 (1938).

2. APPARATUS

The film balance, polonium electrode, and dark field microscope used in the investigation of the mixed films were similar to those used in earlier work in this laboratory.

3. MIXTURES OF COMPONENTS EACH OF WHICH GIVES A CONDENSED FILM

For convenience the different types of films are, in this paper, designated by number as follows: I. Condensed film of very low compressibility, usually solid. II. Condensed liquid film of higher compressibility. III. Transition film with a very high compressibility near the transition point. IV. Liquid expanded. V. Vapor expanded. VI. Gaseous.

The pressure-area relations of a mixed monolayer which consists of two components, each of which forms when alone a condensed film, may be illustrated by the behavior of an equimolar mixture of stearic acid (H St) and stearyl alcohol (St OH) as presented in Fig. 1, and as described below:

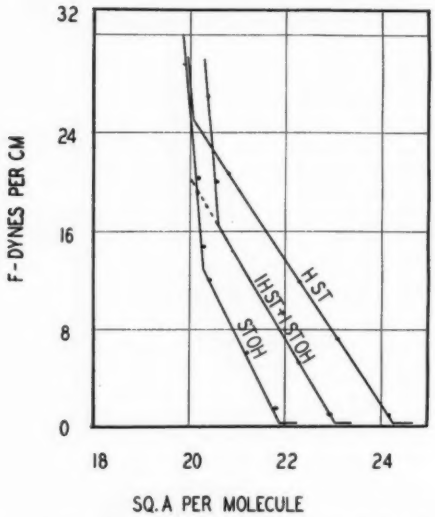

FIG. 1. Mixtures (1 : 1) of condensed films of alcohol and acid (pH = 3) exhibits expansion in solid film only. Note: The experimental points obtained in this work for the first compression of each film lie within the widths of the lines drawn, the dots represent curves obtained by a reduction of the pressure to a low value for one hour and a subsequent recompression of the film.

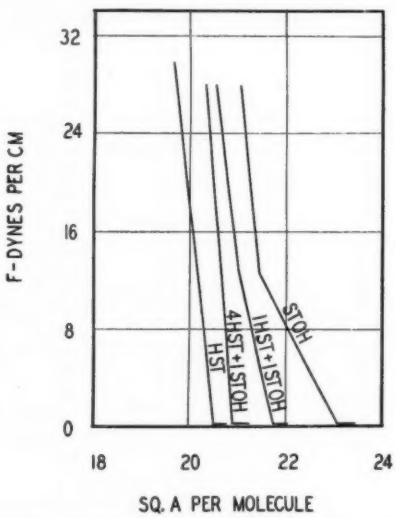

FIG. 2. Mixtures of condensed films of alcohol and calcium stearate (pH = 9.5). The Type II film is eliminated with 80 equivalent percent of calcium stearate, and only the Type I film exists.

1. The Type II, or less condensed film, exhibits a molecular area which is the mean of that given at the same pressure by the pure components. Thus the "limiting areas at zero pressure" as obtained by extrapolation are at 25°C: stearic acid = 24.3, octadecyl alcohol = 21.9, mean value calculated = 23.1, determined = 23.1.

2. The Type I, or more condensed film, has almost exactly the same molecular area in films of either the acid or the alcohol, but for the equimolar mixture the area is much higher (by about 0.75 sq. A). This seems to be due to the fact that the transition II→I occurs in the mixture at a pressure which is much (1.4 dynes) below the mean of the kink points for the films of one component. If the films of Class I are considered as two dimensional solids, then it may be said that the mixed film freezes at a larger molecular area than that of either component.

The experimental points obtained in the work represented by Fig. 1 lie very exactly on the straight lines when these are obtained in the original compression. In order to simplify the figure these points are not given. The dots, which lie very close to, but not so exactly on the lines, were obtained by an additional operation. After the original compression, which gave the linear relations, was completed, the barriers which confined the film were separated widely and the film was allowed to expand for one hour. It was then compressed for a second time, and this recompression gave the data represented by the dots. It is remarkable that the pressure-area relations are so closely the same in the original and the later compression.

4. Effect of Bivalent Ions and of Basic Aqueous Subsolutions (pH = 9.5)

While calcium stearate monolayers have been investigated extensively,[5] the pressure-area relations have been given, so far as we are able to find, in only one paper[6] which presents values for the molecular area which are not sufficiently accurate for our purpose. A more accurate and extensive set of data is presented in this section.

The effect of a basic subsolution which contains sodium without calcium ions is to give not only a condensed film of Type I, but also a lower second limb of the $F-A$ curve which indicates a

[5] R. J. Meyers and W. D. Harkins, Nature **139**, 368 (1937). J. S. Mitchell, E. K. Rideal and J. H. Schulman, ibid. **139**, 626 (1937). J. H. Schulman, ibid. **139**, 626 (1937). C. Robinson, ibid. **139**, 626 (1937). I. Langmuir and V. J. Schaefer, J. Am. Chem. Soc. **59**, 2400 (1937).

[6] W. D. Harkins and T. F. Anderson, J. Am. Chem. Soc. **59**, 2181 (1937).

higher compressibility (Type II). The effect of calcium ion is to eliminate this second type of film and to change it to Type I. With a subsolution with 10^{-3} m $NaHCO_3$, 10^{-4} m $CaCl_2$, and NaOH to give a *p*H of 9.5, the compressibility is reduced to 0.0013 (Fig. 2).

TABLE I. *Increase of area or of surface potential (interaction) above the mean value for mixtures of acids, alcohols, and amines.*

Mixture	*p*H	Area Interaction at Limiting Area (A^2)	Limiting Area (A^2)	Dipole Interaction in mv
Alcohols + Acids (1 : 1)				
18–18	3	+0.02		+33
18–18	9.5	−0.05		+20
18–15	3	−9.6		+2
15–15	3	−4.5		+50
14–15	3	+7.1		+28
18–14	3	−3.7		+29
15–14	3	+5.8		+63 (+3)
14–14	3	+9.5		+42
Acids + Acids (1 : 1)				
20–15	3	−4.3		−27
20–14	3	+2.5		−35
18–14	3	+4.5		—
Alcohol + Amine (1 : 1)				
18–18	3	Approx. −25	21.45	+60
16–18	3	Approx. −25	22.20	+30
14–18	3	Approx. −25	23.60	+26
18–16	3	Approx. −25	22.90	+200
16–16	3	Approx. −25	23.20	+100
14–16	3	Approx. −25	26.25	+200
Acid + Amine (1 : 1)				
18–18	3	Approx. −25	21.6	+200
16–18	3	Approx. −25	(20.4)	+240
15–18	3	Approx. −36	22.8	+105
14–18	3	Approx. −36	22.8	—
18–16	3	Approx. −25	(20.4)	—
16–16	3	Approx. −25	(20.4)	—
14–16	3	Approx. −36	21.6	—
Pure Components				
Alcohols	3		22.0	
18 and 16 acids	3		24.5	
15 and 14 acids	3		47	
18 and 16 amines	3		(Area = 70 A^2 at ½ dyne)	

STEARIC ACID—STEARYL AMINE MIXTURES ON SUBPHASE OF *p*H = 3

6 Mol. S + NH_2 : Mol. HSt	Area at F = 2 dynes (A^2)	Dipole Interaction in mv
(pure $StNH_2$)	55	—
4 : 1	29.2	+140
2 : 1	22.2	+112
1 : 1	20.1	+200
2 : 3	20.8	+103
1 : 3	21.3	+125
1 : 6	23.1	+108
0 (pure HSt)	23.9	—

OCTADECYL ALCOHOL—STEARYL AMINE MIXTURES ON SUBPHASE OF *p*H = 3

Mol. $StNH_2$: Mol. StOH	Area at F = 2 dynes (A^2)	Dipole Interaction in mv
(pure $StNH_2$)	55	—
2 : 1	24.5	+ 30
1 : 1	21.1	+ 60
1 : 2	21.9	+ 60
0 (pure StOH)	21.85	—

The molecular area of this calcium stearate film at 25°C and 0.1 d/cm pressure is 20.5 sq. A, which is practically the same as the extrapolated area at zero pressure for a Type I film of stearic acid (20.6) at the same temperature. On the average each calcium ion attracts two stearate ions but is probably coordinated with the oxygen of four of the carboxyl groups of these ions to give a definite solid lattice. Below the transition pressure of 25 dynes per cm (Fig. 2) the calcium ions have the effect of an increase of pressure on the stearic acid film. Above this pressure the stearic acid and calcium stearate films have practically the same area per equivalent (Figs. 1 and 2).

A monolayer formed from an equimolar mixture of stearic acid and octadecyl alcohol exhibits on this basic subsolution both Types I and II, with the transition pressure at 12.8 dynes at 25°, or practically that of the alcohol. The compressibility of the Type II film is, however, halved, that is from 0.0057 for the pure alcohol to 0.0026 for the mixture. The presence of four molecules of the acid to one of alcohol is sufficient to give enough calcium stearate to eliminate the Type II film, and the compressibility is approximately that found for calcium stearate alone.

At 20 dynes per cm the equivalent mixture of calcium stearate and octadecyl alcohol exhibits an area of 20.8 which is 0.2 sq. A greater than the mean, while the four to one mixture has an area of 20.5 while the calculated area is 20.2.

It is found in general that the liquid film of stearic acid of Type II does not undergo a transition into a Type I (solid) film at *p*H3 if the compression is made slowly, since the liquid film collapses at about the transition pressure. However a sufficiently rapid compression seems to give a Type I film in practically every instance.

5. The Condensing Effects of Alcohols upon Expanded Monolayers of Acids (*p*H = 3)

In mixed films of acids and alcohols the principal types of forces involved are those classified as (1) dipole-dipole, (2) dipole-induced dipole, and (3) van der Waals. Early investigations by

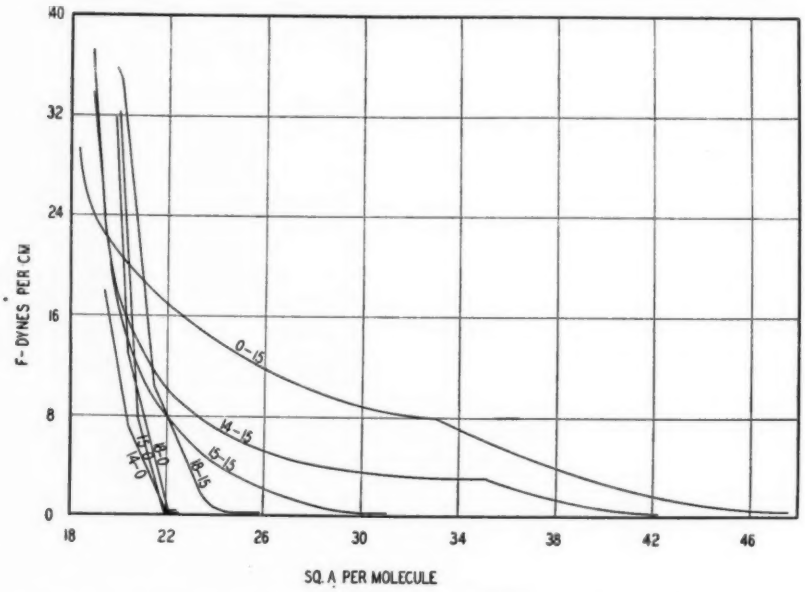

FIG. 3. Mixtures (1 : 1) of condensed alcohol and expanded films of pentadecylic acid. Pentadecylic alcohol eliminates the expanded film of pentadecylic, but not that of myristic acid. The first number gives the number of carbon atoms in the molecule of alcohol, and the second, in the acid.

Harkins and his collaborators[7] indicate that the van der Waals energy of interaction between hydrocarbon chains is, for unit area, of the general order of half that for the dipole-dipole interaction, and that the induced dipole energy is relatively small between hydroxyl or carboxyl, or water, and a hydrocarbon chain. For example, at room temperature the free energy of separation of a hydrocarbon (e.g., octane) from itself, in which van der Waals forces are involved, is the same per unit area as that for the separation of water from octane. The van der Waals forces in the case of water are lessened by the smallness of the water molecules so that van der Waals energy$_{H_2O\text{-}Octane}$+dipole-induced dipole energy$_{H_2O\text{-}Octane}$=van der Waals energy$_{Octane\text{-}Octane}$.

The dipole-dipole interaction between the polar groups of either the acid or the alcohol binds the film firmly to the water. The interaction between the dipoles in the film varies greatly with the relative position of the dipoles. For example, with two equal dipoles the mutual energy is $V=(\mu_1\mu_2/R^3)(\cos\nu-3\cos\theta_1\cos\theta_2)$, where μ is the dipole moment, R the distance between the centers of the dipoles, ν the angle between the vectors of the dipoles and θ_1 and θ_2 are the angles between the straight line connecting the centers of the dipoles and their directions. With dipoles oriented in the same direction in a plane the effect is a repulsion.

Even if the total dipole moments for the alcohol and acid were the same, the orientation and length of the dipoles may be expected to be different, and the size of the group is also different, which affects the value of R. Also the grouping of water molecules around the carboxyl group is undoubtedly different from that around the hydroxyl group.

From this point of view, it is to be expected, especially when one of the substances forms an expanded film, that the molecular interaction will be different in mixtures from that in the one-component monolayers. Thus the molecular area for the mixture may be expected to be either greater or less than that which corresponds to the proper mean value. That there is also a departure from the mean produced by differences in the lengths of the hydrocarbon chains is shown in the figures and in Table I.

[7] W. D. Harkins, F. E. Brown and E. C. H. Davies, J. Am. Chem. Soc. **39**, 354 (1917). W. D. Harkins, G. L. Clark and L. E. Roberts, J. Am. Chem. Soc. **42**, 700 (1920). W. D. Harkins and Y. C. Cheng, J. Am. Chem. Soc. **43**, 35 (1921).

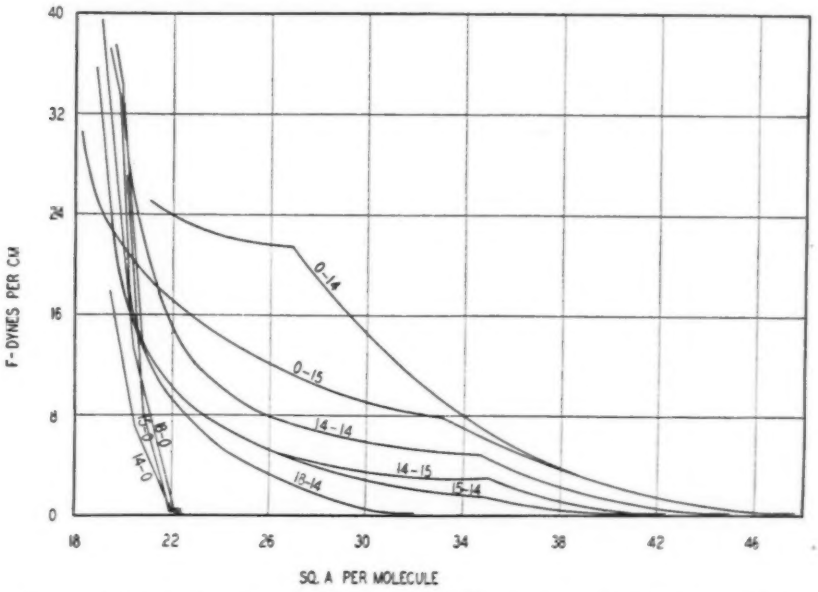

FIG. 4. Mixtures (1 : 1) of condensed alcohol films and expanded films of myristic acid (pH = 3). The curve for myristyl alcohol with pentadecylic (acid (14–15) is added for comparison with the effect produced with interchange of number of carbon atoms in the alcohol and acid). Stearyl alcohol does not condense the myristic acid, while it does the pentadecylic acid film (Fig. 3).

The same type of reasoning indicates that the surface potentials (ΔV) should not in general be additive in mixtures.

Relations of this general type are explained by Schulman and Hughes[8] and Schulman and Rideal[9] as due to compound formation; but that is not the view expressed here.

Alcohols with 14 or more carbon atoms per molecule form highly condensed films of Type I, at high, and II at low pressures. These substances reduce greatly the extent of the expansion in expanded (Type IV) and transition (Type III) films. However, the mixture may exhibit an area either higher (+) or lower (−) than the mean value, and in Table I this is represented as the interaction in sq. A at the limiting area for the film. This is the area at which the pressure begins to rise rapidly above that of the vapor from the film.

In both Table I and Figs. 3 and 4 the number in the first column or on the curve represent first the number of carbon atoms in the hydrocarbon chain of the alcohol, and second, of the acid. Thus 18–15 represents a mixture of octadecyl alcohol and pentadecylic acid. As compared with the mean value the relations which are obtained may be noted as follows:

(1) A contraction occurs if in mixtures with pentadecylic acid the alcohol chain is of the same length or longer than that of the acid.

(2) Expansion is exhibited if the alcohol chain is the shorter.

(3) With myristic acid there is contraction if the alcohol chain is much longer (i.e. 18–14) but expansion if the alcohol chain is one atom longer or of the same length.

It is of considerable interest that in an equimolecular mixture any alcohol of greater length than 14 carbon atoms eliminates the expanded film and leaves only the transition film (15–15, Fig. 3) or the liquid (II) film (18–15). That is, the transition pressure (IV→III) or kink, is depressed to negative film pressures.

It is found (Fig. 4) that equimolecular mixtures of the 14 alcohol with 15 acid, and of 15 alcohol with 14 acid, give the same pressure-area curve for the transition film over a considerable region, but the expanded film exhibits a considerably higher pressure if the acid chain is the longer.

[8] Schulman and Hughes, Biochem. p. **29**, 1243 (1935).
[9] Schulman and Rideal, Proc. Roy. Soc. **B122**, 29 (1937).

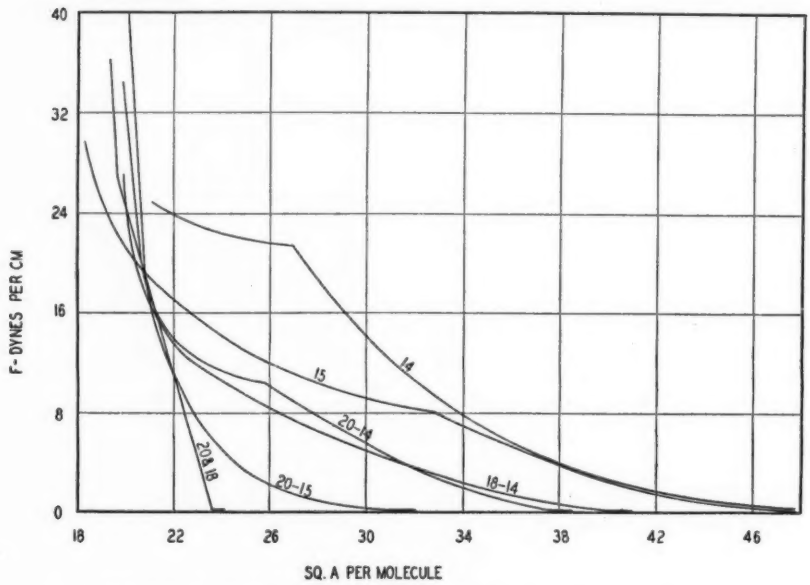

FIG. 5. Mixtures of condensed and expanded acid films (pH = 3). Arachidic, stearic, pentadecylic, and myristic acids. The pressure-area values for the 20–14 and 18–14 mixtures are almost the same, but the position of the transition point expanded transition (IV→III) is affected by an extremely large shift.

With myristic acid stearyl alcohol inhibits the expanded film, but pentadecyl alcohol permits its existence.

Since the molecular interaction is expressed in sq. A at the limiting area it is not surprising that there is an expansion with reference to the mean when the mixed film at this area is an expanded one, and a contraction when the film is of either Class II or III.

If the mixed film is of the transition type and that of the acid expanded, the relation is reversed. Thus at 7 dynes the interaction is −6.2 sq. A for the 14–15 mixture while it is +7.1 at the limiting area.

Thus the sign and magnitude of the interaction depends upon the effect of the mixing upon the state or class of the film which is produced.

Increasing the chain length of the condensing agent has the same effect as a lowering of temperature even though this effect is not apparent with the pure alcohols with from 14 to 18 carbon atoms. Increasing the chain length of the expanded acid has a similar effect.

The deviation from the mean of the surface potential for the alcohol-acid monolayers is positive in all cases, and is smallest in magnitude when the difference in chain length is greatest. The greatest interaction in mv is 63 for the 15 alcohol—14 acid, and 50 for the 15–15 mixture. These are the largest interactions as measured by the potentials.

6. Films of Mixed Acids

Films of mixed acids (Fig. 5) exhibit the same general relations as those which consist of an acid and an alcohol except that long chain acid condenses an expanded film of an acid much less than the alcohol with the same number of carbon atoms. For example, at an area of 26 sq. A the equimolecular mixture of the 18 and 14 acids gives a film pressure of 8.5 dynes/cm, while with the 18 alcohol the 14 acid it is only 3.3 dynes. This is related to the fact that Type II alcohol films are much more condensed than those of the same type with acids.

One component films of arachidic (20) or stearic (18) acid exhibit practically the same pressure area relations for the liquid film, and when mixed in equimolecular proportions with myristic acid give almost the same values. In the case of the mixtures the interaction in terms of the surface potential is negative (Table I), which is the opposite sign from that for alcohol-acid mixtures.

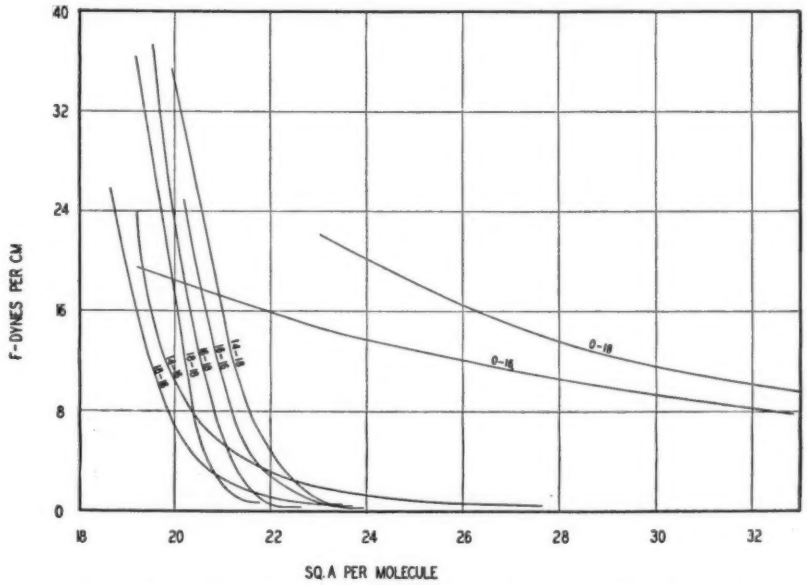

FIG. 6. Mixtures (1 : 1) of condensed alcohol and vapor-expanded amine films (pH = 3). For the one-component alcohol films see Fig. 3 or Fig. 4. The curves at the lower pressures are of the transition type. The first number gives the number of carbon atoms in the alcohol, and the second in the amine, molecule. The 14–16, and 18–16 mixtures have a high compressibility.

In mixtures of the 22–14 acids Adam and Jessop[10] were unable to detect an appreciable condensation but in this work the 20–15 mixture gave a decrease from the mean of 4.3 sq. A at the limiting area, but only 0.25 sq. A at 8 dynes per cm. These involve comparisons of expanded films for the pure 14-component and the mixture. At 12 dynes the condensation is 6.3 sq. A, but here the mixture is in the transition state. These facts indicate that for an understanding of the relations between the films of pure components and the mixtures in all of this work it is essential to study the entire curves as presented in the figures.

7. Positive Ions in Mixed Films (pH = 3)

Alcohol-amine mixtures

The use of amines on dilute acid subsolutions (pH = 3) gives an opportunity to investigate the effect of a positive ion of an organic type. In alcohol mixtures this gives rise to an ion-dipole effect. The pure amines on acids give vapor-expanded films of extremely high expansion, but these are very greatly condensed by the addition of an equal number of molecules of the 14 to 18 alcohols (Fig. 6). Of the mixtures that in which both the amine and the alcohol have 18 carbon atoms gives the closest approach to a solid film of Type I, with an extrapolated area at zero compression of 20.7 sq. A, which is the normal value for solid condensed films. All of the other mixtures give curves of the general type exhibited by transition films of Type III.

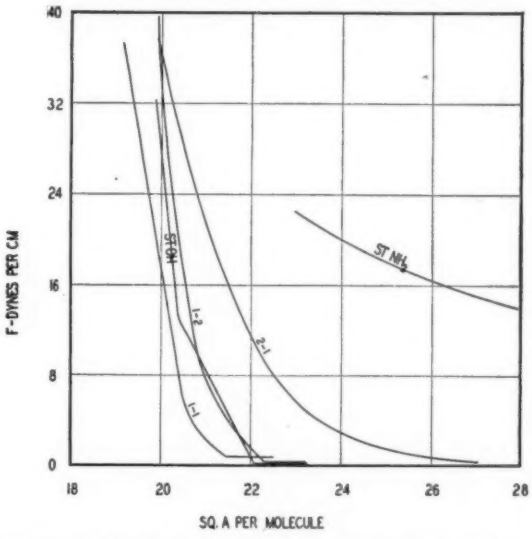

FIG. 7. Effect of proportions in mixed stearyl alcohol and amine films (pH = 3). The first figure gives the number of molecules of amine and the second of alcohol. The 1 : 1 mixture exhibits the greatest condensation.

[10] N. K. Adam and G. Jessop, Proc. Roy. Soc. **A120**, 473 (1928).

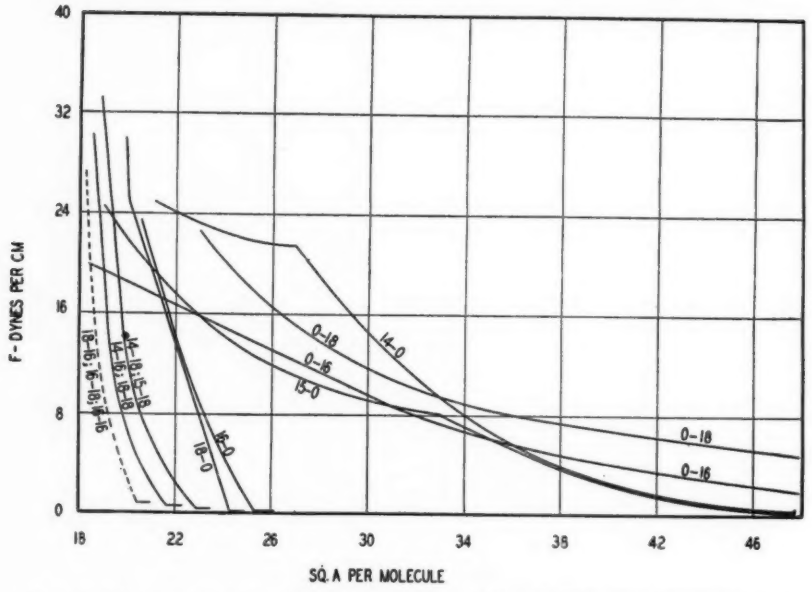

FIG. 8. Mixtures (1 : 1) of acids and amines (pH = 3). The first figure gives the number of carbon atoms in the acid, and the second in the amine, molecule. All of the seven mixtures exhibit pressure-area curves of the same form, and with not very widely differing and very low areas. At the lower pressure all the mixtures give curves of the transition form.

At the low pressure of the limiting area the 14 alcohol and the 16 amine give the highest, and the 18–18 mixture the lowest area, as might have been predicted, but at the higher pressures the order is shifted on account of the fact that the 14–16 mixture is by far the most compressible, as is normal.

Mixtures which contain the amine not only give abnormally low areas at the high pressures, but they also exhibit extremely high positive deviations $\Delta(\Delta V)$ of the surface potential from the mean values. Thus (Table I) the interaction was +200 mv for the 18–16, 100 mv for the 16–16, and 200 mv for the 14–16 mixture, if the first number of each pair refers to the alcohol and the second to the amine. The mixtures with octadecyl (stearyl) amine give potential deviations of the same sign and order of magnitude as those found with alcohol-acid mixtures, that is 25 to 60 mv. The large deviations with cetyl amine as listed above were the maxima, and it is not certain that the films were molecularly homogeneous. This will be investigated later by the use of our ultramicroscopic equipment.

The effect of changing the proportions in the alcohol amine mixtures is exhibited in Fig. 7. It may be noted that the 1 : 1 mixture gives the lowest area, and that one molecule of stearyl alcohol to two of the stearyl amine was not sufficient to give a Type I solid film, though in Fig. 6 it has been shown that 1 : 1 produces the transformation.

Acid-amine mixtures (pH = 3)

When an organic acid is present in the mixture there is the possibility of a chemical action with the positive ion of the amine, so an even more powerful condensing action is to be expected. Thus it is not surprising that a mixture of myristic acid with either cetyl or stearyl amine, both of which when alone form very highly expanded films at 25°C, gives a highly condensed film, but in no case is the relation between film pressure and molecular area linear (Fig. 8). The positive deviation of the surface potential from the mean is very high (Table I) of the order of 200 mv, and is highest for the equimolar mixture.

In the acid : amine mixtures examined, 14–18, 15–18, 16–18, 18–18, 14–16, 16–16, 18–16, there is no evidence of a definite effect of chain length. All of the curves for the mixtures are seen to be practically parallel, and of the same form, and the difference in area is not very significant.

The effect of a change of the relative propor-

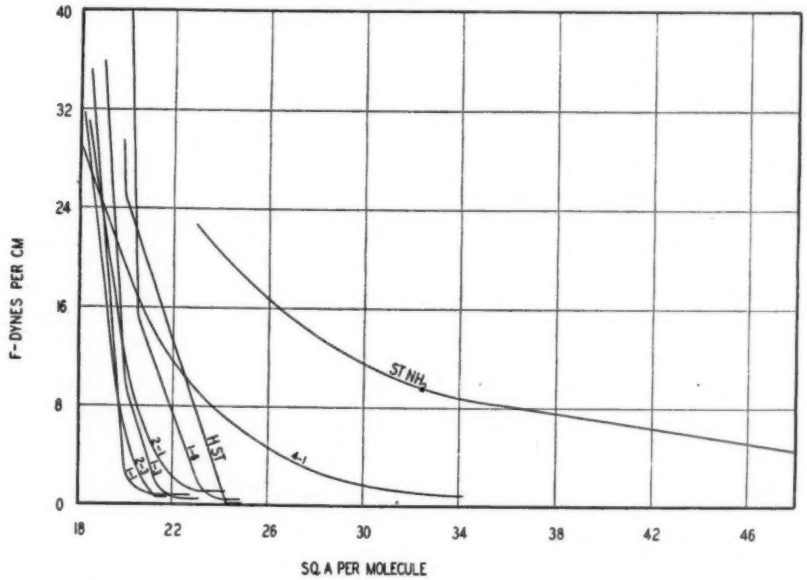

FIG. 9. Effect of proportions in mixed films of stearyl amine and stearic acid (pH = 3). The numbers on the curves give the ratio mole of amine to acid. The 1 : 1 mixture exhibits the greatest condensation with very low molecular areas, and above 3 dynes the low compressibility 0.0023 (at $F=0$ extrapolated) or a Type I film, while the similar value for one-component stearyl alcohol I film is 0.0024. With 75 molar percent of acid the sharp transition II→I or liquid to solid is preserved, but seemingly not with 66⅔ percent.

tions of stearyl amine and stearic acid is presented in Fig. 9, where for example 4 : 1 means 4 molecules of amine to one of acid. The 1 : 1 mixture is found to give the minimum area and the greatest interaction of the potentials (200 mv).

The pressure of the transition for the mixtures Phase II→Phase I is lowered, as the proportion of the amine is increased, from 25 dynes/cm for the pure acid, to 15.4 for one-seventh amine, to 9.8 for one-fourth amine, and the transition point disappears for two-fifths amine or more.

The effect of changes of the proportions in a mixed film of stearic acid and stearyl amine, as given in Fig. 9, is to give a maximum in the potential interaction and a minimum in that of the area for a 1 : 1 proportion.

8. DISCUSSION

It was believed by Adam and Jessop[11] that the condensing action of cholesterol upon expanded films of myristic acid, is due to the "mechanical" action of its large molecules upon the motions of the smaller ones. They found this effect to be small when myristic acid is replaced by substances which give vapor expanded films.

It has been found in our work that shortening the hydrocarbon chain of either the molecules which give condensed or expanded one-component films, increases the expansion of the mixture, as is to be expected on account of the increase in the van der Waals forces with the length of the chain, except when long chain acids and amines are mixed, when the effect disappears, presumably due to compound formation. The condensing effect is greatest with the 1 : 1 mixture and in the potential interaction. This last effect is also a maximum for the 1 : 1 mixture of the amine with the alcohol.

For equal chain length, the acid is found to have a greater condensing effect on the amine than does the alcohol, even though the alcohol itself is more condensed. This is presumably due to compound formation. But with expanded saturated acids the alcohol has a greater condensing effect than an acid; the amine has again the greatest effect, which suggests that a compound may be formed.

[11] N. K. Adam and G. Jessop, Proc. Roy. Soc. **A120**, 474 (1928).

Molecular Interaction in Mixed Monolayers

II. Unstable Mixtures with Unsaturated Acids

ROBERT T. FLORENCE AND WILLIAM D. HARKINS
George Herbert Jones Chemistry Laboratory, University of Chicago, Chicago, Illinois

(Received August 1, 1938)

This investigation concerns the effect of the form of a molecule, with otherwise identical composition and structure, on its binding to the acidic or basic water of the subphase and to the molecules of the film itself. The binding to the water by the carboxyl group should be approximately the same for stearic acid and for the unsaturated acids, oleic and elaidic acid, with the double bond in the middle of the hydrocarbon chain. By compression of the film oleic acid may be squeezed out practically completely, from a mixed monolayer in which a saturated long chain alcohol, acid, or amine is the other constituent. Thus the energy of binding of the oleic acid to the other molecules in the film is weaker than that between the saturated molecules. However, earlier work in this laboratory has shown that the presence of the double bond does not decrease, but very slightly increases, the attraction between molecules.

Thus it seems to be the shape of the molecule which reduces the energy of binding of oleic acid in the film. Oleic acid is a *cis* form, so a nine carbon atom chain R_2 is bent backward with respect to the other $9C$ chain R_1 which ends in the carboxyl group. It may be assumed that the whole molecule is free to rotate, with the carboxyl group in contact with the water, and that the group R_2 is free to vibrate or "flagellate." Thus the oleic acid molecule would occupy a larger area than a saturated acid and this increased distance together with a lessening of the length of the contact between this and the other molecules in the film, decreases greatly the energy of binding. Space models of oleic and elaidic acid have been used in the study of these relations.

By a greater straightening of the chain, as in the trans-compound, elaidic acid, the energy of binding should become intermediate between that of oleic and stearic acid, and much above that for oleic acid. On this basis compression should segregate elaidic acid slightly from the mixed film, but by no means completely, and this is what the experiments demonstrate.

1. Mixtures with Oleic Acid on Acid Subsolutions

MIXTURES of oleic acid with cetyl alcohol, tripalmitin, and triolein have been investigated by Schulman[1] who found that in every case the film was unstable above the collapse pressure of the component which has the lower collapse pressure. Our investigation was undertaken in order to extend the observations to a considerable number of other mixtures, and in an attempt to find an explanation for the phenomenon.

The pressure area relations for mixtures of oleic acid on $0.001N$ sulphuric acid with stearyl alcohol, stearic acid and stearyl amine are presented in Fig. 1.

At a pressure of 5 dynes/cm the molecular area of the mixture is somewhat larger than the mean value (Table I). With any of the mixtures the pressure rises only very slowly as the area is decreased after the collapse pressure of oleic acid is reached. At about this pressure (Fig. 1) lenses, presumably of oleic acid, appear in the field of the dark field microscope used for observation. In a 1:1 mixture the pressure begins to rise abruptly at an area of about 10.5 sq. A for the mixture, which is about 21 sq. A for the substance, stearic acid, stearyl amine, or stearyl alcohol, left in the film. At areas at which lenses begin to be squeezed out, the surface potential (ΔV) remains constant at the mean value for the mixtures which contain the stearic acid or stearyl alcohol. With stearyl amine the potential was 85 mv above the mean value.

After the abrupt rise in pressure obtained after all of the oleic acid had been squeezed out of the mixed film, the potential obtained was very nearly that of the pure stearic acid, stearyl alcohol or stearyl amine, respectively. This is in accord with the hypothesis that the oleic acid has been squeezed out. For example at this final collapse the surface potential for the mixture is 686 mv which is practically the value found for a film of pure stearyl amine.

Before this work was begun a hypothesis was developed to explain the squeezing out of oleic

[1] J. H. Schulman, J. Biochem. **29**, 1243 (1935).

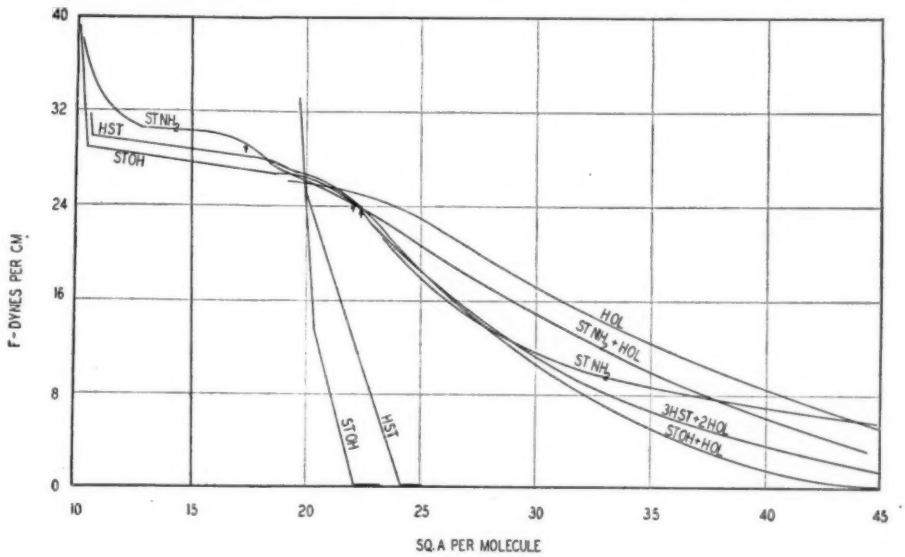

FIG. 1. Pressure-area relations of an oleic acid monolayer, and of mixtures of oleic acid (HOl) with stearyl alcohol (StOH), stearic acid (HSt), and stearyl amine ($StNH_2$) on a subsolution of *p*H 3. The arrows represent the points at which lenses of oleic acid become visible in the ultramicroscope. Since at the extreme left all of the oleic acid has been squeezed out, the figure has been drawn in such a way that the values of the area multiplied by two give the areas for the constituent left in the film: e.g. the almost vertical line at 10.5 sq. A for the mixture of oleic acid and stearyl alcohol indicates that the molecular area for the alcohol left alone in the film is 21 sq. A.

acid from these films. Now oleic acid is a *cis* form of acid with the double bond in the middle of the chain, and elaidic acid is the corresponding *trans* form. The hypothesis predicted that elaidic acid would be squeezed out from similar mixtures with more difficulty and much less completely. Before the relations are discussed it will be convenient to have available the data for mixtures with this acid.

2. Mixtures with Elaidic Acid on Acid Subsolutions (*p*H = 3)

Elaidic acid which is the *trans* form is a solid at ordinary temperatures. Its geometric isomer is the *cis* form, or oleic acid, which is a liquid. Both acids form expanded films at 25° on 0.001N sulphuric acid. The limiting areas are 61 sq. A for oleic and 51.5 sq. A for elaidic acid. At a molecular area of 30 sq. A the film pressure is 17 dynes/cm for oleic, and 18.4 dynes/cm for elaidic acid, but the latter suffers a more definite collapse. The pressure attained at collapse is well known to depend upon the rapidity of compression, but in the special experiment with elaidic acid this occurred at 22 dynes/cm, and 28.6 sq. A (Fig. 2), whereas with oleic acid the collapse was at a much lower area and a higher pressure (Fig. 1). The expansion temperatures have been estimated by Adam[2] as $-30°$ for oleic and $+6°$ for elaidic acid. That collapse occurred with elaidic acid at the values given was indicated by the appearance of a point structure in the field of the ultramicroscope.

The mixtures with elaidic are much more condensed than those with oleic acid. The extremely striking difference appears in the mixtures with stearyl amine. Thus, of the mixtures investigated, those of stearyl amine are the least condensed with oleic, and the most condensed with elaidic acid, and at 5 dynes/cm the area of the former mixture is 1 sq. A greater, and the latter 23.6 sq. A less, than the mean value. This is a remarkable condensing action in which the mixture of two highly expanded films gives a highly condensed film though the condensation is not so great at low pressures as with the saturated acids which form expanded films. At the same pressure the mixture of elaidic acid with stearyl alcohol gives a condensation of 4.6 sq. A, while

[2] Adam, Proc. Roy. Soc. **A101**, 516 (1922).

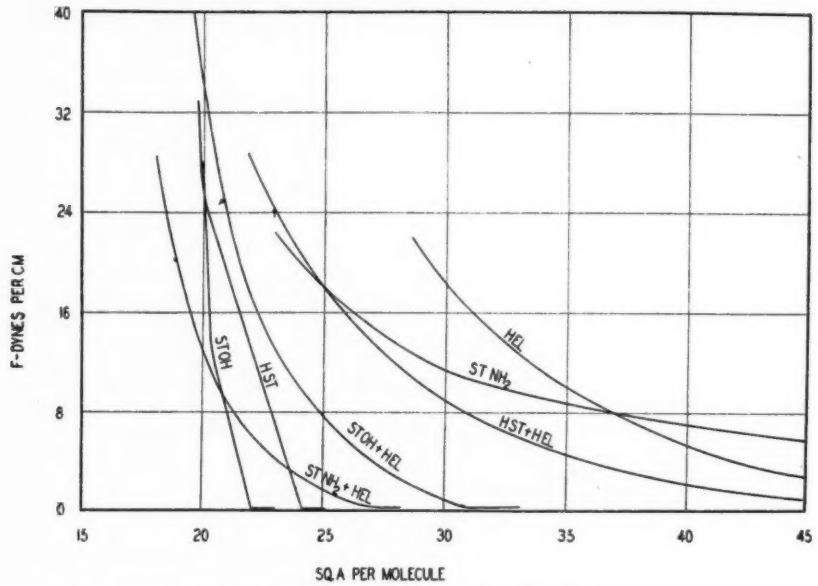

FIG. 2. Mixtures (1 : 1) of elaidic acid with stearyl alcohol, amine, and stearic acid on a subsolution of *p*H 3.

the action of oleic acid is always an expansion: equal to 3 sq. A with stearic acid (2: 3), 1.7 with octadecyl alcohol, and 1.0 with stearyl amine.

The increase of surface potential for mixtures with elaidic acid is 50 mv for stearic acid, 30 mv for octadecyl alcohol, and about 100 mv for the amine.

The behavior of the mixture of the amine with elaidic acid suggests a chemical combination of the two, but that of the mixed film with oleic acid gives no such suggestion.

TABLE I. *Equimolar* mixtures of elaidic or oleic acid with stearyl alcohol, stearic acid, or stearyl amine at* pH = 3.

MIXTURE	AREA INTERACTION AT F = 5 DYNES (A^2)	LIMITING AREA (A^2)	DIPOLE INTERACTION AT LENS PT. (M.V.)	ΔV AT FINAL COLLAPSE (M.V.)
HOl		61.2		+310
*HOl+HSt (2 : 3)	+3.0	50.0	+5	+365
HOl+StOH	+1.7	44.0	+7	+440
HOl+$StNH_2$	+1.0	55.0	+85	+686
HEl		51.5		+250
HEl+HSt	+3.0	47.5	+50	+370
HEl+StOH	−4.6	30.9	+30	+385
HEl+$StNH_2$	−23.6	27.2	(+100)	—
† *Same mixtures on* pH = 9.5.				
HOl		41.0		+225
†HOl+HSt (1 : 1)	+0.5	32.0	+100	+150
HOl+StOH	−1.5	32.0	+20	+347
HOl+$StNH_2$	+6.0	42.0	+5	+525
HEl		(35)		−70
HEl+HSt	Appr. 0	(33)	+60	+230
HEl+StOH	−4.8	23.5	+6	—
HEl+$StNH_2$	−6.1	22.4	+215	+510
HSt		24.3		+385
StOH pH = 3		22.1		+455
$StNH_2$		∞		+680
HSt		20.5		−85
StOH pH = 9.5		23.0		+410
$StNH_2$		23.0		+660

3. MIXTURES WITH OLEIC ACID ON BASIC SUBSOLUTIONS (pH = 9.5)

The subsolution used for these experiments contained 10^{-3} m sodium bicarbonate, 10^{-4} m calcium chloride, and sodium hydroxide to give a pH of 9.5. When oleic acid is spread on this solution, the effect of the calcium ions is not great enough to condense the film of oleate ions, although the expanded film is much less expanded than that of oleic acid on an acidic subsolution. Stearyl amine spreads in a molecular form and at low pressures forms a condensed film of Type II, which at 19.4 dynes and 20.8 sq. A transforms into Type I.

The most remarkable feature exhibited by the mixtures is that although a stearyl amine film is highly condensed, its presence in the oleate film expands the latter even more (Fig. 3). Mixtures

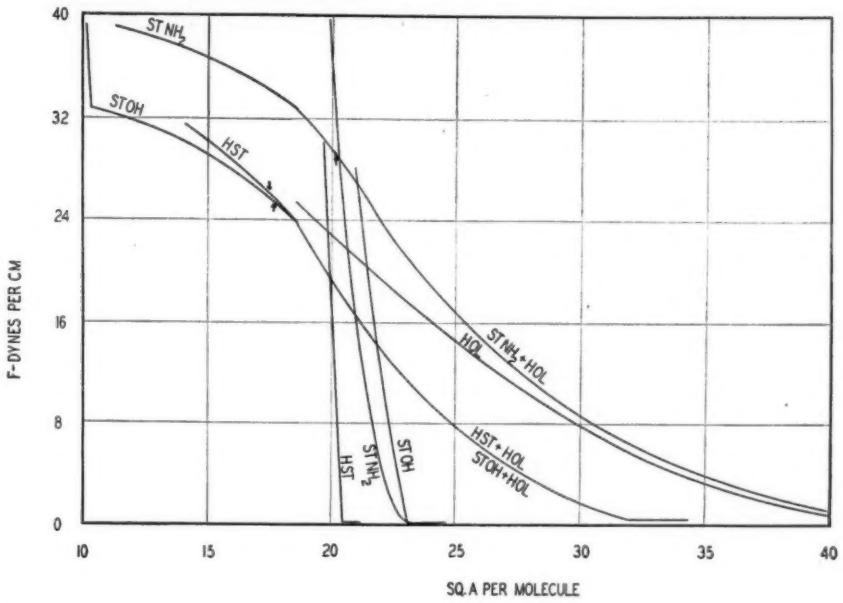

FIG. 3. Mixtures (1 : 1) of oleic acid with stearyl alcohol, amine, and stearic acid on a subsolution of *p*H 9.5 (10^{-3} $NaHCO_3$, 10^{-4} $CaCl_2$ plus NaOH).

with stearic acid or stearyl alcohol are slightly less expanded than on acid subsolutions.

The surface potentials of the mixtures with stearyl alcohol and stearyl amine exhibited almost no departure from the mean, but that with the stearate was 100 mv higher, and passed through a maximum at the lens point for oleic acid. On this subsolution the surface potential is +230 for the oleate, and −85 for the stearate, so forcing the oleic acid out of the film lowers the surface potential.

On further compression the oleic acid was apparently squeezed out of the film, since the pressure began to rise very abruptly in all cases between 20 and 25 A^2 when calculated as if the stearate, stearyl alcohol, or stearyl amine is the only constituent present. Thus the values are practically those for these pure one-component films.

4. Mixtures with Elaidic Acid on Basic Subsolutions (*p*H = 9.5)

If elaidic acid is spread on the same basic subsolution, the 1 : 1 mixed film with stearyl amine is highly condensed, with even smaller areas than that of the pure amine (Fig. 4) instead of being more expanded than the expanded component, or than the mixed film with oleic acid. The elaidate film is itself less expanded (limiting area 35 sq. A) than that of the oleate (41 sq. A). The mixture of the elaidate and stearate is nearly as much expanded as the pure elaidate, but the other mixtures, with the alcohol and the amine are, in contrast with those with the oleate, highly condensed.

The pure elaidate on this subsolution, even although calcium ion is present, is quite soluble, so it is not easy to obtain accurate values for the molecular area, but the film collapses at about 20 to 25 dynes per cm. The surface potential is about −70 mv, while that of the oleate is +230 mv. Neither pressure-area nor the potential *versus* area curve shows a horizontal portion below 40 dynes.

The elaidate-stearate mixture (expanded) is soluble, but the mixtures which form condensed films are only very slightly soluble. Schulman[1] found earlier that one somewhat soluble component may become much less soluble when a stable mixed film is produced.

The potential interaction is +215 mv for the stearyl amine-elaidate mixture, or of the same order as with a saturated acid, but even although the stearyl alcohol-elaidate mixture is highly condensed the interaction is only +6 mv.

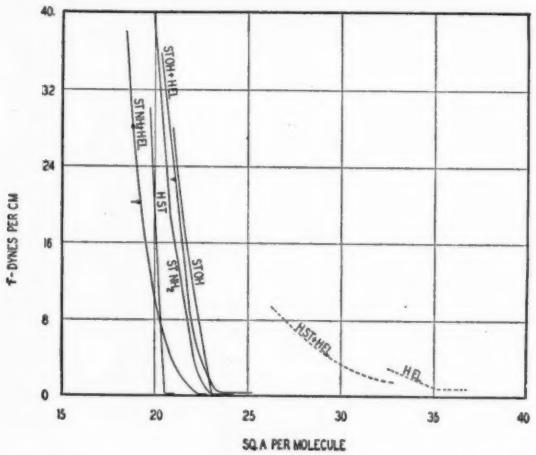

FIG. 4. Mixtures 1 : 1 of elaidic acid with stearyl alcohol, amine, and stearic acid on a basic subsolution (same as for Fig. 3).

While Fig. 4 indicates that the elaidate constituent begins to separate out from the mixtures, as shown by a point structure shown in the dark-field microscope, at 20 dynes/cm with stearyl alcohol, the relations are very different from those in which oleate is present, since this does not bring about a collapse of the film. Obviously very little elaidate separates. It is possible that the extent of the separation would be greater if the film were compressed with extreme slowness.

5. Discussion and Conclusions

The fact that oleic acid is easily squeezed out from its mixtures with substances which give condensed one-component films, was explained by Schulman[3] as due to a "reduction of the adhering qualities between hydrocarbon groups" caused by the presence of a double instead of one single bond in the chain. Since, however, both the work of Harkins and his collaborators[4–6] and modern theory indicate a very slight increase in the primary attraction due to the increased polarity, it is important to see if the difference is due instead to the space relations involved.

Since oleic acid is a ciscompound, it seemed that the bending back of the hydrocarbon chain must increase the distance between an oleic acid molecule and its neighbors, which lessens the attraction between it and the hydrocarbon chains, particularly since the molecule is free to rotate and the doubled-back portions of the hydrocarbon chain may in the mixed film sweep out a larger area. The various orientations which the different groups in both the molecule of oleic and that of elaidic acid may assume by rotation and vibration have been studied by the use of space models, and while the relations are complicated, they seem to justify the conclusion that on the average a molecule of oleic should occupy more area in a monolayer than one of elaidic acid. The plane formulas on paper give a misleading picture as compared with that presented by the space models.

From this standpoint it seemed that the use of the transcompound, elaidic acid, should reduce the effect, but not eliminate it, and the experimental work showed, as has been seen, that this is true. The most marked difference was found on a basic solution with calcium ion, on which the mixture of the two expanded films gave with the elaidate and stearyl amine a highly condensed film, while the oleate-amine mixture was even more expanded than the oleate alone.

On an acid subsolution the film of pure elaidic acid is less expanded at low and more expanded at high pressure than that of oleic acid, that is the former is much less compressible than the latter. The mixtures with elaidic acid are very much the more condensed, and with stearyl amine seems to indicate compound formation, while that with oleic acid does not. As found with saturated expanded acids in the preceding paper, the amine has the greatest condensing effect and the acid the least, with the alcohol intermediate.

[3] J. H. Schulman, Trans. Faraday Soc. **33**, 1118 (1937).
[4] W. D. Harkins, F. E. Brown and E. C. H. Davies, J. Am. Chem. Soc. **39**, 354 (1917).
[5] W. D. Harkins, G. L. Clark and L. E. Roberts, J. Am. Chem. Soc. **42**, 700 (1920).
[6] W. D. Harkins and Y. C. Cheng, J. Am. Chem. Soc. **43**, 35 (1921).

Migration and Photochemical Action of Excitation Energy in Crystals

JAMES FRANCK, *University of Chicago, Chicago, Illinois*

AND

EDWARD TELLER, *George Washington University, Washington, D. C.*

(Received October 1, 1938)

A crystal which has absorbed a light quantum can be treated either as an assembly of molecules or else as a giant molecule. If the exchange of excitation energy between crystal cells is slow as compared to the periods of vibration, the first description is preferable; if it is fast, the second picture is better. Both cases are discussed in connection with the following question: To what extent can excitation energy absorbed by an arbitrary cell of the crystal be used photochemically at a specific point which may be far removed from the absorbing cell? The results are applied to the behavior of polymerized pseudoisocyanines, to the hypothetical photosynthetic unit and to the theory of sensitized photographic plates.

PHOTOCHEMICAL processes in crystals and on crystalline surfaces have been subject recently to several discussions. The fact that according to quantum mechanics the excitation energy may be propagated in a crystal seemed to offer possible explanations for some important photochemical processes. For instance it has been proposed that several quanta absorbed by different molecules in a sensitized photographic plate are propagated to one silver ion and cooperate to dissociate it. In a similar way it has been assumed that in the photosynthetic process in plants thousands of chlorophyl molecules combine to form a photosynthetic unit; light-energy absorbed by any one of them is carried to one and the same CO_2 molecule and effects there photoreduction. In fact, the possibility of a collective interaction of molecules in a crystal with light has not only been postulated by theory, but has also been observed directly in experiments of Scheibe and Jelley on pseudoisocyanine. Here association of molecules into complexes containing a very great number of molecules is accompanied with the appearance of a new narrow absorption band; fluorescence in the wave-length of the incident light and also the phenomenon of quenching have been observed.

Our purpose in the present paper is to discuss the possibilities and limitations of photochemical processes in crystals from a theoretical point of view. The results will be applied to the examples mentioned above.

The interaction of light with crystals and the behavior of crystals in the excited state has been discussed by Peierls[1] and Frenkel.[2] Their results are of fundamental importance in crystal photochemistry. It will be necessary therefore to repeat many points which have been discussed in their papers.

1. PROPAGATION OF EXCITATION. THE EXCITON

A crystal consists of identical elementary cells, which may be atoms, molecules or groups of atoms, molecules or ions. If a crystal is excited, the excitation may be localized in any one of these elementary cells. Such a localized excitation will not represent, however, a stationary state. The coupling between the particles in the crystal and the resonance caused by the identity of the crystal cells has the consequence that the excitation energy will be transferred from one crystal cell to another. A stationary state will be obtained according to Frenkel and Peierls by assuming that any one of the N crystal cells may be excited and that the excitations of the crystal cells shall be superimposed with coefficients which vary with a sine or cosine of the coordinate of the cell measured along any given direction in the crystal. The excitation energy will depend on the wave-length and the direction of the "excitation wave." The lowest excitation energy will be obtained frequently, but not necessarily if the excitation in all the cells is

[1] R. Peierls, Ann. d. Physik **13**, 905 (1932).
[2] J. Frenkel, Phys. Rev. **37**, 1276 (1931); **37**, 17 (1931). Physik. Zeits. Sowjetunion **9**, 158 (1936).

multiplied by the same factor. In the neighborhood of this state, i.e., for "excitation waves" with a wave-length long compared to the lattice distance, the excitation energy will be a quadratic function of the reciprocal wave-length or, more exactly, of the wave number. Choosing the x, y and z coordinate directions in an appropriate way one may write

$$E_{\text{exc}}=E_0+I_x\bar{\nu}_x^2+I_y\bar{\nu}_y^2+I_z\bar{\nu}_z^2. \tag{1}$$

Here $\bar{\nu}_x$, $\bar{\nu}_y$ and $\bar{\nu}_z$ are the components of the wave number in the x, y and z directions, i.e., half the number of nodes per cm which are found if one proceeds along the x, y and z axis respectively. I_x, I_y and I_z are constants proportional to the rates with which excitation energies are exchanged between cells in the x, y and z directions.

There exists an analogy between the excitation waves with an energy expressed by (1) and the de Broglie waves of a material particle. The energy of a particle can be represented by

$$E=E_0+E_{\text{kin}} \tag{2}$$

with

$$\begin{aligned}E_{\text{kin}}&=(p_x^2+p_y^2+p_z^2)/2m\\&=(h^2/2m)(\bar{\nu}_x^2+\bar{\nu}_y^2+\bar{\nu}_z^2).\end{aligned} \tag{3}$$

Here p_x, p_y, p_z are the components of the momentum of the particle and m its mass. In (3) we have used the de Broglie relation

$$p_x=h\bar{\nu}_x \qquad p_y=h\bar{\nu}_y \qquad p_z=h\bar{\nu}_z. \tag{4}$$

It will be seen that the equations connecting the wave number and the energy will become the same for the excitation waves and the matter waves if we have $I_x=I_y=I_z$* and if we set

$$I=I_x=I_y=I_z=h^2/2m. \tag{5}$$

Thus excitation waves will behave as matter waves with a mass defined by (5); in particular the group velocity will be the same in the two cases. Now the group velocity corresponds in the particle picture to the velocity with which the particle represented by the wave picture is moving. Frenkel has proposed to consider the excitation wave as representing a particle, the exciton, having a mass

$$m_e=h^2/2I \tag{6}$$

and moving along with the group-velocity of the excitation waves.

The mass of the exciton may vary from case to case in wide limits according to the value of I. However, the mass will never be of a smaller order of magnitude than the mass of the electron, since the propagation of excitation waves is essentially due to the motion of electrons in their orbits. On the other hand, there is no upper limit to the mass of the exciton: Any great value of the mass may be obtained for sufficiently small values of I, that is, for slow exchange of the excitation energy. If we want to treat the exciton as a particle, the following complications present themselves.

(1) In noncubic crystals $I_x=I_y=I_z$ will not hold. The exciton must then have a mass depending on the direction in the crystal. Along different axes the factors connecting momentum (or wave number) and velocity will be different.

(2) The simple relation (1) holds only for long waves. If the wave-length becomes comparable to the lattice distance, it must be replaced by a more complicated relation amounting to a variation of the mass of the exciton with its velocity. For some wave-lengths the mass of the exciton will even be negative. A negative mass means that if the exciton loses energy, its velocity (i.e., the group velocity) increases and that if it gains energy it will be slowed down.

(3) The state where the excitation of the crystal cells is superimposed with the same coefficient frequently is not the state of lowest energy. In such cases negative masses may be needed to describe the behavior of long waves.

(4) The number of excitons is not conserved. They can be created and destroyed by absorption and emission of radiation or other processes.

(5) If the excited state of a single cell is degenerate an internal degree of freedom of the exciton must be introduced in order to describe the state of the crystal.

Although Eq. (1) is valid only for long excitation waves, we may apply it, nevertheless, to the shortest waves possible in the crystal and obtain thereby an estimate of the total energy range of which an exciton is capable. The shortest possible wave-length is the lattice distance L multiplied by two. Thus we have

* This will be the case for crystals of cubic symmetry.

$\bar{p}^{(\max)} = 1/2L$ and from (1)

$$E^{(\max)} = E_0 + I/4L^2. \quad (7)$$

Using (5) we obtain for the range covered by the exciton energies

$$\Delta E_e = E_{\text{exc}}{}^{(\max)} - E_0 \approx I/4L^2 = h^2/(8L^2 m). \quad (8)$$

The greatest possible range of the exciton energies is obtained if both L and m are small, the minimum value for the latter being of the same order of magnitude as the electronic mass. For the highest possible value of ΔE we therefore obtain a few electron volts, i.e., energies comparable to those of the electrons in the outermost atomic shells. There is, of course, no lower limit for ΔE.

The minimum time, T, required for the excitation to spread to a neighboring lattice point, is closely connected with ΔE. The frequency $\Delta E/h$ will correspond to the fastest possible oscillation of the exciton. T will be one-half times the period of this oscillation

$$T \approx h/(2\Delta E_e) \approx (2hL^2)/I = (4L^2 m)/h. \quad (9)$$

Expressions (6), (8) and (9) offer three different possibilities to interpret the quantity I which we have introduced. According to (6) I is proportional to the reciprocal value of the mass of the exciton. (8), on the other hand, connects I with the breadth of the band of levels in the crystal corresponding to the excited level of a single cell. Finally (9) shows that the greater I is, the shorter will be the time T during which the excitation spreads from one cell to the next.

2. Formation of the Exciton by Absorption of Light

If we want to follow an exciton from its "creation" to its photochemical action the following questions will have to be discussed:

(1) If light is absorbed and an exciton is created, what can be said about its position and its energy?

(2) In what way can the exciton spread to the point of its photochemical action and how can this propagation be disturbed by the lattice vibrations?

(3) Can the exciton be annihilated by emitting its energy in form of radiation or by converting it into heat before it could cause photochemical action?

(4) What effects will occur on disturbed lattice points and surfaces? Most of the proper photochemical processes will fall under this heading.

We shall consider first the creation of an exciton by absorption of light. The wave-length of the light is in general long compared to the lattice distance. The excitation will take place, therefore, on neighboring lattice points with very similar phases, i.e., the coefficient with which the excitation on a definite lattice point has to be multiplied will vary slowly with the lattice point. In such a case we speak about a long wave exciton. These long excitation waves will frequently correspond to the lowest possible value E_0 of the excitation energy and the exciton will have in such cases no kinetic energy to start with. As has been pointed out, however, in the previous section, the state of equal phases may correspond to a high or the highest kinetic energy of the exciton.

In any case, however, the state of equal phases will possess a group velocity equal to zero and correspondingly the excitons' particle velocity vanishes. But if the state of equal phases has the lowest energy, the only way in which the exciton may gain velocity is that it obtains energy from some source, e.g. from lattice vibrations. If, on the other hand, the state of equal phases is a state of high energy, the exciton may lose energy and still be accelerated at the same time.

If distortions and vibrations of the lattice in the fundamental and in the excited electronic state are absent, only long wave excitons will be obtained. The absorption or resonance spectrum may, therefore, appear sharp even though the breadth of the exciton energy band ΔE is great.

Nevertheless there are reasons why other than long wave excitons may be obtained. In the first place, the absorption of light may be so strong that the light can penetrate into the crystal only by a fraction of its wave-length. This may be the case if the absorption is very sharp and if a relatively great oscillator strength of the absorbing electrons is concentrated into a small spectral region. One can hardly expect, however, that the light does not penetrate at least several

crystal layers and the exciton wave-length remains, therefore, long, compared with the lattice distance. The importance of the phenomenon just discussed may be that in such cases the exciton will be created near the surface, i.e., near the place where many photochemical reactions may occur.

A more general reason which causes the creation of short wave excitons is the irregularity in the crystal brought about by lattice vibrations. If a region of the crystal is distorted, both the excitation energy and the energy corresponding to the exchange or propagation of excitons will be affected. Thus even if the light acts in the same phase at all the distorted lattice points they will not absorb light quite similarly and further changes of phase may result by the time the lattice swings back to its equilibrium position.

According to Peierls, two cases must be distinguished. In the first case the perturbation caused by lattice vibrations is smaller than the greater of the two quantities ΔE and the energy range of vibrational quanta of the lattice. In the second case the perturbation of the vibration is greater than both ΔE and any quantum of the perturbing lattice vibrations. The amplitude of the perturbing lattice vibrations will be determined by the temperature if we are above the Debye θ for the corresponding vibration. Below the Debye θ the zero point amplitude must be taken.

In the first case of Peierls primarily long wave excitons will be obtained. Peierls calls such crystals scatterers. In the second case all kinds of exciton wave-lengths will be created. The name used in this case is "absorber." The significance of these names will appear later.

Even if we deal with scatterers there will be a possibility (decreasing with the perturbation by the lattice vibrations) that excitons of shorter wave-lengths may be created. The most probable process will be, however, the creation of a long wave exciton giving a sharp line in the absorption spectrum. The sharp line will be accompanied by a weaker band corresponding to the creation of various short wave excitons. It is necessary, however, that together with any short wave exciton a vibration may appear. The sum of the wave numbers of exciton and crystal vibration must be equal to the wave number of the incident light plus or minus any multiple of the number of lattice points per unit of length. That means that though the phases of the exciton are not equal on neighboring lattice points, they become equal if multiplied by the phases of the vibration which has been excited simultaneously.

The statements in the last paragraph can be formulated somewhat simpler if particles—the vibrational quanta or phonons—will be used to represent the lattice vibrations. The mass of the phonon m_p will be connected with the energy range ΔE_p of the corresponding lattice vibrations by

$$\Delta E_p = h^2/8L^2|m_p|. \tag{8a}$$

The momentum of the phonon will be obtained again from the wave number by multiplication with h. In general several kinds of phonons may exist in a crystal. The number of them is equal to the number of degrees of freedom in a crystal cell. Three of the phonons—corresponding to Debye's acoustical frequencies—will have a rest-energy equal to zero. The absolute value of their average mass will be given, however, by (8a). The other degrees of freedom will correspond in general to phonons with varying rest energies (which we called in case of the exciton E_0). If free rotations are present these will not be described very well by the picture of phonons.

Using the phonon one may express the phase relation discussed above by saying that in the process

$$\text{photon} \rightarrow \text{exciton} + \text{phonon}$$

the momentum must be conserved. This conservation law is, however, only valid modulo the momentum which corresponds to the wave number of the reciprocal lattice.

Using the energies of phonon E_p and the energy range of the exciton ΔE_e, one may subdivide the scatterers of Peierls into phonon scatterers for which $E_p \gg \Delta E_e$ and exciton scatterers for which $\Delta E_e \gg E_p$ and therefore $m_p \gg m_e$. For phonon scatterers several vibrations are completed in a lattice cell before the excitation spreads to the neighboring cell. If in a phonon scatterer an exciton and a phonon are created simultaneously, the energy of the absorbed photon will differ from the energy of a

long wave exciton mainly by the phonon energy. Thus this case corresponds to the application of the spectroscopic principle often called Franck-Condon principle to molecules which have nearly the same equilibrium positions in the excited and fundamental states and which will have mainly $0-0$, $1-1$, $2-2$, $\cdots$ vibrational transitions with relatively weak $0-1$, $1-2$, $\cdots$ and $1-0$, $2-1$, $\cdots$ transitions. There is, however, an essential difference between the case of the molecule and the case of the crystal: In the latter it is possible that the phonon and the exciton created together may separate themselves from each other.

In exciton scatterers the excitation will spread many lattice distances during the time of one vibration. The photon energies for the excitation of long wave and short wave excitons will differ essentially by the kinetic energies of the exciton. In these cases the breadth of the weaker band accompanying the main absorption (which creates a long wave exciton) will be a measure for ΔE_e and m_e, i.e., for the breadth of the region of exciton energies. For phonon scatterers the breadth of adsorption merely measures the energy range of possible E_p values for the disturbing phonons.

Crystals which according to Peierls' definition are absorbers for a certain electronic transition will as a rule produce, together with the exciton, several phonons. Accordingly the absorption will be more uniform lacking the sharp line which corresponds to the strong excitation of a long wave exciton unaccompanied by phonons. Frenkel points out that there will exist in general between the phonons emitted together with the exciton a phase relation of such kind that the lattice will be most strongly distorted around the exciton. Moreover, at least part of the distortion of the lattice will be permanently attached to the exciton. The exciton will be "trapped." This phenomenon has also been discussed by Landau[3] and by v. Hippel.[4]

Absorbers behave as molecules with equilibrium positions differing in the fundamental and excited states. According to the Franck-Condon principle, vibrations will be excited together with the electronic excitation. Since here the zero-point vibration suffices to cause a great perturbation and since the exciton and part of the lattice distortion may remain permanently bound together, it is no longer possible to distinguish sharply between phonon absorbers and exciton absorbers. One may talk, nevertheless, about phonon absorbers if the exciton velocity in the undisturbed lattice would be small compared to the phonon velocity. If, furthermore, the perturbation and trapping in a phonon absorber is effected by internal degrees of freedom of the cell, the spectrum will be very similar to that of an isolated cell. If it is effected by acoustic vibrations, it is similar to what would be the spectrum of a small group of cells.

[3] Landau, Physik. Zeits. Sowjetunion **3**, 664 (1933).
[4] A. v. Hippel, Zeits. f. Physik **93**, 86 (1934).

3. Propagation of an Exciton

In a crystal undisturbed by irregularities or lattice vibrations, an exciton will be propagated like a particle moving freely. The velocity will be the group velocity of the excitation wave.

If perturbation by lattice-vibrations is taken into account, an exciton may emit or absorb a phonon. It may also, with smaller probability, emit or absorb two phonons or absorb a phonon and emit another; i.e., scatter a phonon. For scatterers in which long wave excitons are created almost exclusively, such emissions, absorptions and scatterings will be relatively rare processes. But as the ratio of long wave to short wave excitons produced by light absorption approaches unity, the propagation of the exciton is disturbed more frequently by the lattice vibrations.

There is, however, no strict relation between the mean free path of the exciton and the absorption spectrum. Thus the conservation laws for energy and momentum influence the propagation and the creation of excitons in a different way. Here again phonon scatterers and exciton scatterers have to be distinguished.

If we have an exciton scatterer with $m_e \ll m_p$, an exciton of small mass will emit a heavy phonon. In the emission (absorption or scattering) process, the energy of the exciton will not change much, but its direction of propagation may change very greatly.

In considering the phonon scatterers, a further distinction must be made according to whether

the disturbing lattice vibration—and consequently the emitted phonon—belongs to an acoustic wave or an inner vibration of the lattice cell. If an acoustic wave is emitted for which the rest-energy is equal to zero, $E_p \gg \Delta E_e$ implies $m_p \ll m_e$. Therefore the heavy exciton will emit light phonons and the conservation of energy and momentum requires that the momentum and consequently the energy of the exciton shall not change greatly in an emission process. In such cases the mean free path of the exciton may become short and the exciton will nevertheless be propagated nearly in a straight line.

If the emitted phonon corresponds to an internal vibration the phonon will have in general a rest energy which is greater than its range of kinetic energies. Then it follows from $\Delta E_e \ll E_p$ that the kinetic energy of the exciton does not suffice to emit a phonon of any momentum whatsoever. In such cases the exciton will be propagated in a straight line even though in absorption processes where energy is furnished by the absorbed light a considerable probability exists for creating an exciton and a phonon simultaneously. In the case just mentioned it will be possible that the exciton should be deflected from the straight line by emission of an acoustic phonon. But such emissions might have a small probability. Again a deflection may be caused by the scattering of a phonon which process is never excluded by the conservation laws. But scattering being a double process is improbable and moreover at low temperatures where no phonons are excited initially, scattering becomes impossible. Thus we see that excitons may have a long free path even though in the process of light absorption the creation of short wave excitons is probable.

For absorbers the change in excitation energy produced by zero-point vibration or temperature vibration will be larger than the greater one of the following two quantities: The maximum kinetic energy of the exciton (exciton absorber) and the maximum energy of the phonon (phonon absorber). One may expect in this case that a distortion of the lattice around the position of the exciton will lower the excitation energy and destroy the resonance giving rise to the propagation of exciton or phonon, i.e., the exciton will be trapped.

The position of a trapped exciton may change in two ways. In the first place the thermal vibration of the lattice may bring about an atomic configuration for which resonance is restored. Owing to the irregular nature of temperature motion the exciton will be able to move only to the neighboring cell where it might be trapped again. Thus we are dealing with a diffusion process.

Secondly the temperature may be so low that the energy is not sufficient to excite a phonon. Then the resonance which exists between any two positions in which the exciton may be trapped becomes effective. The trapped exciton may be propagated along a straight line. However, two trapped positions will differ not only in their electronic wave functions but also in the positions of the heavy nuclei. Therefore the transition from one trapped position to a neighboring one will be slow and will correspond to the tunnel effect for the heavy particles which have to slip from one equilibrium position to another. It should be remembered in that connection that a tunnel effect for heavy particles is very improbable; indeed no clean-cut evidence for such a process has been found in physical chemistry.

4. Annihilation of the Exciton in the Normal Lattice

An exciton may be annihilated if it emits light. This is the reverse of the process of creation which we have discussed in §2. In a crystal not disturbed by irregularities or vibrations, an exciton can radiate only if its wave-length agrees with that of the photon to be emitted. The state for which the wave-length agrees with that of the photon will radiate with a very high probability. The lifetime in this state will be that of a single cell if radiating by itself, divided by the number of cells in which the interacting photon and exciton can be described by a pure sine wave and for which, therefore, interference of the emitted light can occur. All the other states of the exciton have to be regarded as metastable.

For a "one-dimensional crystal" (an example will be discussed in connection with the chlorophyll problem) the exciton wave-length for which

destructive interference of the emitted light can take place is limited by the wave-length of the light. Only excitons of shorter wave-length will be metastable. Those of longer wave-length may emit light at an angle to the direction of the crystal.

If we consider an ideal crystal and if the perturbations by lattice vibration are not essential, light can be absorbed only into a state of extremely short lifetime. The light will be re-emitted, therefore, at once without causing any permanent change in the crystal. This means that the crystal will interact with the photon by scattering or rather reflecting it. If, on the other hand, the exciton interacts strongly with the phonons, the light, even if it is re-emitted, will cause in general a permanent change in the crystal. That is the reason why Peierls calls the first kind of crystals scatterers and the second kind absorbers.

The difference between scatterers and absorbers is, of course, a gradual one, as even in scatterers permanent changes may occur in the crystal. That will be, in particular, the case whenever the exciton gets into a metastable state either by the direct (though weak) absorption leading to such states or through absorption into the short life state and subsequent emission or absorption of a phonon. In a metastable state an exciton may be "conserved" and, propagated to the part of the crystal where a photochemical action can take place, it may produce the photochemical effect. It is, therefore, of particular interest to see what is the lifetime of an exciton in a metastable state.

If an exciton in any state will emit or absorb a phonon more readily than a photon and if kT is great as compared to ΔE_e and E_p, then—owing to the possibility that the exciton will be thrown into its short life state—the actual lifetime will be that of a cell radiating by itself. If, on the other hand, an exciton scatterer is considered and if $kT < E_e$, the behavior of the exciton will depend on the question whether its long wave states will have the lowest energies or whether they have high kinetic energies (exceeding kT). In the former case the lifetime of the metastable state will be shorter than the lifetime of the excitation in an isolated cell, since the Boltzmann factor favors the transition of the exciton into the long wave state. In the latter case, however, the Boltzmann factor for the long wave state may become so low that a transition into this state becomes practically impossible. The emission from metastable states will then be due to the fact that during the temperature or zero-point vibrations of the lattice the phases of excitation on the lattice cells are changed. The lifetime of the metastable exciton may then become very long. It can be estimated from the intensity of the weak absorption band which in scatterers accompanies the sharp absorption (or scattering) due to the long wave exciton state.

It might seem possible to assume that these metastable states explain several cases of crystal phosphorescence. However, the lifetime of the metastable states will, in general, not be sufficient for this purpose. For exciton scatterers the lifetime will be that of an excited isolated cell multiplied with $(\Delta E_e/P)^2$ where P is the energy (or more exactly the matrix element) of the perturbation produced by the lattice vibration. The ratio $\Delta E_e/P$ will be of the same order of magnitude as the magnitude of interatomic distances divided by the amplitude of vibration. Thus we have at low temperatures $\Delta E_e/P \approx 10^2$ and $(\Delta E_e/P)^2 \approx 10^4$ and the lifetime of the metastable state will exceed that of an isolated excited cell as a general rule by no more than a factor 10^4.

For phonon scatterers, ΔE_e must be replaced in the above estimate by E_p. A limit for $(E_p/P)^2$ and therefore for the lifetime of metastable states in phonon scatterers can be obtained from the estimate for $(\Delta E_e/P) \approx 10^2$ and from the assumption $\Delta E_e \ll kT$. Thus for room temperature where kT is not much smaller than E_p, the lifetimes of the metastable states in phonon scatterers will not exceed the lifetimes obtained above for exciton scatterers.

For absorbers, if the exciton is trapped, the situation will be entirely different. If the exciton is annihilated by emission of a photon a spherical wave of lattice vibrations will be emitted from the point at which the exciton has been localized. Thus, the final state of the emission process varies with the position of the exciton in the initial state and no interference phenomena are to be expected. An exciton trapped in a certain position will radiate without being disturbed by

the fact that the exciton might have been trapped in another position. The transition probabilities will be comparable to those which one obtains in spectra of polyatomic molecules.

To this general statement a more specific one can be added if in a phonon-absorber the coupling is due to molecular vibrations. In this case the emission will take place from states close to the lowest vibration level in the excited molecule. The fluorescence spectrum may then closely resemble the high pressure fluorescence in the gas or the fluorescence in the solution.

In crystals, as in polyatomic molecules, excitation energy may be converted completely into vibrations and therefore into heat, and the exciton may thus cease to exist without emitting a photon. Such transitions unaccompanied by radiation may occur if potential surfaces cross. If during the trapping processes the nuclei will be displaced strongly from their equilibrium positions, we shall expect these transitions to occur with considerable probability.

It is also possible that instead of the total exciton energy a part of it will be converted into heat or electromagnetic radiation, the remaining energy appearing as a lower excitation energy.

Finally, it will be noticed that in an absorption the exciton energy may be also transformed into chemical energy rather than heat. This must be considered as one type of a photochemical process.

5. Interaction of an Exciton with a Distorted Lattice. The Photochemical Process

If a photochemical process sets in on an atom or molecule differing from the other constituents of the lattice, or if the process proceeds on the surface of the crystal, the photochemical process is essentially an interaction of the exciton with a disturbed lattice point. Such interactions may, of course, also occur without giving rise to photochemical processes.

The case of greatest interest is that of a scatterer. It appears that the exciton may be transported to the point where it can act photochemically with a high velocity and at the point of irregularity it may be trapped giving rise to a photochemical process. We shall investigate the conditions necessary for such a process.

The perturbation of the exciton by lattice vibrations must not be quite negligible otherwise as has been shown in the previous section only long wave excitons of very short life are created. It is best if the long wave excitons have a high kinetic energy so that metastable states may be obtained. By this means the number of excitons lost in fluorescence processes might be reduced.

The photochemical yield will be greatest for phonon scatterers, particularly if the perturbation is due to an internal vibration. The reason is that such interaction may be large and may cause creation of short wave excitons without preventing the exciton from being propagated in a straight line (see §3).

Finally the perturbed lattice point on which the photochemical process will proceed has to fulfill some conditions which we proceed to discuss.

A perturbed lattice point or a perturbed region of the lattice will act on the exciton as a potential acts on a particle. It may attract the particle, it may repel the particle or, finally, the particle may be reflected according to wave mechanics if the potential change occurs too suddenly. In the crystal the first two cases will occur if the excitons on the distorted lattice points are nearly in resonance with excitons on regular points, the difference being smaller than ΔE_e. Reflection will occur, on the other hand, if the distortion has destroyed the resonance. Thus it will be favorable for the photochemical process if on the distorted lattice point the exciton energy is a little lower than on other points. By this mechanism excitons may, for instance, be attracted to the surface of the crystal and if they then emit a phonon they may be left with too little energy to leave the surface. It shall be noted that if a lattice cell is distorted its neighbor will, in general be distorted too. This may act to make the changes of the "potential field" in which the exciton moves less sudden and may make the reflection of an exciton from the "surface" of a distorted region less probable.

It is most favorable for the photochemical process if the time necessary to trap the exciton after it has reached the disturbed lattice point is comparable to the time T given in Eq. (9). If the time necessary for the trapping is much longer than T, the exciton will escape from the disturbed lattice point before it can be trapped. If, on the

other hand, the time of trapping is short compared to T, this short period process will destroy the resonance between the exciton positions on the regular and on the disturbed point. Thus the exciton will be reflected with a great probability before it can reach the distorted lattice point.

Once an exciton reaches a distorted lattice point and is trapped, the photochemical process may occur. If trapping occurs in the undisturbed lattice, the propagation of the trapped exciton to the perturbed lattice cell will be a slow process. In general the exciton will be annihilated by light emission or radiationless transition before it can act photochemically. In addition resonance between the disturbed and undisturbed lattice points is necessary in order that the photochemical process shall occur.

The above discussion shows how many conditions have to be satisfied if we want the absorption of a whole crystal to be used in order to produce photochemical action on a few disturbed lattice points. On the other hand, the photochemical process mentioned at the end of the last section does not require so many conditions. Indeed, it does not differ essentially from a photochemical process in the gaseous state or in solutions.

Applications

Pseudoisocyanines

Propagation of excitons in crystals have been frequently used to explain certain features of absorption and emission spectra. Indeed, it is often unavoidable to assume the propagation of excitation energy (e.g. in some cases of excitation of phosphorescence). But it is probable that in nearly all these cases the energy is transported by electrons.[5]

Clearcut evidence for the specific properties of a freely moving exciton is shown by a strong and sharp absorption of the pseudoisocyanines.[6] It has been shown that the pseudoisocyanines when present in a highly polymerized form possess an absorption band which is absent in the molecular solution. The absorption bands of the molecular solution are separated from this characteristic sharp band by several hundred A units. The sharp band is absent in the dry crystalline form of the pseudoisocyanines but reappears if some water vapor is added. If the polymerized form consists only partly of pseudoisocyanine molecules and partly of a related dyestuff, the new band remains sharp but appears in a shifted position. The band has a half-width of 140–180 cm^{-1} and is, therefore, much sharper than the other absorption bands of these dyes. Fluorescence in the sharp band has been observed both by using the frequency of the band itself and by higher frequencies absorbed by the molecules of the dyestuff. The fluorescence can be weakened by appropriate chemical substitutions. The state of high polymerization and the sharp absorption band can be destroyed in a reversible way by raising the temperature.

Scheibe suggested that the excited state corresponding to the sharp band is a communal electronic state of the polymerized substance. We explain its sharpness by assuming that we are dealing with a scatterer so that light can excite only long wave excitons of a definite energy. The absence of the band in the solution indicates a strong influence of the neighboring molecules in this particular excitation. The behavior of polymerized aggregates consisting of two kinds of molecules is a further proof for the strong coupling. Thus it is very probable that these polymerized dyes are exciton scatterers. For such an exciton scatterer resonance fluorescence is to be expected. Excitation of fluorescence by shorter wave-lengths will be explained by radiationless transitions to the excited state of the sharp band. From the appreciable intensity of this indirectly excited fluorescence and from the absence of afterglow we conclude that long wave excitons have a low energy. The observed breadth of the band may be due to temperature motion of the molecules or to irregularities of the "crystallite." Since the dry macroscopic crystal does not show the new band it is probable that the molecular configuration in the desiccated crystal is not favorable to a fast exchange of excitation energy between the molecules.

The resonance fluorescence seems to have a yield considerably smaller than one. This may be understood in connection with the fact that the

[5] Compare, for instance, results of Riel on luminophores, Ann. d. Physik **29**, 640 (1937).

[6] G. Scheibe and co-workers, Zeits. f. angew. Chem. **49**, 563 (1936); **50**, 51 and 212 (1937); Naturwiss. **25**, 75, 474, 795 (1937); **26**, 412 (1938); Kolloid Zeits. **82**, 1 (1938); E. E. Jelley, Nature **138**, 1009 (1936); **139**, 378, 631 (1937).

polymerized state can be dissociated easily. Though our hypothesis that we are dealing with a scatterer seems to exclude trapping processes, such trappings may occur at points where the "lattice" is strongly distorted. Strong distortions by temperature motion have to be expected in consequence of the ease with which the polymerized state can be destroyed by temperature. As soon as the exciton is trapped its energy may be used for chemical processes, e.g. for the separation of a molecule from the crystallite.

The photosynthetic unit

It has been suggested that in photosynthesis light absorbed by many chlorophyll molecules is utilized for the reduction of a single CO_2. This hypothesis was used to explain certain features of light-saturation and also the apparent absence of a long induction period in weak light. The following detailed picture has been suggested. The chlorophyll molecules are arranged in a one-dimensional crystal to which CO_2 molecules are attached at the ends. Light absorbed in any cell of the crystal must be transported to a CO_2 molecule before being used photochemically. We shall show that it is not easy to reconcile this picture with the behavior of chlorophyll in absorption and fluorescence.

Chlorophyll has two regions of strong absorption in the visible spectrum, namely in the red and in the blue. They appear to correspond to two different electronic transitions. The positions of the absorption maxima vary slightly with the solvent. The variation of the red maximum amounts in molecular solutions to 250 cm^{-1} (6605A–6760A). The maximum in the leaf (6770A) almost coincides with the maximum in methylene iodide solution (6760A). Strong fluorescence has been observed in sufficiently inert solvents. A much weaker fluorescence has been observed in plants. Under stationary conditions during photosynthesis the fluorescence amounts to 0.15 percent of the absorbed radiation. The emitted light is always red independent of the wave-length of the exciting radiation. It follows that the excited state of the absorption in blue will be transformed in that of the red absorption by an internal conversion. Thus the higher excited electronic state has a very short life and we need not consider it in connection with the photosynthetic unit. The absorption in the red region fades out gradually towards short waves whereas near the red end the absorption coefficient drops much more suddenly. For fluorescence the reverse statements hold. The maxima of absorption and fluorescence coincide within close limits while the spectrum extends for several thousand wave numbers in one case towards the violet, in the other towards the red. These facts can be explained immediately if the maximum of absorption and fluorescence is assumed to correspond to the O−O transition, i.e., to a transition from a nonvibrating excited state to a nonvibrating fundamental state. The shape of the curves shows that the equilibria in the excited and fundamental states correspond to somewhat different configurations of atoms in space. The absorption and emission spectra do not differ essentially in the leaf and in solution except for the slight shift of the spectra and the yield of the fluorescence.

The similarity of optical behavior in solution and in the leaf indicates that, if a photosynthetic unit exists, the excitation of its different cells are not strongly coupled, i.e., the kinetic energy of its excitons is small. Thus we are dealing with a phonon scatterer or a phonon absorber. Indeed an exciton scatterer should show a sharp absorption and emission maximum in the leaf for which there is no evidence. The assumption of an exciton absorber would provide no immediate explanation for the similarity between leaf and solution and leads, moreover, to difficulties which will be mentioned later. The decision between a phonon absorber and phonon scatterer depends on the question whether more or less than one vibrational quantum is excited on the average during the electronic transition. Though the maximum apparently corresponds to the O−O band the total intensity of other transitions seems to predominate. Therefore, taking into account the shape of the curves for absorption and emission, the photosynthetic unit should be classified as a phonon absorber or perhaps as an intermediate case between a phonon absorber and phonon scatterer.

Making, however, the assumption that we are dealing with a phonon absorber it is difficult to understand why the yield of fluorescence is so low in the leaf. The half-life of the excited state of

chlorophyll in solution with regard to radiation is about 2.10^{-7} second. Assuming that the half-life in the photosynthetic unit is the same and remembering that the yield of the fluorescence is only 0.15 percent, it will be necessary to assume that the excitation energy must be used in the photosynthetic unit for some radiationless process within the limit of 3.10^{-10} second. Since, furthermore, the quantum yield for photosynthesis approaches under favorable conditions the theoretical value of four quanta, we must conclude that the photosynthetic process is identical with the radiationless process mentioned above, i.e., the photosynthetic process takes place within 3.10^{-10} second. Now the exciton must traverse 10^3 crystal cells before arriving at the CO_2 and therefore the time for propagation from one cell to the next must not be longer than 3.10^{-13} second. Thus it follows from Eq. (9) $\Delta E_e = h/2T$, with $T = 3.10^{-13}$ sec. must be greater than 50 cm^{-1}.

From the vibrational structure in the spectra of chlorophyll *a* and *b* in solutions we obtain $E_p \sim 1000$ cm^{-1}. For a phonon absorber ΔE_e must be smaller that 1000 cm^{-1} for an idealized non-vibrating state in which the atoms of all molecules are held in the same positions. But the propagation in the one-dimensional crystal takes place after the trapping, i.e., after the excited molecule has assumed its *O*th vibrational state around the distorted equilibrium position of the excited electronic state. Then the spreading of the excitation energy to a neighboring molecule must be accompanied by a tunnel effect and ΔE_e will be strongly diminished. According to the argument given above it must remain nevertheless greater than 50 cm^{-1} and we are thus left with a limited range for ΔE_e.

In fact our only possibility to avoid an actual contradiction is to assume (as has been done tacitly in the preceding discussion) that the mean free path of an exciton becomes comparable to the dimensions of the photosynthetic unit as soon as it arrives in the *O*th vibrational state. If, for instance, we assume that owing to collisions with slower vibrations the mean free path is $1000/n$ crystal cells, the exciton shall perform a "brownian motion" with an n times longer duration than that of the propagation on a straight line. Thus ΔE_e for the trapped exciton will become n 50 cm^{-1}. For $n \gtrsim 10$ this is incompatible with our assumption of a phonon absorber.

The assumption of an exciton absorber would lead to even greater difficulties. Here we have to assume $n \approx 1000$ and $\Delta E_e > n \cdot 50$ $cm^{-1} = 5.10^4$ cm^{-1}. In an exciton absorber the time of trapping must be shorter than $h/\Delta E_e$ and the breadth of the spectrum must be greater than ΔE_e. Thus we obtain from our assumption a far too diffuse band. Apart from this, however, it is absurd to assume that the coupling of the excited states measured by ΔE_e is 5.10^4 cm^{-1} and the absorption spectrum is nevertheless practically the same as in a molecular solution.

The only remaining assumption, namely that of a phonon absorber, could be tested by the following experiment. The fluorescence should be excited by a wave-length 6700A leading directly to the *O*th vibration of the excited state. Thus we obtain through direct absorption the "trapped" state of the exciton and at the same time we shall have an excited state for which the phases are the same for all crystal cells. Such a state should radiate in a much shorter time ($\approx 2.10^{-10}$ sec.). Since moreover the photosynthetic unit will remain in this state for a period $(1000/n)h/2\Delta E_e$ and $n \lesssim 10$, we must obtain a fluorescence of at least several percent. This fluorescence will, moreover, belong to the O—O transition and will, therefore, not extend as far towards long waves as the fluorescence hitherto observed. We conclude that according to whether this new kind of fluorescence appears or fails to appear we shall have to conclude that the photosynthetic unit does or does not exist.*

Even on the present basis it seems to us that the existence of the photosynthetic unit is improbable. We have seen that there is left barely sufficient time for the exciton to be transported to the CO_2. We should have to assume further that photochemical action takes place whenever the exciton arrives at the CO_2. This is, however, only possible if the time for trapping the exciton at the CO_2 is just right, i.e., if it is about 3.10^{-13} sec. This same statement must, moreover, hold for all the intermediate stages of photosynthesis.

The sensitized photographic plate

Finally we shall discuss the sensitization of the

* It is planned to carry out this experiment.

photographic plate by dyes which have in the infra-red an absorption analogous to the new band observed with the polymers of pseudo-isocyanines. It has been suggested[7] that two or more excitons are propagated to the same point and cooperate there to split off an electron from the halogen ion. This picture has been used to explain that absorption of light with a much longer wave-length than that absorbed by the silver halide crystal itself can produce a latent image. Though it is generally admitted that in the crystal the migration of electrons is of importance for the photographic process a summation of quanta is in disagreement with experimental evidence and moreover, it is unnecessary.

It has been shown that if the intensity of the light is not too small the effect produced by light on the sensitized photographic place depends in the first approximation on the amount of light, i.e., the product of light intensity and time of irradiation. This fact can be easily understood by assuming that one quantum is sufficient to produce a practically permanent change[8] in the plate. If two quanta would be necessary the effect produced should be proportional to the square of the intensity, and even higher powers should be observed if still more quanta would be needed. If, moreover, the weakest possible intensity is used, for which the dependence on the intensity is still practically linear,[8] less than one quantum per minute is absorbed by a grain in the photographic plate and one should obtain therefore for such intensities a very small quantum yield (probably smaller than 10^{-5}) if two (or more) excitons are necessary to produce an effect on the silver halide.

The production of the latent image by temperature has shown that only 15,000 cal. are needed to obtain the latent image.[9] An immediate necessity of summation of quanta would, therefore, only exist if light with a wave-length longer than 1.9μ would produce the image. The long wave limit of absorption in the crystal does not correspond to the minimum energy necessary to produce a free electron but rather to produce the free electron while keeping the atoms in fixed positions in the lattice.[10] An impact of the second kind such as we may have in a sensitized plate shows similarities to the excitation by temperature. The energy transfer to the crystal can be delayed until the atoms in the crystal get into favorable positions. This will be the case if the dye used for photosensitizing the plate shows fluorescence under suitable conditions.

Another possibility which may be considered is based on the fact that the properties of the ions on the surface are different from the properties of the ions in the interior. Thus the surface ions may absorb light of longer wave-length. This absorption may be weak. But if a strongly absorbing dye is in contact with them, the excitation may be transferred readily from the dye to the crystal surface. The two propositions which we have mentioned certainly do not exhaust the possibilities for explaining the sensitization. They serve only to show that the summation of quanta need not be assumed.

It is possible that some of the photosensitizing dyes, being adsorbed in a monomolecular layer, form a surface crystal which is an exciton scatterer. They would thus be analogous to the pseudoisocyanines. Since, however, the exciton while being propagated would remain in contact with the silver halide crystal, the exciton energies would be available at any time for the photochemical process. An exciton scatterer may be useful for sensitizing the photographic plate for a certain spectral region since it has a particularly strong adsorption in a rather narrow band so that enough light of a suitable wave-length may be absorbed in a monomolecular layer of dye. The adsorption of a phonon scatterer seems to be just as favorable.

[7] G. Scheibe, Naturwiss. **25**, 795 (1934).

[8] *Photographic Plates for Use in Spectroscopy and Astronomy* (Eastman Kodak Co., 1935), p. 12, Fig. 6, plate F.

[9] J. M. Blair and P. A. Leighton, J. Opt. Soc. Am. **24**, 1185 (1934).

[10] A. von Hippel, Zeits. f. Physik **93**, 86 (1934); **101**, 680 (1936).

The Role of Attractive and Repulsive Forces in the Formation of Tactoids, Thixotropic Gels, Protein Crystals and Coacervates

IRVING LANGMUIR
General Electric Company, Schenectady, New York
(Received October 20, 1938)

The formation of tactoids from thixotropic sols, of Schiller layers from iron-oxide sols, the separation of tobacco virus solutions and bentonite sols into two liquid layers and the crystallization of proteins are regarded as examples of unipolar coacervation (micelles having like charges) which must involve attractive forces.

Kallmann, Willstätter, Freundlich, De Boer, Hamaker, Houwink and others have assumed that the attraction is due to van der Waals forces. They have also analyzed the stability of colloid systems by diagrams giving the potential energy as a function of the distance between micelles. It is now shown that the Coulomb attraction between the micelles and the oppositely charged ions in the solution gives an excess of attractive force which must be balanced by the dispersive action of thermal agitation and another *repulsive* force. Thus there is no need to assume long range van der Waals forces. The past use of energy diagrams is criticized because it has ignored the effect of the thermal agitation and the attraction of the "gegenions" in solution. Instead of potential energy it is proposed that osmotic pressure p be used, which includes these previously neglected factors. A maximum in p as the colloid concentration increases is the condition for the separation into two phases (coacervation).

The Debye-Hückel theory (1st approximation) for the osmotic pressure of electrolytes takes into account both these factors and permits a rough calculation of the conditions under which coacervation occurs. The 2nd approximation, which considers particle size, does not agree as well with experiment as the first approximation. The reasons for this lack of agreement are discussed.

The micelles in unipolar coacervates are not in contact, but are separated by relatively large distances (10–5000A). Either a specific repulsive force or a decrease in the Coulomb attraction as the concentration increases (due to decreased charges on micelles) can account for stable coacervates. The assumption of a definite ζ-potential, rather than a definite charge on the micelles, gives automatically just such a decrease in attraction.

The general mathematical theory of coacervation presents great difficulties because the approximations of the Debye-Hückel theory cannot be used. However, the one-dimensional problem of the forces acting between parallel colloidal platelets can be solved rigorously in terms of elliptic integrals. For highly charged particles in sufficiently dilute solutions of electrolytes, the pressure p in the liquid between the two plates is given by $p=(\pi/2)D(kT/eb)^2=8.9\times10^{-7}/b^2$ dynes/cm² where b is the distance in cm between the plates and D is the dielectric constant (81 for water at $T=293°$K). This pressure which tends to force the plates apart is independent of the charge on the plates and on the electrolyte concentration (univalent ions only). Polyvalent ions decrease the force. This force is of the right magnitude to account for the stability of unipolar coacervates. It also furnishes a quantitative explanation of the Jones-Ray effect, by which low salt concentrations decrease the capillary rise in surface tension experiments with water.

Experimental determinations were made of the relaxation times τ for the decay of birefringence in bentonite and vanadium pentoxide sols, after stirring was stopped. In one sample of bentonite, τ varied with the 22nd power of the concentration, while in V_2O_5 sols the exponent was 1.8. The temperature coefficients of τ were also measured and the activation energies were calculated.

A theory of the relaxation of birefringence was developed, according to which the micelles in dilute thixotropic bentonite sols are arranged normally in a cubic lattice (isotropic). Temporary shear in the liquid orients the micelles and produces birefringence although the lattice remains cubic. The experimental data confirm the theory and indicate that the energy barrier opposing reorientation of micelles in a particular bentonite sol varied with the inverse 20th power of the distance between the micelles. With V_2O_5 this exponent was about 4. Further support for the theory was obtained by experiments which gave "angles of isocline" for bentonite particles in a flowing sol that varied from 65° to 78°.

In bipolar coacervates (which contain micelles of unlike polarities) the electric fields and the charges on the micelles *increase* as the micellar concentration increases. When a certain concentration is reached, the field rises to a value so high as to cause increased hydration which holds the micelles apart and gives stability to the coacervate.

WHEN a solution of pure tobacco mosaic virus containing about 2 percent of the protein is allowed to stand for several days, it separates into two phases.[1–5] The lower one, which is the more concentrated, is strongly doubly refracting and consists of a three-dimen-

[1] F. C. Bawden, N. W. Pirie, J. D. Bernal and I. Fankuchen, Nature **138**, 1051 (1936).
[2] J. D. Bernal and I. Fankuchen, Nature **139**, 923 (1937).
[3] F. C. Bawden and N. W. Pirie, Proc. Roy. Soc. (London) **123**, 274 (1937).
[4] F. C. Bawden and N. W. Pirie, Nature **141**, 513 (1938).
[5] M. A. Lauffer and W. M. Stanley, J. Biol. Chem. **123**, 507 (1938).

sional mosaic of small uniaxial liquid crystals arranged in random orientations with respect to each other. The top layer scatters much more light than the lower and is isotropic if undisturbed, but shows double refraction when subjected to shear (streaming double refraction).

During the separation of the liquid into the two phases, spindle-shaped or needle-shaped regions of low or high density, which slowly rise or fall in the solution, appear. The heavier masses which form in the upper part settle to the lower part and there coalesce with one another and with the surrounding liquid which has been enriched in protein by the removal of the lighter masses that have risen into the upper part. In this way the solution gradually separates into two layers which at first have an indistinct transition between them. Gradually, however, the boundary becomes so sharp that it shows distinct total reflection when viewed from a position slightly below the plane of the boundary.

The upper phase in which thermal agitation rapidly brings about a random orientation of the molecules behaves as a slightly viscous, isotropic liquid. If, however, the liquid is made to flow, the shear causes a temporary parallel orientation of molecules, which decays, after the motion stops, with a relaxation time of the order of a second.

The lower phase is a thixotropic gel, which if undisturbed is essentially a solid body made up of uniaxial crystal grains. The more concentrated the original solution, the finer is the observed grain size. The mechanical strength of this gel is very low, for a shearing stress of the order of 10 dynes/cm^2 causes flow. The gel is liquefied by more vigorous stirring, but on standing sets again to a gel and remains birefringent.

X-ray examination[1, 2] has shown that in the lower phase the rod-shaped virus molecules are arranged in a hexagonal close-packed lattice of parallel cylinders. The distance between adjacent molecules decreases continuously from about 500A to about 125A as the concentration of the protein in the solution increases.

The rod-shaped molecules are presumably held in position in the hexagonal lattice by repulsive forces resulting from negative charges on the protein molecules. According to the Debye-Hückel theory the force acting on a charged particle at a distance r from another charged particle is equal to the Coulomb force multiplied by an exponential factor, $\exp(-r/\lambda_D)$, where λ_D, which we may call the Debye distance, varies inversely as the square root of the ionic strength of the electrolyte. Thus the conditions under which the two-phase system forms and the spacing of the molecules in the more concentrated phase should be influenced in marked degree by the presence of electrolytes.

The properties of these tobacco virus solutions appear to be similar in many ways to those exhibited by certain thixotropic sols that have been studied by Zocher, Freundlich, Heller and others.[6–9]

Some thixotropic sols, such as those of V_2O_5, which contain rod-shaped crystalline particles, spontaneously form "tactoids," which are small, sharply defined, spindle-shaped, doubly refracting masses having higher density than the surrounding sol.

Some sols of iron oxide, having disk-shaped particles, when allowed to stand in a vessel with a flat bottom, may yield a separate denser phase in the form of an iridescent layer on the bottom of the vessel. When examined by white light the reflected light is found to be nearly monochromatic. The plate-like particles are thus arranged in parallel layers (Schiller layers) having a uniform spacing which may be as great as 8000A (giving a third-order red reflection).[9]

It has been generally assumed that the forces that hold these Schiller layers apart and the particles of tactoids apart, even at these relatively great distances of several thousand A, are electrostatic forces resulting from the large charges on the colloidal particles.

The properties of the tobacco virus solutions and their behavior during the separation into the two phases show that the phenomena are essentially the same as those involved in the formation of tactoids. In the virus solution, however, the "particle" is a protein molecule of molecular weight of about 50,000,000, while in

---

[6] H. Zocher, Zeits. f. anorg. Chemie **147**, 91 (1925).
[7] H. Zocher and W. Heller, Zeits. f. anorg. Chemie **186**, 75 (1930).
[8] K. Coper and H. Freundlich, Trans. Faraday Soc. **33**, 348 (1937).
[9] P. Bergmann, P. Löw-Beer and H. Zocher, Zeits. f. physik. Chemie **A181**, 301 (1938).

the V_2O_5 sols the particles are needle-like crystals of much larger size.

Bentonite Sols

The monodisperse sols of bentonite that have been prepared by Hauser and Reed,[10] particularly the fractions having the smallest particle size are remarkably thixotropic and, in the presence of minute concentrations of salts, are rheopectic. These sols seem particularly suitable for studies of the nature of the forces that act between colloidal particles. Traces of thixotropic behavior have been observed[10] in presence of salts at concentrations as low as 0.05 percent where the average distance between the particles is of the order of 2000A.

Mr. V. J. Schaefer and I have recently studied some bentonite sols that were prepared in Dr. Hauser's laboratory by Dr. F. J. Norton. The sample that we used was a monodisperse sol whose equivalent spherical diameter was about 300A. These sols were made from a white California bentonite whose analysis gave: SiO_2 39.2 percent; Al_2O_3 0.11 percent; Fe_2O_3 0.15 percent; CaO 15.1 percent; MgO 19.2 percent; ignition loss 22.7. Eighteen different dilutions of a single sample of this sol were made up with concentrations ranging from 0.8 to 2.8 percent (as determined by drying at 105°C). Volumes of 4 ml of each of these solutions were sealed into glass tubes about 0.8 cm inside diameter.

These tubes were shaken and then tilted so that the bubbles passed slowly the length of the tube. They were then placed in a rack and were examined between crossed Polaroids while they were standing undisturbed in a vertical position.

The solutions that contained less than 1.4 percent became isotropic within a couple of seconds, while the birefringence of the more concentrated solutions persisted for a time τ which increased rapidly with concentration. The sol containing 1.40 percent gave $\tau = 3$ seconds and this increased to 12 seconds at 1.50 percent, to 40 seconds at 1.57 percent and to 80 hours at 1.8 percent. The sol containing 2 percent after several hundred hours become isotropic in its upper half, while the lower half remained permanently birefringent, showing a fine mosaic structure of crystal grains having optic axes inclined about 45° to the axis of the tube. With the tube containing the sol of 2.2 percent a sharply defined isotropic portion of about 6 cm depth separated out at the top of the tube. The lower part consisted of the fine grained crystal mosaic. The sols of still higher concentrations appeared to be permanently crystalline throughout. It was only in the concentration range of 2.0 to 2.2 percent that two distinct phases separated after long standing.

The sols that contained from 1.4 to 2.0 percent were thixotropic gels which on standing slowly increased in strength so that (above 1.50 percent) even large bubbles would not move through them when the tubes were inverted. After standing a sufficient length of time, the gels lost their birefringence and became isotropic, but if these gels were shaken very gently or made to oscillate about a horizontal axis they showed temporary birefringence, which disappeared as soon as the agitation stopped. They thus acted essentially like solid elastic bodies which become birefringent when subjected to stress. If the tubes were vigorously shaken, the gel liquefied, and the liquid became anisotropic. It is clear therefore, that, in the case of the bentonite sols, birefringence and the mechanical strength of the gel are not closely associated. With tobacco virus solutions, however, the thixotropy and spontaneous birefringence go together.

It has often been thought[3, 5, 8] that the property of separation into two phases, one of which is isotropic and the other permanently birefringent, is characteristic only of sols having rod-shaped particles. The optical properties of the bentonite sols, however, prove that the particles are flat plates or disks.

It is probable that the repulsive forces between the particles in the bentonite sols, at concentrations above 1.4 percent, cause these particles to assume a lattice-like arrangement (probably a close-packed face-centered cubic type), which gives to the sol its elastic or gel-like properties. This ordered arrangement must start from nuclei and spread to give grain-like lattice regions separated by diffuse boundaries of unordered particles. A very slight shearing motion in the liquid can rotate the grains and allow them to coalesce and so grow in size (rheopexy), but too

[10] E. A. Hauser and C. E. Reed, J. Phys. Chem. **40**, 1169 (1936); **41**, 911 (1937).

great a shearing stress disrupts the grains and causes the gel to become liquid (thixotropy).

Although the center of each particle may thus occupy a definite position in a crystal lattice, the disk-shaped particle, at low concentrations, can rotate freely in all directions. With increasing concentrations, however, the potential energy will be a minimum when the disks have definite orientations.

Let us consider, for example, that the particles are negatively charged, electrically conducting disks arranged in a face-centered cubic lattice, with the appropriate number of univalent positive ions distributed in the aqueous phase in accord with the Poisson and Boltzmann equations. Each particle has 12 equidistant neighbors arranged like the midpoints of edges of a cube about its center. Symmetry considerations seem to indicate that the potential energy of a conducting disk will be a minimum when the axis of the disk lies parallel to any one of the three cubic axes of the lattice.

The induced charges on the disk then cause it to act as an octupole and for other orientations there will be even more poles. The energy barrier that must be overcome if the axis of the disk is to pass from one equilibrium position to another must thus increase with some high power ρ (such as 10 or more) of the ratio d/r, where d is the diameter of the disk and r the distance between the centers of neighboring disks. If the disks are not circular, or if they carry permanent dipole moments, ρ will be reduced, and the magnitude of the energy barrier increased.

Let us use this model in analyzing the changes in properties of bentonite sols that occur with increasing concentration, n, of the particles per cm^3. At very low values of n where the particles are not in lattice positions, there is no energy barrier to oppose free rotation. The Brownian rotation (average angle θ, in time t) should be given approximately by Einstein's equation

$$\theta^2 = kTt/4\pi\eta a^3, \qquad (1)$$

where η is the viscosity of the solvate and a the effective radius of the particle (assumed spherical).

The effective diameter of the particles of the bentonite sols we have made, calculated from the sedimentation rate by Hauser's method[10] was 300A. If the particles are thin circular disks of diameter d and thickness b, the effective diameter d_e should be roughly of the order of magnitude of the geometric mean of d and b. If we take $b = 20$A, which is the spacing of layers in wet clay minerals given by x-ray measurements, we get $d = 4500$A, or 0.45μ.

By Eq. (1) for $\eta = 0.01$, $a = 2.25 \times 10^{-5}$, we find $t = 0.04\theta^2$ second. Thus if the particles are oriented by artificially produced laminar flow in the liquid, this orientation disappears in a small fraction of a second. The relaxation time of about one second which we observed for bentonite concentrations of 0.8 to 1.2 percent may have been due to the persistence of motion in the liquid after passing the bubble through the tube.

The increased time of 3 seconds at 1.4 percent, however, could not have been due to this cause, for the greater viscosity should have decreased the duration of flow. Thus at concentrations of about 1.4 percent the energy barrier has become great enough to interfere with free rotation. At higher concentrations the axes of the disks normally oscillate about equilibrium positions parallel to the 3 lattice axes, but occasionally pass over a barrier to other equilibrium positions with a relaxation time τ given by

$$\tau = A\eta \exp(Ve/kT), \qquad (2)$$

where V is the height of the energy barrier in electron volts, A is a constant and η is the viscosity. Since the rotation of a micelle does not appreciably alter the positions of other micelles, η should be the viscosity of the solvate (water) rather than that of the solution and should thus be independent of the concentration of bentonite.

We may assume that V varies inversely with the ρth power of the distance r between molecules,

$$V = Br^{-\rho}. \qquad (3)$$

By logarithmic differentiation of Eq. (2), remembering that the concentration n varies in proportion to r^{-3}, we obtain

$$d\log\tau/d\log n = (\rho/3)(Ve/kT) = 3870\rho V/T, \qquad (4)$$

if V is in volts.

The increase in τ from 3 to 40 seconds for an increase in concentration from 1.40 to 1.57 percent, which we observed for bentonite sols, cor-

responds to a value of $d \log \tau / d \log n = 22.4$ and thus we obtain, at 20°C, $\rho = 1.70/V$.

The value of V can be determined by Eq. (2) from the temperature coefficient of τ. The sealed off tube containing 1.4 percent of bentonite which had been used for the first determinations of τ was immersed in ice water, the tube was tilted so that the bubble traveled half the length of the tube and back and was replaced in the ice bath. The anisotropy between crossed Polaroids disappeared[11] after 220 seconds. When this was repeated with the tube immersed in water at 40°C the time for the disappearance of anisotropy was 50 seconds.

This 4.4-fold increase in rate for 40°C, or 1.45-fold for 10°C, corresponds to a total activation energy of 6.3 kcal. per mol or an energy barrier of 0.274 volt. But by Eq. (2) we see that we must subtract the activation energy (4.3 cal. or 0.184 volt) which determines the temperature coefficient of the viscosity of water (decrease from 0.01793 to 0.00657, ratio 2.73 : 1, between 0° and 40°). Thus we find the energy barrier for rotation of the particles in the 1.4 percent bentonite sol is $V = 0.084$ volt. Combining this with our previous result $\rho = 1.70/V$, we find that the exponent ρ in Eq. (3) should be $\rho = 20$. This high value is reasonable for charged nearly circular conducting disks and indicates that the orientation of the particles is not caused by permanent dipole moments on these particles. The energy barrier V varies with the $\rho/3$ or 6.7 power of the concentration. Thus taking $V = 0.084$ volt at 1.4 percent we obtain $V = 0.03$, 0.05, 0.13 and 0.21 volt at concentrations of 1.2, 1.3, 1.5 and 1.6 percent respectively.

The development of permanent anisotropy and the separation into two phases which was found to occur at concentrations of 2.0 to 2.2 percent appears to be due to a mutual orienting effect of neighboring disks, which becomes important at high concentrations. The axes of all the disks in a crystal grain thus become parallel, and this alters the forces of interaction between the disks so that a new kind of uniaxial crystal grain is formed having a higher density, leaving a less concentrated isotropic intergranular material.

At concentrations above 2.4 percent the stiffness of the sol was apparently too great to permit the separation of the phases, but microscopic examination would probably have shown the isotropic phase between the crystal grains. A slight rocking or tapping motion would probably accelerate the separation into phases (rheopexy), or moderate centrifugation could be used.

According to these views, the birefringence of the bentonite sols is due to orientation of anisotropic bentonite particles rather than to a dissymmetry of the crystal lattice. The isotropic gels obtained by allowing the sols of concentration less than 2 percent to stand quietly for a time τ are birefringent (instantaneously reversible) when subjected to slight shearing stress (below their elastic limit). If, however, the intensity of the stress exceeds a critical value, permanent shear occurs and the anisotropy then decays slowly with the usual relaxation time τ.

These phenomena prove that the axes of the disks in the isotropic gels are not arranged in random directions, but oscillate about definite *equilibrium axes* which are related to the crystal axes. The effect of a small shearing stress is to displace the equilibrium axes with respect to the crystal axes. Because of the large value of the exponent ρ of Eq. (3) only a very slight distortion of the cubic lattice will be needed to give considerable angular displacements.

If the shearing stress is made sufficiently great, slip planes develop in the lattice and permanent displacement results. Because of the crystal lattice the direction of shearing displacement does not generally coincide with direction of the shearing stresses.

If the gel is subjected to continuously increasing displacements or flow, the gel structure is not necessarily completely broken down. With any given rate of shear a balance will be reached between the rate of growth of crystal lattice and the rate of destruction.

[11] This determination of the temperature coefficient of τ was made about four months after the solutions were sealed into the glass tubes. There had been a gradual change in the properties of the sols during this time, probably due to traces of substances taken up from the glass. During this time the value of τ for the tube containing 1.4 percent increased from 3 to about 100 seconds and similar increases were found with the other tubes. The property of giving two phases after long standing, which was originally observed with the 2.0 and 2.2 percent sols, was also gradually lost. These properties of bentonite solutions are extremely sensitive to traces of salts and other substances.

During this flow the disk-shaped particles become oriented under the influence of two factors. First, the solvate that surrounds the particles is subjected to laminar flow, probably parallel to the slip planes. This tends to orient the planes of the disks parallel to the slip planes. Second, between slip planes, there are distorted lattice arrangements in which the disks take an orientation different from either the direction of the shearing stress or the direction of the slip.

The following simple experiments show that the planes of the bentonite disks do not coincide with the direction of shear and so prove a crystalline structure even in the flowing liquid.

A 2 percent sol of white bentonite was sucked up into a pipette and allowed to flow steadily into a beaker. The birefringence of the sol flowing down through the vertical tubular part of the pipette (8 mm inside diameter) was observed by placing the tube between a pair of crossed Polaroids. These were held by a frame which permitted them to be rotated about a horizontal axis perpendicular to their plane.

When the two planes of polarization made angles of 45° with the direction of flow, the sol gave good transmission along two side bands separated by a darker central band. With lower concentration, 0.8 to 1.2 percent, the central dark band along the tube axis was more distinct than with the higher concentration.

The presence of a dark central band is characteristic of particles which are disks or flat plates. Rods become oriented in the direction of flow which is also the direction of shear, and so give transmission over the whole width of the tube. Disks or plates in a noncrystalline liquid should become oriented with their planes parallel to the tube axis, but perpendicular to the radius of the cylinder through the particle, for these planes are tangent to the surface of shear.

If the particles are circular disks, they should not change the plane of polarization of light passing through the axis of the tube and thus there should be a black band in the axis when the crossed Polaroids are at 45°. If, however, the particles are plates which are longer than they are broad, so that their long axes are oriented parallel to the tube axis, the intensity of the central band should serve as a measure of the ratio of width to length.

Rough observations with 1 percent bentonite sols show that the central band has an intensity perhaps half that of the side bands. This, with our previous observations of scattering, would indicate that the particles are thin flat plates of irregular shapes having lengths which are not large multiples of the widths.

When a vertically flowing sol is observed between crossed Polaroids having vertical and horizontal planes of polarization, one should expect to get no transmission with either rod-shaped or disk-shaped particles. Actually, however, the 2 percent bentonite sols show distinct transmission (perhaps $\frac{1}{4}$ as intense as with 45° Polaroids) in two side bands with a narrow completely black band between them. If the Polaroids are rotated slightly to the right (clockwise), the central black band moves to the right and becomes broader until at a Polaroid rotation of 12° the whole right side of the tube appears uniformly black, while the left side has increased considerably in brightness. A counter-clockwise rotation blackens the left side.

These phenomena prove that the planes of the disks in the flowing bentonite sol a rearranged so that they lie tangent to the surfaces of cones whose apexes (of half-angle 12°) point in the direction of flow.

The angle of 12° did not seem to vary appreciably with the rate of flow. In fact, with the 2 percent sol, the effect persisted indefinitely after the flow had stopped entirely. However, a noticeable increase in brightness appeared instantly if flow was allowed to start again. The intensity of the light became much less when the concentration of the sol was reduced, but even at 0.8 percent the effect could still be observed and the angle was still about 12°.

A similar effect was observed with the tube (8 mm inside diameter) of 1.4 percent bentonite sol (which had been used to study the temperature coefficient of τ) when this tube was placed vertically in ice water after having been made isotropic by immersion in water at 40°. After 20 to 60 seconds, examination between crossed Polaroids at 0° and 90° showed two broad side bands; the *left* one became black when the Polaroids were rotated 25° in a clockwise direction. This indicated that the disks lay on a 25° cone with apex up. The effect gradually died

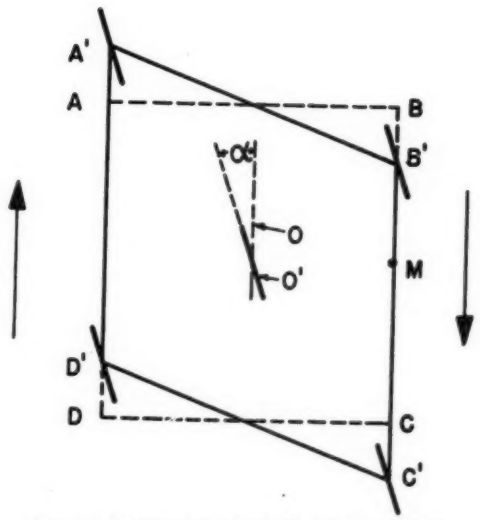

FIG. 1. Orientation of micelles due to shear.

away after a few minutes. After the sol had become isotropic at 0°C, immersion in the 40°C bath caused the side bands to reappear, but now the apex of the cone pointed downward.

These effects are due to vertical convection currents set up within the tube when its temperature is changed. Thus, when the tube is placed in ice water there is a thin layer of descending liquid close to the walls and a central upward return flow.

The direction of inclination of the bentonite disks with respect to the plane of shear is in every case that which we might expect by the following hypothesis. Take two neighboring points in the liquid which initially lie on a normal to the plane of shear. The vector or line connecting these points sweeps through two opposite quadrants of a plane which is perpendicular to the plane of shear and parallel to the direction of shear. We find that the plane of the bentonite particles is perpendicular to the plane containing the vector, and the line of intersection of these two planes, which we may call the line of inclination, lies within the quadrants swept through by the vector and makes an angle α with the line of shear (same angle with plane of shear).

The probable mechanism of the tilting of the disks can be illustrated by Fig. 1. The square $ABCD$ represents the cross section through the center of a cube which has a micelle at the center O and one at the midpoint of each edge. If the liquid is subjected to shear, as shown by the arrows, the square $ABCD$ is changed into the parallelogram $A'B'C'D'$. Since the micelles at B' and D' are brought closer to the micelle at the center O, the repulsive forces between them are increased. Thus the micelle at O becomes inclined through an angle α, as shown by O'. If the points B' and C' move downward with uniform velocity while A' and D' move upward, α should pass through a maximum and fall to zero when B' reaches M, a point midway between B and C. During the rest of the travel while B moves from M to C, α will be negative. Thus the average value of α should be zero.

However, because of the repulsive forces between the particles, B' will not move with uniform velocity, but will take longer to travel from B to M than from M to C, since it slips through the surrounding liquid in accord with Stokes law. The average angle α will thus be inclined in the direction shown by O' in the figure. A further development of this theory should make it possible to calculate the viscosity of bentonite sols in terms of the distance between the particles and the charges on the particle. We plan to obtain experimental data by which to test these theories.

Let us now consider the optical effects that occur when the tube containing the bentonite sol is dipped into ice water. We should expect that in a layer extending from the wall of the tube to the cylindrical surface where the downward velocity is a maximum, the bentonite particles should be tilted so that their planes intersect the axis below the particle (cone apex downward). Between this surface of maximum downward velocity and the axis of the tube, the planes of the disks should intersect the axis above the level of the particle (cone apex up). In repeating the experiments with the tube plunged into ice water, careful examination between crossed Polaroids showed the presence of very narrow bands near the walls where the particles have the opposite inclination to those nearer the axis.

The lack of parallelism between the axes of rod-shaped micelles and the direction of shear has been studied in detail for V_2O_5 sols by Freundlich, Zocher[12–14] and others.

[12] H. Freundlich, F. Stapelfeldt and H. Zocher, Zeits. f. physik. Chemie **114**, 190 (1924).
[13] H. Freundlich, H. Neukircher and H. Zocher, Kolloid Zeits. **38**, 43, 48 (1926).
[14] H. Zocher, Kolloid Zeits. **37**, 336 (1925).

A "cross of isocline" [15] (Wirbelkreuz) was observed when the sol was placed between coaxial cylinders, one of which rotated, and was examined between crossed Nicols in a direction parallel to the axis. This cross was displaced with respect to the planes of polarization by an angle, which Edsall calls the angle of isocline: This is the complement of the angle α which we have used to measure the inclination of the particles to the direction of shear.

The data show that the angle α is close to zero with old V_2O_5 sols. New sols give angles up to 45°, which decrease at high rates of shear but are nearly independent of concentration.

The differences which we observed between the values of α for the bentonite flowing in the pipette (12°) and for the tube in which temperature changes produced convection currents (25°) are undoubtedly due to this dependence of α on the rate of shear.

All the studies of bentonite which have been discussed so far were made with a sample of bentonite sol prepared in July, 1938. Recently Dr. Norton, in Schenectady, has prepared another monodisperse sol from white California bentonite in distilled water. The effective spherical diameter of the particles is approximately the same, 300A, as was found for the sol made previously. However, this new sample shows gel-like properties at considerably lower concentrations. Using sols ranging from 0.80 to 1.20 percent, we have measured the times of disappearance of the birefringence at 0°, 20°, and 40°. A summary of the data obtained is given in Table I.

The three values τ_0, τ_{20} and τ_{40} for a given concentration were plotted on semilogarithmic paper against $1/T$ and straight lines were drawn which best represented these points. The value of τ at 20°C and the ratio τ_0/τ_{40} obtained from each of these lines are given in the 2nd and 3rd columns of Table I. By Eq. (2) the energy barrier V was calculated as given in the 4th column. Plotting these values of V against the concentration on double logarithmic paper a straight line was obtained whose slope was -3.46. Three times this, or 10.4, should correspond to the value of ρ in Eq. (3).

TABLE I. *Time, τ, for disappearance of birefringence in bentonite sols at 20°C and the temperature coefficient of τ from measurements at 0° and 40°C.*

CONCENTRATION PERCENT	τ_{20} SEC.	τ_0/τ_{40}	V VOLTS	V CALC. VOLTS	τ CALC. SEC.
0.80	—	—	—	0.042	1.5
.920	4.2	—	—	.068	4.6
.968	8.	4.25	0.082	.082	8.
1.065	31.	5.1	.116	.114	28.
1.112	59.	5.6	.133	.134	62.
1.137	260.	—	—	.144	96.
1.160	>1000.	—	—	.156	145.

When the values of log τ from the data in the 2nd column in the table were plotted against log n a straight line was obtained having a slope 14.3. The mean value of V over the range from 0.97 to 1.11 percent is 0.104 volt. Substituting these values into Eq. (4), we obtain $\rho=10.5$, in agreement with the value of ρ from the temperature coefficient.

Using $\rho=10.5$ in Eq. (3) we calculate V as given in the 5th column of Table I. These values agree well with those calculated from the temperature coefficients. Substituting these values of V into Eq. (2) and choosing a single appropriate value of A, we obtain τ as given in the 6th column. Up to a concentration of 1.11 percent the agreement with the experimental data of the 2nd column is excellent, but at higher concentrations the observed values of τ increase much more rapidly than those calculated. In fact, at 1.16 percent permanent birefringence already sets in.

Dr. Norton finds that with this sol in concentrations from 1.2 to 1.5 percent, a sharply defined polycrystalline phase separates out in about 24 hours of quiet standing or after only 10 minutes of centrifuging. The bounding line is a sharp horizontal plane, and if the tube (6 mm diameter) is tilted, the boundary moves with the tube, but after several minutes in the tilted position the crystalline phase flows sufficiently to bring the boundary nearly back to a nearly horizontal plane. Analysis of the top and bottom phases in one of the tubes gave 1.16 and 1.35 percent, respectively.

A tube 2 cm diameter, 15 cm long was half-filled with a series of bentonite sols of decreasing concentrations. Birefringence could be observed on tilting the tube to a horizontal position even at concentrations as low as 0.05 percent.

[15] J. T. Edsall, J. Biol. Chem. **89**, 315 (1930).

Comparing these data with those given by the first bentonite sample, we note that the value of ρ is only a little more than half as great as the value 20 previously found; the concentration at which $V=0.080$ volt is now about 1.0 percent, whereas formerly it was 1.5 percent, and the lowest concentration at which separation into phases occurs is 1.2 instead of 2.0 percent.

The data of Table I indicate that the theory which led to Eqs. (2) and (4) is quite accurately applicable to these bentonite sols, so that the exponent ρ should be an important characteristic of sols of this type. The variations in ρ may be due to changes in the average shape of the micelles, the lower value presumably corresponding to more elongated particles.

We intend to make further studies of these bentonite sols determining the dependence of ρ on the presence of low concentrations of salts and on particle size.

Vanadium Pentoxide Sols

The bentonite sols whose properties we have investigated constitute perhaps the most striking example of sols containing disk-shaped particles.

For comparison we have studied vanadium pentoxide sols which have rod-shaped particles. We have used a sol, containing 2.0 percent of V_2O_5 in distilled water, which was made up 17 years ago. This was diluted with distilled water to give a series of solutions of different concentrations. When these were allowed to flow through the tube of a pipette (8 mm inside diameter) and examined between crossed Polaroids, birefringence was observed which persisted for several seconds after the flow was stopped, even at a concentration as low as 0.002 percent V_2O_5.

With increasing concentration, the time τ required for the disappearance of the birefringence after stopping the flow increased with the 1.8th power of the concentration at concentrations in the neighborhood of 0.015 percent, and still more rapidly at concentrations of 0.02 percent. At 0.015 percent τ was 120 seconds. This increase with the 1.8th power of the concentration may be compared to the corresponding exponents 22.4 and 14.3 which we observed with the bentonite sols.

With solutions of concentrations of 0.010, 0.015, and 0.020 percent we measured the temperature coefficient of τ between 0° and 40°C. The temperature coefficient increased with increasing concentration: Thus the ratios τ_0/τ_{40} were 2.9, 3.5 and 4.1, at the concentrations of 0.010, 0.015 and 0.020 respectively. Allowing for the temperature coefficient of η in accordance with Eq. (2), we find that V is negligibly small at 0.01 percent and increases to 0.046 volt at 0.015 percent and to 0.089 volt at 0.020 percent. Applying Eqs. (3) and (4), as for the bentonite, we find the best fit with the data is obtained when we choose $\rho=4$ for V_2O_5 sols as compared to $\rho=20$ and $\rho=10.5$ for the two bentonite sols. The experimental data, however, do not agree with the equations as well as in the case of bentonite, so that $\rho=4$ is a rough approximation.

There are at least two reasons why the equations are not so accurately applicable to the V_2O_5 sols. In the first place the sol had not been made monodisperse by centrifugation, and therefore contained particles having a wide range of sizes. Secondly, the mechanism by which the particles lose their orientation in the V_2O_5 sols is in many ways different from that which we have postulated for bentonite sols, so that the assumptions underlying Eq. (3) are not strictly applicable. Furthermore, the average distance between the particles, which are lined up in parallel directions in the anisotropic sol, does not necessarily vary in proportion to $n^{-\frac{1}{3}}$ as it does for bentonite, but may vary with n^{-1} if the end-to-end distance between rod-shaped oriented particles is independent of concentration.

We can readily understand why the concentrations at which perceptible persistence of orientation is observable is so much lower with the V_2O_5 sols than it is with the bentonite. For the rod-like particles, with diameters very small compared to their lengths, the length of the rods will be greater than the lateral distances between them even at relatively great dilutions. With the more compact bentonite disks, however, the diameter of the disk becomes comparable with the distance between the particles only at very much higher concentrations.

Let us consider a V_2O_5 sol of parallel rod-shaped particles of such concentration that the average lateral distance between the particles is

a little less than the average length of the particles. If a single particle has its longitudinal axis turned through 90°, the ends of the particle are forced between pairs of adjacent parallel molecules. The potential energy resulting from the repulsion between the displaced molecule and its neighbors will depend upon the lateral distances between molecules. However, this energy will not vary with a high power of this distance. The problem is closely related to that of the potential energy of two charged cylinders of small diameter whose axes are separated by a distance r but are respectively parallel to two axes that are at right angles to one another. (90° skew angle). The value of ρ corresponding to the variation of this potential with r should have a relatively low value.

At higher concentrations the displaced molecules are brought close to more than four other molecules. At very low concentrations, on the other hand, the lateral distance between molecules should be greater than the length of the rods, and therefore ρ probably increases. Thus for V_2O_5 ρ should not be constant over a wide range, as in the case of bentonite.

When the old V_2O_5 sol that we used flows through the tube of a pipette it acts as a uniaxial crystal. Thus it transmits no light between the crossed Polaroids when these are in the 0–90° position. When the Polaroids are turned to the 45° position, the transmitted light reaches a maximum but shows no trace of the central dark band which was observed with the bentonite sols, and which we attributed to the disk-like nature of the bentonite particle.

We must thus conclude that in this V_2O_5 sol, flowing with moderate velocity through a tube, the particles are completely oriented, parallel to the direction of flow so that $\alpha=0°$. This agrees with previous conclusions[12] that α is close to zero for very old V_2O_5 sols in which the particles have great lengths. In such sols, as in tobacco virus solutions,[2] there is probably no regularity of micelle arrangement in directions parallel to their length, so that the forces illustrated by Fig. 1 which cause the tilting are absent. In new V_2O_5 sols, however, the shorter particles permit a three-dimensional rather than a two-dimensional lattice arrangement and so give $\alpha \neq 0$.

Protein Crystals and Tactoids

Our observations with tobacco virus and bentonite lead us to believe that the separation of thixotropic gels into two phases on standing is a common phenomenon among sols which consist of highly charged particles or molecules. Bernal and Fankuchen[2] consider that Stanley's so-called needle-shaped crystals of tobacco mosaic virus protein are paracrystals, or sharply defined regions consisting of an anisotropic liquid phase. It seems preferable, however, to recognize the fact that they are tactoids, thus extending the definition of tactoid to include cases where the particles are large molecules.

There seems to be no advantage in regarding a tactoid as a type of liquid crystal; it appears to be essentially a solid crystal, often having such low mechanical strength that it appears to flow like a liquid. The lower phases that separate from a 2 to 3 percent tobacco virus solution or a 1.2 to 2.0 percent bentonite solution are built up of interlocking tactoids which form crystal grains giving a structure much like that observed with single-phase metallic alloys. The structure is permanent if undisturbed and Brownian movement is absent. Yet if the test tube containing the sol is tilted slightly, the phase boundary remains or soon becomes horizontal, showing the exceedingly low mechanical strength of this thixotropic gel.

Tactoids which are formed from more concentrated solutions (or by the addition of salts, as in the case of tobacco virus crystals) may have such high mechanical strength that they would normally be regarded as solids. Tobacco virus "crystals" have two characteristics which seem to distinguish them from most other crystals: (1) The distance between molecules increases continuously as the water content increases. (2) The molecules are not regularly spaced along a direction parallel to the long axes of the molecules.

The first of these characteristics seems to be a general property of protein crystals. Recent x-ray studies[16] of lactoglobulin, tobacco seed globulin, chymotrypsin and haemoglobin have shown that the volume of the unit crystallographic cell shrinks by 27 to 42 percent when

[16] D. Crowfoot, D. Riley, Nature **141**, 521 (1938); D. Crowfoot, I. Fankuchen, ibid. **141**, 522 (1938); J. D. Bernal, I. Fankuchen, M. Perutz, ibid. **141**, 523 (1938).

crystals of these proteins are dried in the air. This shrinkage is accompanied by a disordering of the structure, since the smallest observable x-ray spacings increase progressively from about 2A up to 20A.

The second characteristic of tobacco virus crystals (lack of order along optic axis) is not observed with the other protein crystals and appears to be caused by the unusually great length of the rod-shaped virus molecules.

The fact that a high but indefinite water content forms an essential part of protein crystals justifies us in regarding them all as tactoids. According to this concept, each protein molecule, which is surrounded by an envelope that may contain several thousand water molecules, is held in a position of equilibrium by repulsive forces resulting from charges on the molecule.

Coacervates

Bungenberg de Jong and his co-workers have published[17] a large number of papers in recent years dealing with the unmixing or coacervation of liquids into two phases. The most striking examples of this kind are furnished by colloidal solutions containing both positive and negative micelles. For example, if a dilute solution of gelatin (positive micelles) is mixed with a dilute solution of gum Arabic (negative micelles), droplets of a liquid phase separate out. We shall call this bipolar coacervation.

Numerous other examples are given where a colloid having charged particles is coacervated by the addition of a salt containing polyvalent ions of opposite sign. For example, if a solution of strontium chloride is mixed with ammonium molybdate, a second liquid phase is formed. This we shall call unipolar coacervation.

When ammonia gas is led into a strong solution of potassium or rubidium carbonate or tripotassium phosphate, a two-phase system is formed, which has been studied in detail by Jänecke.[18] Undoubtedly these are also examples of coacervation (probably bipolar).

Another interesting unipolar coacervate has been called to my attention by Dr. E. P. Partridge. When a strong solution of sodium hexametaphosphate is mixed with a strong solution of calcium chloride, the liquid separates into two isotropic layers, the lower being a very viscous liquid. In this case the negative ions are undoubtedly of very high molecular weight, while the positive ions are sodium ions.

The separations of tobacco virus and of bentonite sols into two phases seem to be typical examples of unipolar coacervation. On this basis we should also look upon tactoids as coacervates. Protein crystals are merely solid coacervates.

Bungenberg de Jong has classified various types of coacervation and has given a "working hypothesis" for the mechanism of their formation. In the case of "complex coacervates," which we call bipolar, the attractive forces between the positive and negative colloidal particles can account for their gathering together in a separate phase. However, since these coacervates usually contain 80 to 90 percent water and are liquid, it is necessary that there should be some repulsive force that prevents the positive and negative particles from coming into contact. The hypothesis is made that the intense electric field draws the dipole water molecules into the spaces between the particles and so holds them apart. The theories of Bungenberg de Jong are not so satisfactory when applied to the unipolar coacervates such as strontium, molybdate, calcium hexametaphosphate, tobacco virus and bentonite.

Attractive and Repulsive Forces in Unipolar Coacervates

We have seen from our consideration of the bentonite sols that large negatively charged colloidal particles, because of the repulsive force they exert upon one another, tend to become arranged in a definite crystal lattice. These forces can cause elasticity and anisotropy of thixotropic gels and tactoids and the disappearance of the Brownian movement. However, the spontaneous gathering together of particles into tactoids or into birefringent liquid phases indicates the presence of long range *attractive* forces, which under some conditions can outweigh the effect of repulsive forces.

Kallmann and Willstätter[19] assumed that van

[17] H. G. Bungenberg de Jong, Kolloid Zeits. **79**, 223, 334 (1937); **80**, 221, 350 (1937). These articles give references to and a summary of about 30 previous papers.

[18] E. Jänecke, Zeits. f. Elektrochemie **33**, 518 (1927).

[19] H. Kallmann and M. Willstätter, Naturwiss. **20**, 952 (1932).

der Waals attractive forces between colloidal particles might be of sufficient range and intensity to account for the formation of tactoids.

This idea has been accepted by Freundlich[20] and has been developed quantitatively,[21, 22] and applied to colloid systems[23] by H. C. Hamaker. He calculates that the potential of the van der Waals attraction between two thick flat plates separated by the distance d should vary with d^{-2}. In the case of equal spheres he finds that the potential energy is of the order of kT when the distance between the surfaces of the spheres is 0.1 to 0.5 of their diameter. These calculations, however, are based on the very improbable assumption that these forces involve a kind of "action at a distance" and are not influenced by the medium through which they are transmitted.

Hamaker analyzes the characteristic properties of colloids by means of diagrams in which the potential energy of the forces acting between two colloid particles is given as a function of the distance between them. He then regards this total potential as resulting from the superposition of the potentials of attractive and of repulsive forces. He believes[24] that the repulsion is due to the electric charges on the particles in accord with the Debye-Hückel theory, while the attraction is the result of van der Waals forces and is independent of the charge or the ion content of the solution. Adding the two potentials, he shows that a minimum potential may occur when the particles are at distances of the order of 1000A.

Houwink[25, 26] makes a similar analysis of the repulsive electrostatic forces and the attractive van der Waals forces to explain the properties of colloids and in particular the yield value.

In a recent paper Bergmann, Löw-Beer and Zocher[27] have calculated the repulsive forces due to the charges between Schiller layers of tungstic oxide sols and have equated these to the gravitational force. To obtain the repulsion they used a modification of the Gouy-Debye-Hückel theory. They considered only experimental data in which separate phases do not appear. They make the statement that electrostatic forces cannot explain the attractive forces in gels having micelles which all have similar charges.

The authors of these theories of colloidal structure recognize the repulsive forces between micelles of like charges and take it as axiomatic that this charge must be balanced by a long range attractive force which is not of electrostatic origin. They agree that the only conceivable attractive force that will meet their needs is the van der Waals force.

It will be shown in the following pages that there are at least three fundamental fallacies involved in this use of energy diagrams to analyze the stability of colloids.

(A) No direct account is taken of the thermal agitation which by itself would tend to cause the colloid particles and the ions to be dispersed throughout the liquid giving an osmotic pressure $p=\sum nkT$.

(B) The attraction between the charged micelles and the ion atmosphere of opposite sign which extends throughout the intervening liquid is ignored or neglected although it exceeds the repulsive force between the micelles.

(C) The electric charges on the micelles are assumed to be constant, whereas they must be, in general, dependent on the concentration of the micelles.

Let us analyze the general problem of the forces and energies responsible for the stability of colloids. We will first consider a colloidal solution having large positive micelles of charge z_1e, while the equivalent opposite charge is distributed throughout the intermicellar liquid in the form of negative ions of charge $-z_2e$. Let this solution be confined by a piston which is permeable to water but impermeable to both the micelles and to the ions. On the other side of the piston we assume there is pure water.

If the forces due to the interaction of the charges could be neglected, the pressure on the piston (Factor A) would be

$$p=(n_1+n_2)kT, \tag{5}$$

[20] H. Freundlich, *Thixotropy* (Paris, 1935).
[21] H. C. Hamaker, Physica **4**, 1058 (1937).
[22] H. C. Hamaker, Recueil des Travaux Chimiques des Pay-Bas **57**, 61 (1938).
[23] H. C. Hamaker, Recueil des Travaux Chimiques des Pay-Bas **56**, 727 (1937).
[24] H. C. Hamaker, Recueil des Travaux Chimiques des Pay-Bas **56**, 1 (1937).
[25] R. Houwink and W. G. Burgers, *Elasticity, Plasticity and Structure of Matter* (Cambridge University Press, 1937). See especially pp. 338–343.
[26] *Second Report on Viscosity and Plasticity* (Committee of the Academy of Sciences at Amsterdam) (Nordermann Publishing Company, N. Y., 1938). See pp. 233–237, of Chapter 4 by R. Houwink.
[27] P. Bergmann, P. Löw-Beer and H. Zocher, Zeits. f. physik. Chemie **181A**, 301 (1938).

where n_1 and n_2 are the concentrations of the micelles and of the ions, respectively. Since the total charge must be zero, we have

$$n_1 z_1 = n_2 z_2 \tag{6}$$

and thus Eq. (5) becomes

$$p = (1 + z_1/z_2) n_1 kT. \tag{7}$$

This force which is due merely to thermal agitation or Brownian movement is not a repulsive force between particles and so is not explicitly considered in a theory such as Hamaker's which is based on potential energy diagrams.

The second factor (B), which takes into account the effect of the electric charges, can be illustrated by considering a sodium chloride crystal. The distance between any ion in this lattice and its oppositely charged neighbor is less than the distance between the ion and its nearest neighbor of like sign. The attractive forces between unlike ions thus exceed the repulsive forces between like ions so that the crystal lattice should tend to shrink.

From simple dimensional considerations it is obvious that the effect of the Coulomb forces alone is to reduce the size of the lattice. Thus a crystal lattice built up of positive and negative point charges ($z_1 e$ and $-z_2 e$, respectively) has an energy per ion (of any given type) equal to

$$E = -\kappa z_1 z_2 e^2/a, \tag{8}$$

where κ is a constant depending upon the type of lattice, and a is the lattice constant. From this it follows that as a decreases, the energy decreases without limit so that stable equilibrium can occur only if some *repulsive force* other than the Coulomb interaction is called into play.

Exactly the same consideration must apply to a colloidal solution (unipolar) which has micelles of one sign with small ions of the opposite sign distributed within the intermicellar liquid. The interaction of these charges, just as in the sodium chloride crystal, gives an excess of attractive force and in order to have equilibrium it will be necessary not to have an additional *attractive* force, such as the van der Waals force postulated by Hamaker, but some new kind of *repulsive* force.

It is natural, therefore, that as the concentration increases, the effect of the attractive forces should exceed the dispersing tendency of the Brownian movement and tend to cause the colloid to draw together into a more condensed phase (unipolar coacervate). If no other repulsive force than that which acts between particles in contact were involved we should expect the colloid to form a dense precipitated solid mass from which the water has largely been expelled. Of course, this is just what happens when the concentration of a sodium chloride or other salt solution is increased too much; the salt crystallizes out in an anhydrous form or with a small amount of water of crystallization.

To account for the existence of unipolar coacervates which contain large amounts of water, we must either find some long range repulsive force or we must be able to show that the electrostatic attractive force is such a function of the distance between particles that a state of equilibrium can be reached (Factor C).

Equation (8), from which we concluded that the electrostatic force would tend to cause the separation of a dense phase, was based on the assumption that the charges on the particles remain constant when the distance between the particles is varied. Now in the case of colloidal particles it is probable that the charge on the micelles decreases as the concentration of the colloid increases. From the viewpoint of Eq. (8), therefore, we can see that if $z_1 z_2$ decreases faster than a decreases, the potential energy will rise at increasing concentrations so that there may be a definite concentration which gives a stable second phase.

A complete theory of the interaction of micelles with ionic atmospheres covering the whole range of concentrations would present insuperable mathematical difficulties. However, a very concentrated colloid phase in equilibrium with a dilute phase can be treated by an elementary consideration of two simple limiting cases.

In the theory of the potential distributions in the neighborhood of tungsten filaments in caesium vapor, which I have considered elsewhere,[28] there are many features which are fundamentally related to those of colloids. A tungsten filament in equilibrium with a given pressure of caesium has a definite electron emission and positive ion emission at a given tem-

[28] I. Langmuir, Phys. Rev. **43**, 224 (1933).

perature. In the interior of the caesium vapor at a large distance from the tungsten surface there are equal concentrations, n_0, of caesium ions and electrons, so there is no space charge. Taking the potential of this plasma to be zero, the potential of the tungsten filament is a function only of its temperature and of the caesium vapor pressure. It does not depend upon the size or shape of the tungsten surface. One could, for example, have fine tungsten particles distributed in any manner through the space and the potential of every surface would be the same. This corresponds then to the ζ-potential of colloidal particles. Abramson[29] has shown that the ζ-potential of quartz particles on which a given protein is adsorbed is independent of the size or shape of these particles.

Now let us consider that we bring some of the tungsten particles (or micelles in a colloid) so close together that their ionic atmospheres overlap. Since the ζ-potentials remain constant, it is necessary that the charges on the particles shall decrease.

Take, for example, a two-phase colloidal system in which a semi-permeable membrane, to which pressure can be applied, separates the two phases. Let the membrane be permeable to electrolytic ions but impermeable to the micelles of the colloid. In the dilute phase at sufficiently large distances from the micelle, the concentrations of positive and negative ions, both assumed univalent, will each be equal to n_0.

If the micelles are positively charged and have a potential V_1 (the ζ-potential), the concentration of negative univalent ions very close to the surfaces of the micelles is given by the Boltzmann equation

$$n_n = n_0 \exp (V_1 e/kT) = n_0 \exp \eta_1, \qquad (9)$$

where for convenience we have put

$$\eta = Ve/kT = 11{,}600\, V/T, \qquad (10)$$

if V is expressed in volts. Similarly the concentration of positive univalent ions is

$$n_p = n_0 \exp (-V_1 e/kT) = n_0 \exp (-\eta_1). \qquad (11)$$

In the ordinary approximate form of the Debye-Hückel theory η is assumed to be numerically small compared to unity. We wish, however, to consider colloids which have highly charged micelles, for these are the ones which show the separation into two phases (unipolar coacervation). For such colloids $\eta_1 \gg 1$, since the ζ-potential is far greater than the value 0.025 volt which corresponds to kT at room temperature according to Eq. (10). Close to the surface of a positive micelle, in a region where $\eta > 2$, the concentration of positive ions, by Eqs. (9) and (10), is negligible compared to that of the negative ions, so that there is a sheath of firmly bound negative ions surrounding the positive micelle.

At larger distances, where the potential is less than about 0.04 volt, positive as well as negative ions are present and the conditions postulated in the Debye-Hückel theory are fulfilled. It thus appears that the properties of the dilute phase can be treated by the Debye-Hückel theory if one replaces the micelle with its large positive charge by a point charge having an appropriate fictitious charge. This effective charge is roughly equal to the charge on a micelle reduced by the firmly bound negative ions in the sheath.

Fuoss[30] has shown that ion association of this kind plays an important part in the theory of the properties of electrolytes in solvents of low dielectric constant. It also becomes important in solvents of high dielectric constant such as water, if one of the ions has a charge high enough to give a potential above about 0.07 volt.

Let us now examine the conditions that exist within the concentrated phase which is in equilibrium with the dilute phase. Since the potential V_1 of the particles in this phase must be the same as that of similar particles in the dilute phase, we see that the limiting concentration n_1 of negative ions close to the surface of the particles has the same value as for the particles in the dilute phase.

If the particles in the concentrated phase are brought very close together, the charge carried by the solvate between the micelles, since n_n cannot exceed n_1, must decrease about in proportion to the volume of this solvate included in this denser phase, and there must be a similar decrease in the positive charge on the micelles. When the concentration of the micelles becomes very high, the whole phase tends to acquire a nearly uniform potential throughout, close to V_1, and the

[29] H. A. Abramson, *Electrokinetic Phenomena* (Chemical Catalog Co., New York, 1934). See especially pp. 111–114.

[30] R. M. Fuoss, Trans. Faraday Soc. **30**, 967 (1934); Chem. Revs. **17**, 27 (1935).

charges on the particles and in the solvate become very small. At the phase boundary, however, there is a sharp drop in potential so that, according to the Poisson equation, there must be an electric double layer. In the denser phase the electric forces may become negligible in determining the pressure p which would then be given by

$$p_1 = n_1 kT = n_0 kT \exp(V_1 e/kT). \quad (12)$$

This theory then enables us to calculate a limiting pressure which can exist within the condensed phase as the concentration increases.

If desired, this pressure can be described as a repulsive force existing within the concentrated phase. It has the characteristics of the repulsive force that we have found necessary to counteract the excess of electrostatic attractive forces within the colloid.

At somewhat lower concentrations of the colloid than those we have just considered, the potential V in the intermicellar spaces will range between V_1 at the surface of the micelles to some lower minimum value V_M at points in the liquid which are farthest from the micelles. The pressure within the concentrated phase will then have some value intermediate between p_1 and p_M where p_M can be calculated from Eq. (12) by replacing V_1 by V_M. As the micelle concentration decreases the charge on the micelles increases, and an increasingly large role is played by the electrostatic forces.

The Debye-Hückel Theory (1st Approximation) Applied to the Dilute Phase

The approximate conditions required for the appearance of two phases can be derived from the Debye-Hückel theory of osmotic pressures.[31] A calculation of this kind has already been made[32] for the case of highly ionized caesium vapor at high pressures. The equations that were developed, modified by the introduction of the dielectric constant and the unequal charges on positive and negative ions, are applicable to colloidal solutions.

The osmotic pressure p in an electrolytic solution according to the 1st-order approximation given by Debye and Hückel is

$$p = kT\sum n_i - e^2\sum(n_i z_i^2)/6D\lambda, \quad (13)$$

where λ, which we may call the Debye distance, is

$$\lambda = [DkT/4\pi e^2\sum(n_i z_i^2)]^{\frac{1}{2}}. \quad (14)$$

Elimination of λ between these two equations gives

$$p = kT\sum n_i - (\tfrac{1}{3})(\pi e^6/D^3 kT)^{\frac{1}{2}}[\sum(n_i z_i^2)]^{\frac{1}{2}}. \quad (15$$

The first term in the second member of this equation represents the pressure of all the ions, according to the ideal gas law, as if there were no electric forces. The second term gives the (1st-order) effect of the electric charges. It should be noted that the sign of this term is always negative, indicating that the effect of the interaction of the charges is equivalent to a net electric attraction and not a repulsion as was assumed in the theories of colloid structure that have been cited.

We have previously derived Eqs. (5), (6) and (7) for the effect of Factor A (thermal agitation) in the case of large positive ions of charge $z_1 e$ and concentration n_1 with small negative ions of charge $-z_2 e$ and concentration n_2. We can now apply Eq. (15) to modify these equations to take into account Factor B (electric interaction). Eliminating n_2 from Eq. (15) by means of Eq. (6), we obtain in place of Eq. (7)

$$p = (1+z_1/z_2)n_1 kT - (\tfrac{1}{3})(\pi e^6 D^3 kT)^{\frac{1}{2}} z_1^{\frac{1}{2}}(z_1+z_2)^{\frac{1}{2}} n_1^{\frac{1}{2}}. \quad (16)$$

By choosing appropriate units for p and n_1 this equation can be written in the simple form

$$p = 3n - 2n^{\frac{1}{2}}, \quad (17)$$

for which a plot is given by the curve $OBCG$ in Fig. 2. The maximum, found from Eq. (17) by placing $dp/dn = 0$, is located at $n=1$, $p=1$. In a similar way the maximum value of p according to Eq. (16) occurs when

$$n_1 = 4(DkT)^3/\pi e^6 z_1^3 z_2^2(z_1+z_2) \quad (18)$$

and

$$p_M = 4kT(DkT)^3/3\pi e^6 z_1^3 z_2^3. \quad (19)$$

The straight line OA in Fig. 2 corresponds to the ideal gas law (Factor A) and the deviations of the curve OBC from this line are due to the electric effects (Factor B).

[31] P. Debye and E. Hückel, Physik. Zeits. **25**, 97 (1924).
[32] Reference 28, p. 226.

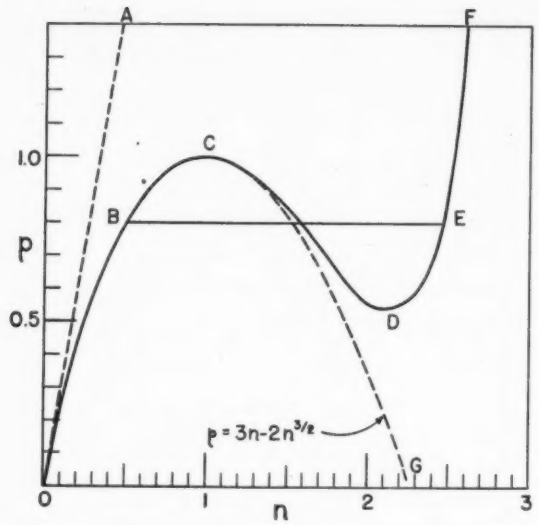

FIG. 2. Pressure-concentration curve illustrating conditions for coacervation.

If, p reaches a maximum at one value of n_1, it is certain that at still higher values of n_1 it must have a minimum value, since p must rise to very high values when the particles come into contact. Thus, if there is a maximum in p, the curve must have some such shape as *OBCDEF*. The location of the portion *DEF* will be determined by repulsive forces between particles or by (Factor C) a decrease in z_1 at high values of n_1. We shall give further consideration to *DEF* in a later section.

The portion *CD* of the curve between the maximum and minimum values of p is a region of instability, just as in the van der Waals theory of the continuous transition between the liquid and gaseous states. Therefore, whenever a maximum occurs we have conditions which necessarily cause two phases to appear as indicated by the points B and E with the horizontal line connecting them. The exact location of both B and E must depend upon the shape of the whole intermediate part of the curve *BCDE*. The theory of the *CD* portion must present almost insuperable mathematical obstacles, but the theories of the two limiting cases corresponding to the portions *OBC* and *DEF* are far simpler and can probably be developed without great difficulty. Eq. (16) is a first approximation to such a theory for the portion *OBC*.

In the case of many colloids, Factor C, which has an effect like that of a repulsive force of the type illustrated by Eq. (12), may come into play before the concentration has reached the value given by Eq. (18), and this may prevent the occurrence of the maximum in p. The curve then shows a point of inflection while the slope is still positive. This corresponds to a liquid-gas system above its critical temperature. Under these conditions two phases will not occur until such high concentrations are reached that repulsive forces due to contact come into play.

Let us consider an aqueous solution ($D=81$, $T=293°$K) containing w grams per ml of a substance, of molecular weight M, whose molecules dissociate into one positive ion of charge z_1e and z_1/z_2 negative ions each having a charge $-z_2e$. Then Eq. (18) takes the form

$$w_M = 6.15\times10^{-3} M/z_1^3 z_2^2(z_1+z_2). \qquad (20)$$

Here w_M is the value of w that corresponds to the maximum at C in Fig. 2.

Table II gives data calculated by Eq. (20) for a few typical salt solutions and colloids. In the first three examples w_M has been calculated from the known values of z_1 and z_2. The fact that these values of w_M are of the same order of magnitude as the solubilities of common inorganic salts illustrates the importance of the factors which we have considered in the derivation of this theory. There are several reasons why exact values for the solubility cannot be given by Eq. (20). The true equilibrium point B in Fig. 2 corresponds to a concentration which is necessarily lower than at the point C in the curve by an amount that depends upon the whole curve *BCDE*. Thus if the condensed phase at E is of

TABLE II. *The concentrations, w_M, in g per ml which give a maximum osmotic pressure for solutions of various types. Based on Eq.* (20).

EXAMPLE	SOLUTION	M	z_1	z_2	w_M	c ($z_3=z_4=1$)
1	NaCl	58	1	1	0.180	3.1 molar
2	$BaCl_2$	208	2	1	0.053	0.8
3	$MgSO_4$	120	2	2	0.006	0.19
4	Protein	35,000	4	1	0.67	0.19
	"	"	6	1	0.14	0.085
	"	"	6	2	0.031	—
5	Tobacco virus	5×10^7	53	1	0.04	0.0011
6	Bentonite	10^9	133	1	0.02	2×10^{-4}
7	Spheres 1μ diameter	6×10^{11}	660	1	0.020	—
	"	"	660	2	0.005	—

unusually high stability (for example $BaSO_4$) the solubility may be far less than given by Eq. (20). On the other hand, hydration of the ions, as illustrated by the water of crystallization in $MgSO_4 7H_2O$, may increase the solubility above w_M. Of course, we must consider also that the Debye-Hückel theory on which Eq. (20) is based cannot be expected to apply accurately to solutions as concentrated as those in the first three examples.

A protein of molecular weight of 35,000 has been chosen for Example 4. It was assumed that the protein gives micelles of charge z_1 and univalent ions, $z_2=1$, in solution. With $z_1=4$ or 6 we obtain values of w_M of 0.65 or 0.14, respectively. Thus the theory indicates that proteins of this molecular weight could be highly soluble in water if they have charges on the micelles which do not exceed about 6. If very low concentrations of divalent ions, $z_2=2$, are present the solubility would decrease to about one-quarter. It is known[33] that proteins such as egg albumin have values of z_2 that are positive when the pH of the solution is below the isoelectric point and negative for values of pH above the isoelectric point. The rate of change of the charge is about 8 units for each unit of pH. Thus, the value $z_2=6$ corresponds to pH values which differ from the isoelectric point by about 0.8 unit. It is seen that the effect of low salt concentrations as calculated by Eq. (20) is in general accord with the Schulze-Hardy rule.

In Example 5 with tobacco virus having a molecular weight of 50,000,000, we choose for w_M a value twice that at which coacervation was observed. We then calculate $z_1=53$. Of course, Eq. (20) cannot hold accurately in this case for it was based on the assumption of spherical molecules, and it is known that tobacco virus molecules are long rods. However, the order of magnitude of the calculated value of z_1 seems reasonable.

The molecular weight of bentonite sols is of the order of 10^9, and if we again take for w_M twice the concentration (1 percent) needed for coacervation we calculate $z_1=133$.

The last example is that of a colloidal solution of spheres 10^{-4} cm in diameter, of density 2, and therefore molecular weight 6×10^{11}. Here to get coacervation in a 1 percent solution a charge $z_1=660$ is required. The presence of divalent ions of the opposite polarity would give coacervation at a concentration only one-quarter as great.

[33] L. S. Moyer and J. C. Abels, J. Biol. Chem. **21**, 331 (1937).

The Effect of Added Salts

Besides the ions of charge z_1e and $-z_2e$, let us assume that we have also a concentration of some salt, giving per unit volume n_3 positive ions with a charge z_3e and n_4 negative ions with a charge $-z_4e$. Then in addition to Eq. (6) we have the condition

$$n_3z_3=n_4z_4. \tag{21}$$

Substitution of these values into Eq. (15) gives an expression for p in terms of n_1 and n_3. If we take the partial derivative of p with respect to n_1 and equate this to zero, we obtain an equation which enables us to calculate roughly the concentration of protein or of salt which will correspond to the maximum C in Fig. 2. This equation is

$$\begin{aligned} n_1z_1(z_1+z_2)+n_3z_3(z_3+z_4) &= 4(DkT)^3/\pi e^6z_1^2z_2^2 \\ &= 2.79\times10^8D^3T^3/z_1^2z_2^2. \end{aligned} \tag{22}$$

An increase in the amount of added salt thus decreases the colloid concentration at which p becomes a maximum. The concentration c, in mols per liter, needed to reduce n_1 to zero, is given by

$$c=6.15/z_1^2z_2^2z_3(z_3+z_4)^2. \tag{23}$$

The last column of Table II gives values of c calculated from Eq. (23) assuming that the ions of the added salt are univalent ($z_3=z_4=1$). Concentrations only one-quarter as great of a di-di-valent salt would be needed. This would indicate that ordinary proteins are sensitive to salts in 100 to 200 millimolar concentrations, while bentonite sols, in accord with observations, are affected in their coacervation properties by far lower concentrations.

Debye-Hückel 2nd Approximation. Effect of Particle Size

The approximate form of the Debye-Hückel theory that we have used has shown that electrostatic forces result in a net attraction that can

account at least qualitatively for unipolar coacervation.

Debye and Hückel, in a kind of second approximation, have considered the effects of the finite sizes of the ions. Their expression for the osmotic pressure[34] in the case where the charge and diameter of the micelle (z_1 and a) are large compared to the corresponding values for the ions of opposite sign is

$$p = n_1 kT z_1/z_2 - e^2 n_1 z_1^2 \sigma/6D\lambda, \quad (24)$$

where σ is given by

$$\sigma = 3\beta^{-3}[1+\beta-(1+\beta)^{-1}-2\ln(1+\beta)], \quad (25)$$

$$\beta = a/\lambda \quad (26)$$

and a is the effective distance of nearest approach of the negative and positive particles or ions. In the present case a is approximately the *radius* of the micelle.

Equation (24) can be brought to a simpler form by substituting

$$B = e^2 z_1 z_2/2DkT = 3.50\times10^{-8} z_1 z_2 \text{ cm}, \quad (27)$$

if we take $D=81$, $T=293°$K. Here B is the "Bjerrum[35] radius," within which the potential energy (to remove an ion to ∞) exceeds $2kT$. We thus obtain

$$p = n_1 kT(z_1/z_2)(1-B\sigma/3\lambda). \quad (28)$$

By differentiating with respect to λ, taking p, n_1, and σ as dependent variables, by making use of Eqs. (25), (26), (14), and by putting $dp/d\lambda=0$, we find, without making further approximations, that p becomes a maximum when the following condition is fulfilled:

$$a/\lambda+\lambda/a+2 = B/2a. \quad (29)$$

TABLE III. *Conditions under which p is a maximum. By Eqs.* (32), (29), (25), (28) *and* (34).

a/λ	$wz_1/\rho z_2$	B/a	σ	$1-B\sigma/3\lambda$	$\eta_1 z_2$
0.4	0.0027	9.8	0.598	0.220	14.0
0.6	.0071	8.53	.486	.169	10.7
0.8	.0132	8.10	.403	.130	9.0
1.0	.021	8.00	.341	.068	8.0
1.2	.030	8.07	.293	.056	7.4
1.4	.040	8.23	.254	.0242	6.8
1.6	.051	8.45	.223	−.005	6.5

[34] P. Debye and E. Hückel, Physik. Zeits. **24**, 185 (1923). See especially Eqs. (37) and (33).
[35] N. Bjerrum, Trans. Faraday Soc. **23**, 433 (1927).

The value of a/λ can be expressed in terms of B/a by combining Eqs. (14) and (27):

$$(a/\lambda)^2 = 8\pi a^3 n_1 (B/a)(z_1/z_2). \quad (30)$$

If ρ is the density of the micelles and w the concentration of the sol in grams per ml, then

$$w = (4\pi/3)a^3 n_1 \rho \quad (31)$$

and therefore in place of Eq. (30) we have

$$(a/\lambda)^2 = 6(wz_1/\rho z_2)B/a. \quad (32)$$

The potential V_1 at the surface of the micelle of radius a according to Debye and Hückel is

$$V_1 = ez_1/Da(1+a/\lambda). \quad (33)$$

Combining this with Eqs. (10) and (27)

$$\eta_1 = 2B/az_2(1+a/\lambda). \quad (34)$$

In order that p shall have a maximum value as n_1 increases Eq. (29) must be satisfied. The minimum value that B/a can have is 8 and this is reached when $a=\lambda$. Column 3 in Table III gives B/a for other values of a/λ. The 5th column shows that the coefficient of n_1kT in Eq. (28) becomes negative for $a/\lambda>1.6$, indicating that the Debye-Hückel equation is not applicable to such high concentrations which make λ small compared to the radius of the micelle. The Debye-Hückel theory, although it is frequently used under such conditions, cannot be expected to be valid for large values of $\eta_1 z_2$ for in its derivation $\epsilon^{\eta z}$ was replaced by $1+\eta z$.

At low values of a/λ, $\eta_1 z_2$ increases to very high values. The conditions for the validity of the theory are most nearly fulfilled for values of a/λ from 1.0 to 1.4. Here the value of B/a is approximately 8, and thus by Eq. (27) the charge on the micelles needed to give a maximum value of p is roughly $z_1 = 2\times10^8 a/z_2$.

With these large charges, considerably larger than we calculated in Table II, the concentrations needed for coacervation by column 2 are very much lower than found in Table II and are lower than given by experiment.

Potential Distribution Near Plane Surfaces

In connection with previous studies of metallic surfaces in caesium vapor at high temperature,

the following equation was derived[28] for the potential distribution:

$$\theta = -ln \tanh (\eta/4), \tag{35}$$

where

$$\theta = x/\lambda, \tag{36}$$

x being the distance from the plane surface and λ the Debye distance given by Eq. (14).

Equation (35) is a special solution of the fundamental equation

$$2\frac{d^2\eta}{d\theta^2} = \epsilon^{\eta} - \epsilon^{-\eta} \tag{37}$$

for the case that the potential gradient vanishes at $x = \infty$.

A plot of Eq. (35) is shown in Fig. 3 by the curve $ABCD$. For low values of η Eq. (35) approaches the limiting form

$$\eta = 4\epsilon^{-\theta}, \tag{38}$$

whereas for high values of η the limiting curve is

$$\theta = 2\epsilon^{-\eta/2}. \tag{39}$$

These two curves are given in Fig. 3 by FCD and ABE.

The curve FCD, as given by Eq. (38), corresponds to the Debye-Hückel theory. Thus we can replace the actual potential V_1 of a large colloid particle, having approximately a plane surface ($a \gg \lambda$), by the corresponding potential calculated from the curve FCD, and, for values of η less than about 1.5, obtain the same potential distribution as if we used the Debye-Hückel theory.

The portion of the curve AB rises to infinity at $\theta = 0$. Thus apart from a very small displacement $\Delta\theta$ the potential distribution near a charged surface is independent of the charge, provided the potential corresponds to values $\eta > 5$.

From this theory it follows that the potential distribution around large particles, at distances greater than about 0.8λ, can be calculated by the ordinary Debye-Hückel theory if one replaces the true value of η_1 by the fictitious value $\eta_f = 4$. For large spherical particles with $\eta_1 > 5$ ($V_1 > 0.125$ volt) we may put $\theta = (r-a)/\lambda$ and obtain from Eq. (38)

$$V = 4kT/e \exp [-(r-a)/\lambda]. \tag{40}$$

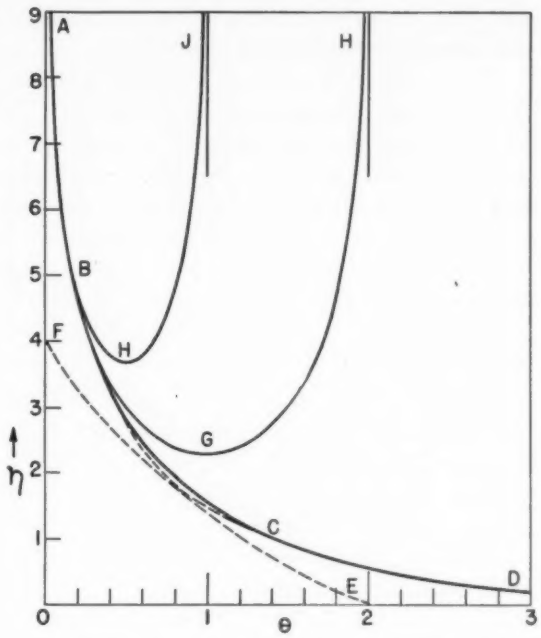

FIG. 3. Potential distributions between parallel plates in an electrolyte.

The potential distribution about a point charge according to the approximate Debye-Hückel theory is

$$V = (ez_1/Dr) \exp (-r/\lambda). \tag{41}$$

Since $r \gg \lambda$ we can replace r in the coefficient of the exponential factor by a and then by eliminating V between (40) and (41) we find

$$z_1 = (4DkTa/e^2) \exp (a/\lambda)$$
$$= 0.57 \times 10^{-8} a \exp (a/\lambda). \tag{42}$$

Thus, if we take a point charge $z_1 e$ as given by Eq. (42) and apply the simple potential distribution law of Eq. (41) we will obtain the same distribution as is given by Eq. (40) for all values of r greater than a. The charge z_1, however, will have to be greater than that needed if we were dealing with an ion of radius a.

We are now in a position to make a comparison between the two forms of the Debye-Hückel theory which we have used corresponding to Tables II and III or to the first and second approximations which we shall refer to as A and B. Let us assume that z_1 in each case is so chosen that the potential distributions are the same for $r > a$. The essential difference between

the two theories is that they give entirely different distributions for values of $r<a$.

Thus in Case A within the sphere of radius a there will be a distribution of ions of the opposite sign to that of the micelle, so that this is a kind of storage space for ions. As the concentration increases, the number of ions that are drawn into this space increases. The effect of this withdrawal of ions from solution is to decrease the pressure p from the value given by Eq. (7).

In the Case B the effect of taking a finite radius a is to exclude ions from the interior of the sphere so that the storage space is absent. Therefore, as the concentration increases, fewer ions are bound by the charges on the particles than in Case A. We see, therefore, the physical reason for the marked difference between the calculated data of Table III and the theoretical and experimental data of Table II.

The problem before us is to consider the mechanism of unipolar coacervation. This phenomenon will naturally occur best in colloids whose particles are highly charged, so that we may take $\eta_1>5$. We see from Fig. 3 that close to the surface of the particle where $\theta<1$ the potential rises faster than the Debye-Hückel curve *FCD*. Thus close to the surface of the micelle there will actually be a higher concentration than was given by the theory B. This excess of bound ions close to the surface produces an effect equivalent to that of the storage space in Case A.

For this reason, Theory A, which assumes a point charge, for high values of η_1 will presumably give a better approximation than Theory B. A closer comparison of the data of Tables II and III suggests that Theory A gives too great a storage space, while Theory B gives none. It would seem, therefore, as though a further development, which we may call Theory C, would be desirable in which we take, instead of a point charge, at the center, a sphere of radius a_2 where $a_2<a$. Then the charge z_1 on this smaller sphere can be chosen to make the storage space between the two spheres approximately equivalent to that which is due to the difference between the two curves *ABCD* and *FCD* in Fig. 3.

In Theory C we can still use Table III by replacing a by a_2. If we take $a_2=a/8$ we would make $B/a=1$ and would bring η to values where the Debye-Hückel theory would be applicable.

In this way, by choosing a suitable value for a_2/a, we can cover transitions between Theories A and B. Of course, closer examination might show that in place of Eq. (25) we would have some other relation to give σ in terms of a/λ. It is also possible that the ratio a_2/a should be a function of the concentration. It hardly seems worth while to develop a theory along such lines until we have far better quantitative experimental data on unipolar coacervation with colloids having particles of known character.

For the present we may conclude that neither of the two forms A or B of the Debye-Hückel theory that has been proposed is applicable quantitatively to the problem of coacervation. The A theory fits available data far better than the B theory, and there are good theoretical reasons why this should be true. Moreover, it is clear that the attractive forces given by the Debye-Hückel theory are of the right order of magnitude to account for unipolar coacervation. The lack of quantitative agreement gives no reason to assume that unipolar coacervation involves other than Coulomb forces.

From the foregoing attempts to apply the Debye-Hückel theory to unipolar coacervation it appears that the separation into two phases occurs under conditions where a/λ and B/a are each approximately equal to unity. Under these conditions the charge z_1 which must be assumed to exist on a fictitious micelle having a radius $a_2=0.2a$ is of the order of 1 unit for each A unit in the diameter $2a$.

Some of these conclusions are closely related to those of a recent paper by Fuoss[36] where he finds critical transitions in the distribution of ions when $a/\lambda=0.72$ and where $B/a=2$. We may conclude that if coacervation occurs it generally occurs under about these conditions. If, however, it fails to occur with rising concentrations, this will probably be in general because of factors such as repulsive forces of the type given by Eq. (12) or forces dependent upon the hydration of the ions.

[36] R. M. Fuoss, J. Am. Chem. Soc. **57**, 2604 (1935).

Repulsion Between Parallel Planes

Equation (35) is the solution of the differential Eq. (37) for the case where $d\eta/d\theta=0$ at $\theta=\infty$. Let us now consider the problem of two positively charged parallel planes at distance b apart. A complete solution of Eq. (37) can be had in terms of elliptic functions. For our present purposes, however, we are interested in the case where $\eta\gg1$, so that we can neglect $\epsilon^{-\eta}$ in Eq. (37). The general solution then becomes

$$\theta=2\exp(-\eta_M/2)\tan^{-1}[\exp(\eta-\eta_M)-1]^{\frac{1}{2}}, \quad (43)$$

where θ is now measured from the median plane at which η has a minimum value η_M.

If we place $\eta=\infty$ we obtain the value of θ at one of the planes.

$$\theta_1=b/2\lambda=\pi\exp(-\eta_M/2). \quad (44)$$

Now, the planes have forces acting upon them due to the pressure of the ions and to the electric field. The sum of these two forces must, however, be constant across the space between the planes.

The potential distributions between the planes for the two cases where $b=2\lambda$ and $b=\lambda$ are given in Fig. 3 by the curves $ABGH$ and $ABHJ$ respectively. At the median plane where $\theta=0$, $d\eta/d\theta=0$ and there is no electric field. If, then, we get the pressure of the ions at this median plane, we obtain the total forces acting upon the plates. According to Eq. (9), we then have for the concentration n_M at the midpoint

$$n_M=n_0\exp\eta_M. \quad (45)$$

The pressure $p=n_MkT$ is then given by

$$p=(2\pi\lambda/b)^2n_0kT, \quad (46)$$

but according to Eq. (14)

$$\lambda=[DkT/8\pi e^2n_0]^{\frac{1}{2}}=3.07\times10^{-8}c^{-\frac{1}{2}}\text{ cm}, \quad (47)$$

if $D=81$, $T=293$ and c is the molar concentration. By eliminating λ between these equations we obtain

$$p=(\pi/2)D(kT/eb)^2=8.90\times10^{-7}/b^2\text{ dynes/cm}^{-2}. \quad (48)$$

There is thus a repulsive force which is proportional to the surface area and varies inversely as the square of the distance b between the surfaces. This pressure is independent of the charge on the plates and of the ionic concentration provided the potential V_1 is great enough to make $\eta_1\gg\eta_M\gg1$ and the concentration is low enough to make $\lambda>b/3$. These restrictions on the general validity of Eq. (48) result from the neglect of the last term, $e^{-\eta}$, in Eq. (37), and the assumption $\eta_1=\infty$ in the derivation of Eq. (44).

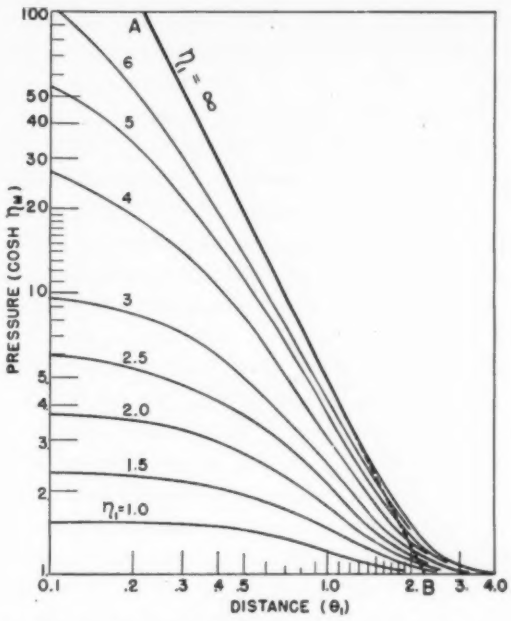

FIG. 4. Double logarithmic plot of the pressure between two plates as a function of the distance between them, for given values of the potentials V_1 on the plates. The actual values of p can be obtained from these data by Eqs. (52), (44), (47) and (10).

If we put

$$K=\exp(-\eta_M) \quad (49)$$

and replace η by a new variable ϕ defined by

$$\sin\phi=\exp[-(\eta-\eta_M)/2], \quad (50)$$

integration of Eq. (37), without simplifying assumptions, gives

$$\theta=2K^{\frac{1}{2}}[F(\pi/2, K)-F(\phi, K)], \quad (51)$$

where $F(\phi, K)$ is the elliptic integral of the first kind for which tables are available.

The exact expression for the pressure is

$$p=2n_0kT\cosh\eta_M=(\pi/2)D(kT/eb)^2R, \quad (52)$$

where

$$R=2(\theta/\pi)^2\cosh\eta_M. \quad (53)$$

When $R=1$, Eq. (52) reduces to Eq. (48).

The variation of pressure with the distance between the plates is illustrated in Fig. 4 which has been constructed by means of Eq. (51). The ordinates, on a logarithmic scale, measure cosh η_M, which, according to Eq. (52), varies in proportion to the pressure acting between the plates. The abscissas, also on a logarithmic scale, give θ_1, which, by Eq. (44), measures the distance b between the plates. The straight line AB corresponds to the inverse square law of Eq. (48).

The deviations from this limiting expression are of two kinds. When $\theta > 1.5$, or $b > 3\lambda$, the pressure may rise above the values given by Eq. (48); *viz.*, R may exceed unity. These deviations, however, are only 17 percent at $b = 4\lambda$. At still greater values of b the pressure rapidly approaches the limit $2n_0kT$.

The second factor, the approach of η_M to its limiting value η_1, causes the curves in Fig. 4 to break away from the straight line AB at low values of θ_1 and to become approximately horizontal. When $\eta_M > 2$ (or cosh $\eta_M > 3.8$) a good approximation may be had by using Eq. (43) without assuming that $\eta_1 \gg 1$. Substitution of K and ϕ, as defined by Eqs. (49) and (50), into Eq. (43) gives

$$\theta = 2K^{\frac{1}{2}}(\pi/2 - \phi). \tag{54}$$

The shape of the curves for small values of θ_1, where η_M approaches its limit η_1, may be had by assuming that $\eta_1 - \eta_M \ll 1$ in Eq. (50). Eq. (54) then becomes

$$\theta_1^2 = 4(\eta_1 - \eta_M) \exp(-\eta_M). \tag{55}$$

The limit of p at low θ_1, shown by Eq. (55) and by the curves of Fig. 4, corresponds to the pressure p_1 given by Eq. (12).

The whole of the pressure calculated from Eq. (52) cannot be regarded as a true repulsive force between the plates. Consider, for example, two colloid particles in the form of plates of widths large compared to λ. If these, with their faces parallel, are brought within a distance 3λ there is a pressure between them given by Eq. (52), but on the outer surfaces of each particle there is a pressure $2n_0kT$ acting in the opposite direction. The net repulsive force between the particles thus corresponds to a pressure p_r given by

$$p_r = 2n_0kT(\cosh \eta_M - 1). \tag{56}$$

It has been shown in a recent note[37] that these equations can also be used to calculate the pressure exerted by a solid surface upon the air-water interface of a film of water on this surface. This accounts apparently quantitatively for the Jones-Ray effect according to which very low concentrations of salts lower the capillary rise in surface tension measurements.

Repulsive Forces Between Micelles in Colloids

These equations for the forces between parallel planes are directly applicable to theories of the structure of laminar coacervates such as those formed in iron oxide and tungstic oxide sols that show Schiller layers.

The force given Eq. (48) is of the right magnitude to account for the formation of these coacervates. Thus if $b = 5000$A, we calculate $p = 350$ dynes/cm^2 which is a reasonable osmotic pressure for colloids of this kind. For example, if we assume $z_2 = 1$, $z_1 = 1000$ and $p = 350$, Eq. (7) gives $n_1 = 10^{13}$ per cm^3 (roughly 10^{-8} molar). A sol containing 5 percent by weight of plate-shaped particles 2000A square, of a thickness 250A and density 5 (molecular weight 3×10^8) gives this value of n_1.

The theory of repulsive forces which has been developed in the foregoing pages has been limited to the one-dimensional case to avoid the serious mathematical difficulties involved in the analogous 2- and 3-dimensional problems. The results obtained indicate that forces of the same general nature are effective in all types of unipolar coacervation, whether they involve 1-, 2- or 3-dimensional structures. There are, however, some differences that should be pointed out.

Three types of coacervates may be recognized which differ in the lattice arrangement of their particles:

One-dimensional coacervation. Iron oxide and tungstic oxide coacervates (Schiller layers) have plate-shaped particles arranged in parallel planes (1-dimensional lattice) with no regularity of distribution within the plane.

Two-dimensional coacervation. The tobacco virus coacervates and V_2O_5 tactoids are examples in which the rod-shaped micelles are arranged in

[37] I. Langmuir, Science **88**, Nov. 5 (1938).

a 2-dimensional lattice without regularity in an axial direction.

Three-dimensional coacervation. The white bentonite sols, although they contain plate-like micelles, form coacervates whose particles are arranged in a 3-dimensional lattice. There are probably numerous other cases where particles are in 3-dimensional amorphous arrangements (isotropic liquids).

In each case the dilute phase in equilibrium with the coacervate has a 3-dimensional amorphous arrangement of its micelles. This fact seems to be essential for the coexistence of the two phases. To make this clear let us consider the possibility of coacervation in a 1-dimensional system such as that represented in Fig. 4. A plot of p against $1/\theta$ should give a kind of "equation of state" that can be compared to Fig. 2. According to the theory we have given we see, however, that for the 1-dimensional system (Fig. 4), there can be no maximum value of p at large values of θ_1 (low concentrations) and therefore a separation into two phases cannot occur.

The actual existence of 1-dimensional coacervates therefore depends upon the 3-dimensional character of the dilute phase. This means that certain dilute 3-dimensional sols must have higher osmotic pressures p than more concentrated 1-dimensional coacervates.

This difference between the 1- and 3-dimensional phases appears to depend upon the fact that ion association in a 3-dimensional electrolyte becomes negligible at infinite dilution but this does not occur in a 1-dimensional system. Thus in the phase having the 3-dimensional structure the pressure by Eq. (7) is large because z_1 is large, but in the phase having the 1-dimensional structure the effective charge z_1 may be smaller because many of the ions are bound more firmly by the particles (greater ion association).

A complete theory of even 1-dimensional coacervation must therefore involve a calculation of the pressure in a phase having a 3-dimensional arrangement of micelles.

The Potential V_1 and the ζ-Potential

It is known[29] that the ζ-potential, which is calculated from the electric mobilities of particles, is generally much less than the thermodynamic or electrochemical potential. What value should be used for V_1 in the equations that have been derived?

It is of interest that practically all the values of ζ given in Abramson's book[29] lie below a rather definite limit of 100 mv. This corresponds to $\eta=4$, which is the value at the point F in Fig. 3 where a very rapid rise in η begins.

By differentiation of Eq. (39) we find that the potential gradient at the surface of a large particle is given by

$$dV/dx = -(kT/e\lambda)\exp(\eta_1/2) = -(0.025/\lambda)\exp(\eta_1/2)\ \text{volts/cm.} \quad (57)$$

With a 10^{-5} M salt solution, $\lambda=10^{-5}$ cm and the potential gradient corresponding to $\eta_1=4$ is then 19,000 volts/cm.

In a discussion of the dielectric constants of dilute salt solutions Debye[38] has calculated that strong electric fields near the ions cause a dielectric saturation. The effect is the same as if the water in regions of field strength exceeding 150,000 volts/cm contributed nothing to the dielectric constant. Actually, of course, the loss of dielectric power is gradual and Debye gives a curve showing the calculated values of D as a function of the distance from the center of the ion.

It is perhaps possible that fields of the order of 20,000 volts/cm which exist when $\eta_1>4$ cause an interference in the motions of ions which accounts for the limitation in the observed values of ζ. Probably far higher potential gradients, of the order of 150,000 volts/cm (corresponding to $\eta_1=8$), are needed to give a layer of water of hydration (impenetrable to ions).

It seems therefore that when ζ is small, V_1 and ζ are equal, but when ζ approaches its limit of about 100 mv, V_1 can rise considerably above 100 mv. Contact potential measurements of monolayers of proteins and fatty acid derivatives on water give potentials as high as 400 mv. It seems that similar or even higher potentials must be active in many colloids.

Bipolar Coacervation

The cases of coacervation most intensively studied by Bungenberg de Jong have been those in which there are colloidal particles of both

[38] P. Debye, *Polar Molecules* (Chemical Catalog Co., New York, 1929), p. 118.

signs. With these bipolar coacervates, if V_1 is to remain unchanged for particles of both kinds, the electric fields and the charges on the micelles increase when the concentration increases, whereas with unipolar coacervates the fields decrease. The fact that the particles in the bipolar coacervates remain separated by considerable distances and do not come into contact proves the presence of some other kind of repulsive force than that given by Eq. (48). Hydration seems to be the most reasonable explanation.

The very intense fields that develop when the particles come close together are apparently able to draw water in between the particles and so hold them apart.

It seems, therefore, that Bungenberg de Jong's working hypothesis for this type of coacervation should be accepted. It should be noted that in bipolar coacervates the particles are far closer together than they are in such unipolar coacervates as bentonite, tobacco virus and iron oxide sols.

DECEMBER, 1938 JOURNAL OF CHEMICAL PHYSICS VOLUME 9

Quadrupole Contributions to London's Dispersion Forces

HENRY MARGENAU
Sloane Physics Laboratory, Yale University, New Haven, Connecticut
(Received August 27, 1938)

The contribution of terms in R^{-8} and R^{-10} to the dispersion forces is expressed by a simple, approximate formula (Eq. (7)) involving only measurable quantities (polarizability, absorption frequency, oscillator strength). The formula is applicable when the dispersion curve of the substance can be represented with the use of a single resonant frequency. Numerical values of the terms in question are calculated for a number of molecules (Table II). Except in the case of the alkalies, where the convergence of the sequence in inverse powers of R fails at distances around 6A, the R^{-10} term is generally negligible, while the R^{-8} term contributes appreciably in the region of the van der Waals minimum.

FOR large distances of separation (R), the interaction energy of two neutral molecules is given with good approximation by C_1/R^6, where C_1 is a coefficient which may be calculated with considerable precision for simpler molecules and atoms. For the case where the dispersion curve of the substance in question is given with sufficient accuracy by an expression involving but a single resonant frequency, ν, London[1] has derived the particularly simple and beautiful formula:

$$C_1 = -\tfrac{3}{4}h\nu\alpha^2, \qquad (1)$$

which, in applications, has proved fairly successful.

On the other hand, it is known that C_1/R^6 is only the first term of an expansion to which multipoles contribute higher powers in $1/R$. In detailed investigations, and especially when attention is given to values of the intermolecular distance in the neighborhood of the van der Waals minimum, these higher power terms are important. I wish to point out in this note that, under the conditions for which (1) is valid, equally simple formulas are available for the coefficients of the higher terms.

Expression (1) is derived most directly with the use of a model which possesses only a single frequency, the simple harmonic oscillator.[1] The state function for two three-dimensional isotropic oscillators, infinitely far apart, and vibrating in quantum states n_1, n_2, n_3, and n_4, n_5, n_6, respectively, is given by

$$\psi(n_1 \cdots n_6) = \prod_1^6 H_{n_i}(\beta^{\frac{1}{2}} x_i) \exp\left[-(\beta/2)x_i^2\right], \qquad (2)$$

where the x_i stand for the 6 coordinates of the two oscillators, each referred to the center of mass of its molecule. The parameter β measures

[1] F. London, Zeits f. physik. Chemie **B11**, 222 (1930); Trans. Faraday Soc. **33**, 8 (1937).

the stiffness of the oscillators; elementary theory shows it to be related to the polarizability α and the classical frequency ν as follows:

$$\beta = e^2/\alpha h\nu. \tag{3}$$

As the two molecules approach, a perturbation $V = V_1 + V_2 + V_3 + \cdots$ is called into play, where[2]

$$V_1 = -(e^2/R^3)(2z_1z_2 - x_1x_2 - y_1y_2),$$

$$V_2 = (3e^2/2R^4)[(x_1^2 + y_1^2 - 2z_1^2 - 2x_1x_2 - 2y_1y_2)z_2 - (x_2^2 + y_2^2 - 2z_2^2 - 2x_1x_2 - 2y_1y_2)z_1],$$

$$V_3 = \tfrac{3}{4}(e^2/R^5)[3x_1^2x_2^2 + 3y_1^2y_2^2 + x_1^2y_2^2 + y_1^2x_2^2 - 4(x_1^2 + y_1^2)z_2^2 - (4x_2^2 + y_2^2)z_1^2 + 8z_1^2z_2^2 + 4(x_1x_2y_1y_2 + 4x_1x_2z_1z_2 + 4y_1y_2z_1z_2)].$$

The z axis of both molecules is here chosen parallel to R.

A perturbation calculation leads to the results desired. The first-order energy is zero because the average of V over the normal state vanishes. To compute

$$E^{(2)} = \sum_\lambda{}' \frac{|V_{0\lambda}|^2}{E_0 - E_\lambda},$$

we only require the following formulas for the elements of the individual coordinate matrices:

$$x_{01} = (2\beta)^{-\frac{1}{2}}; \quad (x^2)_{00} = (2\beta)^{-1};$$
$$(x^2)_{02} = 2^{-\frac{1}{2}}\beta^{-1}.$$

Elements not listed here either do not appear or are zero. Distinction between the coordinates is unnecessary because the oscillators are taken to be isotropic. The unperturbed energies, E_λ, are given by

$$E_\lambda = h\nu \sum_{i=1}^{6} (n_i + \tfrac{1}{2}).$$

In Table I we show (1) the excited states $\psi(n_1 \cdots n_6)$ for which $V_{0\lambda}$ is different from zero, (2) the corresponding energy difference $E_\lambda - E_0$, (3) the value of $V_{0\lambda}$. It will be noticed that V_1 causes the ground state to combine only with doubly excited states, V_2 with triply, and V_3 with quadruply excited states. This means that there is no collusion between the three terms in V; each produces cleanly its own order of approximation, and there are no terms with powers of $1/R$ intermediate between those appearing in the result. The parentheses in the first column contain the quantum numbers of the functions in question; they refer to $x_1y_1 \cdots z_2$, in that order. Finally, we are using the abbreviations $p_1 = -e^2/R^3$, $p_2 = 3e^2/2R^4$, $p_3 = \frac{3}{4}e^2/R^5$.

Adding up the squares of the elements and dividing by $(E_0 - E_\lambda)$ we obtain

$$E^{(2)} = -\frac{3/2}{2h\nu}\frac{p_1^2}{\beta^2} - \frac{5}{3h\nu}\frac{p_2^2}{\beta^3} - \frac{70}{4h\nu}\frac{p_3^2}{\beta^4},$$

which, on inserting the values of the p's and of β (Eq. (3)), becomes

$$E^{(2)} = -\frac{3}{4}\frac{\alpha^2 h\nu}{R^6} - \frac{15}{4}\frac{\alpha^3(h\nu)^2}{e^2R^8} - \frac{315}{32}\frac{\alpha^4(h\nu)^3}{e^4R^{10}}. \tag{4}$$

The division of elements in Table I shows, of course, that the same result could have been obtained by squaring V_1, V_2 and V_3, computing 0-0-elements, and dividing by $2h\nu$, $3h\nu$ and $4h\nu$, respectively.

The next step is to generalize this expression so as to make it valid for the case where each

TABLE I.

FUNCTIONS	$(E_\lambda - E_0)/h\nu$	$V_{0\lambda}$	
(100,100)	2	$-(2\beta)^{-1}p_1$	Elements of V_1
(010,010)	2	$-(2\beta)^{-1}p_1$	
(001,001)	2	$2(2\beta)^{-1}p_1$	
(200,001)	3	$\frac{1}{2}\beta^{-\frac{1}{2}}p_2$	Elements of V_2
(020,001)	3	$\frac{1}{2}\beta^{-\frac{1}{2}}p_2$	
(002,001)	3	$-\beta^{-\frac{1}{2}}p_2$	
(100,101)	3	$-2(2\beta)^{-\frac{1}{2}}p_2$	
(010,011)	3	$-2(2\beta)^{-\frac{1}{2}}p_2$	
(001,200)	3	$\frac{1}{2}\beta^{-\frac{1}{2}}p_2$	
(001,020)	3	$\frac{1}{2}\beta^{-\frac{1}{2}}p_2$	
(001,002)	3	$-\beta^{-\frac{1}{2}}p_2$	
(101,100)	3	$-2(2\beta)^{-\frac{1}{2}}p_2$	
(011,010)	3	$-2(2\beta)^{-\frac{1}{2}}p_2$	
(200,200)	4	$3\cdot\frac{1}{2}\beta^{-2}p_3$	Elements of V_3
(020,020)	4	$3\cdot\frac{1}{2}\beta^{-2}p_3$	
(200,020)	4	$\frac{1}{2}\beta^{-2}p_3$	
(020,200)	4	$\frac{1}{2}\beta^{-2}p_3$	
(002,200)	4	$-4\cdot\frac{1}{2}\beta^{-2}p_3$	
(002,020)	4	$-4\cdot\frac{1}{2}\beta^{-2}p_3$	
(200,002)	4	$-4\cdot\frac{1}{2}\beta^{-2}p_3$	
(020,002)	4	$-4\cdot\frac{1}{2}\beta^{-2}p_3$	
(002,002)	4	$8\cdot\frac{1}{2}\beta^{-2}p_3$	
(110,110)	4	$4\cdot(2\beta)^{-2}p_3$	
(101,101)	4	$16\cdot(2\beta)^{-2}p_3$	
(011,011)	4	$16\cdot(2\beta)^{-2}p_3$	

[2] H. Margenau, Phys. Rev. **38**, 747 (1931). The three terms here retained are known as dipole-dipole, dipole-quadrupole, and quadrupole-quadrupole energies.

molecule contains several oscillating charges, all having the same frequency. Let the number of electrons be f. The modification of (2) is obvious; instead of (3) we have

$$\beta = fe^2/\alpha h\nu.$$

V_1, V_2 and V_3 must be modified by attaching to all coordinates labeled 1, another subscript i, to those labeled 2 another subscript j, and then summing over both i and j independently from 1 to f. There will then be many more functions in Table I, and the matrix elements there listed will be repeated f^2 times. On adding them up as before, there emerges a factor f^{-1} in the second, and f^{-2} in the third term on the right-hand side of (4), the first term being unaltered. The final formula therefore reads

$$E^{(2)} = -\frac{3}{4}\frac{\alpha^2 h\nu}{R^6} - \frac{15}{4}\frac{\alpha^3(h\nu)^2}{fe^2R^8} - \frac{315}{32}\frac{\alpha^4(h\nu)^3}{f^2e^4R^{10}}. \quad (7)$$

The meaning of f here is perfectly clear; it is the oscillator strength of the transition of energy $h\nu$. As a concession to the structure difference between real molecules and our simple model we must permit f to be nonintegral. Moreover, this quantity is always known from the dispersion formula whenever $h\nu$ is known. This is an advantage not shared by the results of variational calculations, which often involve the number of electrons in the outer shell in a rather ambiguous way.

Equation (7) may, of course, be written in a way such that $h\nu$ does not appear, because of an elementary relation between α, $h\nu$ and f, holding for a molecule with a single absorption frequency. In fact, for a collection of simple oscillators, as well as an ideal molecule with single ν,

$$\nu = (e/2\pi)(f/\alpha m)^{\frac{1}{2}}.$$

When this is introduced in (7) that equation becomes

$$E^{(2)} = -\frac{3}{4R^6}\hbar e\left(\frac{f\alpha^3}{m}\right)^{\frac{1}{2}} - \frac{15}{4R^8}\hbar^2\frac{\alpha^2}{m} - \frac{315}{32R^{10}}\frac{\hbar^3}{e}\left(\frac{\alpha^5}{fm^3}\right)^{\frac{1}{2}}. \quad (7')$$

The first term on the right represents the formula of Slater and Kirkwood,[3] except that the oscillator strength appears in place of their parameter N, the number of electrons in the outer shell. It is thus apparent that for molecules having a single ν, N should really be replaced by f.

The manner in which we have derived formula (7) shows clearly its limit of validity: it arises from the fact that it contains only a single frequency. One must also remember that the error committed in approximating the dispersion curve with the use of a single frequency is magnified in each succeeding term of (7), because these terms involve increasingly higher moments of the total spectral intensity distribution. But it seems that one may trust this formula as a guide somewhat beyond the limitations implied in its derivation, since it contains only measurable quanties not peculiar to the simple oscillator model. Remarks by Van Vleck[4] on the use of the oscillator model in deriving corrections to the Clausius-Mosotti law are illuminating in this connection.

To test it, we refer to the case of He, where the dispersion curve can be represented with sufficient accuracy if the single quantum $h\nu = 24.4$ e-volts is employed, and where the dipole-quadrupole term is known from other calculations.[2, 5] The f value associated with ν is 1.1. We write Eq. (7) in the form $E^{(2)} = C_1R^{-6} + C_2R^{-8} + C_3R^{-10}$. Of primary interest is C_2/C_1, which has the value 1.53×10^{-16} cm^2. The most accurate calculation of this quantity is probably the one by Page, who finds 1.75×10^{-16} cm^2. This agreement is to be regarded as satisfactory.

In Table II may be found the calculated values of C_1, C_2 and C_3 for a number of molecules, together with the data used for $h\nu$, α and f.[6] The numerical results are based on Eq. (7), not (7′). The two forms often give slightly different results because the experimental value of α does not agree exactly with that extrapolated from

[3] J. C. Slater and J. G. Kirkwood, Phys. Rev. **37**, 682 (1931).

[4] J. H. Van Vleck, J. Chem. Phys. **5**, 556 (1937). See especially p. 564.

[5] C. H. Page, Phys. Rev. **53**, 426 (1938).

[6] The frequencies and f values used here and in Table II are taken chiefly from C. and M. Cuthbertson's investigations. Tabulations and a good survey of matters relating to the dispersion curve may be found in the article by K. L. Wolf and K. F. Herzfeld, *Handbuch der Physik*, Vol. 20 (1928).

TABLE II.

	$h\nu$ e-volts	$\alpha\times10^{24}$	f	$C_1\times10^{60}$	$C_2\times10^{76}$	$C_3\times10^{92}$	$C_2/C_1\times10^{16}$	$C_2/C_1\times10^{16}$*
Ne	25.7	.39	2.37	4.67	6.9	5.3	1.47	1.46
A	17.5	1.63	4.58	55.4	120	136	2.17	3.0
Kr	14.7	2.46	4.90	107	275	370	2.55	3.08
Xe	12.2	4.00	5.61	233	710	1120	3.04	
H_2	(14.5)	.81	(1.5)	11.4	31	45	2.7	
N_2	15.8	1.74	4.61	57.2	120	130	2.08	
O_2	13.6	1.57	3.11	39.8	96	120	2.41	
CO_2	15.5	2.86	5.70	152	410	590	2.72	
CH_4	14.1	2.58	4.60	112	310	440	2.77	
NH_3	11.7	2.24	2.72	70	236	410	3.37	
Cl_2	12.7	4.60	6.55	321	1000	1630	3.10	
HCl	13.4	2.63	4.25	111	320	480	2.89	
HBr	12.1	3.58	4.71	185	600	1000	3.24	
HI	10.5	5.4	5.30	370	1360	2700	3.7	
Na	2.08	29.7	1	2190	47600	530000	21.7	
K	1.60	(49)	(1)	4600	127000	1800000	28	

* Values according to Buckingham, reference 7.
Numbers in parentheses are uncertain.

the dispersion formulas here employed. Absolute units are implied throughout (energy expressed in ergs). The numbers appearing under $C_2/C_1\times10^{16}$ may be defined as the ratio of dipole-quadrupole to dipole-dipole energy at a hypothetical distance of separation equal to 1A (where, of course, they are physically meaningless because of other overpowering interactions).

Very refined variational calculations of van der Waals forces including the coefficient C_2 have recently been made by Buckingham.[7] The last column contains his values of C_2/C_1 for the rare gases he considered. In judging the agreement one should recall that the range of uncertainty even in C_1 is still fairly large. (Thus, London[1] obtains for He, $C_1=1.22\times10^{-60}$ against Buckingham's $C_1=1.63\times10^{-60}$.) Also, if Buckingham's method is applied to the oscillator model, it gives a value of C_2/C_1 which is 28 percent too great. In view of these facts the agreement seems good.[8]

Two general conclusions of some interest may be drawn from Table II. First, the term in R^{-8} is always of appreciable magnitude in the region of the van der Waals minimum, while the term in R^{-10} is quite generally negligible. Second, for the alkalies, Na and K, the quadrupole forces are particularly strong in relation to the R^{-6} forces. Indeed the indication is that the R^{-8} term is equal to the R^{-6} term at an intermolecular distance of about 5A. Here, the last term in (7) also gains importance; it contributes about half as much as the first. This means that the series expansion for V has little significance for these atoms, except at larger distances of separation.

Unfortunately, no simple formula is available for expressing the first-order forces which are of prime importance in the critical region. The approximation of infinite forces at the gas kinetic collision distance is most inadequate. It gives the appearance of success if, as a compensating error, the dipole-quadrupole forces are neglected. In general, then, if formula (7) is to be used, the first-order forces must be introduced either from detailed calculation[9] or by a method such as that adopted by Born and Mayer,[10] and by Sponer and Bruch-Willstätter.[11]

[7] R. A. Buckingham, Proc. Roy. Soc. **A160**, 94 (1937).
[8] It is quite possible that our values of C_2/C_1 are a little low because of our choice of $h\nu$. For consistency, this was taken wherever possible from the same authors (Cuthbertson); their values have a tendency to be smaller than those listed by other investigators.

[9] P. Gombar, Zeits. f. Physik **93**, 378 (1935). H. Jensen, Zeits. f. Physik **101**, 164 (1936).
[10] M. Born and J. E. Mayer, Zeits. f. Physik **75**, 1 (1932).
[11] H. Sponer and M. Bruch-Willstätter, J. Chem. Phys. **5**, 745 (1937).

Internal Rotation of Propane and Propylene; the Origin of the Internal Restricting Potentials

G. B. KISTIAKOWSKY, J. R. LACHER* AND W. W. RANSOM
Mallinckrodt Chemical Laboratory, Harvard University, Cambridge, Massachusetts
(Received November 11, 1938)

BY the "hot wire" technique[1,2] we have studied the heat capacities of propane and propylene down to 148°K. A novel refinement of the method made possible the calculation of the heat capacities (with not more than one percent error) even at the higher temperatures where the accommodation coefficient ratios deviate from unity. Selecting for propane the same vibrational frequencies as used by Pitzer[3] and for propylene a set suggested by Professor E. B. Wilson, Jr. (3000(6); 1648(1); 1415(2); 1297(1); 920(1); 432(1); 580(1); 1300(1); 1200(1); 1100(1); 900(3); 700(1)), the contribution of the internal rotation has been calculated in the usual manner and is plotted in Fig. 1. The curves in the figure give the isothermal dependence of the rotational heat capacity upon the restricting potential, drawn for two temperatures from the table of Pitzer;[4] the same curves apply to both molecules since their effective moments of inertia are nearly equal.

Propane shows a systematic trend of the apparent potential with temperature, which is even more pronounced when the vibrational assignment of Kemp and Egan[5] is used. The inconstancy is unquestionably due to a combination of improper frequency selection and of error in the experimental heat capacity. We expect to report in the near future the results of another experimental study made with a more accurate method at higher temperatures, but in the meantime it is entirely safe to conclude that propane possesses an internal potential of from 3200 to 3600 cal. per methyl group. This conclusion is in complete accord with the deduction of Pitzer[3] and of Kemp and Egan[5] (3300±400), based on comparisons of the third law and statistical entropies.

In propylene the restricting potential is seen to be about 600 to 800 cal. This is in accord with Pitzer's conclusion that the potential is less than 800 cal.[3] but the present method goes further than that and shows very conclusively the impossibility of reconciling a sixfold equipotential-minimum curve with the experimental data. A threefold minimum, on the other hand, agrees well with the new data.

One is thus led to believe that only one hydrogen atom—for instance the adjacent (secondary) one—hinders the rotation of the methyl group, although one of the hydrogen atoms of the $=CH_2$ group is at practically the same distance. But this conclusion is inconsistent with the findings on tetramethyl methane and some other compounds and thus we are led to discard the idea of hydrogen interactions as the cause of restricting potentials and to propose instead a different and more general formulation.

According to the new postulate the restricting potentials are due to an interaction which has hitherto not been explored with the aid of wave mechanics—an *interaction of electron pairs forming single bonds on adjacent polyvalent atoms*. If the evidence offered by Bartholomé and Karweil[6] on the symmetry character of ethane proves to be correct, the interaction is such as to give energy minima for a location of bonds in the same plane. The essential point in this interpretation is that *electron pairs forming double bonds do not take part in this orienting interaction*. The reason is as yet not clear but possibly the lack of axial symmetry of a double bond is responsible.

With this hypothesis in mind one sees readily why ethane and propane have rather similar potentials while that of propylene (and of the butenes-2[3]) is only about one-third as large. For tetramethyl methane Pitzer[3] finds a potential of

* Present address: Department of Chemistry, Brown University.

[1] Kistiakowsky and Nazmi, J. Chem. Phys. **6**, 18 (1938).
[2] Kistiakowsky, Lacher and Stitt, J. Chem. Phys. **6**, 407 (1938).
[3] Pitzer, J. Chem. Phys. **5**, 473 (1937).
[4] Pitzer, J. Chem. Phys. **5**, 469 (1937).
[5] Kemp and Egan, J. Am. Chem. Soc. **60**, 1521 (1938).
[6] Bartholomé and Karweil, Zeits. f. physik. Chemie, **B39**, 1 (1938).

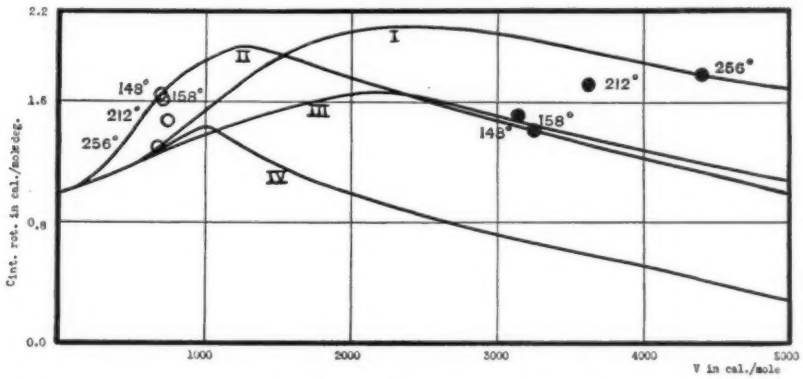

FIG. 1. Curves I and II, the dependence of heat capacity due to restricted internal rotation upon the restricting potential, $V = V_0(1-\cos 3\varphi)$. Curves III and IV, same but $V = V_0(1-\cos 6\varphi)$. Open circles, experimental values for propylene. Filled circles, experimental values for propane.

ca. 4200 cal. Although the value may be somewhat changed on a more exhaustive study of the vibrational frequencies of this molecule, it suggests that the orienting action of the C−C electron pairs is more energetic than is that of the C−H pairs; a slight increase of potential from ethane to propane is also evidence in favor of this.

The work of Schumann and Aston[7] on acetone and isopropyl alcohol is further confirmation of our ideas. They find that in acetone the restricting potentials are only 1000 cal. per methyl group, hence experimentally identical with that of propylene; indeed in both molecules the central carbon atom has only one single-bond electron pair contributing to the orienting interaction. In isopropyl alcohol the calculation is more uncertain because of *ad hoc* assumptions concerning the restriction of rotation of the hydroxyl hydrogen, but the calculations of Schumann and Aston indicate it as probable that the methyl groups are restricted to an extent not very different from that of propane.

The evidence on hydroxyl group is as yet rather contradictory. In methyl alcohol, where the uncertainties of vibrational assignment should have the least effect on the calculation of the restricting potential, the latter appears to be of the order of 2000 to 3000 cal.[8] Hence the interaction of an O−H electron pair with the C−H pairs is much more intense than that of another C−H electron pair. It may be however that unshared electron pairs of oxygen (and that of nitrogen in CH_3NH_2) also contribute to the interaction energy. For isopropyl alcohol Schumann and Aston[7] calculate 5000 cal. The figure may be materially in error but the trend is perhaps real, being due to a still stronger interaction with the C−C bonds. For ethyl alcohol Schumann and Aston[9] deduce 10,000 cal. This value seems to be entirely out of line and we venture to predict that a more complete study will revise it downward.

The findings of Beach and Palmer[10] that dichloroethylene has a potential of at least 5000 cal., indicates that the C−Cl bond has a rather strong interaction, but more certain data on this and other halogen compounds are needed. The C−H bonds have thus the least effect of all the studied bonds. Finally, the observations of Aston, Siller and Messerly[11] on methyl amine, where again a large restricting potential is needed to reconcile the third law and the statistical entropy, may be cited as evidence for the necessity of including the orienting bond interactions in considerations of all molecules capable of internal rotations.

[7] Schumann and Aston, J. Chem. Phys. **6**, 485 (1938).
[8] Kassel, J. Chem. Phys. **4**, 493 (1936); Halford and Pecherer, *ibid.*, **6**, 571 (1938); but see Borden and Barker, *ibid.*, **6**, 553 (1938).
[9] Schumann and Aston, J. Chem. Phys. **6**, 480 (1938).
[10] Beach and Palmer, J. Chem. Phys. **6**, 639 (1938).
[11] Aston, Siller and Messerly, J. Am. Chem. Soc. **59**, 1743 (1937).

A Note on the Raman Spectra of Nitrogen*

CHARLES E. MILLER
Department of Chemistry, Columbia University, New York, N. Y.
(Received October 30, 1938)

FOLLOWING the successful concentration of the N^{15} isotope in this laboratory,[1] plates were taken of the Raman spectra of ordinary nitrogen to see if the method could be used to determine the alternating intensity ratio of N_2^{15}. Although excellent rotational Raman spectra were obtained, it was found that a clear-cut determination of the N^{15} nuclear spin could not be made in this way because of the greatly increased number of lines that would result from the mixture of three isotopic molecules. However, as the only published values for the ground state rotational transitions of nitrogen are those of Rasetti,[2] it seemed worth while to record the frequency and intensity values obtained.

The Raman tube and mercury arcs used were those described by Teal and MacWood.[3] A Hilger E-1 quartz prism spectrograph, which was maintained at constant pressure and temperature, and contained mercury vapor to absorb the exciting line Hg, λ2537, was used to make the exposures. A stream of carbon dioxide was passed between the reflector and Raman tube to prevent the formation of ozone. The slit width was 0.03 mm, and the nitrogen pressure four atmospheres. A strong exposure could be obtained in 20 hours on a rapid plate (Eastman Ortho-Press), but in order to get better resolution a 100-hour exposure was made on a process plate.

The rotation spectrum is shown in Fig. 1, and a microphotometer tracing obtained from it in Fig. 2. The intensity relation for a rotation Raman transition of this type is given by Placzek and Teller[4] as:

$$I = I_0^0 \frac{\frac{3}{2}\frac{(J+1)(J+2)}{(2J+1)(2J+3)}(2J+1)g_j e^{-(E\,\mathrm{rot.}/kT)}}{Q},$$

where I_0^0 is the total intensity of the O−O band, g_j the nuclear spin factor, and Q the state summation. Intensities could not be measured directly as the plate was not calibrated for this purpose. However, as the darkenings for most of the lines fall on the linear portion of the sensitivity curve, darkenings have been plotted against log intensity (theoretical) with the result shown in Fig. 3. Points for lines too close to Hg λ2537 for intensity measurement, or too faint to lie on the

* Publication assisted by the Ernest Kempton Adams Fund for Physical Research of Columbia University.
[1] Thode and Urey, J. Chem. Phys., to be published.
[2] Rasetti, Proc. Nat. Acad. Sci. **15**, 515 (1929); Phys. Rev. **34**, 367 (1929).
[3] Teal and MacWood, J. Chem. Phys. **3**, 760 (1935).
[4] Placzek and Teller, Zeits. f. Physik **81**, 209 (1933).

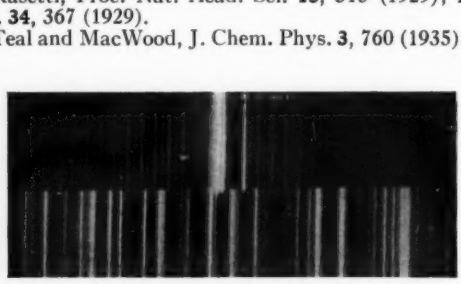

FIG. 1. O−O nitrogen rotation band.

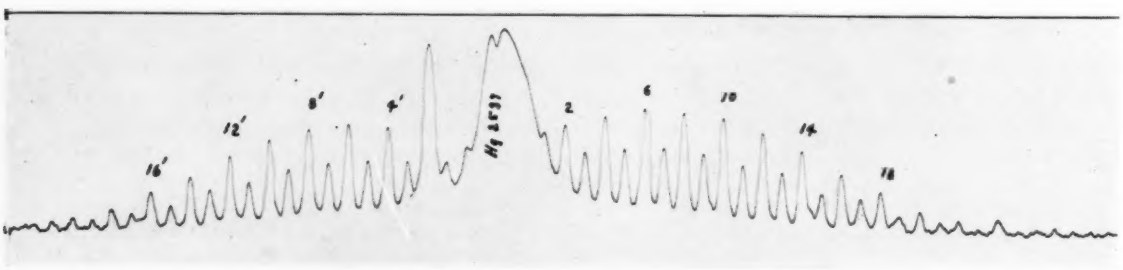

FIG. 2. Microphotometer tracing of nitrogen O−O band.

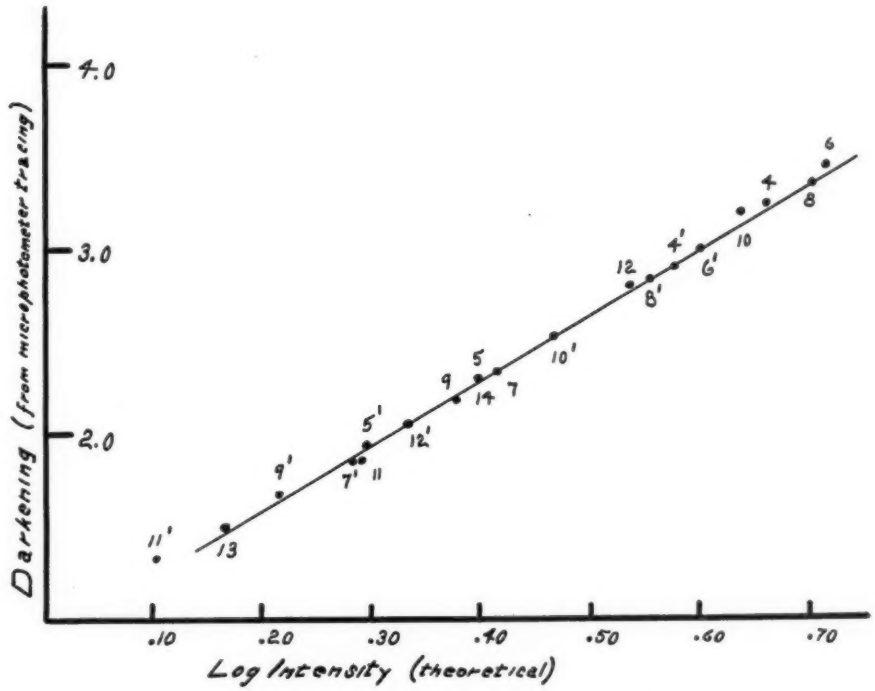

FIG. 3. The figures on the curve give initial J values for Stokes and Anti-Stokes lines. Primed values refer to Anti-Stokes lines.

linear part of the curve, have been omitted. This would seem to give a good experimental test of the equation of Placzek and Teller. Regardless of the plate characteristics it is seen that the transitions from $J=5$ and 14, which have the same theoretical intensity, give the same darkening. Measured and calculated intensities for hydrogen have been compared by Raman and Bhagavantam.[5]

The spectrograph has a dispersion of 2.7A/mm in the region near λ2537. Rotational frequency shifts first obtained showed differences between corresponding Stokes and Anti-Stokes lines too large to be accounted for by an error in plate measurement. This was traced to errors as large as 0.02A in the values given for the iron arc wavelengths in this region. The final calibration was made using the iron lines of wave-length 2519.628, 2530.694, and 2542.887A, given by Meggers and Humphreys[6] to 0.0005A, and the results corrected to vacuum. The frequency of Hg λ2537 was taken as 39412.76 cm^{-1}, this being an average value for symmetrically displaced Stokes and Anti-Stokes lines. The values of B_e

TABLE I.

	This Paper		Rasetti		
(J)	Stokes cm^{-1}	Anti-Stokes cm^{-1}	Stokes cm^{-1}	Anti-Stokes cm^{-1}	Calculated cm^{-1}
2	27.8				27.9
3	35.8	35.8			35.8
4	43.7	43.6		44.0	43.8
5	51.7	51.7			51.7
6	59.7	59.8	60.0	59.9	59.7
7	67.7	67.7			67.6
8	75.7	75.6	76.0	76.5	75.6
9	83.7	83.5			83.5
10	91.5	91.3	92.1	91.8	91.5
11	99.3	99.5			99.4
12	107.2	107.3	108.2		107.4
13	115.4	115.6			115.3
14	123.2	123.3	124.2		123.3
15	131.2	131.6			131.2
16	139.1	139.3			139.1
17	146.7	—			147.1
18	154.8	155.0			155.0

$B_0=1.980\pm0.002$ cm^{-1}, (this paper)
$B_0=1.992\pm0.005$ cm^{-1}, (Rasetti)
0–1 vibration frequency = 2328.3 cm^{-1}, (this paper)
0–1 vibration frequency = 2330.7 cm^{-1}, (Rasetti)
(Calculated values contain a first-order correction term with $D_e=5.8\times10^{-6}$ cm^{-1}.)

[5] Raman and Bhagavantam, Ind. J. Phys. **6**, 353 (1931).
[6] Meggers and Humphreys, Bur. Standards J. Research **18**, 543 (1937).

were obtained after adding to each frequency a correction term $=D_e(4J+6)(3J^2+3J+3)$, the value of D_e being obtained theoretically[7] from the vibration frequency as 5.8×10^{-6} cm^{-1}. This correction, while somewhat uncertain, amounts to only 0.17 cm^{-1} at $J=18$. Measured and calculated values of the rotation frequencies are given in Table I. B_0 was obtained using the value 0.018 cm^{-1} for α, as given by Jevons.[8] The value for the 0–1 vibration frequency was found to be 2328.3 cm^{-1}.

[7] Jevons, Report on Band Spectra of Diatomic Molecules, The Physical Society, (1932) p. 27.

[8] See reference 7, p. 284.

Correction: On the Paramagnetic Conversion of Parahydrogen and Orthodeuterium in the Presence of Nitrous Oxide (The Magnetic Moment of the Deuteron)

L. Farkas and U. Garbatski
Department of Physical Chemistry, The Hebrew University, Jerusalem
(J. Chem. Phys. **6**, 260 (1938))

THE title of the article referred to above should have read "Nitric Oxide" instead of "Nitrous Oxide."

LETTERS TO THE EDITOR

This section will accept reports of new work, provided these are terse and contain few figures, and especially few halftone cuts. The Editorial Board will not hold itself responsible for opinions expressed by the correspondents. Contributions to this section should not exceed 600 words in length and must reach the office of the Managing Editor not later than the 15th of the month preceding that of the issue in which the letter is to appear. No proof will be sent to the authors. The usual publication charge ($3.00 per page) will not be made and no reprints will be furnished free.

The Dielectric Polarization of Formic Acid Vapor

Some time ago, C. T. Zahn[1] studied the dielectric polarization of formic acid vapor between 71°C and 150°C. We have re-investigated this, with an improved apparatus,[2] and, in view of the recent interest in the separate properties of the monomer and dimer of this acid,[3] we think it timely to give a preliminary report of our observations, which are not in agreement with those of Zahn.

Dielectric polarization as a function of pressure was measured between 37.5°C and 127°C. Measurements at 37.5°, 53.9°, 64.4° and 74.2° were over a sufficiently broad pressure range to permit the determination of the polarizations of the monomer and dimer, P_1 and P_2, from the relation $P=P_1f_1+P_2f_2$. P is the apparent polarization at the mole fractions f_1, f_2, which are calculated from the vapor density data of Coolidge.[7] The "least squares" results and probable errors are:—

t°C	P_1	P_2
37.5	42.1±0.9	32.0±0.5
53.9	44.2±0.2	31.7±0.2
64.4	45.2±0.3	31.8±0.3
74.2	44.7±0.3	33.3±0.6

The figure for the temperature 64.4° shows a typical series of results. Those at 95° and 127° do not permit of such an extrapolation, but by assuming $P_2=32.0$ cc one obtains for P_1, 43.6 and 42.0, respectively. (The measurements at these temperatures are so close to the $f_2=0$ axis, that the values of P_1 are not very sensitive to the value assumed for P_2.) There is some indication from the 95° results that P_2 has risen to 36–38 cc, but this is not very certain.

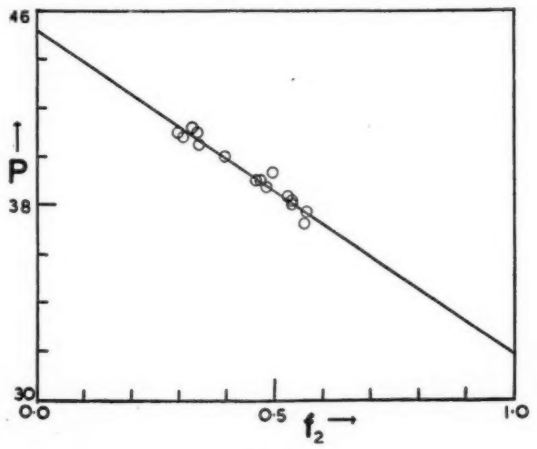

FIG. 1.

The polarization of the monomer appears first to rise with temperature and then to diminish, the maximum being at about 70°. This behavior suggests that in the temperature range studied, there is a transition from one state to another of higher energy and higher dipole moment.[4] The transition is perhaps from a low energy state in which the "hydroxyl" hydrogen atom is locked *cis* to the "carbonyl" oxygen, owing to resonance and hydrogen bonding forces to a high energy state in which either the hydrogen atom is fixed *trans* to the "carbonyl" oxygen[5] or is free to rotate around the "hydroxyl" oxygen. This latter case is somewhat analogous to that of ethylene dichloride.[6]

If one of these interpretations is correct, it is to be expected that:—

(a) The infra-red spectrum of formic acid monomer at 40°C would be different from that at 140°C.[3]

(b) Depending upon the relation between the energy difference for the two postulated structures, and the amount of zero point energy in each, the polarization temperature behavior of monomeric "half-heavy" formic acid HCO_2D might well be different from that for the ordinary monomer.

The polarization of the dimer is either constant or increases with temperature. We therefore disagree with Zahn who concluded tentatively that the dimer has a permanent dipole moment. The difference of 15.5 cc between the total polarization and the electron polarization is probably atom polarization, since it has recently been demonstrated that in such molecules as this, where large moments are opposed and may readily be changed with respect to one another, large values for the atom polarization are to be expected.[2]

We hope, in the near future, to modify our apparatus to measure larger changes of dielectric constant from vacuum, so that more precise information may be obtained as to the polarization of the dimer at high temperatures.

I. E. COOP
N. R. DAVIDSON
L. E. SUTTON

Dyson Perrins Laboratory,
Oxford, England,
November 4, 1938.

[1] Zahn, Phys. Rev. **37**, 1516 (1931).
[2] Coop and Sutton, J. Chem. Soc. 1269 (1938).
[3] Bonner and Hofstadter, J. Chem. Phys. **6**, 531 (1938). Hofstadter, J. Chem. Phys. **6**, 540 (1938).
[4] Zahn, Phys. Rev. **35**, 1056 (1930).
[5] Marsden and Sutton, J. Chem. Soc. 1383 (1936).
[6] Lennard-Jones and Pike, Trans. Faraday Soc. **30**, 830 (1934).
[7] Coolidge, J. Am. Chem. Soc. **50**, 2166 (1928).

Dipole Moment and Surface Potentials

In a previous note[1] it was stated that films of ω-bromohexadecanoic acid show large negative surface potentials. These films afford relatively favorable conditions for the comparison of dipole moment and surface potential data. A more detailed investigation showed, however,[2] that the free acid films are remarkably unstable, a certain degree of soap formation being a necessary condition for the existence of stable films. The best results were obtained in the presence of polyvalent cations. The instability of the free acid films is undoubtedly connected with the repulsive forces acting between the similarly orientated C−Br dipoles. As little is known about the structure of fatty acid films on neutral or slightly alkaline solutions in the presence of polyvalent cations, we tried to stabilize the ω-bromoacid films by mixing the ω-bromoacid with an excess of the unsubstituted compound. The mixed films obtained in this way are stable up to a concentration of 50 percent of the ω-bromoacid and possess interesting properties. A series of surface potential-area curves obtained with mixtures of palmitic acid with increasing quantities of $Br(CH_2)_{15}COOH$ on 10^{-2} norm. HCl are given in Fig. 1. The admixture of the ω-compound causes a large decrease of the positive surface potential observed with palmitic acid; with higher concentrations the surface potential becomes negative, but this negative effect disappears if the surface area is increased and a curious change of the sign of the surface potential is observed on expansion of the film. Similar series of curves were obtained with palmitic acid $+Br(CH_2)_{12}COOH$, $Br(CH_2)_{14}COOH$ and $I(CH_2)_{14}COOH$ and cetyl alcohol $+Br(CH_2)_{14}OH$. In the latter case the influence of the ω-compound on the surface potential is especially large, the potential becoming negative on addition of 25 percent of the ω-alcohol. The addition of the ω-compounds causes a gradual transition of the film to the expanded state. The resistance of the films of acids to pressure is thereby strongly decreased; for instance, the maximum pressure obtained with 90 percent $CH_3(CH_2)_{14}COOH$+10 percent $Br(CH_2)_{15}COOH$ is 12.7 and with 75 percent $CH_3(CH_2)_{14}COOH$+25 percent $I(CH_2)_{14}COOH$ 7.2 dynes per cm. The mixed alcohol films are much more stable and pressures up to 30–40 dynes per cm can be obtained.

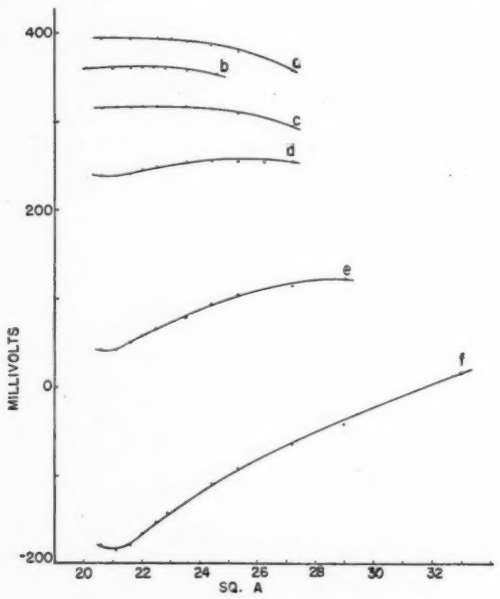

FIG. 1. *a*—palmitic acid, *b*—2%, *c*—5%, *d*—10%, *e*—25%, *f*—50%. $Br(CH_2)_{15}COOH$.

TABLE I.

FILM	$\bar{\mu}\times10^{18}$
$Br(CH_2)_{15}COOH$ +palmitic acid	0.95
$Br(CH_2)_{12}COOH$ +palmitic acid	0.82
$I(CH_2)_{14}COOH$ +palmitic acid	0.97
$Br(CH_2)_{14}OH$ +cetyl alcohol	1.25

The effective dipole moment per C−Br linkage $\bar{\mu}$ was calculated in the following way. Let us denote by V_0 the surface potential of the film of the unsubstituted compound, by V_1 the surface potential of the mixed film, the total number of molecules per cm² being equal in both cases, then

$$\bar{\mu}=(V_0-V_1)/4\pi n,$$

where n is the number of the molecules of the ω-compound per cm². The values of $\bar{\mu}$ obtained in this way for different concentrations of the ω-compound in the film were extrapolated to zero concentration; the results are given in Table I. The area per molecule was 20.5A² (maximum compression). The method outlined here is quite similar to the usual calculation of dipole moments from measurements of dielectric constants of solutions in a nonpolar solvent, which leads to values between 1.8 and 1.9×10^{-18} for the C−Br linkage in different normal bromosubstituted hydrocarbons.

The values obtained in this way especially in the case of the alcohol films, are much closer to the accepted values of the dipole moments than those usually obtained from surface potential data. The lower values obtained with acids are perhaps connected with a partial collapse of the films at strong compressions, as indicated by the low resistance to compression of these films. If we assume in the alcohol film a normal angle of 54° 44′ between the C−Br linkage and the water surface, the value of $\bar{\mu}$ in Table I had to be increased by a factor of $1 : \sin 54° 44' = 1.22$, which leads to a value of 1.53×10^{-18} for the dipole moment of the C−Br linkage.

The samples of the ω-compounds used with the exception of $I(Cu_2)_{14}COOH$ were kindly supplied to one of us by Dr. M. Stoll, Geneva.

M. GEROVICH
A. FRUMKIN
D. VARGIN

Electrochemical Laboratory,
University of Moscow,
Moscow, U. S. S. R.,
October 31, 1938.

[1] M. Gerovich and A. Frumkin, J. Chem. Phys., **4**, 624 (1936).
[2] M. Gerovich and D. Vargin, Acta Physicochimica URSS **8**, 63. (1938).

The Equivalent Conductances of Europium Chloride and of Europium Nitrate

In recent notes in this journal[1, 2] some experiments on the spectra of solutions of trivalent europium have been reported. From these experiments it was noted[3] "that the salts of europium are revealing bonds which are permanently oriented;" yet from the close resemblances among the rare earths in general, it would not be too much to assume that the salts of europium are just as strong electrolytes as those of lanthanum. Unfortunately, however, since no thermodynamic data, such as freezing-point lowering or conductance measurements, existed on europium salts, this assumption could not be checked. As has also been pointed out,[1] we wish to "look upon europium as an indicator for the symmetries of the fields about the other rare earth ions." It was considered advisable, therefore, to carry out electrical conductance measurements on solutions of europium salts. These results could then be compared with the corresponding data on other rare earth salts, so that in case of conformance, any phenomena connected with the electrical character of the europium ion could be considered characteristic of the rare earth ions in general. Comparison with the conductances of the corresponding lanthanum salts should be particularly significant since lanthanum salts have always been considered typical trivalent electrolytes.

The europium salts used were prepared from samples of europium oxalate presented by Dr. H. N. McCoy for our researches. The oxalate was ignited to the oxide, a slight excess of nitric or hydrochloric acid added, and the substances were heated on a hot plate for at least three hours after all of the excess acid had evaporated. In this way large masses of crystals of europium nitrate and europium chloride, respectively, were obtained.

The data obtained (Table I) have been plotted in Fig. 1

TABLE I. *Equivalent Conductances at 25°C.*

Europium Nitrate		Europium Chloride	
N	Λ	N	Λ
.07277	91.6	.07100	101.0
.03639	100.0	.03550	108.2
.01820	108.1	.01775	115.3
.00910	115.2	.00888	121.6
.004550	122.1	.004438	127.4
.002275	128.0	.002219	132.1

together with values for the corresponding lanthanum salts at 25°C converted from Öholm's data[4] at 20°C. Inspection shows that the europium curves are "normal" in all respects. In fact in the case of europium chloride the conductances are so similar to those of lanthanum chloride, that on the scale to which the graph is drawn, it is impossible to distinguish the curves. If lanthanum chloride is a strong electrolyte, europium chloride must certainly be one also. If lanthanum chloride is "completely ionized," europium chloride must also be "completely ionized."

Similarly in the case of the nitrate curves, the graph of the europium salt is similar both in magnitude and shape to that of the lanthanum salt. Furthermore, the europium nitrate conductivities, carried out over the range of concentration from $0.02N$ to $0.0007N$, show no abnormalities, yet it is during this region that the spectrum of the nitrate shows the change from the "nitrate-structure" to the "chloride-structure."

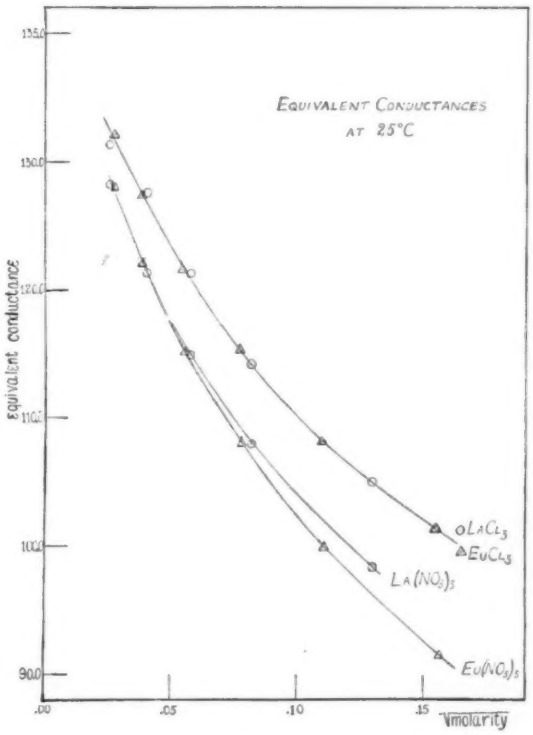

FIG. 1.

Comparison of the experimental results with rough data on the electrical conductivities of rare earth salts besides those of lanthanum shows similar agreement.

Conductance data thus show that in electrical properties the europium ion is typical of the rare earth ions. It is thus quite reasonable to assume that the electrical properties of europium ion revealed by its spectra are characteristic of the other rare earth ions also.

I. M. KLOTZ

Jones Chemical Laboratory,
University of Chicago,
Chicago, Illinois,
October 27, 1938.

[1] S. Freed and S. I. Weissman, J. Chem. Phys. **6**, 297 (1938).
[2] S. Freed and H. F. Jacobson, J. Chem. Phys. **6**, 654 (1938).
[3] S. Freed, J. Chem. Phys. **6**, 655 (1938).
[4] L. W. Öholm, Soc. Sci. Fennica, Acta and Comm. Phys. Math. **9**, 2 (1936).

Correction: The Effect of Structure upon the Reactions of Organic Compounds. Temperature and Solvent Influences

(J. Chem. Phys. **4**, 613 (1936))

On page 615, in the eighth line from the bottom of column 1 the word small should be substituted for the word large.

LOUIS P. HAMMETT

Columbia University,
New York City,
September 14, 1938.

The Nuclear spin of N^{15}

A sample of heavy ammonia with about 36 percent N^{15} which was furnished us by Professor H. C. Urey yielded the bands of $N^{15}-N^{15}$ with sufficient strength to determine the spin of N^{15}. Almost all the bands of $N^{15}-N^{15}$ are so confused with bands of $N^{14}-N^{15}$ and $N^{14}-N^{14}$, or are so complex, that the rotational structure is not sufficiently open for reliable intensity measurements (see R. W. Wood and G. H. Dieke,* where the analysis of the $N^{14}-N^{15}$ bands is given). A notable exception is the $1\rightarrow 0$ band of the negative band (N_2^+), the head of which is at 3582.3A for $N^{14}-N^{14}$, 3587.4 for $N^{14}-N^{15}$, and 3592.5 for $N^{15}-N^{15}$. The P branch of the latter band is completely free from overlapping with other bands and, except for the lines at the very head, is completely resolved in the second order of our 21-foot grating with 30,000 lines per inch and a dispersion of about 0.6A per mm. The alternating intensities of successive rotational lines are plainly visible. In order to determine the spin a detailed measurement of the intensities is superfluous, as it is only necessary to distinguish between a few definite ratios (3 to 1 for $i=\frac{1}{2}$, 2 to 1 for $i=1$, 5 to 3 for $i=3/2$, etc.) and therefore a simplified method of intensity comparison can be used. We placed a rotating sector directly in front of the plate so that it would cut down the intensity of the lower half of the lines to one-third its original value. The microphotometer then showed that the intensities of the strong lines, when reduced to a third of their original intensity, fell on the same smooth curve as the unreduced weak lines. This proves that the intensity ratio is 3 : 1 and this was confirmed by trying other ratios of the rotating sector. Lines in other bands which are free from other lines can also be used for this purpose.

The nuclear spin of N^{15} is therefore $\frac{1}{2}$. This agrees with what should be expected, as ${}_7N^{15}$ can be obtained from ${}_8O^{16}$ (which has no spin) by taking away one proton. And whereas in $N^{14}-N^{14}$ the even numbered lines are the strong ones, it is just the reverse for $N^{15}-N^{15}$, which shows that, in agreement with expectation, the N^{15} nuclei obey Fermi-Dirac statistics.

A detailed analysis of the whole band system will appear later.

We wish to express our most sincere thanks to Professor Urey for the heavy nitrogen which made this investigation possible.

R. W. Wood
G. H. Dieke

The Johns Hopkins University,
Baltimore, Maryland,
November 16, 1938.

* R. W. Wood and G. H. Dieke, J. Chem. Phys. **6**, 734 (1938).

Addendum: Primary Processes in Photodecomposition

(J. Chem. Phys. **6**, 416 (1938))

It should have been mentioned in our discussion of the formaldehyde decomposition that, since 1932, Norrish has on several occasions expressed the opinion that the predissociation in the discrete region is spontaneous.[1]

Milton Burton
G. K. Rollefson

University of California,
Berkeley, California,
September 26, 1938.

[1] Norrish, Acta Physicochimica **3**, 173 (1935); Trans. Faraday Soc. **30**, 105 (1934); Proc. Roy. Soc. London **A146**, 257 (1934).

J. C. Halford

THE JOURNAL OF CHEMICAL PHYSICS

VOLUME 6 NUMBER 12

DECEMBER, 1938

Published by the

AMERICAN INSTITUTE OF PHYSICS

Incorporated

LANCASTER, PA., AND NEW YORK, N. Y.

CONTENTS

J. CHEM. PHYS. 6 (1938) DECEMBER

Diffuse Electron Diffraction Patterns . . . . . J. T. BURWELL 749
Ultraviolet Absorption Bands Ascribed to HNO_3 . . . . D. M. NEWITT AND L. E. OUTRIDGE 752
Infra-Red Absorption of Carboxylic Acids in Solution. I. Qualitative Features . . . . . M. M. DAVIES AND G. B. B. M. SUTHERLAND 755
Infra-Red Absorption of Carboxylic Acids in Solution. II. Intensities . . . . . M. M. DAVIES AND G. B. B. M. SUTHERLAND 767
Infra-Red Study of Omega-Hydroxyundecanoic Acid in Carbon Tetrachloride . . . . . MANSEL M. DAVIES 770
Infra-Red Bands of Methylamine and the Phenomenon of Free Rotation . . . . . H. W. THOMPSON AND H. A. SKINNER 775
Kinetics of OH Radicals Determined by Their Absorption Spectrum. IV. Pressure Broadening and the Line Spectrum as Background . . . . . O. OLDENBERG AND F. F. RIEKE 779
Alpha-Particle Reactions in Carbon Monoxide, Oxygen and Carbon Dioxide Systems . . . . . JOSEPH O. HIRSCHFELDER AND HUGH S. TAYLOR 783
Slow Electron Scattering and the Apparent Electron Affinity of Mercury . . . . . J. H. SIMONS AND R. P. SEWARD 790
Energy of the Triatomic Hydrogen Molecule and Ion, V. . . . . JOSEPH O. HIRSCHFELDER 795
Integrals Required for Computing the Energy of H_3 and of H_3^+ . . . . . JOSEPH O. HIRSCHFELDER AND CORNELIUS N. WEYGANDT 806
Reaction of Hydrogen Atoms with Carbon Tetrachloride JOHN E. VANCE AND W. C. BAUMAN 811
Calculation of Bond Strengths from Photochemical Evidence . . . . . MILTON BURTON 818
Optical Activity of Secondary Butyl Alcohol . . . . . EVERETT GORIN, JOHN WALTER AND HENRY EYRING 824
Kinetic Approach to the Theory of Conductance of Infinitely Dilute Solutions, Based on the "Cage" Model of Liquids . . . . . MILTON J. POLISSAR 833
Equation for Transference Numbers . . . . . THEODORE SHEDLOVSKY 845
Molecular Interaction in Mixed Monolayers on Aqueous Subsolutions. I. Mixtures of Alcohols, Acids and Amines . . . . . WILLIAM D. HARKINS AND ROBERT T. FLORENCE 847
Molecular Interaction in Mixed Monolayers. II. Unstable Mixtures with Unsaturated Acids . . . . . ROBERT T. FLORENCE AND WILLIAM D. HARKINS 856
Migration and Photochemical Action of Excitation Energy in Crystals . . . . . JAMES FRANCK AND EDWARD TELLER 861
Role of Attractive and Repulsive Forces in the Formation of Tactoids, Thixotropic Gels, Protein Crystals and Coacervates . . . . . IRVING LANGMUIR 873
Quadrupole Contributions to London's Dispersion Forces . . . . . HENRY MARGENAU 896
Internal Rotation of Propane and Propylene; the Origin of the Internal Restricting Potentials . . . . . G. B. KISTIAKOWSKY, J. R. LACHER AND W. W. RANSOM 900
Note on the Raman Spectra of Nitrogen . . . . . CHARLES E. MILLER 902
Correction: On the Paramagnetic Conversion of Parahydrogen and Orthodeuterium in the Presence of Nitrous Oxide (The Magnetic Moment of the Deuteron) . . . . . L. FARKAS AND U. GARBATSKI 904

Letters to the Editor:

Dielectric Polarization of Formic Acid Vapor . . . I. E. COOP, N. R. DAVIDSON AND L. E. SUTTON 905
Dipole Moment and Surface Potentials . . . . . M. GEROVICH, A. FRUMKIN AND D. VARGIN 906
Equivalent Conductances of Europium Chloride and of Europium Nitrate . . . . . I. M. KLOTZ 907
Correction: The Effect of Structure upon the Reactions of Organic Compounds, Temperature and Solvent Influences . . . . . LOUIS P. HAMMETT 907
Nuclear Spin of N^{15} . . . . . R. W. WOOD AND G. H. DIEKE 908
Addendum: Primary Processes in Photodecomposition . . MILTON BURTON AND G. K. ROLLEFSON 908

Author Index to Volume 6 909
Analytic Subject Index to Volume 6 915
Volume Table of Contents i

LANCASTER PRESS, INC., LANCASTER, PA.